UNIVERSITÉ DE STRASBOURG

ÉCOLE DOCTORALE DES SCIENCES DE LA VIE ET DE LA SANTÉ
INSTITUT DE BIOLOGIE MOLÉCULAIRE DES PLANTES UPR-CNRS 2357

THÈSE

présentée par :

Joelle MAKARIAN

soutenue le : 2 décembre 2016

pour obtenir le grade de : **Docteur de l'Université de Strasbourg**

Mention : Sciences de la Vie et de la Santé

Discipline : Aspects Moléculaires et Cellulaires de la Biologie

Rôle du facteur d'initiation eIF3h dans la réinitiation de la traduction et dans la pathogénèse virale chez les plantes

THÈSE dirigée par :
Mme. RYABOVA Lyubov — Directrice de recherche, Université de Strasbourg, IBMP-CNRS

RAPPORTEURS EXTERNES :
M. MEYER Christian — Directeur de recherche, INRA-Centre Versailles-Grignon
M. POOGGIN Mikhail — Directeur de recherche, CIRAD- Montpellier

EXAMINATEUR INTERNE :
M. HEINLEIN Manfred — Directeur de recherche, Université de Strasbourg, IBMP-CNRS

فكم عينٍ لنا سهرتْ وجفنٍ في دياجينـــا

وكمْ في ليلنا الساجي، أضـأنَا الكتْب تالينَـــا

ونام النـــــاسُ لكنا صحبْنا النجمَ راعينَا

فقرطاسٌ نسامـــرهٌ ، وقرطَـاسٌ يسلِّينا

و مسألةٌ تداعبُنا ، و أخـرى قد تبكِّـــينا

و نرقى بالنجـاحِ إلى مقـامات تعلِّيـنا

تخرُّجنا شراعُ النصر حـادٍ باتَ هـــادينا

فمنْ في قلبه عزمٌ كعـزمٍ باتَ يذْكيـــنا

ومن في عينِـه مجد تراءى في مراميـــنا

شربْنا العلمَ مصبَحَنا ، و بالآداب ممسيـــنا

" تهانيـنا تهانيـنَا ، و هذا الفوزُ يكفـينَا "

ACKNOWLEDGEMENTS

The guidance, support and participation of many people led my PhD work reach the desired accomplishment. First of all, I would like to express my sincere gratitude to my advisor Dr. Lyuba Ryabova for her continuous guidance and support during my PhD study and related research, for her patience, motivation and immense knowledge. Without her comments and advices, I would not have been able to advance further in my project. I could not have imagined having a better advisor for my thesis work.

Also, I would like to thank my thesis committee members Drs. Christian Meyer, Mikhail Pooggin and Manfred Heinlein. Their valuable knowledge, achievements and perspectives in my research field of study widened my scientific vision and broadened the research domain.

Special gratitude to Dr. Mikhail Schepetilnikov for all his time, valuable ideas and discussions thus, making my research journey and experience fruitful and productive. In addition, I would like to thank Dr. Eder Mancera for his training, help, and stimulation. Also, many sincere appreciations go to my lab colleagues for their support and for maintaining a joyful working environment.

In addition, I would like to express my gratitude to my friends and sisters Yasmine Jabaly, Zeinab Wehbe, Batoul Srour, Ola Srour, Nedal Taha and Rania Noureddein for being next to me in my tough and happy times throughout my stay in France.

To the “Dr. to be” Wael Bazzi, thank you for your continuous listening and motivation and for being beside me during my PhD journey. You have been a constant pillar of support, always encouraging when times were hard. Thank you for the really happy and funny moments we spent together my dear, it will be stuck in my mind forever.

Last but not least, no words can explain the amount of love and gratitude I hold to my parents whom I dedicate this work. To my mother, your dream to see your second daughter graduate

as a “Dr” is fulfilled with your continuous prayers. To my father, your support throughout my life is priceless. I promise you to always make you proud. To my sister, thank you for being next to me in every step I take and for all your advices, much love to you and your family.

LIST OF ABBREVIATIONS

Abbreviation	Term
ABCE-1	ATP-binding cassette protein-1
ARF	Auxin response factor
CaMV	Cauliflower mosaic virus
CSN	COP9 signalosome
eIF	Eukaryotic initiation factor
GTP	Guanosine-5'-triphosphate
IRES	Internal ribosome entry site
MAV	MiniTAV, Minimal transactivation domain
MBD	Multiple protein binding domain
ORF	Open reading frame
uORF	Upstream open reading frame
sORF	Short open reading frame
ORMV	Oilseed rape mosaic virus
PABP	Poly-A binding protein
PIC	Preinitiation complex
mRNA	Messenger RNA
Met-tRNA^{Met}i	Methionine initiator transfer RNA
pgRNA	Pre-genomic RNA
tRNA	Transfer RNA
RISP	Reinitiation supporting protein
RPL24	Ribosomal protein L24
S6K1	Eukaryotic ribosomal protein eS6 kinase-1
TAV	Transactivator/viroplasmin
TC	Ternary complex
TOR	Target of rapamycin
TuMV	Turnip mosaic virus
TURBS	Termination Codon Upstream Ribosome-Binding Site
UTR	Untranslated region
40S	Small ribosomal subunit
60S	Large ribosomal subunit
80S	80S ribosome

LIST OF CONTENTS

PREFACE

Short upstream open reading frames (uORFs) – located in the 5'-untranslated region (5'UTR) of mRNAs – are important regulators of gene expression. uORFs are involved in the control of groups of genes coding for potent proteins such as cytokines, growth factors, protein kinases, and transcription factors. Translation of mRNAs harboring multiple uORFs within their 5'-leader regions occurs via the mechanism of translation reinitiation. Although production of two or more long polypeptides from the same RNA via translation reinitiation is a very rare event in eukaryotes, reinitiation can occur if the first ORF is small, and this reinitiation event is usually less efficient. Often, uORFs are used to down-modulate the production of potent or toxic proteins. The efficiency of reinitiation is controlled by structural mRNA features, such as the size of the upstream ORF (less than 30 codons), and the availability of initiation factors. A possible explanation for the inhibitory effect of a longer ORF on reinitiation efficiency when compared with that of a small one might be due to the preservation of initiation factors on the terminating ribosome after a short translation event. Preserved factors help 40S ribosomal subunits to resume scanning and/or allow them to remain steady for any possible reinitiation event. Among these factors, eukaryotic initiation factor 3 (eIF3) plays the most important role. eIF3 assists the most of translation initiation steps and participate in re-acquirement of critical factors *de novo* that would allow reinitiation to occur.

In view of the small size of viral genomes, viruses often exploit non-canonical translational mechanisms to “decompress” their condensed genetic information. So far, there is no evidence that viruses and particularly plant viruses inhibit host translation in favor for their own mRNAs translation. Therefore, to ensure optimal production of their gene products, viral RNA must compete with cellular mRNAs for the host translational machinery. *Cauliflower mosaic virus* (CaMV) is a member of the *Caulimoviridae*, the sole family of plant pararetroviruses. The CaMV DNA genome is transcribed into two major transcripts: the 35S polycistronic RNA and the 19S monocistronic RNA. Interestingly, CaMV has developed an alternative translation initiation strategy to overcome cellular barriers to polycistronic translation that is prohibited under normal circumstances in eukaryotes. The CaMV factor transactivator/viroplasmin (TAV) is a rule-breaker that up-regulates the plant reinitiation machinery to its own needs. All these features make CaMV an interesting model to study translation reinitiation strategies and essential host factors. TAV binds and mediates target of rapamycin (TOR) activation that gives us opportunity to study upstream effectors TOR in plants. TOR mediates temporal control of cell growth by activating anabolic processes such as ribosome biogenesis, protein synthesis, transcription, and nutrient uptake, and by inhibiting catabolic processes such as autophagy and ubiquitin-dependent proteolysis. TOR, a critical sensor of nutritional and cellular energy and a major regulator of cell growth is a large serine/threonine protein kinase.

One of eIF3 subunits, eIF3h is an important reinitiation factor that becomes active in reinitiation, if phosphorylated via the TOR signaling pathway. In plants, eIF3h strongly increases reinitiation competence of uORF-containing mRNAs (uORF-RNAs), for example those encoding transcriptional factors, the auxin response factors (ARFs) and the basic zipper transcription factors (bZIPs) via unknown mechanisms. Importantly, translation reinitiation and auxin-mediated organogenesis are severely compromised by mutations in

eIF3h. The function of eIF3h is very specific to reinitiation—the subunit h is required for reinitiation after short ORF translation, but not for cap-dependent translation initiation events. The fact that eIF3h is a phosphorylation target of the TOR signaling pathway allow us to link reinitiation and signal transduction events. It was proposed that TOR functions in polysomes to maintain the active S6K1 (and thus eIF3h) phosphorylation status that is critical for translation reinitiation after short ORF. However, the mechanism of eIF3h function in reinitiation after short ORF translation remains to be elucidated.

The main aim of my thesis is to study the mechanism of eIF3h function in reinitiation of translation after short uORFs, along with its role in both TAV-mediated transactivation of polycistronic translation after long ORFs and during CaMV infection. To understand translation initiation mechanisms, first, I will present a brief overview of the basic translational phases-initiation, elongation and termination, and canonical translation (re)initiation factors known in eukaryotes. Second, I will describe in details the main players in reinitiation after short ORF translation in plants, as well as reinitiation after long ORF translation mediated by CaMV TAV. My work will introduce and highlight eIF3h as a new factor required for CaMV amplification and a critical reinitiation factor essential for both cellular and viral reinitiation events.

I. INTRODUCTION

In translation, the genetic code demonstrates the communication between the sequence of nucleotides in a gene and the corresponding amino acid sequence that it encodes. This communication is achieved with high organization and complexity, where the ribosome reads the sequence of the mRNA to assemble the corresponding protein. This mechanism requires the displacement of the tRNA within the ribosome and requires various quality check steps. Three main phases complete the translational process: the initiation, the elongation and the termination phase. The initiation of translation is considered to be the most complex and is highly regulated. The elongation phase is the stepwise addition of amino acids to the growing protein chain that requires function of the elongation factors, the ribosome and the aminoacyl-tRNAs along the mRNA. This phase ends, when the ribosome encounters one of the three stop codons (UAA, UGA or UAG) allowing the termination phase to start (BROWNING AND BAILEY-SERRES 2015). In some cases, after the termination of translation ribosomal subunits can resume scanning and initiate at a downstream AUG codon on the same mRNA (FUTTERER AND HOHN 1996).

1. General overview of translation

1.1 Initiation phase

Initiation of translation begins with the binding of the eukaryotic initiation factor 1 (eIF1), eIF1a, eIF5 and eIF3, the ternary complex (TC) consisting of the methionyl-tRNA (Met-tRNAi) and the GTP-bound eukaryotic initiation factor (eIF2) to the small 40S ribosomal subunit (40S) to form the 43S preinitiation complex (43S PIC) (Figure 1.1-1) (KLANN AND DEVER 2004). 43S PIC is loaded on the mRNA near the 5'-cap in a process facilitated by eIF3, eIF4B and eIF4F to form the 48S PIC. The eIF4F complex is composed of the cap-binding protein eIF4E, the scaffold protein eIF4G and the RNA helicase eIF4A. The 48S PIC scans along mRNA until it encounters the initiation codon (AUG) in a favorable initiation sequence context (GALLIE 2002; SCHEPETILNIKOV *et al.* 2011). Codon-anticodon pairing triggers eIF5-dependent hydrolysis of eIF2-bound GTP (conversion of GTP-eIF2 to GDP-eIF2 accompanied by the release of phosphate) and release of GDP-bound eIF2. The next step is the recruitment of the large ribosomal subunit (60S) by eIF5B and formation of the 80S ribosome that enters the elongation phase of protein synthesis (PISAREV *et al.* 2007; HINNEBUSCH AND LORSCH 2012).

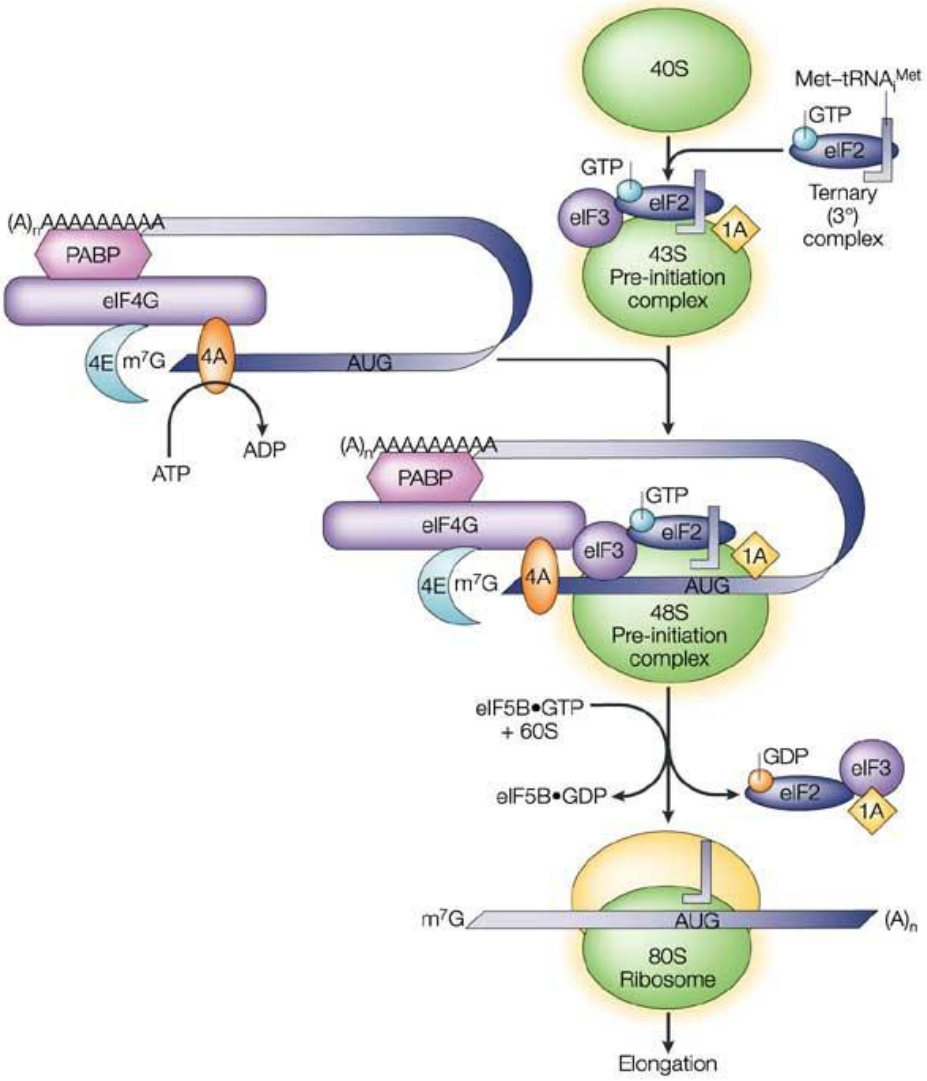

Figure 1.1-1 Pathway of translation initiation in eukaryotes
GTP-bound eIF2 and methionyl–initiator transfer RNA (Met–tRNAi^{Met}) form a ternary complex (TC), which together with eIF3, eIF1 eIF1A associate with 40S to generate a 43S pre-initiation complex (43S PIC). The cap-binding complex, which consists of eIF4E (4E), eIF4G and eIF4A (4A) binds to the 7-methyl-GTP (m7GTP) cap structure at the 5' end of a messenger RNA (mRNA). eIF4G also binds to the poly(A)-binding protein (PABP), thereby bridging the 5' and 3' ends of the mRNA. This mRNA circularization and the ATP-dependent helicase activity of eIF4A are thought to promote the binding of 43S PIC to the mRNA, which produces a 48S pre-initiation complex. Following scanning of 43S PIC to the AUG start codon, codon-anticodon interaction triggers hydrolysis of eIF2-bound GTP and eIF2 release. GTPase eIF5B is required for 60S recruitment to 48S PIC. Resulting 80S is competent for translation elongation and protein synthesis. *Modified from Eric Klann & Thomas E. Dever (2004), Nature Reviews Neuroscience 5, 931-942*

1.2 Elongation phase

Translation elongation is an evolutionarily conserved process, consisting of three major steps: decoding, peptide bond formation and tRNA–mRNA translocation (RODNINA AND WINTERMEYER 2009; RODNINA AND WINTERMEYER 2016). Following the 80S placement on the mRNA and the Met-tRNA occupation of the P site, the ribosome then chooses its aa-tRNA coupled to eEF1A-GTP and targeting its corresponding codon in the ribosomal A site (DEVER AND GREEN 2012; RODNINA AND WINTERMEYER 2016). Interaction between codon-anticodon at the A site triggers eEF1A release, GTP hydrolysis and peptide bond formation between the peptidyl-tRNA and aminoacyl-tRNA leaving a deacetylated tRNA in the P site (BROWNING AND BAILEY-SERRES 2015; RODNINA AND WINTERMEYER 2016). The newly synthesized peptidyl-tRNA and the deacylated tRNA occupying the A site and P site, respectively, shift to their subsequent positions (P and E sites) by a process termed translocation that requires eEF2-GTP binding and GTP hydrolysis (DEVER AND GREEN 2012; DOERFEL *et al.* 2013). Now, the A site is ready to accept a new aa-tRNA and start the next elongation cycle.

1.3 Termination phase

Translation termination occurs when a stop codon (UAA, UGA or UAG) enters the A site of the ribosome indicating that the end of the coding sequence is reached. Mainly two factors catalyze termination in eukaryotes, eukaryotic release factor (eRF1) and (eRF3) that sense the stop codon (Figure 1.3-1) (STANSFIELD *et al.* 1995; RODNINA 2010; DEVER AND GREEN 2012). eRF1 (class I release factor) plays role in a highly sensitive way to recognize the stop codon and peptidyl-tRNA hydrolysis, while eRF3 (class II release factor) is a translational GTPase (ATKINSON *et al.* 2008). When the ribosome encounters a stop codon, the eRF3-GTP-eRF1 occupies the ribosomal A site, acting as a lock to prevent the entry/binding of any

eIF1A-aa-tRNA complexes (BROWNING AND BAILEY-SERRES 2015). It was shown that the eRF1 has a highly similar structure to a tRNA-shaped protein factor made up of three domains (CHEN *et al.* 2010), where the amino-terminal domain is responsible for the codon recognition feature due to the presence of a distal loop with a conserved NIKS motif that is hypothesized to decode stop codons (CHAVATTE *et al.* 2002). On the other hand, eRF3 speeds up peptide release and increases termination efficiency depending on GTP hydrolysis (ALKALAEVA *et al.* 2006; EYLER AND GREEN 2011). eRF3-bound GTP hydrolysis depends on whether eRF1 is bound to the ribosome, which explains why eRF1 has been proposed to act as a GTP hydrolysis inhibitor (PISAREVA *et al.* 2006). A recently discovered eukaryotic ribosome release factor, ATP-binding cassette E (ABCE1) induce polypeptide release and split 80S on mRNA-bound 40S and 60S (DEVER AND GREEN 2012; PREIS *et al.* 2014). In the end, molecular details are still missing to explain the fate of the translation complex when termination is finished. However, it is known that termination is usually followed by ribosome release, but, if the preceding ORF is short, resumption of scanning followed by a reinitiation at further downstream AUG might occur (ROY AND VON ARNIM 2013).

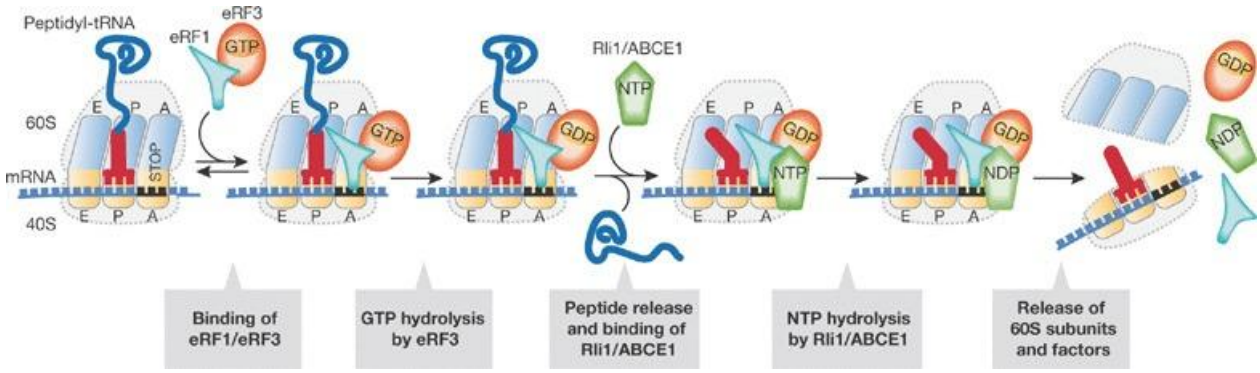

Figure 1.3-1 Pathway of translation termination in eukaryotes
During termination, translating ribosomes contain peptidyl-tRNA in the P site and expose a stop codon in the A site. The stop codon is recognized by termination factor eRF1, which enters the ribosome together with eRF3-GTP. After GTP hydrolysis, catalysed by eRF3, the peptide is released from the peptidyl-tRNA with the help of eRF1. The point at which Rli1/ABCE1 binds to the ribosome is unknown, but the order shown is consistent with the effect of the factor on both termination and recycling. After NTP hydrolysis by Rli1/ABCE1, the 60S subunit and factors dissociate from the 40S subunit. Finally, tRNA and mRNA are released from the 40S subunit with the help of initiation factors. *Modified from Marina V Rodnina (2010) EMBO Reports 3,143-4*

1.4 Eukaryotic translation recycling and reinitiation

By definition, recycling is the mechanism that is undertaken once the fully synthesized polypeptide is released (DEVER AND GREEN 2012). This process is regulated by initiation factors in both bacteria and eukaryotes. Once termination is accomplished, three main factors remain bound to the mRNA: the 80S ribosome, the deacylated tRNA and the release factor eRF1. For recycling to proceed, both subunits of the ribosome must dissociate, eRF1 in addition to deacylated tRNA should be released. In fact, an important protein, ABCE1 induces polypeptide release upon combining with eRF1 following the eRF3-GDP release (Figure 1.4-1) (DEVER AND GREEN 2012; PREIS *et al.* 2014). This step induces a conformational change in eRF3 allowing it to be positioned in the peptidyl transferase center (PTC) to induce the release of the polypeptide and ribosome recycling (PISAREV *et al.* 2010). Furthermore, studies performed in yeast and mammals spot light onto the importance of ABCE1 in engaging the multifactor complex (MFC) consisting of eIF1, eIF2, eIF3 and eIF5 to the 40S ribosomal subunit after the ribosome dissociation. Also, it was shown that some mammalian proteins (Ligatin) can promote the release of deacylated tRNA and mRNA from

40S recycled subunits after ABCE1-mediated dissociation of the ribosomal complexes into subunits (SKABKIN *et al.* 2010).

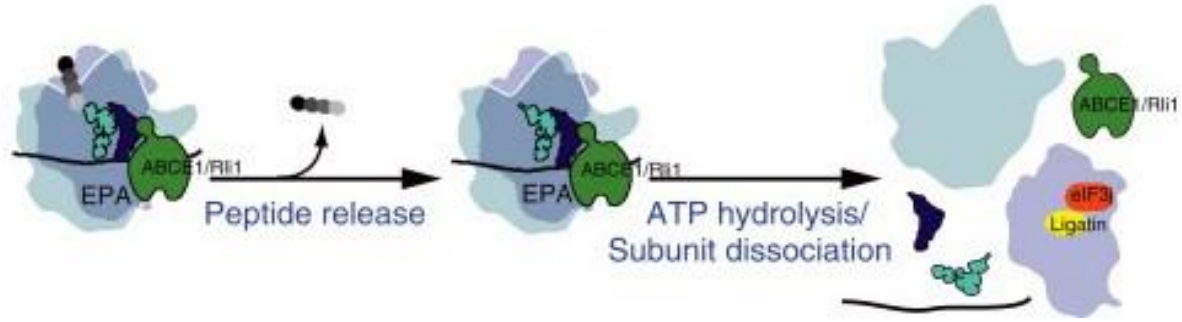

Figure 1.4-1 Model of eukaryotic recycling
In this model the large ribosomal subunit is drawn as transparent to visualize tRNAs, factors, and mRNA binding to the decoding center at the interface between the large and small subunit. Also, the positions of the mRNA, tRNAs, and factors are drawn on the ribosome. Upon stop codon recognition, the eRF1:eRF3:GTP ternary complex binds to the A site of the ribosome, GTP hydrolysis occurs, and eRF3 is released. ABCE1/Rli1 binds and facilitates the accommodation of eRF1 into an optimally active configuration. *Modified from Dever and Green (2012) Cold Spring Harb Perspect Biol 4(7):a013706*

However, in some cases partial dissociation or incomplete recycling of the complex may enable loosely bound 40S ribosomal subunits to reestablish a PIC and restart the initiation process of translation known as "reinitiation" (Figure 1.4-2) (DEVER AND GREEN 2012; BROWNING AND BAILEY-SERRES 2015; YOUNG *et al.* 2015). In mRNAs having one ORF, an incomplete recycling mechanism might happen at the termination codon allowing scanning to occur along the 3' untranslated region (3'-UTR), and enabling the transfer of the 40S subunit to the 5'-UTR and thus leading to translation of the same ORF again (DEVER AND GREEN 2012). Studies revealed that after termination, the eIF1, eIF1A, eIF3 and eIF2-Met-tRNA remain bound with the 40S ribosomal subunit followed by bidirectional scanning by the 40S or 80S complex, allowing initiation to occur at an AUG codon downstream or upstream (SKABKIN *et al.* 2013). In addition, studies revealed that PABP, eIF4G and eIF4E

interact with each other in very specific yet poorly understood way to bring the 5' and 3' ends of the mRNA into close proximity (TARUN AND SACHS 1996). Some hypothesis suggest that the aim of these interactions is to protect the mRNA from potential degradation, and promoting translation again (SACHS AND DAVIS 1989). Other studies suggest that intra- and inter molecular base pairing is important for translation reinitiation to occur. For example, it was shown that two short sequence motifs within the "termination upstream ribosomal binding site" (TURBS) were found to be essential for reinitiation (LUTTERMANN AND MEYERS 2009). Also, analysis on human mRNAs having small upstream ORFs revealed the presence of reinitiation sites downstream the AUG codons implying the availability of potential alternative ORFs (KOCHETOV *et al.* 2008).

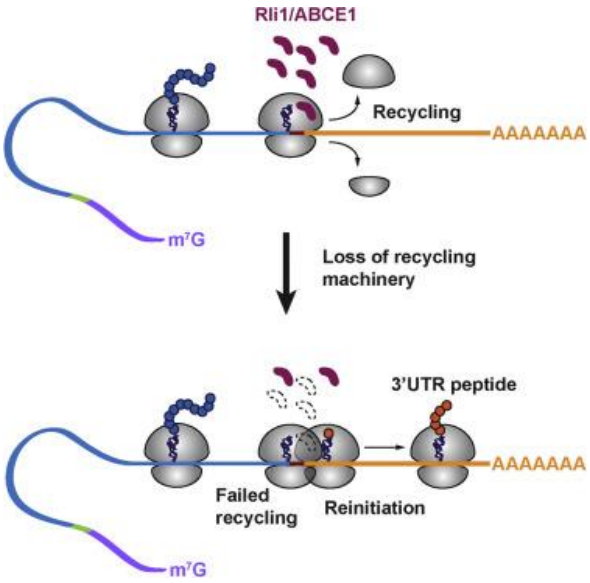

Figure 1.4-2 Loss of recycling machinery leads to reinitiation
Unrecycled ribosomes enter mRNA 3'UTRs and reinitiate translation without start codon preference to produce small peptides. 80S ribosome levels in 3'UTRs are enhanced when ribosome recycling is compromised and under stress conditions, suggesting that modulation of recycling helps shape the proteome in response to environmental perturbations. *Young et al., (2015) Cell 4,872-84*

2. Translation factors

2.1 Canonical initiation factors

a. eIF4F Complex

The loading of the 43S PIC to the mRNA is promoted by a cap-binding complex eIF4F (all eukaryotes) and eIFiso4F (plant specific) (HINNEBUSCH AND LORSCH 2012; VALASEK 2012). eIF4F is composed of 2 major subunits: the cap-binding protein eIF4E and the large scaffolding protein eIF4G in addition to a minor subunit eIF4A, an RNA-dependent RNA helicase of the DEAD-box family (BROWNING AND BAILEY-SERRES 2015). In plants, the eIF4F isoform "eIFiso4F" share functional and structural similarities. It consists of two subunits, the small cap binding complex eIFiso4E and the large scaffold protein eIFiso4G, but lacks the PABP binding site (BROWNING 1996). The presence of two isoforms in plants (eIF4F and eIFiso4F) may spotlight onto differences at the level of their biological activities. Many studies demonstrated that both eIF4F and eIFiso4F might have evolved specific abilities to regulate mRNA translation. However, this is not well elucidated (BROWNING AND BAILEY-SERRES 2015).

eIF4E Three forms of cap-binding proteins are present in higher plants, eIF4E, eIFiso4E (plant-specific) and 4EHP (4E homologous protein) (RUUD *et al.* 1998). Both eIF4E and eIFiso4E belong to class 1 cap-binding protein (JOSHI *et al.* 2005). eIF4E recognizes the methylated guanine residue on the 5' end of the mRNA (BROWNING AND BAILEY-SERRES 2015).

Many plant viruses use eIF4F or eIFiso4F for their replication. For example, it was revealed that the 5' linked protein (VPg) of potyviruses show direct interactions with eIF4E and other components of the eIF4F complex (JIANG AND LALIBERTE 2011). Point mutagenesis of the VPg domain suggests that its binding to eIFiso4E is crucial for virus propagation in

plant. However, the VPg protein of the *Rice yellow mottle virus* was discovered to directly interact with eIFiso4G rather than eIF4E isoforms. In general, eIF4E and eIF4G are described as host factors during viral infections, but their role in plant resistance is still unclear (WANG AND KRISHNASWAMY 2012).

eIF4G eIF4G contains one to three HEAT domains (1 in yeast, 2 in plants and 3 in mammals) indicating a possible evolution of the complex (HERNANDEZ AND VAZQUEZ-PIANZOLA 2005). These domains interact with proteins such as eIF4A, eIF4B, eIF3 and PABP to prepare for the binding of the 40S subunit to the mRNA resulting in scanning initiation (HINNEBUSCH AND LORSCH 2012). In addition, eIF4G induces a "closed" eIF4A conformation which is critical for efficient recruitment of the 43S PIC to the mRNA 5' via direct interaction with eIF3 (PISAREV *et al.* 2007).

In plants, the eIF4G and its isoform eIFiso4G have different molecular weights of 180 kDa and 86 kDa respectively. eIFiso4G also show HEAT domain interactions with eIF4A, eIF4B and PAPB similar to those of eIF4G. However, eIFiso4G differs significantly, when compared to mammalian or yeast interactions (GALLIE 2014).

eIF4A It belongs to the DEAD box helicase family and was defined as "the godfather of helicases". It is a non RNA dependent ATPase that has local functions to open short RNA duplexes recruited by eIF4E near the 5'UTR (MARINTCHEV 2013). Its helicase activity is enhanced by eIF4B (RNA binding protein) and by combining the heterodimeric complex eIF4F (HINNEBUSCH AND LORSCH 2012). eIF4A along with eIF4G and eIF4B, interact with the 5' end of the mRNA and unwind the secondary structure upon ATP hydrolysis to prepare for 43S PIC recruitment (PARSYAN *et al.* 2011; ANDREOU AND KLOSTERMEIER 2014). An additional function for eIF4A appears at the level of removing the RNA binding proteins while the PIC is still in the scanning process (PARSYAN *et al.* 2011; MARINTCHEV 2013; ANDREOU AND KLOSTERMEIER 2014). In plants, eIF4A is loosely integrated with the eIF4F

complex. Many studies suggested hypothetical roles of RNA helicases in translation; however, the exact role has not yet been elucidated (BROWNING AND BAILEY-SERRES 2015).

b. eIF1 group

This group includes the eIF1 (SUI1 in yeast) and eIF1A. Both factors are involved in maintaining the structure and assembly of the 43S PIC. Both factors are small in size (single polypeptides / 12-17 kDa and highly conserved in eukaryotes. The orthologs of eIF1 and eIF1A in prokaryotes are the initiation factors IF3 and IF1, respectively (VALASEK 2012; BROWNING AND BAILEY-SERRES 2015).

eIF1 and eIF1A Once the initiation codon (AUG) is recognized, eIF1 binds the 40S subunit at the level of the P site and prevents the ternary complex (TC) from fully occupying the P site of the 43S PIC (NANDA *et al.* 2013; MARTIN-MARCOS *et al.* 2014). Similarly, eIF1A precludes Met-tRNAiMet from binding the P site until the identification of the initiation codon is done (NANDA *et al.* 2013). The function of recombinant wheat eIF1 in multifactor complex (MFC) formation *in vitro* is highly similar to that in yeast and mammals (SOKABE *et al.* 2012; HINNEBUSCH 2014). The MFC complex composed of eIF1, eIF2, eIF3 and eIF5 can be formed before its binding to 43S PIC. In plants, eIF1A binds the 40S subunit independently of MFC binding. However, eIF1 interacts with both eIF5 and eIF3c (DENNIS *et al.* 2009). Both factors were also shown to be involved in stress tolerance in conditions of overexpression of both their encoding genes.

eIF1A structure is characterized by the β-barrel OB-fold and the α-helical domain. Its central region is bound to the A site of 40S, while the N- and C-terminal tails protrude towards the P site. Mutations within the mammalian OB-folds and α-helical domains decrease RNA binding capabilities and 40S scanning efficiency (FEKETE *et al.* 2007).

c. eIF5 group

This group includes two main factors, eIF5 and eIF5B, involved in initiation and precisely in the start site recognition and codon-anticodon base pairing. Both factors are conserved between mammals and plants.

The main role of eIF5 is to promote eIF2-bound GTP hydrolysis within 43S PIC upon start codon recognition. Regarding its structure, it is made up of two main domains—N-terminal (NTD) and C-terminal (CTD) connected by a linker (CONTE *et al.* 2006). NTD contains a zinc finger motif required for eIF2 GTPase activation (ALONE AND DEVER 2006; NANDA *et al.* 2013). CTD contains a HEAT domain that interacts with eIF2β and is necessary for eIF2-guanosine interaction (JENNINGS AND PAVITT 2010). In yeast, CTD of eIF5 interacts with eIF4G to induce mRNA-43S PIC binding and assists the scanning process (SINGH *et al.* 2012). In plants, eIF5 is poorly studied, but it can play a role in MFC formation (DENNIS *et al.* 2009).

eIF5B (IF2 in prokaryotes) promotes 60S joining step as a result of eIF5B-bound GTP hydrolysis. Upon recognition of the initiation codon, eIF5 promotes eIF2-bound GTP hydrolysis that leads to eIF2 release (ALLEN AND FRANK 2007). eIF5B-bound GTP hydrolysis promotes 60S binding to 40S and eIF1A release. Additional properties of mammalian eIF5B include a chaperon function (RASHEEDI *et al.* 2010; SURAGANI *et al.* 2011).

d. eIF3 group

eIF3 is made up of 13 subunits in higher eukaryotes and in plants (eIF3a to eIF3m) and has a molecular weight of 800 kDa (Figures 2.1-1) (DES GEORGES *et al.* 2015; SMITH *et al.* 2016). In contrast, in yeast, eIF3 contains only 5 orthologs of the mammalian subunits (eIF3a, eIF3b, eIF3c, eIF3g and eIF3i) that have been suggested to form the core of eIF3 in all eukaryotes

(Table 2.1-1) (HINNEBUSCH 2006; MARCHIONE *et al.* 2013). In humans, the core of eIF3 is made up of 8 subunits (a, c, e, f, h, k, l and m) (SIRIDECHADILOK *et al.* 2005; SUN *et al.* 2011). eIF3 interacts with several eIFs such as eIF1 and eIF4G (VALASEK 2012). It plays a role at practically each step of translation initiation—promotes TC recruitment to 40S, 43S PIC binding to mRNA, the scanning process (HERSHEY 2015). In mammals, eIF3 alone can interact with 40S, when other eIFs are not present, and prevent assembly of 60S and 40S subunits (Figure 2.1-2 and 2.1-3) (DES GEORGES *et al.* 2015). However, recent studies revealed that this function of eIF3 depends on other factors such as eIF1, eIF1A, TC and RNA oligonucleotides. In addition, eIF3 induces TC assembly, if Met-tRNAi^{Met} is a limiting factor. Its function in TC recruitment to 43S PIC is further promoted by eIF1 and eIF1A (CHAUDHURI *et al.* 1999; KOLUPAEVA *et al.* 2005). Moreover, mammalian eIF3 was implicated in mRNA recruitment via direct interaction with the internal segment of eIF4G, which allows 40S-bound eIF3 to interact with the eIF4F-mRNA complex (LAMPHEAR *et al.* 1995; IMATAKA *et al.* 1997).

The eIF3 preinitiation complex functions as a scaffold to coordinate a phosphorylation function of TOR. When active, TOR associates with the eIF3 complex, and phosphorylates eIF3-bound inactive S6K1. S6K1, when phosphorylated by TOR, dissociates eIF3. Indeed, insulin treatment of nutrient-replete cells allows the binding of mTOR to eIF3-containing PIC that correlates with a phosphorylation step that activates S6 kinase 1 (S6K1) (HOLZ *et al.* 2005). Furthermore, a connection between brassinosteroid signaling and eIF3 mode of action was suggested. Although eIF3i was revealed as a target of brassinosteroid insensitive receptor kinase (BRI1), the role of phosphorylated eIF3i in eIF3 function is still unknown (JIANG AND CLOUSE 2001; EHSAN *et al.* 2005).

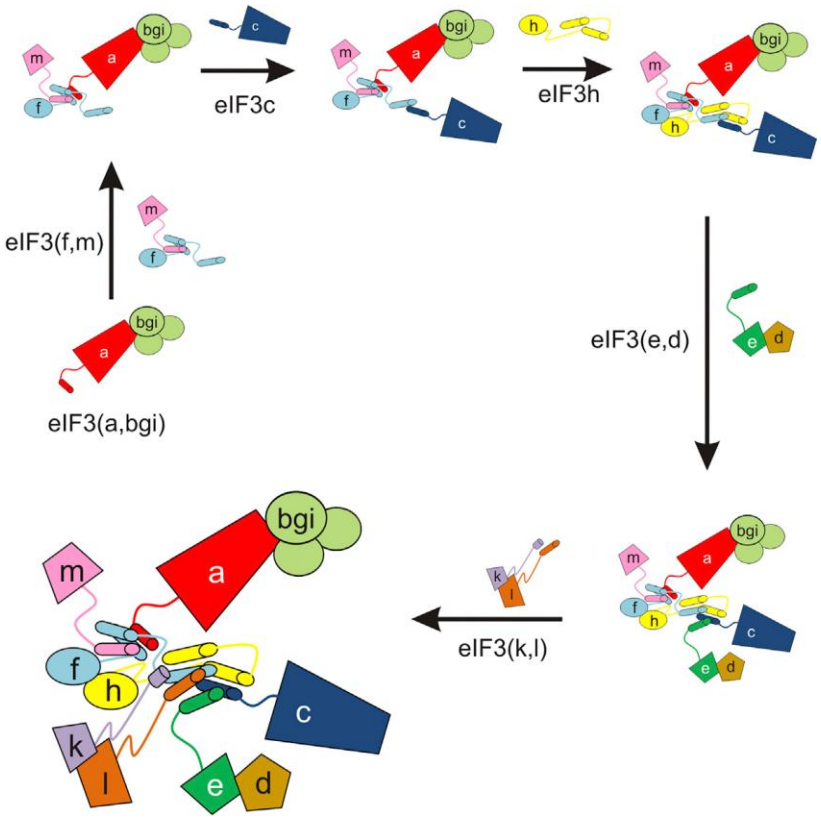

Figure 2.1-1 Main assembly pathway for human-like eIF3

Cartoon scheme showing the ordered assembly of eIF3. Helical bundle formation is guided by the C-terminal helices of the indicated subunits. The (b,g,i) subcomplex assembles with eIF3a, followed by joining of eIF3(f, m), the subunit c, the subunit h and eIF3(d, e). *Modified from Smith et al., (2016) Cell 6,886-96*

Unified nomenclature	*S. cerevisiae* + MW	*H. sapiens*	*S. pombe*	*A. thaliana*	Consensus motif
eIF3a	**Tif32—110 kDa**	**p170**	**p107**	**p114**	**PCI**
eIF3b	**Prt1—90 kDa**	**p116**	**p84**	**p82**	**RRM**
eIF3c	**Nip1—93 kDa**	**p110**	**p104**	**p105**	**PCI**
eIF3d	–	*p66*	*Moe1*[a]	*p66*	–
eIF3e	–	p48	*Int6*[a]	*p51*	*PCI*
eIF3f	–	p47	*Csn6*	*p32*	*MPN*
eIF3g	**Tif35—33 kDa**	**p44**	**Tif35**	**p33**	**RBD**
eIF3h		p40	*p40*[b]	*p38*	*MPN*
eIF3i	**Tif34—39 kDa**	**p36**	**Sum1**	**p36**	**WD repeats**
eIF3j	*Hcr1—35 kDa*	*p35*	–	–	–
eIF3k	–	*p28*	–	*p25*	*PCI*
eIF3l	–	*p67*	–	*p60*	*PCI*
eIF3m	–	*GA17*	*Csn7B*[b]	–	*PCI*

Table 2.1-1 Summary of eukaryotic eIF3 subunits

The 'conserved' core subunits are highlighted in bold type, the 'functional' core subunits are underlined, and the 'dispensable' ones are in italics. *MPN* Mpr1p and Pad1p N-terminal conserved domain; *PCI* 26S proteasome, COP9 signalosome and eukaryotic initiation factor eIF3 conserved domain; *RBD* RNA-binding domain; *RRM* RNA-recognition motif; *S6K1* ribosomal protein S6 kinase 1; *WD* conserved regions of approximately 40 amino acids typically bracketed by Trp–Asp

a Subunits contained in *S. pombe* Int6 eIF3 complex

b Subunits contained in *S. pombe* Csn7B eIF3 complex

Modified from Marchione et al., (2013) CellMol Life Sci 19,3603-16

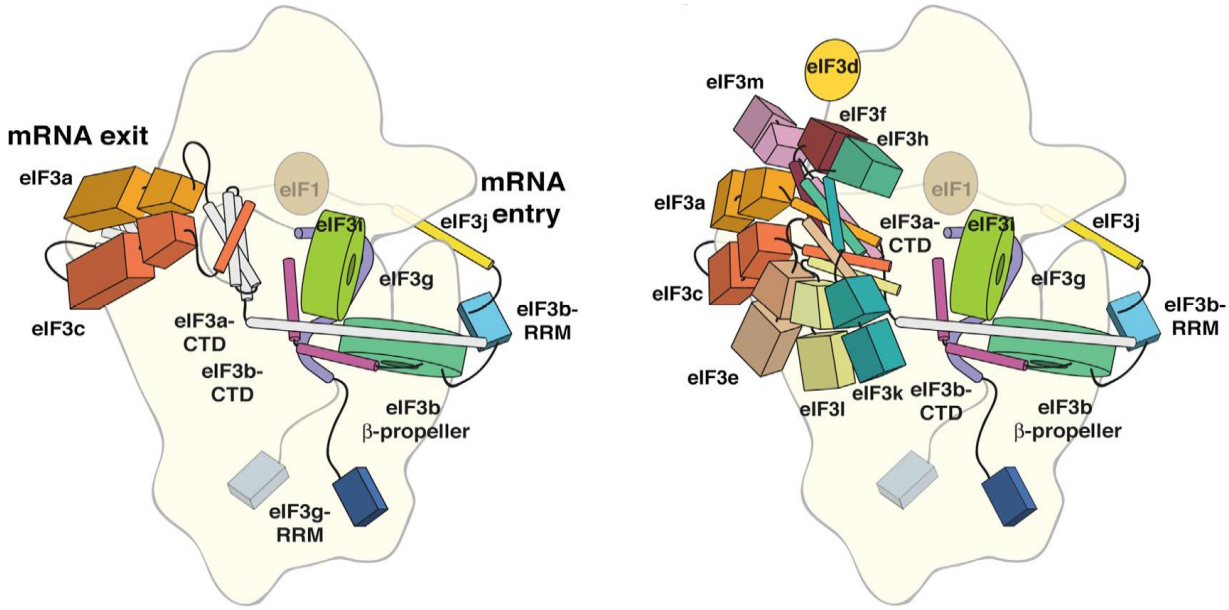

Figure 2.1-2 Placement and interactions of eIF3 components on 40S
Model of eIF3 subunit positions within 43S PIC (40S-eIF1-eIF3) in the yeast (left panel) and mammals (right panel). *Modified from Ezberger et al., (2014) Cell 5,1123-35*

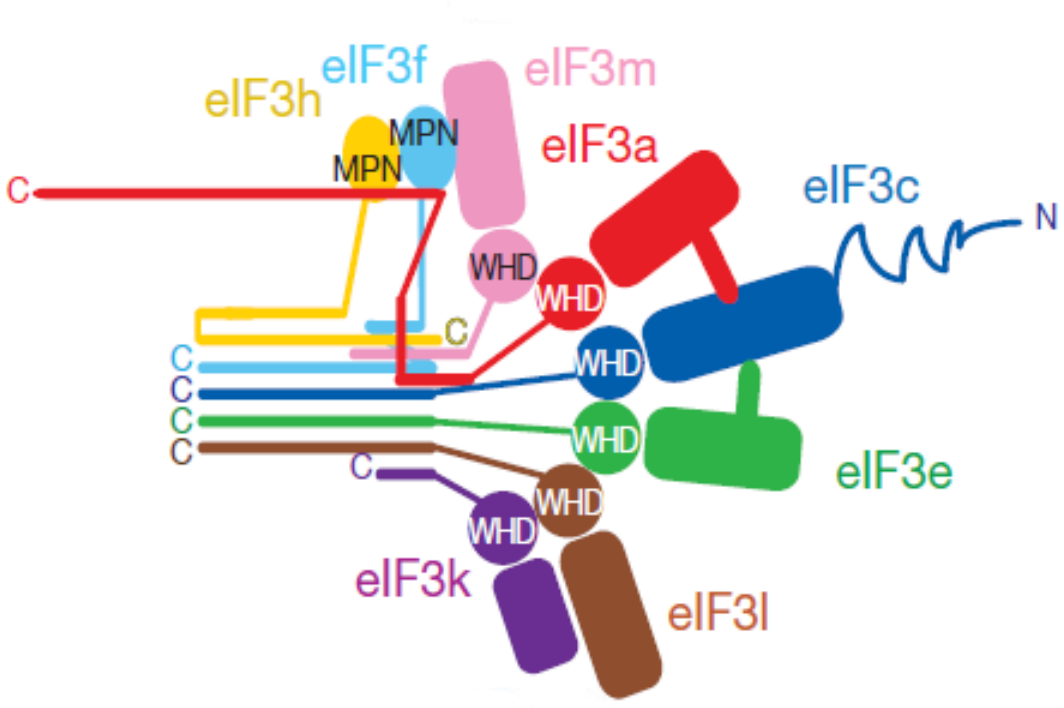

Figure 2.1-3 Two-dimensional representation of the eIF3 octamer core
The helical bundle is represented by colored bars. Zig-zagged line on eIF3c indicates possibly unstructured N-terminal tail. *Modified from des Georges et al., (2015) Nature 7570,491-5*

Some similarities exist between eIF3, the 26S proteasome lid and the COP9/signalosome, which are known as PCI complexes. Motifs known as PCI and MPN domains are present within the 8 core proteins of the PCI complex (PICK *et al.* 2009). In higher eukaryotes, PCI domains are also present within the eIF3 subunits a, c, e and l. On the other hand, eIF3 subunits k and m have α-helixes domains; f and h have MPN domains, b, d and g have RNA Recognition Motif (RRM) domains (CUCHALOVA *et al.* 2010). eIF3g has a zinc-binding domain (HINNEBUSCH AND LORSCH 2012; VOIGTS-HOFFMANN *et al.* 2012; HASHEM *et al.* 2013). In yeast, eIF3 is also involved in the termination process and reinitiation of translation (PISAREV *et al.* 2007; BEZNOSKOVA *et al.* 2013).

In plants (wheat and *Arabidopsis*), eIF3 biochemical analysis revealed strong similarities in terms of the number of subunits and their sequences to the mammalian eIF3 (HEUFLER *et al.* 1988; BURKS *et al.* 2001). In fact, eIF3m and eIF3l were originally described in plants (BURKS *et al.* 2001). Similar to the mammalian eIF3, studies on *Arabidopsis* eIF3 revealed strong similarities between eIF3, the 26S proteasome and COP9 signalosome (KARNIOL *et al.* 1998). These collaborations among the PCI complex proteins indicate additional unknown functions for eIF3 subunits to control translation and protein degradation (KIM *et al.* 2001). Mutations in the only gene encoding eIf3e or eIF3f cause male gametophytic lethality (YAHALOM *et al.* 2008; XIA *et al.* 2010).

eIF3a and eIF3c eIF3 a and c are the largest among eIF3 subunits, which were implicated in maintaining the assembly of the complex (SUN *et al.* 2011; SMITH *et al.* 2013). Both eIF3a and eIF3c are important for VacV protein synthesis and virus spreading. eIF3a acts as a translational regulator for proteins in S phase (DONG *et al.* 2009). Interesting that the PCI-MPN domain of eIF3a is not located near the C terminus, which protrudes from the rest of the complex and involved in assembly of the PCI-MPN octamer in humans (SUN *et al.* 2011). Removal of eIF3a C-terminus disrupted its eIF3 association (SMITH *et al.* 2016). In

addition, it was shown that eIF3a interacts with the internal ribosome entry site (IRES) of hepatitis C virus (KIEFT *et al.* 2001). Also, eIF3a ensures mRNA binding by 43S PIC *in vivo*.

eIF3c can stabilize interactions outside the bundle with other subunits (SMITH *et al.* 2016). It enters eIF3 as a complex with eIF3e (MORRIS-DESBOIS *et al.* 1999). Interestingly, eIF3c depletion negatively affects eIF3e phosphorylation and its recruitment to the eIF3 complex (WALSH AND MOHR 2014).

eIF3b eIF3b overexpression triggers up-regulation of several other subunits and formation of several specific subcomplexes like (d, e, k and l), which changes the rates of cap-dependent versus cap-independent translation initiation and can cause cancer (SILVERA *et al.* 2010). In *S. cerevisiae*, eIF3a and eIF3b were found to be essential during G1-S phase of the cell cycle (EVANS *et al.* 1994; KOVARIK *et al.* 1998). In addition, deletion of eIF3b leads to a decrease in protein synthesis, which can indicate that eIF3b is required to maintain the integrity of the eIF3 complex.

eIF3d Crystal structure analysis of the cap-binding domains of eIF3d revealed unexpected homology to endonucleases playing a role in RNA turnover. eIF3d is involved in a cap-dependent pathway of translation initiation in a human cell line. Indeed, eIF3d interacts with cap and requires for the assembly of the translation initiation complex on special mRNAs such as *c-Jun* (cell proliferation regulator) (LEE *et al.* 2016). Moreover, eIF3d was found to interact with CDC48 in yeast, which can abolish cell cycle progression (OTERO *et al.* 2010).

eIF3e eIF3e seems to play multiple roles indicating that it's a regulatory subunit. *eIF3e* gene was initially identified as an integration site for mouse mammary virus (MARCHETTI *et al.* 1995). Transgenes mimicking truncated eIF3e alleles are oncogenic and can induce breast cancers (PEREZ *et al.* 2005). During antiviral defense in mammalian cells, eIF3e interacts with specific p56-like proteins to promote translational inhibition (GUO *et al.*

2000). Furthermore, it was demonstrated that a reduction in eIF3e levels prevents eIF3d joining the eIF3 complex. In *Schizosaccharomyces pombe*, eIF3e has special roles in cell differentiation in fission yeast since its knockout affects spore formation (BANDYOPADHYAY *et al.* 2000). Interestingly, in fission yeast, two eIF3 complexes with and without eIF3e were discovered (ZHOU *et al.* 2005). Furthermore, eIF3e plays role in *Arabidopsis* embryogenesis. As stated earlier, *eIF3E* gene deletion (*AtelF3e*) in *Arabidopsis* leads to male gametophytic lethality thus, spotting its role in male gametogenesis (YAHALOM *et al.* 2008). On the other hand, over expressing *eIF3e* gene impacts seed formation by causing developmental arrest of light-grown seedlings, causes problems in floral development and plays negative regulatory roles in translation (YAHALOM *et al.* 2008). Also, eIF3e was shown to interact with CSN (highly conserved protein sequences) in *Arabidopsis*. CSN plays role in maintaining eIF3e levels that are required for normal development of the plant and protein translation (PAZ-AVIRAM *et al.* 2008).

eIF3f eIF3f is considered to be the regulatory subunit of the eIF3 complex. It is a member of the Mov34 family, which contains the Mpr1/Pad central motif (HOFMANN AND BUCHER 1998). eIF3f function within the eIF3 complex is not yet well established. Interestingly, upon eIF3f overexpression, HIV-1 replication and the activation of apoptosis in melanoma and pancreatic cancer cells were down regulated. This indicates the eIF3f role as suppressor of cell proliferation, but positive apoptosis effector (SHI *et al.* 2006). Furthermore, eIF3f was found to activate rRNA degradation via direct interaction with nuclear ribonucleoprotein K (WEN *et al.* 2012). In addition, eIF3f was shown to play major roles in controlling signaling pathways involved in determining muscle size (CSIBI *et al.* 2008). As I said before, eIF3 is a key factor in the S6K1 phosphorylation by mTOR (HOLZ *et al.* 2005; HARRIS *et al.* 2006). Here, eIF3f is a scaffold that connects the mTOR/raptor complex via conserved TOS motif during terminal muscle differentiation (CSIBI *et al.* 2010). Hyper-

phosphorylation of S6K1 leads to its binding to eIF3f. In conclusion, eIF3f is a key factor in skeletal muscle mass regulation (Figure 2.1-4) (SANCHEZ *et al.* 2013).

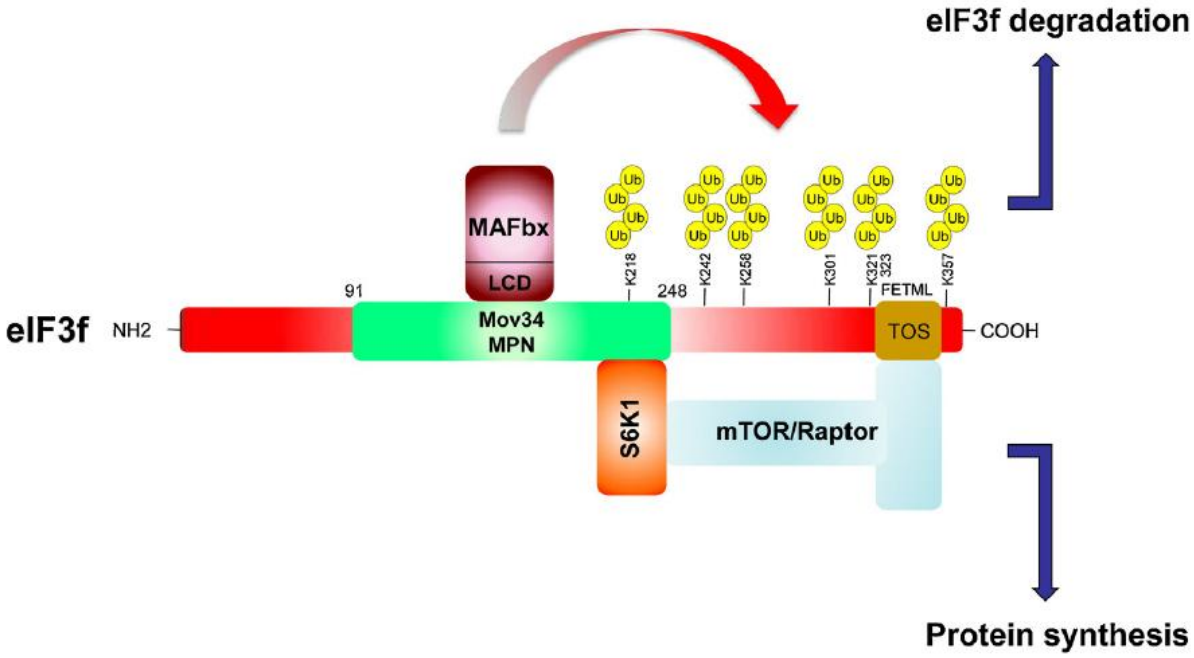

2.1-4 Physical links between eIF3f, mTOR-raptor, S6K1 and MAFbx in skeletal muscle
The ubiquitin ligase MAFbx/atrogin-1 physically interacts with the Mov34 domain of eIF3f and contributes to its ubiquitinylation within the C-terminal region and its subsequent degradation by the proteasome during muscle wasting. The Mov34 domain also interacts with the inactive hypo-phosphorylated form of S6K1. Under nutrient rich conditions, the mTOR/raptor complex binds to TOS motif of eIF3f and can phosphorylate and activate S6K1. Active S6K1 is released from the eIF3 complex, further activated and phosphorylates its downstream targets in translation to promote protein synthesis. Thus, eIF3f acts as a scaffolding protein allowing mTORC1-dependent activation of S6K1 upon insulin or growth hormone stimulation of muscle cells. *Modified from Sanchez AM et al., (2013) Int J Biochem Cell Biol 10,2158-62*

The function of eIF3f in plants is not well characterized. However, in *eIF3f* expression levels were found elevated in pollen grains, pollen tubes, embryos and root tips in *Arabidopsis*. Note that some mutations within *eIF3f* lead to embryogenesis defects (XIA *et al.* 2010). eIF3f was implicated in binding to eIF3e and eIF3h suggesting eIF3f function in cell growth and differentiation as a part of the eIF3 complex (XIA *et al.* 2010).

eIF3g eIF3g is a core subunit of eIF3. In yeast, eIF3g was documented as a factor important for translation (PHAN *et al.* 2001). eIF3 promotes translation initiation in part via eIF3g interaction with Paip1 (PABP-interacting protein) in mammals (MARTINEAU *et al.*

2008). In *Arabidopsis*, eIF3g overexpression enhances stress tolerance in (SINGH *et al.* 2013). Interesting that eIF3g functions in unusual mechanism of virus-activated reinitiation after long ORF translation that operates in Cauliflower mosaic virus (CaMV; PARK *et al.* 2001). CaMV translation tranactivator/ viroplasmin binds eIF3 via eIF3g and promotes eIF3 accumulation in polysomes (PARK *et al.* 2001). Interestingly, eIF4B outcompetes TAV for eIF3g binding, and thus, interacts with TAV after eIF4B release from 40S (PARK *et al.* 2004).

eIF3h eIF3h has a molecular weight of 40 kDa. In *Arabidopsis*, eIF3h plays a crucial role in translation of specific transcripts that harbor uORFs within their 5'-UTRs (ZHOU *et al.* 2010). For example, eIF3h augments the reinitiation capacity of mRNAs that encode basic zipper transcription factors (bZIPs) (KIM *et al.* 2004). Strikingly, eIF3h is dispensable for basal translation, but it is essential for reinitiation after short ORF translation (KIM *et al.* 2004).

eIF3i and eIF3j Although deletion of eIF3i or eIF3g in HeLa cells has no impact on the rate of protein synthesis (MASUTANI *et al.* 2007), eIF3i was found to be essential for translation in yeast (PHAN *et al.* 2001). The mammalian eIF3j acts as a regulatory subunit that is inhibitory for the scanning process in eukaryotes (MIYAMOTO *et al.* 2005), but it is a non-essential in budding yeast.

eIF3k and eIF3l eIF3k is the smallest subunit in the eIF3 complex. The non-conserved subunits eIF3k and eIF3l are so called assessory proteins that has no impact on the activity of the complex as a whole, but might playing a role in the translational regulation of specific mRNAs in specific conditions (MASUTANI *et al.* 2007). eIF3k is found in both the cytoplasm and the nucleus indicating that it can shuttle between compartments according to the cell cycle needs (SHEN *et al.* 2004). Moreover, eIF3k stabilizes eIF3l in the cell (SMITH *et al.* 2013).

eIF3m The complex of eIF3a and eIF3c directly interacts with several subunits containing the PCI domain including eIF3m (26S proteasome, COP9 and eukaryotic initiation factor eIF3 conserved domain) to form a stable PCI/MPN octamer structure (SUN *et al.* 2011).

2.2 Elongation factors

Translation elongation requires a number of elongation factors—eukaryotic elongation factor 1A (eEF1A, homolog of bacterial EF-Tu), eEF1B (homolog of bacterial EF-Ts), eEF2 (homolog of bacterial EF-G) and eEF5 (prokaryotic homolog EF-P) (DOERFEL *et al.* 2013; GUTIERREZ *et al.* 2013). eEF1A is the most abundant protein in eukaryotic cells that constitutes approximately 1% of the total protein in the cell (LOPEZ-VALENZUELA *et al.* 2004). eEF1A has function in apoptosis, proteolysis and viral propagation (SASIKUMAR *et al.* 2012). eEF1B has three orthologs in plants (eEF1Bα, eEF1Bβ and eEF1Bγ) (SASIKUMAR *et al.* 2012). Similar to eEF1A, eEF1B is also involved in viral replication process (WANG AND KRISHNASWAMY 2012). It is suggested that conformational change in eEF2 structure along with GTP hydrolysis causes the ribosome to unlock and allows the mRNA and tRNA to move smoothly for a second round of the elongation step (DEVER AND GREEN 2012). eEF5 (bacterial ortholog EF-P) facilitates the elongation step by providing efficient insertions for proteins enriched with proline and glycine residues (NANDA *et al.* 2009; DOERFEL *et al.* 2013). In addition, eEF5 is the only eukaryotic protein that contains a hypusine post-translational modification, which is initially derived from spermidine. This modification ensures stable activity of eEF5 and minimizes the distance between proline residues and the PTC (GUTIERREZ *et al.* 2013).

2.3 Termination factors

a. eRF1 and eRF3

eRF1 (class I release factor, bacterial homolog RF1 and RF2), resembles tRNA in terms of structure. Its main role is to recognize all three stop codons in the A-site of mRNA. In plants (*Arabidopsis*), the RFs are encoded by three *AteRF1* genes (CHAPMAN AND BROWN 2004). *AteRF-1* overexpression leads to silencing of all three *AteRF1* genes (*AteRF-1*, *AteRF-2* and *AteRF-3*), which in turn causes distorted spacing between inflorescence stems and ultimately leads to the "broomhead" phenotype (broom-like appearance) (PETSCH *et al.* 2005).

3. The TOR signaling pathway in eukaryotes

3.1 TOR complexes and their roles in mammals and plants

Target of rapamycin (TOR), a member of the phosphatidylinositol 3-kinase-related kinase (PIKK) family, is a Serine/Threonine protein kinase, a central regulator of cell growth, proliferation, and survival (JEWELL AND GUAN 2013). Rapamycin produced by the bacterium *Streptomyces hygroscopicus* is anti-fungal, anti-cancer and immunosuppressive compound that inhibits TOR, if bound to FKBP12, via the rapamycin-FKBP12 complex binding to the FRB domain of TOR (VEZINA *et al.* 1975; WULLSCHLEGER *et al.* 2006). Initially, TOR was discovered in yeast for resistance to rapamycin as an inhibitor of T cell proliferation and activation (HEITMAN *et al.* 1991). TOR is encoded by two genes *TOR1* and *TOR2* in yeast, and one single gene in mammals. In mammals, TOR is involved in formation of two structurally and functionally similar complexes mTORC1 and mTORC2. mTORC1 complex contains mTOR, the scaffold protein Raptor (Regulatory-Associated Protein of mTOR), mLST8 (mammalian Lethal with Sec13 protein 8), PRAS40 (Proline-Rich AKT Substrate 40 kDa) and Deptor (DEP-domain-containing mTOR-interacting protein). mTORC2 complex contains, in addition to mTOR, mLST8 and DEPTOR that are present in both complexes,

Rictor (Rapamycin-insensitive companion of mTOR), mSIN1 (mammalian Stress activated protein kinase (SAPK) Interacting Protein 1) and Protor (Protein observed with Rictor) (Zoncu et al., 2011). TORC1 is rapamycin sensitive, and it positively regulates translation, transcription, ribosomal biogenesis, while negatively affects autophagy. In mammals, TORC1 promotes cell differentiation and growth. In contrast, TORC2 is not susceptible to rapamycin and activates cytoskeleton reorganization and cellular survival mechanisms by regulating glucose metabolism and apoptosis (XIE AND GUAN 2011). Interestingly, as in mammals, a single TOR gene is present in *Arabidopsis*, and both species share 75% similarity at the level of the amino acid sequence in the kinase domain (MENAND *et al.* 2002). In many cancers, mTOR signaling is dysregulated, strongly suggesting involvement in tumorigenesis and human metabolic dysfunctions (ZONCU *et al.* 2011). mTORC1 responds to amino acids such as glutamine, insulin and growth factors via the PI3K-phosphoinositide-dependent kinase 1 (PDK1)-AKT pathway to regulate proliferation and cell growth by induction of anabolic pathways (transcription, ribosomal biogenesis and translation) and inhibition of autophagy. The N-terminal half of mTOR is composed of approximately 20 tandem repeats of Huntingtin, EF3, PP2A and TOR1 (HEAT) motifs involved in protein-protein interactions. HEAT repeats are followed by FRAP, ATM, TRRAP and the kinase domain which is in turn made up of FKBP12-rapamycin binding (FRB) domain, catalytic site and the FATC domain (LIKO AND HALL 2015). In general, HEAT domains bind the 45S rRNA promoter region to induce ribosome biogenesis (REN *et al.* 2011). Most of mTORC1 functions are mediated by its two direct downstream substrates—S6 kinase (S6K) and eIF4E-binding protein (4E-BP) (WULLSCHLEGER *et al.* 2006; XIE AND GUAN 2011; LAPLANTE AND SABATINI 2012).

On the other hand, mTORC2 functions are not well-known due to the presence of the rapamycin-insensitive companion of mTOR (RICTOR). TORC2 is mainly involved in

regulating cell growth by controlling cytoskeleton structure and polarity in addition to glucose metabolism like its yeast ortholog (TORC2) (WULLSCHLEGER *et al.* 2006; LAPLANTE AND SABATINI 2012; CORNU *et al.* 2013).

In plants, the specific components of the TOR complex have not been well characterized since plant TOR is much less sensitive to rapamycin. Thus, TOR studies have been delayed in plants. It was mentioned in (XIONG AND SHEEN 2012) that the use of rapamycin at high concentration (10 µM) somewhat improves TOR sensitivity to rapamycin in *Arabidopsis* mesophylls protoplasts or seedlings. However, overall data suggest that TOR is involved in regulation of transcription, translation, metabolism, stress and immune responses in plants that lead to induction of more than 100 genes involved in different mechanisms (XIONG AND SHEEN 2012). *Arabidopsis* TOR encodes several factors of TORC1 besides TOR kinase (Figure 3.1-1) (ROBAGLIA *et al.* 2012). These factors include the regulatory associate protein of target of rapamycin (RAPTOR1/RAPTOR2) (DEPROST *et al.* 2005; MAHFOUZ *et al.* 2006), the lethal with sec thirteen protein 8 (LST8-1/LST8-2) and the FK506 binding protein (FKBP12) (MOREAU *et al.* 2012). It was also shown that RAPTOR interacts with the ribosomal protein S6 kinase (MAHFOUZ *et al.* 2006). *Arabidopsis* TOR loss of function (AtTOR) or RAPTOR loss of function are embryonic lethal. Inhibition of TOR activity by rapamycin results in leaf senescence, inhibition of organ growth and a decrease in ribosomal RNA synthesis and translation. On the other hand, overexpressing TOR promotes root and shoot growth in addition to an increase in seed formation (DEPROST *et al.* 2007; REN *et al.* 2012).

Up to date several TOR downstream targets have been characterized in plants: S6K1/S6K2, 40S ribosomal protein S6 (RPS6A/B), type 2A-phosphatase-associated protein 46kDa (TAP46), and epidermal growth factor receptor binding protein (ErbB-3) (TURCK *et al.* 2004; DEPROST *et al.* 2005; MAHFOUZ *et al.* 2006; ROBAGLIA *et al.* 2012). In addition to

its role in S6K phosphorylation, *Arabidopsis* TOR is capable of phosphorylating the human 4E-BP1/4E-BP2, which suggests the presence of a conserved functional TORC1 in plants (XIONG AND SHEEN 2012; XIONG *et al.* 2013). Unlike in mammals, there is no clear evidence for the presence of TORC2 in plants due to the absence of the core component RICTOR and the stress-activated mitogen-activated protein kinase protein-1 (MAPK1). However, plants might have a functional equivalent of TORC2, but this is not yet elucidated. In addition, the molecular cascades by which TOR kinase functions in plants are still vague (Figure 3.1-2) (XIONG AND SHEEN 2014) due to the complexity and limitation of techniques to measure TOR kinase activity and due to the lethality of null *tor* mutants. Interestingly, the TOR kinase domain can partially rescue embryonic lethality of null *tor* mutants (REN *et al.* 2011). In mammals and plants, TOR is sensitive to ATP-competitive chemical inhibitors such as Torin-1 (SCHEPETILNIKOV *et al.* 2013) and AZD-8055 (MONTANE AND MENAND 2013).

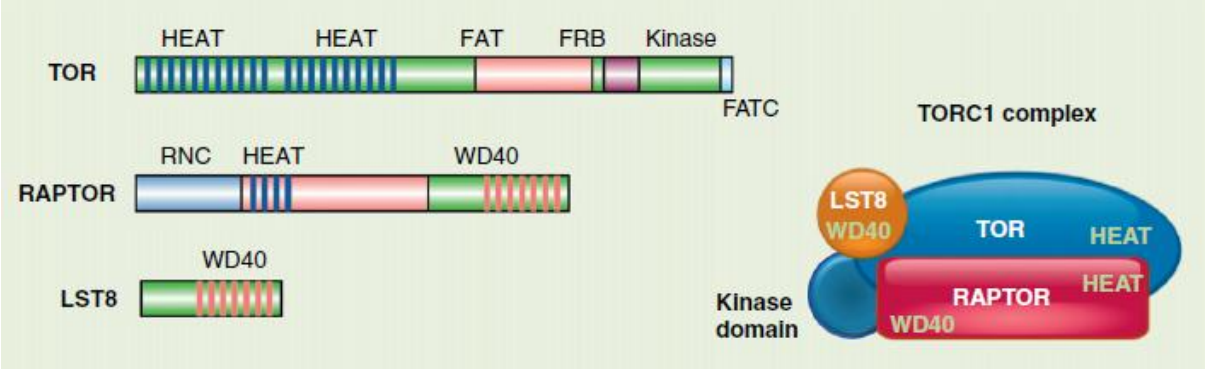

Figure 3.1-1 Structure of the components of the TORC1 complex
TOR (Target of Rapamycin) is a protein kinase that associates with the RAPTOR/KOG1 (Regulatory-associated protein of mTOR/Kontroller of growth 1) and LST8/GbetaL (Lethal with Sec13 8/Protein G beta subunit like) to form the conserved TORC1 complex. The *Arabidopsis* TOR protein contains many tandem HEAT repeats (Huntingtin, Elongation Factor 3, A subunit of PP2A phosphatase and TOR1) followed by the FAT (FRAP, ATM, TRRAP kinases), FRB (FKBP12-rapamycin binding), kinase and FATC (FAT-C-terminal) domains. The TOR kinase is a member of the Phosphoinositol 3-kinase (PI3K)-like family (PIKK). *Modified from Robalgia et al., (2012) Curr Opin Plant Biol 3,301-7*

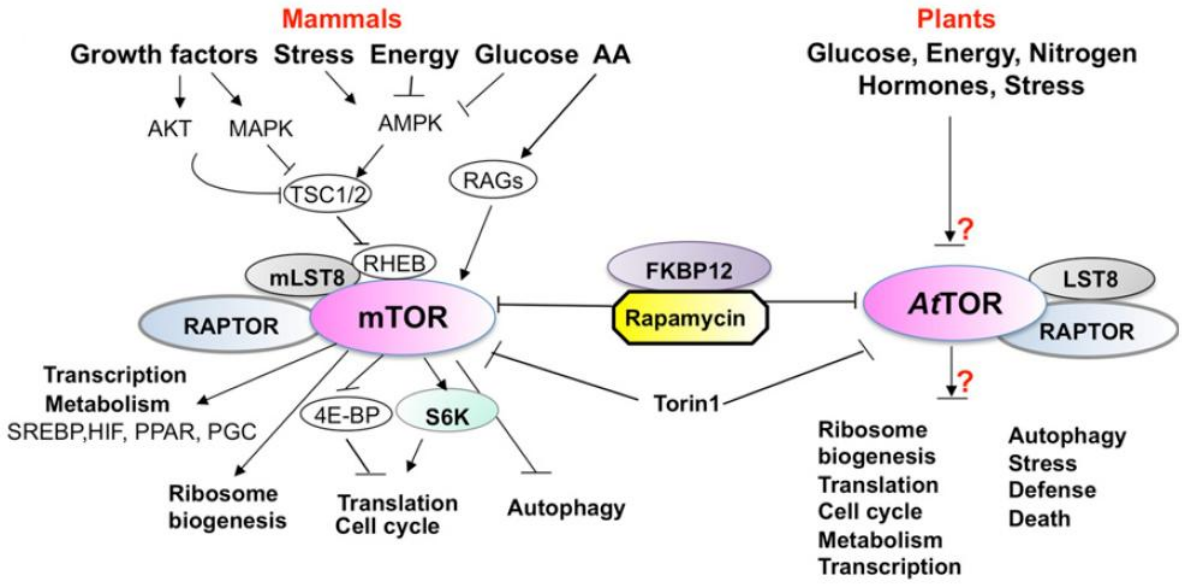

Figure 3.1-2 TOR signaling in *Arabidopsis* and mammals
Plant and mammalian TOR signaling networks - AA, Amino acid; FAT, FRAP, ATM, and TRRAP domain; FATC, Carboxy-terminal FAT domain; HEAT repeats, Huntingtin, Elongation factor 3, subunit of protein phosphatase 2A and TOR1; HIF, hypoxia-inducible factor; PGC, peroxisome proliferator-activated receptor-g coactivator; PPAR, peroxisome proliferator-activated receptor; RNC, Raptor N-terminal Conserved/ putative Caspase domain; SREBP, sterol regulatory element-binding protein; TSC1/TSC2, tuberous sclerosis1/tuberous sclerosis2;WD40 repeat domain *Modified from Xiong and Sheen (2014) Plant Physiol 2,499-512*

3.2 The role of TOR in cap-dependent translation initiation in mammals

a. TOR downstream targets - eIF4E-binding proteins (4E-BPs) and the ribosomal protein S6 (eS6) kinase - in translation initiation

TOR downstream targets S6Ks and 4E-BPs are directly phosphorylated by mTORC1 that regulates their function in protein synthesis control. The S6K1 seems to be phosphorylated by TOR at the hydrophobic motif residue Thr389, and fully activated by phosphorylation within its catalytic domain residue Thr229 in the T-loop by PDK1 (MAGNUSON *et al.* 2012). In mammals, several S6K1 downstream targets were identified—RPS6 that is phosphorylated at five Ser residues (Ser 235, ser236, ser240, ser244, ser 247) by S6K in TOR-responsive manner. 4E-BPs (4E-BPs 1,2,3) are characterized as translation repressors of cap-dependent translation initiation—their activity is modulated by TOR phosphorylation—unphosphorylated 4E-BPs outcompete eIF4G for eIF4E binding, thus blocking eIF4F complex formation that leads to repression of cap-dependent translation initiation. Upon TOR activation, TOR phosphorylates 4E-BPs and abolishes their binding to eIF4E thus restoring eIF4F complex formation and translation initiation (GINGRAS *et al.* 1999; GINGRAS *et al.* 2001).

In plants, TOR is activated in response to glucose (Xiong *et al*, 2013), the plant hormone auxin (SCHEPETILNIKOV *et al.* 2013), and the pathogenicity factor, Cauliflower mosaic virus (CaMV) protein TAV (SCHEPETILNIKOV *et al.* 2011) via as yet uncharacterized signal transduction pathways. However, the TOR-S6K1 cascade is conserved since plant TOR phosphorylates S6K1 at Thr449 (XIONG AND SHEEN 2012; XIONG *et al.* 2013). 4EBP orthologs have not been identified in plants. Although plants harbor several proteins that contain canonical eIF4E-binding site and interact with eIF4E such as lipoxygenase 2 (FREIRE *et al.* 2000) and mammalian ortholog of BTF3 (beta subunit of the nascent polypeptide-associated complex) in plants (FREIRE *et al.* 2000; FREIRE 2005), these eIF4E-binding

proteins are not targets of TOR signaling. Interestingly, TOR is required to promote translation of uORF-mRNAs in plants (SCHEPETILNIKOV *et al.* 2013) and virus-activated reinitiation after long ORF translation that operates within the 35S polycistronic pregenomic RNA in *Cauliflower mosaic virus* (CaMV; (SCHEPETILNIKOV *et al.* 2011)).

b. S6K1 downstream targets in eukaryotes - RPS6, eIF4B and others

AGC kinases are Serine/Threonine kinases fall into three major groups—pro-directed, basophilic and acidophilic, where S6Ks are capable of phosphorylating basophilic motifs (R/KxR/KxxS/T). S6K1 is a major kinase that phosphorylates the r-protein RPS6—the most phosphorylated ribosomal protein. In mammals, S6Ks are presented by two protein kinase isoforms $p70^{s6k}$/$p85^{s6k}$. Both isoforms $p70^{s6k}$ and $p85^{s6k}$ are encoded by the same transcript, but initiated at two different AUG codons. In fact, $p85^{s6k}$ has an additional 23 amino acids at its N-terminus, which is sufficient for its nuclear localization (DUFNER AND THOMAS 1999). The phosphorylation of Thr388/389 is widely used in animal and human studies as a marker for the TOR kinase activity. It was demonstrated that eIF3 acts as a platform for S6K1 phosphorylation by mTORC1 (HOLZ *et al.* 2005). In the inactive state, S6K1 but not mTORC1 binds to the non-polysome-associated eIF3 complex. Upon activation, mTORC1 is loaded on polysomes, where it phosphorylates S6K1 at Thr389 triggering its detachment from eIF3 followed by further activation by PDK1 (HOLZ *et al.* 2005).

In *Arabidopsis*, two S6K equivalents are present with over 87% sequence homology. S6K1 and S6K2 have conserved phosphorylation sites as in mammals. S6K1—a downstream target of TOR and the homolog of p70 S6 kinase—is present in the cytoplasm and phosphorylates the r-protein eS6 (MAHFOUZ *et al.* 2006). When TOR is active, it phosphorylates S6K1 at Thr449 (SCHEPETILNIKOV *et al.* 2011). On the other hand, S6K2 is nuclear due to the presence of bipartite signals that promote its nuclear localization. Moreover, its function is restricted to the phosphorylation of the nuclear form of r-protein

bound to the chromatin (FRANCO AND ROSENFELD 1990; MAHFOUZ *et al.* 2006). Phosphorylation sites of eS6 vary between different species. Six Ser sites are present in humans and mice (Ser235, Ser236, Ser240, Ser242, Ser244 and Ser247) (MEYUHAS 2008). In mammals and yeast, two conserved phosphorylation sites are present (Ser235 and Ser236). Two isoforms of eS6 (eS6a and eS6b) are present in plants. Both harbor several phosphorylation sites at Ser240 being documented in cell culture assays as a common site for both (CARROLL *et al.* 2008). In *Arabidopsis* seedlings, additional phosphorylation sites for eS6a include Thr127, Thr249, Ser 237, Ser240, and Ser247 while additional sites for eS6b include Thr127, Ser237 and Ser240 (REILAND *et al.* 2009). Recent studies highlighted more phosphorylation sites for both isoforms at Ser229 and Ser231 (BOEX-FONTVIEILLE *et al.* 2013). In addition, it is noteworthy to indicate that the phosphorylation levels of eS6 are relatively higher during day hours (BOEX-FONTVIEILLE *et al.* 2013), upon UV exposure and increased CO_2 concentrations (CASATI AND WALBOT 2004; BOEX-FONTVIEILLE *et al.* 2013). On the other hand, it is reduced upon hypoxia and increased temperature (SCHARF AND NOVER 1982). Recent publication suggests that Ser240 and may be Ser237 are phosphorylated by S6K1 in TOR-responsive manner (DOBRENEL *et al.* 2016). However, more studies are required to identify all TOR –responsive phosphorylation sites within RPS6.

A second S6K1 downstream target is eIF4B. The Ser422 phosphorylation site of eIF4B is involved in mRNA translation control—phosphorylation of this site augments the helicase activity of eIF4A, and eIF4B recruitment to the 48S PIC (HOLZ *et al.* 2005; WILKER *et al.* 2007). Additionally, the programmed cell death (PDCD4) tumor suppressor protein binds to eIF4A and inhibits its helicase activity. In contrast, PDCD4 phosphorylated at Ser67 by S6K1 is rapidly degraded to abolish its inhibitory effect on eIF4A (YANG *et al.* 2004). Additional S6K1 phosphorylation targets include the eukaryotic elongation factor 2 kinase (eEF2K); an

inhibitor of translation elongation Aly/Ref-like target (SKAR) that promotes S6K1 binding to the newly synthesized mRNAs (RICHARDSON *et al.* 2004).

4. Reinitiation after short ORF translation in mammals

The process of reinitiation after a short uORF translation in mammals was initially discovered when studies were ongoing to understand the process of ribosomal scanning. It was found that inserting a stop codon of few base pairs downstream of the 5'-proximal AUG can activate translation again at the second AUG (KOZAK 1984). Actually, long intercistronic regions are more efficient for reinitiation and the efficiency of initiation at the second AUG codon increased upon an increasing distance, if longer than 80 nucleotides between the inserted stop codon and AUG (KOZAK 1987). On the other hand, reinitiation efficiency decreases when the length of uORF increases (LUUKKONEN *et al.* 1995). Also, when the race of the elongation process through the uORF is decreased upon the addition of cyclohexamide or due to the presence of secondary structures, efficiency of reinitiation is reduced, which ultimately leads to ribosome pausing (KOZAK 2001). In plants, in the case of the *Arabidopsis* transcription factor GBF6, when sucrose binds the emerging uORF peptide, it induces ribosome pausing and thus a decrease in translation initiation at the coding sequence (RAHMANI *et al.* 2009). All this sheds light onto the importance of time, but not the length, in translating the uORF for reinitiation efficiency. In prokaryotes, ribosomes bind mRNA internally at the Shine-Dalgarno sequence located upstream of the AUG codon, and their scanning ability is not high. Thus, prokaryotic uORFs largely do not impact downstream translation initiation (LOVETT AND ROGERS 1996). The main role of uORFs could be to fine-tune translation efficiencies of the main ORFs. Also, uORfs might block translation of the main ORF in specific circumstances.

4.1 uORF number and distribution among eukaryotic mRNAs

In mammals and plants, uORFs are abundant as, particularly, when compared to yeast. Approximately, 45% of the mammalian genes encode mRNAs harboring at least one uORF as compared to only 13% in yeast (CALVO *et al.* 2009; INGOLIA *et al.* 2009). Studies revealed that increasing the length of intercistronic space from 16 to 64 nucleotides increases the efficiency of reinitiation from 16% to 38%. The average size of a uORF or an intercistronic spacer is 52 ± 23 or 68 ± 77 nucleotides, respectively. In humans, translation initiation at near-cognate, non-AUG initiation codons preceding the coding regions is present in 54% of the transcripts. In fact, the chance of an mRNA harboring more than one uORF increases with the length of the 5'-UTR region, although the occurrence of upstream AUGs (uAUG) does not associate with the size of the 5'-UTR (IACONO *et al.* 2005). In some cases, the presence of one or several uORFs depends on alternative splicing of the transcript or transcription initiation from various alternative promoters. Studies from deep sequencing analyses from yeast extracts highlighted the presence of high numbers of uORFs with no AUG initiation codons, but nearby equivalent codons appeared to be translated efficiently (INGOLIA *et al.* 2009). In mammals, approximately all uORFs allow reinitiation steps to occur not depending on precise uORF sequence. However, often mRNA specific sequences can modulate efficiency of rescanning. In yeast, the uORF that allows reinitiation to occur is the 5'-proximal uORF1 of all the four GCN4 mRNAs with an efficiency reaching 50% (Figure 4.1-1) (VILELA *et al.* 1998; JACKSON *et al.* 2012). The first uORF is always translated regardless of the nutritional conditions. Nucleotides upstream and downstream the uORF1 have been revealed to interact with yeast eIF3, which is necessary for 40S retention on mRNA after uORF termination (SZAMECZ *et al.* 2008; MUNZAROVA *et al.* 2011). Recently, it was demonstrated that the subunit eIF3h can boost reinitiation after translating a reinitiation-permissive uORF (ROY *et al.* 2010).

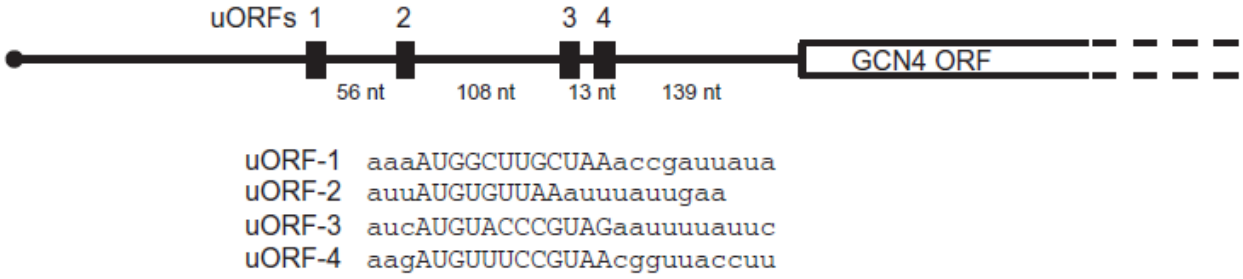

Figure 4.1-1 Position and configuration of uORFs in yeast GCN4 mRNA
Position and spacing of the four uORFs in yeast GCN4 mRNA - The sequences of the four uORFs are shown in upper case, with flanking sequences in lower case. *Modified from Jackson et al., (2012) Adv Protein Chem Struct Biol 86,45-93*

In mammals, the dependence of reinitiation on eIF2-TC is manifested by the mammalian ATF4 and ATF5 mRNAs. This transcript encodes for a basic zipper transcription factor (bZIP) and harbors 2 uORFs in the 5'UTR region. uORF1 is a three-amino-acid-long, while uORF2 is 59-amino- acid-long and overlaps the main *ATF4* ORF (VATTEM AND WEK 2004). Both uORFs are reinitiation-permissive, when eIF2 is phosphorylated by PKR-like endoplasmic reticulum kinase (PERK). When eIF2-TC is available in normal conditions, uORF1 is translated. Since the length of the uORF2 is long and it overlaps *ATF4* ORF, the ribosomes will be recycled at the termination codon leading to ribosome pausing and thus the continuation of scanning is altered (KOZAK 2001). Under stress conditions, the phosphorylation of eIF2α augments, which in turn reduces eIF2-TC concentrations and allows the 40S ribosomal subunit to bypass the uORF2 AUG codon which ultimately leads to reinitiation to start at *ATF4* mORF (main ORF) (Figure 4.1-2) (VATTEM AND WEK 2004; SOMERS *et al.* 2013).

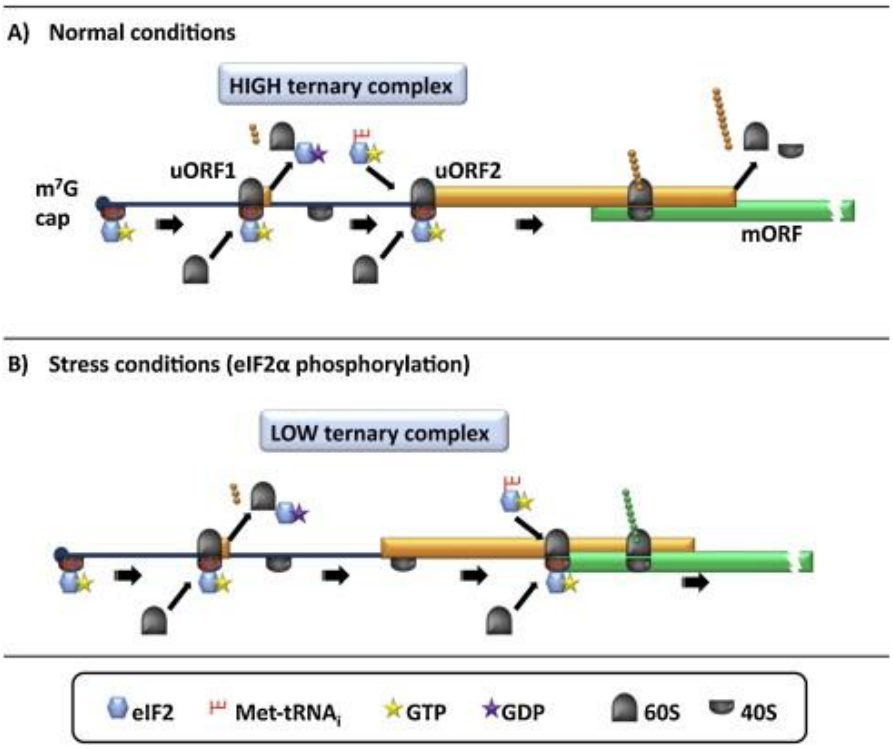

Figure 4.1-2 Reinitation mechanism of ATF4 mRNA translation
(A) Under normal conditions (abundant eIF2-TC), ribosomes have been translated uORF1 may reinitate—40S remains attached to the transcript and can resume scanning downstream. eIF2B acts as a GEF to eIF2-GDP, exchanging the GDP for GTP. Due to the abundant eIF2-TC availability the 40S ribosome reacquires a ternary complex before uORF2 allowing reinitation at uORF2 AUG codon thus, preventing translation of the ATF4 mORF. (B) Under stress conditions, which elevate eIF2α phosphorylation, uORF1 is translated as described above. However, eIF2α phosphorylated at Ser51 irreversibly binds eIF2B reducing the available pool of eIF2-TC. In this case, 40S scanning progresses further along the transcript before reacquiring eIF2-TC, thus bypassing the start codon of uORF2. Reinitiation at the ATF4 mORF is abolished. *Modified from Somers et al., (2013) Int J Biochem Cell Biol 8,1690-700*

4.2 RNA cis-elements and trans-factors promoting reinitiation after uORF translation in mammals

The *cis* sequences and *trans*-acting factors can modulate mechanisms of reinitiation after short ORF translation. First, 5’ and 3’-UTRs flanking the mRNA coding sequence may contain strong secondary structures such as hairpins and pseudoknots that play a regulatory roles, protein binding sites, IRES-dependent elements and uORFs within the 5’-UTR or localization elements and poly-A tail in the 3’UTR (PICHON *et al.* 2012). Efficient recognition of the start codon requires the Kozak consensus sequence that gives the most

favorable initiation context (GCC**R**CC*AUG***G**; R represents a purine base). Second, translation initiation factors that have been recruited during the first initiation event, may remain associated with translating ribosomes during several elongation cycles, albeit loosely, and participate in reinitiation of translation. Indeed, ribosomes that remain attached to crucial factors are capable of rescanning again upon the 60S ribosomal subunit detachment at the termination phase (JACKSON *et al.* 2012). However, employment of IRES elements, which initiation depends on different sets of eIFs, allowed identification of eIF4F (eIF4G) as reinitiation factors.

Indeed, no reinitiation occurred when the system was lacking specifically eIF4G, but this was rescued by adding eIF4G p50 fragment which harbors the central domain required to interact with eIF3 and eIF4A (POYRY *et al.* 2004). This indicates that the eIF4G-eIF3-40S complex is necessary for the reinitiation step to occur. Other factors like eIF5B and eIF1A are released from the ribosome upon GTP hydrolysis and are not essential for the reinitiation step (PESTOVA *et al.* 2000; MYASNIKOV *et al.* 2005). Moreover, other factors such as TDE (translational depression element) interact with PABP and eRF3 to form a complex that stops termination of uORF and promotes reinitiation.

4.3 Translational control by uORFs

Until now, known uORFs vary in terms of length, number, distance from the 5'-cap, their positioning within the 5'-UTR, secondary structures, and the distance between the stop codon and the start site (Figure 4.3-1) (SOMERS *et al.* 2013).

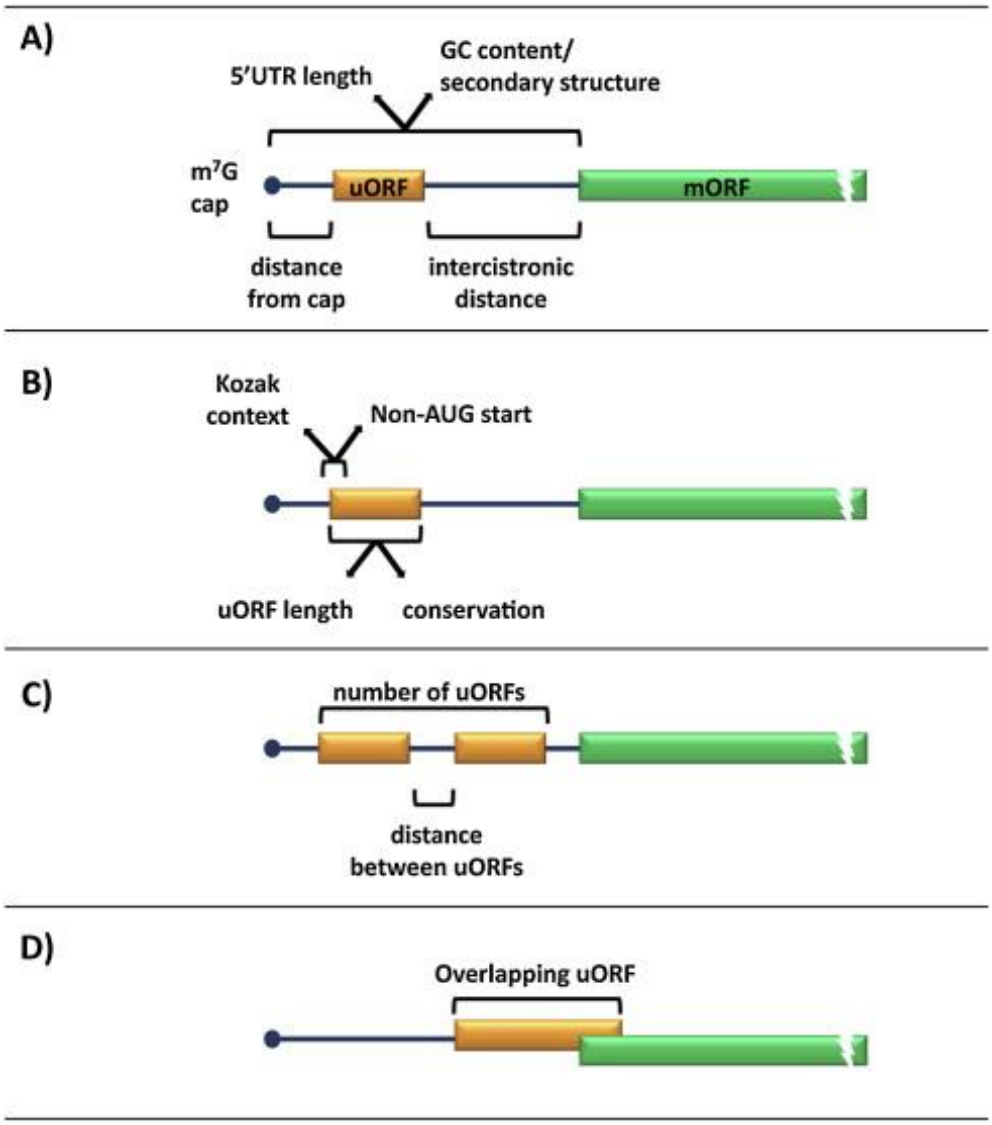

Figure 4.3-1 Properties may contribute to a uORF's role in the translational control of a mORF
Multiple properties may contribute to uORF role in the translational control of a main ORF. These include the length of the 5'UTR, the secondary structure and GC content; consideration of where the uORF is situated, including the distance from the cap and the intercistronic distance between the termination of the uORF and the mORF (A). The sequence and context of uORF might be important, the strength of the surrounding Kozak context and the uORF length and its conservation. Conservation of uORFs may indicate a role for the peptide coding sequence of the uORF (B). Longer 5'UTRs tend to have multiple uORFs, so considering the distance between these uORFs is important (C). Lastly, some uORFs do not terminate within the 5'UTR; rather they overlap with the main ORF. These uORFs, if recognized by ribosomes, will inhibit the main ORF translation (D). *Modified from Somers et al., (2013) Int J Biochem Cell Biol 8,1690-700*

Furthermore, alternative mechanisms are involved in translation of uORF-containing mRNAs (SOMERS *et al.* 2013). uORF2 nucleotide sequence can slow down ribosomal scanning towards to main ORF of mRNA that encodes methionine synthase (mRNA harbors two inhibitory uORFs; within the leader region (Figure 4.3-2) (COL *et al.* 2007; SOMERS *et al.* 2013). In general, secondary structures slow down ribosomal scanning since more time is required for AUG codon recognition and uORF translation.

uORF products are either expressed at very low levels or degraded (OYAMA *et al.* 2007; SLAVOFF *et al.* 2013). This makes the detection of peptide expressed from the uORF very difficult and limited. In fact, studies by mass spectrometry revealed only 7 uORFs peptides in human cells that can interfere with translation *in cis* or *in trans* (OYAMA *et al.* 2007). These are specific uORF products MYCNOT arising from the $MYCN^{\Delta 1b}$ transcript detected in fetal but not adult brains (BESANCON *et al.* 2009). Some uORF encoded peptides can abolish main ORF translation in *cis* (Figure 4.3-2). For instance, 6 codon uORF within S-adenosyl-methionine decarboxylase (*AdoMetDC*) mRNA that encodes peptide MAGDIS block ribosomes at the termination step (RYABOVA AND HOHN 2000; LAW *et al.* 2001).

In some cases uORFs can be bypassed by ribosomes via leaky scanning mechanisms, ribosomal hopping or shunting (RYABOVA AND HOHN 2000) (Figure 4.3-2). One example demonstrates that increased levels of phosphorylated eIF2α (CALKHOVEN *et al.* 2000; PALAM *et al.* 2011) decreases levels of active eIF2-TC.

Internal ribosome entry site (IRES)

IRES and IRES factors allow the ribosome to initiate internally regardless of cap-dependent translational events (PICHON *et al.* 2012). An example, *Cat-1* mRNA is translated internally when the glucose amino acid is in shortage. The prerequisite is translation of a 48-codon uORF that is necessary for a maximal IRES activity (FERNANDEZ *et al.* 2001; YAMAN *et al.* 2003) (Figure 4.3-2).

Non-sense mediated mRNA decay (NMD)

The elimination of transcripts containing a premature termination codon occurs via the non-sense mediated decay (NMD) process. Stop codons located 50 base pairs upstream of an exon-exon junction will be eliminated during the first round of translation by NMD (Fig 4.3-2) (REBBAPRAGADA AND LYKKE-ANDERSEN 2009). It was suggested that uORFs can activate the NMD pathway via adding termination codons at the 5' leader sequence.

Many diseases are associated with mutations within uORFs. For example, *MDM2* is an oncogene that inhibits function of a tumor suppressor p53. MDM2 is encoded by 2 transcripts of different sizes (uORF-less short and 2 uORF containing long transcripts). Increased translation of the short transcript triggers an increased production of MDM2 protein, which is associated with breast cancers. Statistical analysis revealed that in 70% of oncogenes, uORFs are common (SPRIGGS *et al.* 2010).

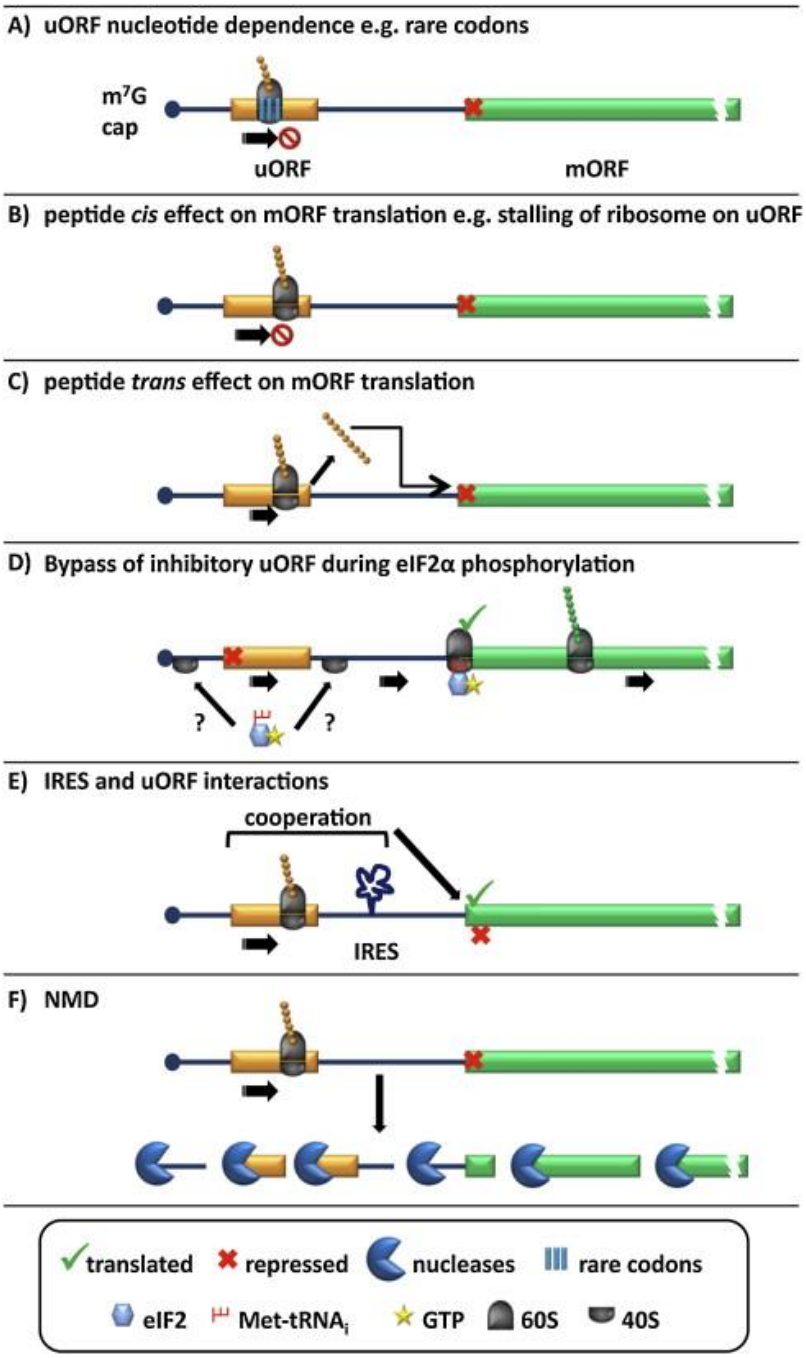

Figure 4.3-2 The roles of uORFs in translational control
uORFs have been characterized to perform a number of different roles. (A) The nucleotide sequence can have a predominant role in uORF translatability by encoding for rare codons that cause the ribosome to stall (*methionine synthase*) or the potential involvement of such sequences in secondary structure or RNA motifs (*UCP2*). The peptide product of uORFs can have *cis* regulatory functions, for instance causing the stalling of ribosomes (*AdoMetDC* and *CHOP*) (B), or by the *trans* repression of the mORF (*AS, β2 adrenergic receptor* and *vasopressin V1B receptor*) (C). (D) Bypass of an inhibitory uORF has been observed under stress conditions and is dependent on eIF2α phosphorylation. An interesting possibility for how this may occur is the loading of the 40S without an eIF2-TC which it acquires as it scans (E) Interactions that involve both uORFs and IRES elements within 5'UTRs can cause expression of the mORF (*Cat-1*) or repression of particular splice variants (*VEGF-A*). (F) Approximately 35–50% of uORF containing transcripts undergo selective degradation by NMD (e.g. *ATF4*, *CHOP* and *IFDR1*). *Modified from Somers et al., (2013) Int J Biochem Cell Biol 8,1690-700*

5. uORF-containing mRNAs in plants

5.1 Reinitiation factors in plants, their phosphorylation by TOR

In plants, translation is controlled by many parameters originating from nutritional, biotic and abiotic stresses (environmental changes, starvation, pathogens) and small metabolites (KAWAGUCHI AND BAILEY-SERRES 2002). The ribosome usually dissociates the mRNA when it reaches a termination codon, leading to translation termination. However, in *Arabidopsis* approximately 30% of the mRNAs contain one or more uORFs in the 5' UTR with a total of 23,463 uORFs (Table 5.1-1) (KIM *et al.* 2007; VON ARNIM *et al.* 2014). A small percentage of uORFs show an evolutionally conserved peptide sequence (CP-uORFs), which has ability to stop the ribosome movement often at the termination codon by a nascent peptide, when positioned at the ribosome exit channel (RAHMANI *et al.* 2009). Normally, CP-uORFs regulate translation of main ORF through external signals such as sucrose and polyamines (HANFREY *et al.* 2005; RAHMANI *et al.* 2009). In addition, some uORFs can regulate translation via metabolic control. For example, the efficiency of translation of phosphoethanolamine N-methyltransferase, a phosphatidyl-choline enzyme is decreased upon the addition of colchicines thanks to a conserved peptide encoded by CP-uORF within 5'-UTR (TABUCHI *et al.* 2006). Polyamines (organic cations) can impact start codon sensing and serve as substrates for specific post-translational modifications in the cell (IVANOV *et al.* 2010). The translation of leucine zipper transcription factor AtbZip11 involved in sugar metabolism can be down regulated by sucrose sufficiency that acts via repressor uORF2b (WIESE *et al.* 2004). uORFs that overlap the main ORF can induce the NMD pathway. This is consistent with the assumption that long uORFs suppress translation reinitiation and induce the NMD pathway, while short uORFs allow reinitiation and suppress NMD (ROY AND VON ARNIM 2013).

Gene AGI # Functional class	Number of uORFs CPuORF class[a]	uORF affects[b]	uORF lengths (codons)	Other characteristics
A. Transcription factors				
AtbZip11 At4g34590 S-type bZip	4 uORFs CPuORF HG1	Translation	18, 42, 5, 19	42 amino acid (aa) CPuORF peptide detected in vitro; sucrose exacerbates repression;
Opaque-2 Maize bZip	3 uORFs	Translation	3, 21, 20	uORFs in cluster repress translation redundantly
myb7 Rice Myb	1 uORF	Translation	40	uORF repression depends on downstream spacer sequence; peptide detected in vitro
ATR1 At5g60890 Myb	3 uORFs	mRNA level	33, 3, 4	33 amino acid uORF reduces mRNA level; uORF mutant allele from suppressor screen (*atr1-d*)
R/Lc Maize basic helix loop helix	1 uORF	Translation	38	Peptide involved in repression; poor reinitiation
SAC51 At5g64350 Basic helix loop helix	5 uORFs CPuORF HG15	mRNA level (NMD)	20, 16, 48, 53, 6	CPuORF truncation from 53 to 3 amino acids rescues expression and thermospermine deficiency; uORF mutant allele from suppressor screen (*sac51-d*)
HsfB1/HSF4/TBF1 At4g36990 Heat shock factor	2 uORFs CPuORF HG18	Translation	15, 36	CPuORF has 36 amino acids
ARF3/ETTIN At2g33860 Auxin response factor	2 uORFs	mRNA level (minor) Translation	92, 5	Large uORF1 peptide detected in vitro; *ARF3* translation stimulated by RPL24 and eIF3h
ARF5/MONOPTEROS At1g19850 Auxin response factor	6 uORFs	Translation	3–23	*ARF5* translation stimulated by RPL24 and eIF3h
ATH1 At4g32980 BELL-type homeodomain	4 uORFs	Translation	9, 12, 13, 1	uORF cluster with 7 uAUGs
ABI3 At3g24650	3 uORFs		26, 11, 12	Cluster of 3 uORFs inhibits *ABI3* expression
MtHAP2-1 *Medicago* C/EBP	3 uORFs	mRNA level	62, 50, 34	uORF cluster in alternatively spliced intron; uORF1 peptide binds and represses its own mRNA

Table 5.1-1 Examples of uORF-containing mRNAs and their putative functions in plants
a. The homology group (HG) of the CPuORF is indicated.
b. If nonsense mediated decay was also shown, it is indicated by NMD.
Modified from von Armin et al., (2014) Plant Sci 14,1-12

a. TOR

Because previous studies demonstrate that auxin mediates phosphorylation of TOR—treatment of 7 dag seedlings by auxin leads to activation and phosphorylation of TOR at S2424 (SCHEPETILNIKOV *et al.* 2011; SCHEPETILNIKOV *et al.* 2013)—it becomes possible to monitor behavior of active TOR in translation initiation/reinitiation. Accordingly, auxin-treated plants support high levels of reinitiation after uORF translation (SCHEPETILNIKOV *et al.* 2013). As it was proposed (KOZAK 2001; JACKSON *et al.* 2012), reinitiation after uORF translation depends on the participation of certain eIFs supporting reinitiation that are recruited during the initiation event at uORF and then not released during the short time required for sORF translation, thus suggesting that these factors should accumulate in polysomes, if reinitiation is efficient. These eIFs associated with post-termination ribosomes

can then regenerate reinitiation-competent 40S complexes capable of scanning to the next ORF, rebinding the ternary complex (TC) along the way. Indeed, analysis of 48S PIC and polysomes of plants treated with auxin revealed that these associate with increased levels of active TOR phosphorylated at Ser2424. In contrast, germination and growth of *Arabidopsis* on the medium containing TOR inhibitors—either Torin-1 or AZD-8055—abolished TOR phosphorylation and its loading on polysomes, but promotes loading of inactive S6K1 instead. Thus, as in mammals, 48S PIC and polysomes serve as platforms for S6K1 phosphorylation by TOR in *Arabidopsis*. Interestingly, active TOR maintains phosphorylation of reinitiation supporting protein (RISP) in polysomes, also in TOR inhibitor sensitive manner. Taking data together, eIF3-48S PIC/ polysomes interacts with S6K1, if TOR and S6K1 are not active, but with TOR, if TOR is activated. Thus, plant-eIF3 can associate with both TOR and S6K1 in dynamic order of events that provides a base for S6K1 phosphorylation by TOR (HOLZ *et al.* 2005; SCHEPETILNIKOV *et al.* 2013). TOR mediates phosphorylation of S6K1 at the TOR specific hydrophobic residue T449, which in turn phosphorylates reinitiation specific factor eIF3h at residue S178 (see below) that induces reinitiation of post-terminating ribosomes of short uORFs in response to auxin (SCHEPETILNIKOV *et al.* 2013) (Figure 5-1.1) Furthermore, TOR is required for virus-activated reinitiation after long ORF translation that operates on the polycistronic 35S RNA of CaMV under control of TAV (SCHEPETILNIKOV *et al.* 2013) (see below).

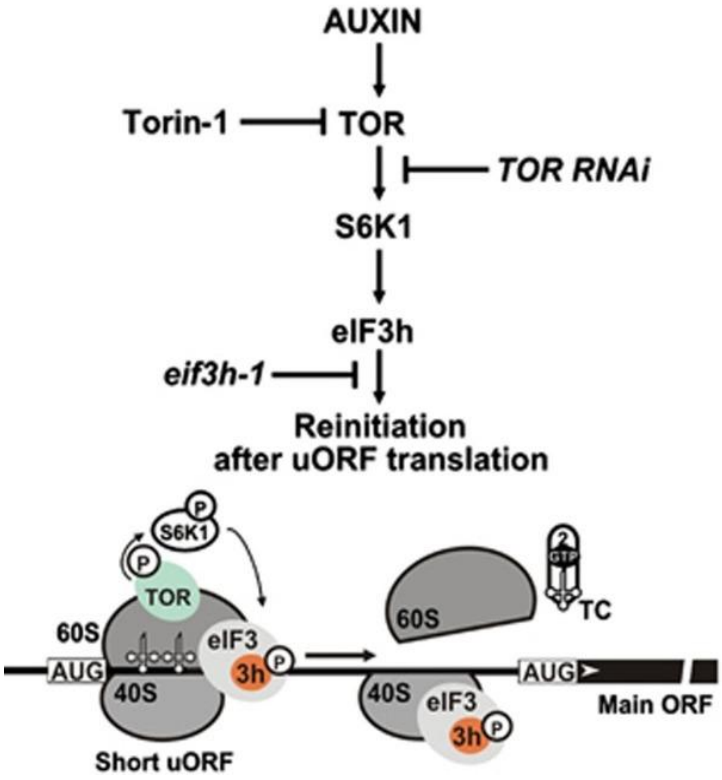

Figure 5.1-1 Auxin-responsive TOR function in reinitiation after uORF translation
Torin-1 application, or TOR deficiency, or eIF3h C-terminal deletion inhibit reinitiation at the steps indicated. *Modified from Schepetilnikov et al., (2013) EMBO J 8,1087-102*

Two plant proteins were suggested to fulfill function of reinitiation promoting factors. In plants, eIF3 non-core subunit h (eIF3h) and the 60S protein RPL24 increase the reinitiation competence of uORF-containing mRNAs (uORF-RNAs) encoding two families of transcriptional factors—auxin response factors (ARFs) and basic zipper transcription factors (bZIPs) (KIM *et al.* 2004; NISHIMURA *et al.* 2005; ZHOU *et al.* 2010). Both translation reinitiation and auxin-mediated organogenesis are compromised severely by mutations in either eIF3h or RPL24.

b. RISP

The reinitiation supporting protein (RISP) was discovered as a partner of CaMV TAV as a result of *Arabidopsis* cDNA libray screening with TAV as bait (THIEBEAULD *et al.* 2009). RISP contains the pattern RGRLES (phospho-Ser/Thr preceded by Lys/Arg at positions 5 and

3) that is phosphorylated by S6K1 at S267; phosphorylation of RISP at this site by S6K1 improves RISP binding to TAV. Thus, RISP interacts with TAV and promotes virus-activated reinitiation after long ORF translation. Additionally, RISP binds two eIF3 subunits—a and c through the N-terminal α-helical H2 domain of RISP, and this complex was implicated in stimulating of viral polycistronic translation in plants. In addition to its interaction with eIF3a/ eIF3c, RISP is capable of binding the 60S ribosomal subunit via the RPL24 C-terminus. When bound to eIF3, RISP is found attached to 40S, indicating that it enters translation initiation at the step of 43S PIC or 48S PIC formation. Thus, RISP and TAV collaborate to promote reinitiation by TC or 60S recruitment to 40S (THIEBEAULD *et al.* 2009). Knockout of one (*RISPa*) out of two gene copies results in a viral replication delay and reduced TAV-mediated transactivation in protoplasts further validating the role of RISP in CaMV-mediated reinitiation after long ORF translation.

The proposed model states that after translation termination, the RISP-TAV complex might mediate contacts between 40S and 60S and promote retention of 60S by the 40S scanning ribosome via RPL24. The shift from scanning to reinitiating ribosome is not well understood, but upon start codon recognition, the contacts between RISP-TAV and RPL24 will be destroyed allowing the shift to occur (Figure 5.1-2) (THIEBEAULD *et al.* 2009).

Studies suggest that TAV interacts and activates TOR, which in turn phosphorylates S6K1 and induces the subsequent phosphorylation of RISP at S267, which strengthens its binding to RPL24. In the presence of TAV, phosphorylated TOR associates with polysomes that correlates with high loading of phosphorylated RISP in polysomes (SCHEPETILNIKOV *et al.* 2011). In contrast, TAV lacking the TOR binding site, is still able to promote loading of RISP to polysomes. But due to TAV inability to interact and thus promote TOR activation, RISP accumulating in polysomes is not phosphorylated (SCHEPETILNIKOV *et al.* 2013).

c. eIF3h

eIF3h induces and facilitates translation reinitiation of mRNAs that harbor uORFs within their 5'-UTRs, that was shown for auxin response factors (ARFs) and basic zipper transcription factors (bZIPs) (KIM *et al.* 2004; ZHOU *et al.* 2010). It plays a regulatory function is response to exogenous sources of sugars and to hormones and it is mainly accumulated in roots and flowers.

Mammalian and plant eIF3h have similar motifs (REKNFS^{178}/KEKDFS^{183}) present in many Akt and S6K1 substrates, and it was demonstrated that both homologs are phosphorylated (SCHEPETILNIKOV *et al.* 2011; HERSHEY 2015). Mammalian phosphorylated eIF3h accumulates in cancer cells (HERSHEY 2015), while in *Arabidopsis*, eIF3h phosphorylation occurs through TOR signaling cascade and the eIF3h phosphorylation step leads to eIF3 accumulation in polysomes (SCHEPETILNIKOV *et al.* 2013). eIF3h may contribute to different steps of reinitiation—the resumption of scanning and start codon recognition at the downstream uORF.

Thanks to *eif3h-1* mutant that carries the carboxyl-terminal truncation of eIF3h and thus having defects in translation of specific mRNAs harboring several uORFs within the 5' leader sequence, but not mRNAs which translation initiation occurs via cap-dependent mechanism (KIM *et al.* 2007). *eif3h-1* contains an insertion of a T-DNA in the 10th exon of *eif3h* gene downstream to Ser254, which led to repression at both translational and transcriptional levels, and resulted in growth delays, mainly in vegetative and root development, the flowering process in addition to morphological defects that decrease fertility and hypersensitivity to the hormone ABA. The bZIP11 leader contains multiple uORFs, where uORF2a is the only uORF indispensable for eIF3h dependent translation as compared to other uORFs. However, removal of uORFs 2b, 3 or 4 also decreases repression by uORFs in *eif3h-1*. uORF2b is an inhibitory peptide that blocks main ORF of *AtbZip11*

translation at high sucrose concentrations (RAHMANI *et al.* 2009). Here, sucrose acts as an external signal that regulates translation (WIESE *et al.* 2004).

eif3h displays defects related to defects in auxin responses indicating a link between auxin and eIF3h. A similar characteristic were found for *ARF5* mutants and *eif3h-1* —one or two asymmetric cotyledons (ZHOU *et al.* 2010). On the other hand, one valve was absent in *eif3h* mutants a characteristic similar to *ARF3* mutation. In addition, flowers in *eif3h* mutant plants contain 4 to 5 stamens instead of 6 (KIM *et al.* 2004).

Interestingly, in *eif3h-1* polysomal association of uORF-containing RNAs is influenced by the length of the main coding region. Thus, the contribution of eIF3h to polysome binding depends on the repressive effect of uORFs and the length of main ORFs. Thus, efficient translation of above mRNAs depends on intact eIF3h structure (KIM *et al.* 2007). mRNAs coding for ribosomal proteins are among the least dependent on eIF3h for polysome binding.
Studies also suggested important interactions between eIF3h and COP9 signalosome (CSN). In yeast, co-immunoprecipitation assays with an antibody against eIF3h revealed two CSN subunits (CSN4 and CSN5) (KIM *et al.* 2004). In plants, similar phenotypes are found for *eif3h* and CSN mutants; both abolish growth and development after germination. Furthermore, the *fus6/CSN-11* line, which is known to have decreased levels of CSN, showed growth retardations similar to *eif3h* mutant phenotypes. Thus, a possible interaction between both complexes (eIF3h and CSN) might spot light on the possible collaboration and cellular activities in inducing translation initiation and protein turnover.

5.2 The reinitiation factor RPL24

A plant ribosomal protein (RPL24) of the large 60S ribosomal subunit is encoded by the *SHORT VALVE1* gene. It belongs to a category of ribosomal proteins present in archaebacteria and eukaryotes, but not in prokaryotes. RPL24 was implicated in 60S subunit

joining in yeast (DRESIOS *et al.* 2000). It becomes famous in translation research, when it was demonstrated that RPL24 is critically required for translation of mRNAs that encode auxin response transcription factors ARF5/MONOPTEROS (participates in formation of the apical-basal axis) and ARF3/ETTIN (establishing the dorsoventrality of the leaves) (SESSIONS AND ZAMBRYSKI 1995; HARDTKE AND BERLETH 1998). It is well known that ARFs boost the expression of many auxin response genes when bound to their promoter regions (ULMASOV *et al.* 1997). However, ARFs can trigger repression of auxin response gene transription (ULMASOV *et al.* 1999; TIWARI *et al.* 2003).

Studies revealed that deletions in *RPL24B/SHORT VALVE* (STV) lead to defects in organ initiation, gynoecium structure and vascular patterning that are linked to ARFs 3 and 5 mutants (NISHIMURA *et al.* 2005). A defect in auxin response is characterized by the pin-formed shoots phenotype due to mutations in *ARF5* gene (PRZEMECK *et al.* 1996). As eIF3h, intact RPL24 improves both ARF3 and ARF5 expression. Similar to eIF3h, translation efficiency of *AtbZip11* is strongly reduced by a deletion in (*STV*) gene. Thus, *ARF3* and *ARF5* translation is affected in both mutants *rplb24* and *eif3h*, implying that the presence of uORFs within leader regions serves as employees for eIF3h and RPL24.

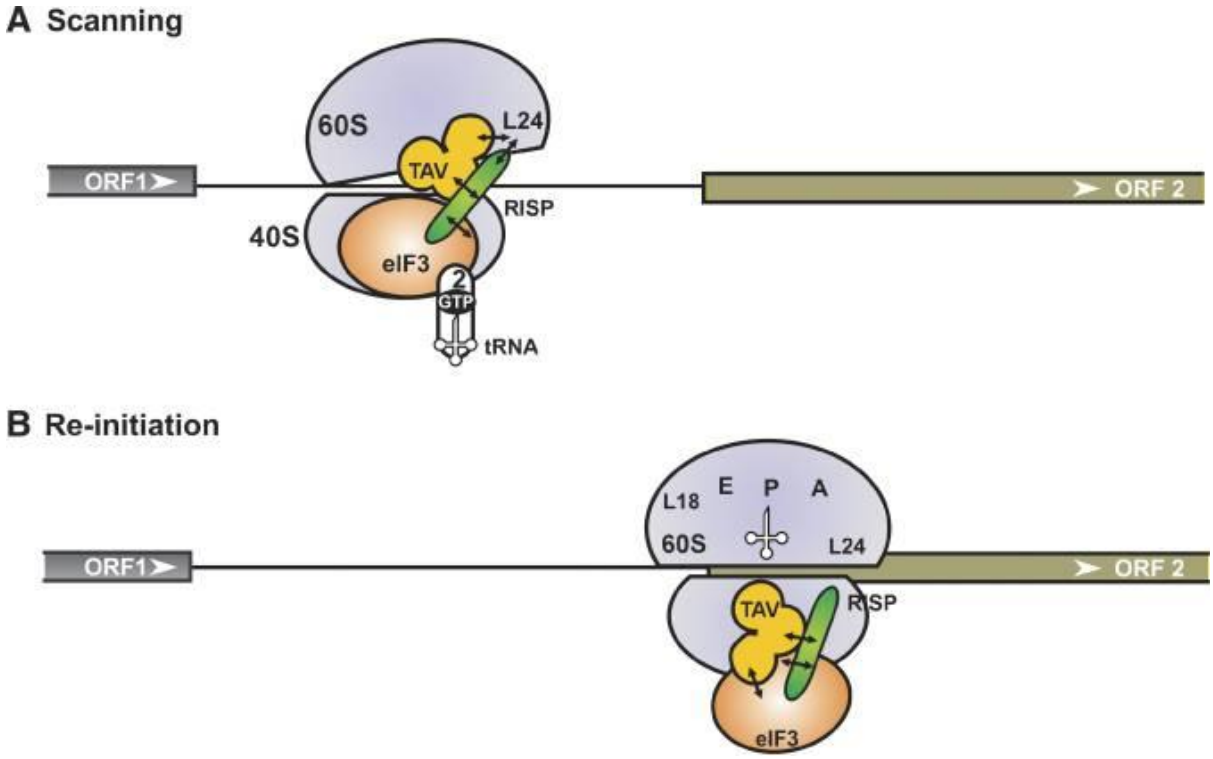

Figure 5.1-2 Proposed model of re-initiation supporting protein (RISP) function in 60S recruitment during virus-activated re-initiation
During ORF1 elongation, the RISP–transactivator viroplasmin (TAV)–80S complex can be stabilized by transfer of TAV– RISP–eIF3 to the solvent surface of 60S through TAV binding to L18/L13. During termination, the TAV–RISP–eIF3 complex is relocated back to 40S to reconstruct a pre-initiation complex (PIC) competent for re-initiation. (A) RISP TAV establishes a bridge between 40S-bound eIF3 and 60S through the ribosomal protein L24, preventing, for a short time, removal of 60S. During scanning, RISP bridges the relaxed 40S–60S interactions through contact with 40S-bound eIF3, while simultaneously stabilizing TAV–L24 contacts (open conformation of 80S). This open 80S conformation allows eIF3-bound 40S to continue scanning and search for a downstream start codon. (B) Codon–anticodon recognition and positioning of Met-tRNAiMet in the ribosomal P-site would then displace TAV and RISP from L24 followed by the formation of 80S ready for elongation. eIF3, TC, RISP, TAV, L24, 40S and 60S are indicated. *Modified from Thiébauld et al., (2009) EMBO J 20,3171-84*

5.3 uORFs affect plant development and organogenesis

All aboveground plants arise from stem cells in the primary shoot apical meristem (SAM). SAM is important for the production of lateral organs such as leaves, branches and flowers. In *Arabidopsis*, the proliferation of stem cells is highly regulated by feedback loop formed by WUSCHEL (WUS), a homeodomain transcription factor and the CLAVATA ligand-receptor system. SAM stem cells are highly controlled by the CLAVATA-WUSCHEL (CLV-WUS) cascade (AICHINGER *et al.* 2012). CLV3 is an extracellular peptide synthesized in the central

zone of SAM, it acts as a ligand for the receptor kinase CLV1. Their interaction leads to the restriction of the spatial expression of WUS, which in turn induces the expression of CLV3 and forms a negative feedback loop to maintain the stability of the stem cell population (BRAND *et al.* 2000; GUO *et al.* 2010). Several mRNAs involved in the maintenance of the apical meristem harbor uORFs that make the translational process relying partially on eIF3h. For example, the *eif3h-1* mutant displays a number of defects in SAM maintenance, ranging from problems in the positioning and the polarity of the organ to a huge enlargement in SAM size and failure to initiate the synthesis of new organs. In flowering plants, the enlargement of SAM is less prominent, but other characteristics such as defects in organ positioning are still observed. This suggests that *Arabidopsis* eIF3h plays a role in morphogenesis, homeostasis and organogenesis (Figure 5.3-1). These studies revealed that eIF3h promotes efficient translation of mRNAs that encode the leaf transcription factor *AS1* and *CLV1*. Both mRNAs harbor several uORFs in their 5'-UTR. C-terminal truncation of eIF3h strikingly reduces translation of *CLV1* and disturbs the feedback required for SAM maintenance and organogenesis.

CLV1 mRNA harbors 4 uORFs of 16, 4, 1 and 12 codons, respectively, that would inhibit the main ORF substantially in *eif3h-1* plants, triggering decrease in translation of *CLV1* that leads to an increase of *WUS* transcription, which in turn will activate *CLV3* transcription that will ultimately lead to the observed expansion in SAM (ZHOU *et al.* 2014). *AS1* mRNA contains 3 uORFs. A decrease in the expression of this gene results in the appearance of wrinkled leaves, a phenotype observed in *eif3h* mutants. Mutations in other genes also result in meristem enlargement and over proliferation, such as silencing of the Homeodomain-Zipper class III transcription factors involved in adaxial leaf determination. It is noteworthy to indicate that *CLV1* interacts with other receptor kinase encoding genes such as *CORYNE, TOADSTOOL* and *CLAVATA2*. In addition, *WUS* is controlled by other genes

like *CORONA* and *SPLAYED* (GREEN *et al.* 2005; KWON *et al.* 2005). Strikingly, *CORONA* contains 8 uORFs within 5'-UTR.

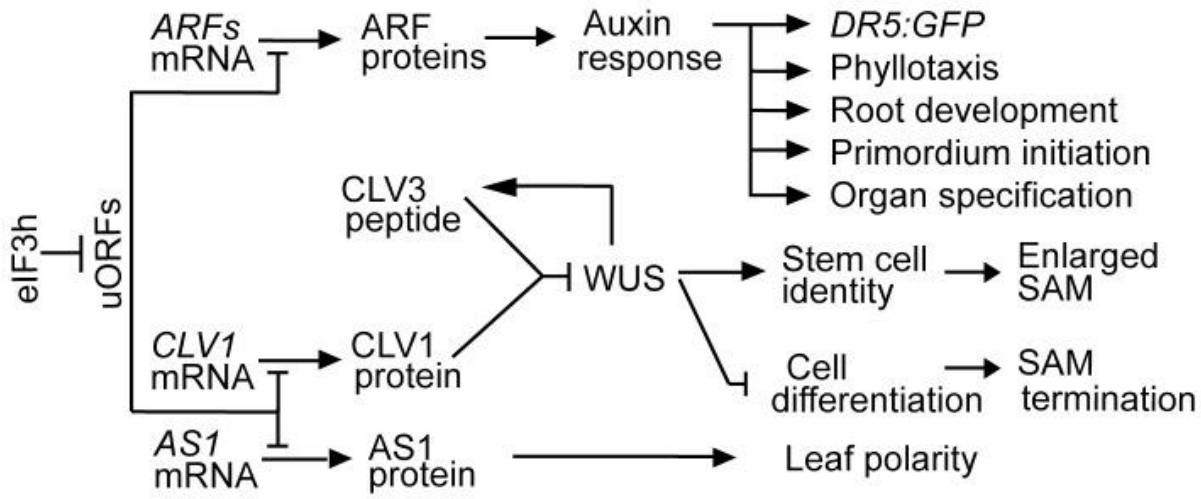

Figure 5.3-1 Role of eIF3h in *Arabidopsis* SAM maintenance and auxin response
By overcoming the translational repression by uORFs, eIF3h promotes the translation of ARFs and CLV1 and AS1, and therefore plays an important role in SAM maintenance and organogenesis. *Modified from Zhou et al., (2014) PLoS One 4,e95396*

6. Viral reinitiation after long ORF translation in eukaryotes

6.1 Reinitiation after long uORF translation in calicivirus virus, influenza B virus and transposon LINE-1

Viruses use many mechanisms to synthesize the maximum number of proteins encoded by their limited genomes. Reinitiation after long ORFs is very rare in mammals as compared to reinitiation after short ORFs. Unlike prokaryotes, mammalian ribosomes in general cannot translate downstream cistron of bicistronic mRNA. However, translation of the second ORF is possible if (1) an IRES element is located within an intercistronic region, allowing the binding of ribosomes internally upstream of the start site of the second ORF; (2) the first uORF is short (less than 30 codons; (KOZAK 2001; POYRY *et al.* 2004).

A rare case of reinitiation after long ORF translation was found operating within the bicistronic subgenomic mRNA of mammalian *Caliciviridae* family of positive-strand RNA

viruses. This family includes the feline calicivirus (FCV) and the rabbit hemorrhagic disease virus (RHDV), where so-called termination-reinitiation mechanism was studied in details. FCV RNA is around 7700 nucleotides long and contains 3 long ORFs—RNA replicase, two capsid proteins VP1/ VP2 and a protease. VP1 and VP2 are encoded by two tandem ORFs within the subgenomic RNA, where VP2 is encoded by the second ORF. VP2 is indispensable for infectivity (SOSNOVTSEV *et al.* 2005). Studies revealed that VP2/VP1 ratios vary among members of the calicivirus (LUTTERMANN AND MEYERS 2007). In general, these two ORFs overlap by 4 nucleotides (AUGA…). However, some exceptions are present in Norwalk virus or bovine calicivirus (Figure 6.1-1) (PÖYRY *et al.* 2007).

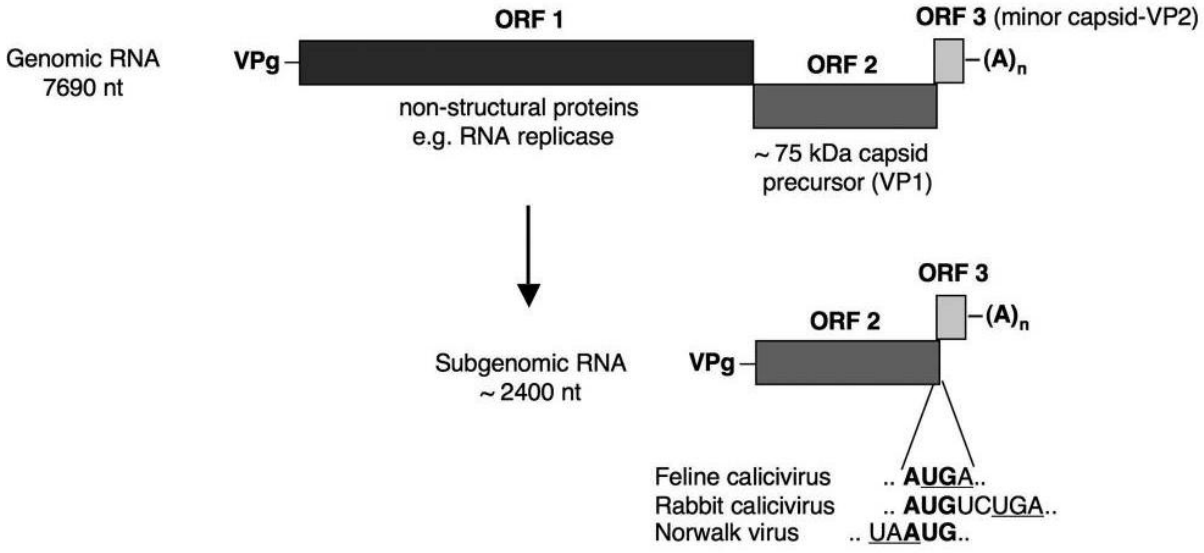

Figure 6.1-1 Diagrammatic map of FCV genomic (virion) and subgenomic RNAs
The ORF structure of the virion (genomic) RNA – The ORF2/ORF3 overlap sequence of FCV subgenomic RNA is given, together with with the largest (RHDV) and smallest (Norwalk virus) overlaps found in other caliciviruses. *Modified from Pöyry et al, (2007) Genes Dev 23,3149-62*

VP2 expression depends on a reinitiation process and can occur only after translation of ORF1 (PÖYRY *et al.* 2007). The so-called TURBS motif (80 nucleotides, Termination Codon Upstream Ribosome-Binding Site) located within the 3'-terminus of ORF1 coding region is

essential for ORF2 translation via termination-reinitiation (LUTTERMANN AND MEYERS 2007). Its position close to the ORF2 AUG codon increases ORF2 translation efficiency. TURBS may promote termination-reinitiation via eIF3 binding (POYRY *et al.* 2007).

Normally, 60S has to dissociate 40S-mRNA during termination of translation to be ready to initiate at further downstream ORF specifically. The model states that 60S is then captured by TURBS until 40S recruits TC, and delivered to 40S-TC for VP2 ORF initiation. In addition, TURBS motif was implicated in direct binding to 40S ribosomal subunit via 18S ribosomal RNA (LUTTERMANN AND MEYERS 2007).

A second case of reinitiation after long ORF was reported for an influenza B virus M2 RNA, where TURBS of 40 nt is also present (POWELL *et al.* 2008). The presence of similar TURBS elements in caliciviruses and influenza B virus speaks in favor of evolutionary conservation. Another example is the M2 RNA of pneumoviruses, where these two ORFs overlap by 32 nucleotides and reinitiation occurs at any AUG codon localized further upstream of the first ORF stop codon (AHMADIAN *et al.* 2000).

Finally, non-long repeat retrotransposons possesses two ORFs with overlap either UAAG or AUGA, and a secondary structure element downstream of the second initiation site is necessary for reinitiation (KOJIMA *et al.* 2005). Long Interspersed Element-1 (LINE-1 or L1) retrotransposons encode proteins essential for their movement (ORF1p and ORF2p). Here, *ORF2* translation occurrs also by termination/reinitiation mechanism. The 40S subunit scans over the inter-ORF spacer and reveal a *cis*-acting sequence(s) in the 5' end of *ORF2* that is used to position ribosomes at or near the *ORF2* initiation codon (ALISCH *et al.* 2006).

6.2 Virus-activated reinitiation after long ORF translation

a. CaMV genome

Cauliflower mosaic virus (CaMV) belongs to the *Caulimovirus* genus, a member of the plant pararetrovisruses. It can infect Crucifer species and Solanaceous species (DAUBERT *et al.* 1984). CaMV contains a circular double-stranded DNA molecule of about 8.0 kbp carrying single-stranded interruptions and sequence discontinuities at precise locations within the (+) and (-) strands that forms minichromosomes in the nucleus of infected cells. CaMV genome has seven major open reading frames that are overlapped or separated by few nucleotides, except for ORF 6 which lies between the two intergenic regions.

CaMV genome is transcripted by the cellular RNA polymerase II from 35S and 19S promoters localized within the large and small intergenic regions into two polyadenylated and capped transcripts: the 35S pregenomic RNA (pgRNA) and 19S subgenomic RNA. The 35S pgRNA is used as a template for reverse transcription and mRNA for translation of viral proteins; it is capped and polyadenylated. However, it has a polycistronic nature and harbors an atypical leader sequence containing up to 600 nucleotides and 9 small ORFs (sORFs). The number of sORFs varies between various CaMV strains; and size of peptides encoded by sORFs ranges between 2 and 35 amino acids (POOGGIN *et al.* 1999).

CaMV encodes six functional proteins, but the product of ORF 7 was not detected in plants. Cell-to-cell movement protein (Mov or P1), which forms tubules within the plasmodesmata, is encoded by ORF1. Mov allows the movement of CaMV particles between cells. The aphid transmission factor (Atf or P2) is encoded by ORF2. It has a size of 18 kDa and it is a major factor of electron-lucent inclusion bodies. In addition, it is not essential for viral replication (Figure 6.2-1). ORFs 3 and 4 encode the virion-associated protein (Vap) and the capsid protein precursor (CP or GAG), respectively. Vap is 15 kDa and essential for infectivity. Mov, Atf and Vap play role in virus transportation within the cell and from cell to

cell and are dispensable for CaMV replication (HOWARTH *et al.* 1981). However, Gag and Pol are essential for replication and they share structural similarities with the retroviral Gag and Pol. Gag, precapsid protein of 56 kDa (CP56) is 489 amino acids long. Several processing steps lead to three main capsid protein species, CP42, CP39, and CP37 (named after their respective mobilities. A polyprotein of 78 kDa contains a protease, reverse transcriptase and RNAse functions (Pol or P5) is encoded by ORF5. The final ORF (ORF6) encodes P6 or translation transactivator/ viroplasmin (TAV) (ROTHNIE *et al.* 1994). TAV is the most abundant viral protein with a size of 62 kDa having no homology with other proteins. It is a main component of viral inclusion bodies known as viroplasms, required for protein synthesis, reverse transcription and virion assembly. It is essential and multifunctional protein—required for CaMV replication, morphogenesis, stabilization of viral proteins and critical for translation of viral polycistronic mRNA (PARK *et al.* 2001; THIEBEAULD *et al.* 2009; SCHEPETILNIKOV *et al.* 2011). TAV promotes virion assembly via interaction with Gag and Pol, plays major roles in viral pathogenesis, is the main symptom determinant of CaMV (Figure 6.2-2) (HULL AND SHEPHERD 1976; HIMMELBACH *et al.* 1996). Notably, TAV can physically interact with Chloroplast Unusual Positioning1 (CHUP1), a plant protein that contributes to the movement of chloroplasts along microfilaments (OIKAWA *et al.* 2003). CaMV induces a variety of symptoms such as chlorosis, vein clearing and stunting ranging between mild and severe depending on the viral strain and environmental conditions (MELCHER 1989).

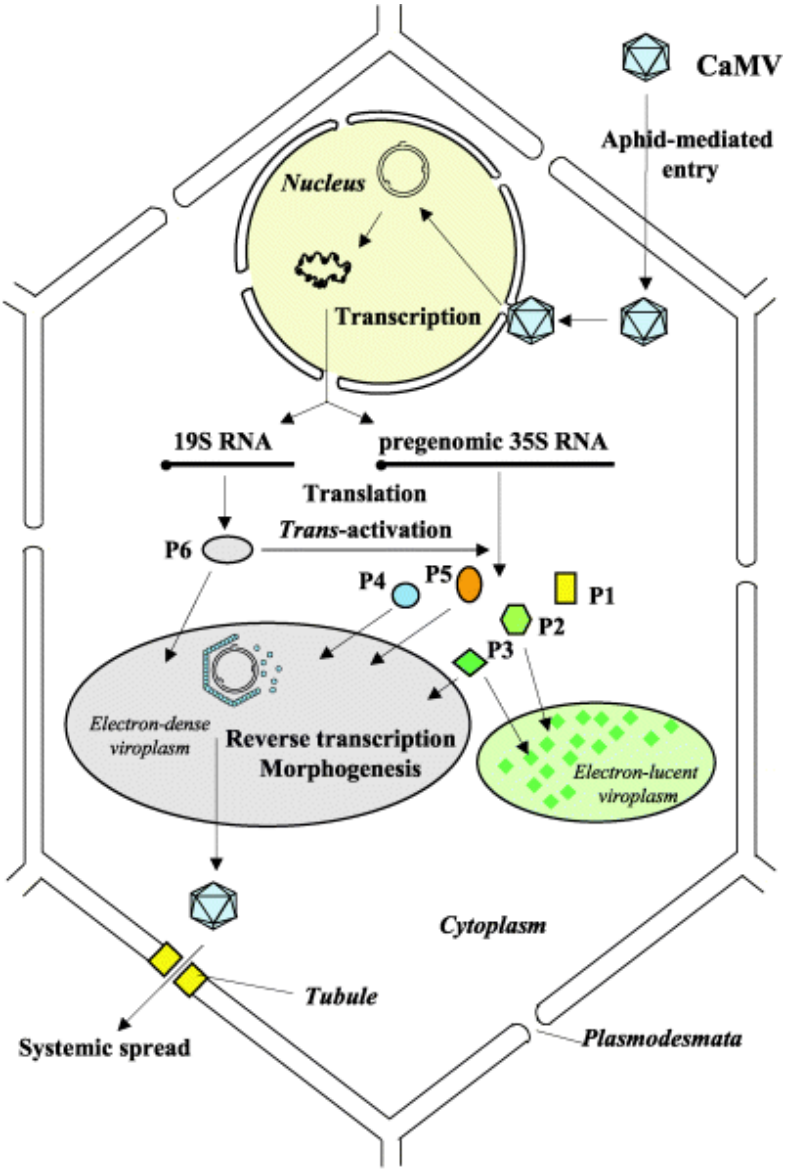

Figure 6.2-1 The multiplication cycle of CaMV
The main steps of the viral cycle are: (a) aphid-mediated entry of the virus into the host cell, (b) NLS mediated transport of CaMV particles to the nuclear pore, (c) import of the viral DNA into the nucleus, (d) reparation of DNA sequence discontinuities and association with histones to form a mini chromosome, (e) transcription of the viral DNA by cellular RNA polymerase II, (f) translation of the 19S RNA and 35S RNA (g) replication of the genome and morphogenesis of viral particles in the electron dense viroplasms, and (h) cell to cell movement of virus particles through tubules, targeting to the nucleus and aphid uptake. *Modified from Haas et al, (2002) Mol Plant Pathol 6,419-29*

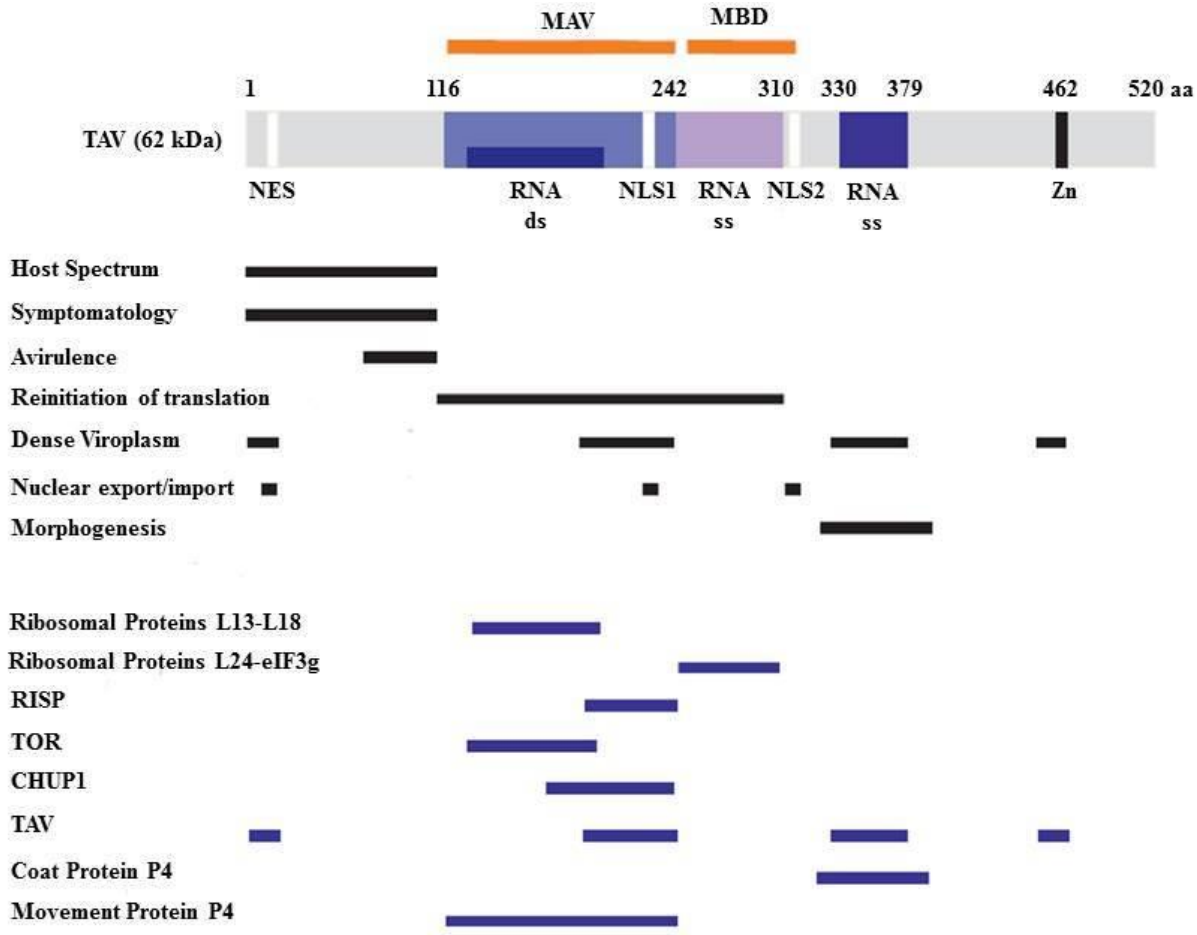

Figure 6.2-2 Schematic representation of the TAV domain map
Lines indicate the positions of regions involved in the function of TAV and in interactions with viral and cellular partners. Zn: Zinc-finger motif - MBD: Multiple binding domain - MAV: Mini TAV, the minimal region required for transactivation of polycistronic translation – RNAds: RNA Binding Domain – NES: nuclear export signal – NLS: nuclear localization signal. *Modified from Bouton et al, (2015) Virologie 3,119-39*

b. Translation strategies of CaMV in expression of the 35S pregenomic mRNA. The role of translational transactivator/viroplasmin (TAV)

Two CaMV promoters direct the production of the terminally-redundant pregenomic 35S RNA and the 19S subgenomic RNA encompassing ORF VI. The 35S RNA, alternatively used as a replicative intermediate or as a polycistronic mRNA for expression of viral proteins, consists of a 600 nt long leader sequence containing several AUG codons, followed by seven tightly-arranged long ORFs encoding all of the viral proteins. The 19S subgenomic RNA encodes a transactivator/viroplasmin, TAV, essential for translation of the 35S pgRNA

(Figure 6.2.3). The 35S RNA is translated thanks to two alternative translation strategies—a ribosomal shunt (FUTTERER *et al.* 1993) and virus-activated reinitiation after long ORF translation (BONNEVILLE *et al.* 1989; SCHOLTHOF *et al.* 1992).

Ribosome shunt is a special mechanism of translation initiation that combines features of the 5′-end dependent scanning and internal initiation (RYABOVA *et al.* 2002; RYABOVA *et al.* 2006). Shunt was the best studied in the *Cauliflower mosaic virus* (CaMV) (FUTTERER *et al.* 1990; FUTTERER *et al.* 1993) and *Rice tungro bacilliform virus* (RTBV) (FUTTERER *et al.* 1996). Initiation of translation on the 35S RNA is 5'-cap-dependent (Fütterer and Hohn, 1991; Schmidt-Puchta et al., 1997), and leads first to recognition of the AUG of sORF A within the leader sequence (POOGGIN *et al.* 2000; RYABOVA AND HOHN 2000). The leader is folded into a strong elongated hairpin structure that together with sORFs represent major obstacles to ribosomes that scan from the 5'-capped end (POOGGIN *et al.* 2000; RYABOVA AND HOHN 2000).

Ribosomal shunt. To avoid these obstacles CaMV exploits the shunting strategy that includes several steps: (1) 40S binding to the capped 5′-end of the 35S RNA, scanning along the leader sequence until it encounters the first AUG—the start codon of short ORF A (sORF A); assembly of 80S followed by translation of sORF A; (2) during short elongation event reinitiation supporting factors, including eIF3 stay ribosome-associated, while RNA helicase activities released; (3) termination at the stop codon of sORF A that is located upstream of the base of the stem-loop structure; (4) the released 40S subunit (shunting ribosome) has lost initiation factor(s) able of melting the secondary structure and accordingly linear scanning is paused by structure; (5) the shunting (bypass) of the 40S subunit over the structured region; (6) the shunting ribosome resumes scanning just downstream of the stem-loop structure at a shunt landing site and reaches the AUG start codon of the first long viral ORF (ORF VII), where translation is re-initiated. eIF3 bound to the shunting ribosomes assists 40S to resume

scanning and initiate directly downstream of the shunt landing site even at a non-AUG codon (RYABOVA AND HOHN 2000). Although shunt functions without TAV, it increases shunting efficiency by about three folds (FUTTERER *et al.* 1993; POOGGIN *et al.* 2000; POOGGIN *et al.* 2001) as manifested by improved translation of the first long ORF (ORF VII downstream of the 35S RNA leader), probably by increasing the reinitiation capacity of shunting ribosomes.

TAV-mediated reinitiation of translation. The main function of TAV in viral translation is to promote translation of several consecutive long ORFs on the polycistronic 35S RNA via reinitiation (BONNEVILLE *et al.* 1989; PARK *et al.* 2001), when ribosomes do not disassociate after translation of the first ORF but reinitiate translation of the subsequent ORF one by one (DIXON AND HOHN 1984; BAILEY-SERRES *et al.* 1986). Thus, translation of ORF VII and further downstream ORFs occurs via reinitiation (RYABOVA *et al.* 2002). TAV is required for reinitiation to occur when shunting is over (BONNEVILLE *et al.* 1989).

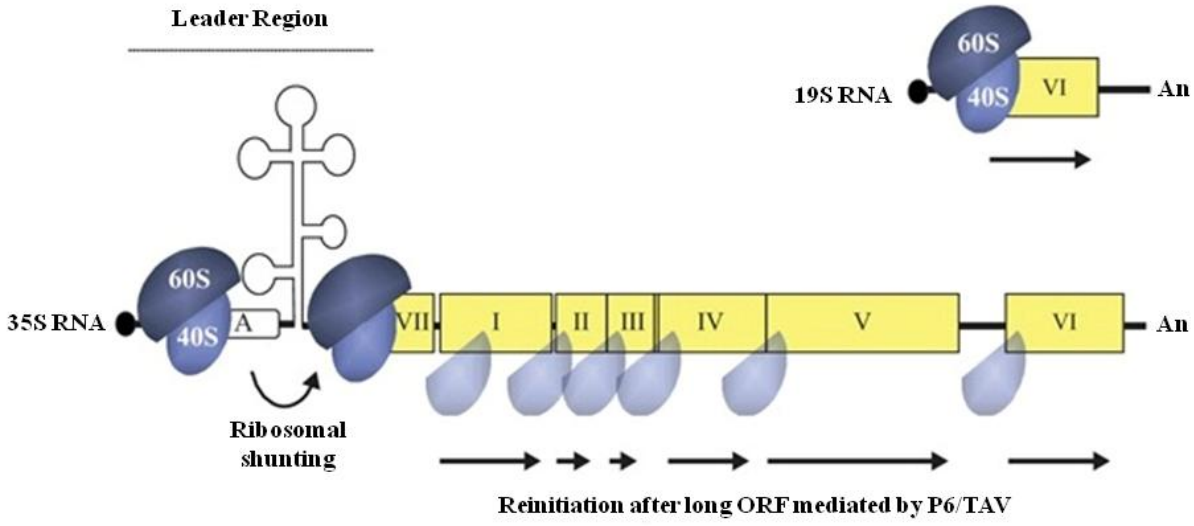

Figure 6.2-3 Schematic representation of the structural organization of the 35S and 19S RNA. Two non-canonical translation strategies used to express the 35S RNA, the shunt of the ribosome and the re-initiation of translation. Box A represents the sORF A (3 codons), the full translation of sORF A is required to allow the ribosomal shunting. The secondary structure of the leader region contains other sORF (not represented). *Modified from Bouton et al, (2015) Virologie 3,119-39*

Unlike the case of GCN4, TAV mediated reinitiation is independent on the distance between the two ORFs and occurs equally in a efficient way either directly after translation termination when the two ORFs are linked by an AUGA quadruplet or when the second ORF is located as far as 600 nucleotides further downstream (FUTTERER AND HOHN 1991).

The central region of TAV molecule is essential for transactivation, and can be divided into two parts: the N-terminal part (miniTAV) and the C-terminal—multiple protein binding domain (MBD). MiniTAV alone can maintain a minimal transactivation levels (20-25%) and it can interact with two 60S ribosomal proteins, the L18 and L13. MBD increases the level of transactivation by 70-75% (PARK *et al.* 2001). In addition, TAV interacts with eIF3 via its subunit g. MiniTAV can bind double stranded RNA due to its high similarity with the N-terminal eukaryotic RNase H1 domain (CERRITELLI *et al.* 1998). TAV was shown to be involved in the second and subsequent initiation events, but not the first translation initiation event (PARK *et al.* 2004).

In reinitiation, maintaining the initiation factors by 40S during short ORF elongation event would help 40S to resume scanning and acquire TC. TAV likely binds initiating ribosomes at the 60S joining step, when eIF4B that outcompetes TAV for eIF3g binding is released. Thus, formation of the TAV–eIF3 complex is formed via competition between TAV and eIF4B for eIF3 binding—the eIF4B and TAV binding sites on eIF3g overlap. Indeed, TAV-mediated transactivation is negatively affected in plant protoplasts upon eIF4B overexpression (PARK *et al.* 2004). The function of TAV in reinitiation after long ORF translation would be to promote eIF3 retention on translating ribosomes during the long elongation event to ensure rapid recruitment of TC after termination of first ORF translation.

c. Dissection of TAV functional domains

The process of translation reinitiation after long ORFs requires a critical step allowing the interaction between TOR and TAV which in turn maintains viral fitness. TOR is considered a host protein that is crucial for TAV function during CaMV cycle. Studies documented that TOR-deficient plant resist viral infections, since the interaction between TAV and TOR is essential to induce infectivity. Only functional TOR can promote TAV-mediated efficient reinitiation. TAV works by inducing the hyperactivation of TOR and the subsequent phosphorylation of S6K1. Upon TOR activation, it binds to polyribosomes in parallel with the accumulation of eIF3 and RISP in the polysome. This process depends on TAV and allows RISP to get highly phosphorylated at S267 which is a step essential for its function. In TAV mutants, TOR is not recruited to the polyribosome, RISP is not phosphorylated and thus reinitiation does not occur (SCHEPETILNIKOV *et al.* 2011). TOR is capable of binding TAV via the HEAT repeats. Sub-cloning the *Arabidopsis* TOR encoding gene and its 5' and 3' terminal fragments (NTOR encoding the entire HEAT repeat; CTOR encoding the sequence for the kinase domain) revealed that NTOR interacts with TAV through an RNA-binding motif (dsR, aa 136-182) within the minimal transactivation domain (MAV) (DE TAPIA *et al.* 1993). TAV dsR is necessary for binding with TOR, and the mutation of dsR domain abolishes the binding to TOR. TOR activation and phosphorylation of S6K1 at T449 and RISP at S267 upon TAV overexpression are eliminated by removal of the TOR binding site within MAV, or by the TOR-specific inhibitor Torin-1 (SCHEPETILNIKOV *et al.* 2011). The importance of eIF3 in 40S binding to mRNA and scanning is considered to be the entry point for its function in reinitiation. The interaction between the transactivator viroplasmin TAV of Cauliflower mosaic virus (CaMV) and eIF3 via its subunit g is essential for reinitiation to occur. In fact, eIF3 can bind the 80S ribosome when TAV is present, through attaching to the 60S subunit and thus allowing eIF3 to move along the ORF with the ribosome (PARK *et al.*

2001). In addition, CaMV reinitiation factor (TAV) was shown to also interact with RPL24A (paralog of RPL24B) to induce translation reinitiation of downstream ORFs of the CaMV 35S RNA, which is translated efficiently by TAV (PARK *et al.* 2001). The intercistronic space in ARF3 and ARF5 are 61 and 91 nucleotides respectively, which make them capable for efficient reinitiation as compared to the 60 nucleotides intercistronic space in the case of CaMV 35S RNA (FUTTERER *et al.* 1989).

d. TAV partners in reinitiation after long ORF translation - eIF3g, TOR, RISP, 40S and 60S ribosomal subunits

The process of reinitiation after long ORF translation operating on CaMV 35S pgRNA depends on TAV (RYABOVA *et al.* 2006; THIEBEAULD *et al.* 2009). The regulation of the reinitiation process in CaMV requires the interaction between TAV and the translation machinery of the host. In addition, TAV interacts with TOR to trigger TOR phosphorylation and activation of the TOR signaling pathway (SCHEPETILNIKOV *et al.* 2011). The TAV molecule can be dissected on several domains (Fig. 6.2-2). The main transactivation domain includes the minimal transactivation domain (MAV) that contains an RNA-binding motif (dsR, aa 136-182) (DE TAPIA *et al.* 1993), and the multiple protein binding domain (MBD) immediately downstream of MAV. Interesting that MAV domain expressed at high levels in plant protoplasts can promote the residual level of reinitiation after long ORF translation (DE TAPIA *et al.* 1993). Several mutations within MAV abolished transactivation of polycistronic translation. Both MAV and MBD domains interact with the host cell translation machinery. MAV binds TOR via the dsR domain and interacts with RISP via the C-terminus of MAV (THIEBEAULD *et al.* 2009). MBD is responsible for interaction with eIF3g and the 60S ribosomal protein RPL24—eIF3g outcompetes RPL24 for TAV binding (PARK *et al.* 2001). It was proposed that RISP is a cofactor of TAV—both proteins interact with eIF3 and RPL24.

Strikingly that RISP interact with RPL24 via the C-terminal half, while TAV interacts with its N-terminal domain; while the eIF3 subunit g associates with TAV (PARK *et al.* 2001), and subunits a and c—with RISP (THIEBEAULD *et al.* 2009). In TAV transgenic plants, high levels of TAV, eIF3 and RISP are found in polysomes. Data suggest that TAV maintains binding of RISP and eIF3 to polysomes during the long elongation event. As I said before TOR activated via TAV also bihds polysomes and maintains phosphorylation of RISP (SCHEPETILNIKOV *et al.* 2011). Mutant TAV which is defective in RISP binding cannot induce reinitiation in a transient manner or for viral amplification in plant protoplasts. Interestingly, when RISP is phosphorylated, it preferentially associates with TAV and RPL24, while its dephosphorylation favors eIF3g binding. Thus, TAV preferentially binds phosphorylated RISP to maintain and stabilize the complex at the level of the polyribosome. Accordingly, RISP stimulates TAV-mediated reinitiation only in its phosphorylated state (SCHEPETILNIKOV *et al.* 2011). Earlier studies suggest that eIF3 binds the exposed site of the 40S subunit during translation initiation, and this interaction stays for several cycles during the elongation step (KOZAK 2001). So, TAV can stabilize this binding during long elongation.

6.3 Model of TAV function in reinitiation after long ORF translation

The recent model of the mechanism of reinitiation after long ORF translation is based on several publications (PARK *et al.* 2001, THIEBEAULD *et al.* 2009, SCHEPETILNIKOV *et al.* 2011; 2013) is following. TAV mediates activation of TOR in TAV transgenic plants. Similar to mammals, TOR can use eIF3-PIC as a platform for phosphorylation of S6K1. S6K1 further activated by PDK1, phosphorylates RISP. TAV enters polysomes soon after the 60S joining step stabilizing weakly polysome-associated eIF3 and phosphorylated RISP, prevents their dissociation from actively translating ribosomes. During elongation, TAV-eIF3-RISP complex can be translocated from the 40S subunit to the 60S subunit upon TAV binding L18.

During termination of the first ORF, the eIF3-TAV-RISP-P complex is shifted back to the reinitiating 40S subunit (Figure 6.3-1) (SCHEPETILNIKOV *et al.* 2011).

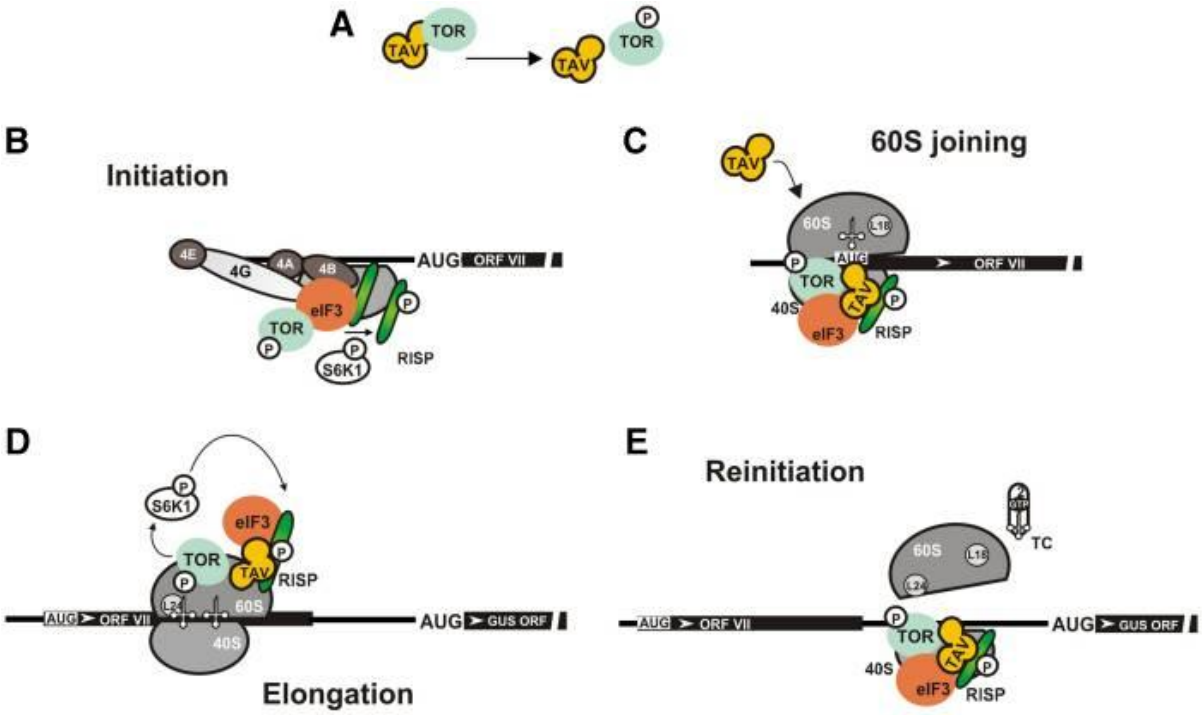

Figure 6.3-1 Provisional model of TAV/TOR function in reinitiation after translation of a long ORF

(A) TAV maintains TOR in a constitutively activated state. (B) Activated TOR binds eIF3-PIC to trigger S6K1 and RISP phosphorylation. (C) TAV joins 40S-associated eIF3 during the 60S-joining step via interactions with eIF3 and RISP-P. (D) TAV retains eIF3/RISP on the elongating ribosome, likely by transferring to the rear side of 60S. Activated TOR with or without TAV binds polysomes and maintains the phosphorylation state of RISP. (E) TAV/eIF3/RISP-P is relocated back to 40S via eIF3/40S interaction to form a reinitiation-competent 40S capable of resuming scanning and 60S/TC recruitment. *Modified from Schepetilnikov et al, (2011) EMBO J 7,1343-56*

The main aim of my PhD project was to understand the role of eIF3h in plant and CaMV virus- promoted translation reinitiation events. To understand eIF3h function in reinitiation, I investigated the role of C- and N domains of eIF3h in reinitiation after short ORF translation and, tested whether eIF3h is required for TAV-activated polycistronic translation and for viral pathogenesis.

II. RESULTS

2.1 Article 1: eIF3 subunit h is required for viral reinitiation factor TAV to promote reinitiation after long ORF translation

Joelle Makarian, Ola Srour, Eder Mancera-Martinez1, Mikhail Schepetilnikov and Lyubov A. Ryabova*

Institut de Biologie Moléculaire des Plantes du CNRS, Université de Strasbourg, 67084 Strasbourg Cedex, France

eIF3 subunit h is required for viral reinitiation factor TAV to promote reinitiation after long ORF translation

Joelle Makarian, Ola Srour, Eder Mancera-Martinez1, Mikhail Schepetilnikov and Lyubov A. Ryabova*

Institut de Biologie Moléculaire des Plantes du CNRS, Université de Strasbourg, 67084 Strasbourg Cedex, France

*To whom correspondence should be addressed:
lyuba.ryabova@ibmp-cnrs.unistra.fr

[1]Present address:
CNRS, Institut de Biologie Moléculaire et Cellulaire, Architecture et Réactivité de l'ARN UPR9002, Université de Strasbourg, 67084 Strasbourg, France

2.1.1 Abstract

Translation of mRNAs that harbor upstream open reading frames (uORFs) within their leader regions operates via a reinitiation mechanism. In plants, reinitiation is up regulated by the target of rapamycin (TOR) signaling via phosphorylation of the subunit h of initiation factor 3 (eIF3). The *eif3h-1* mutant expressing the C-terminally truncated eIF3h while maintaining high translation initiation efficiency is not active in reinitiation. *Cauliflower mosaic virus* (CaMV) pregenomic polycistronic RNA is translated via an exceptional mechanism of reinitiation after long ORF translation under control of CaMV protein TAV, which ensures activation of TOR. To find the link between underlying mechanisms, we examined eIF3h function in cellular and viral context.

Here we show that eIF3h, if phosphorylated, has a role in recruitment of eIF3 into actively translating ribosomes that is a prerequisite for formation of reinitiation-competent ribosomal complexes. C-terminal truncation of eIF3h abolished its integration into the eIF3 complex and eIF3 loading on polysomes as manifested by the eIF3 core subunit c. We also show that eIF3h as a putative target of TOR/S6K1 binds S6K1 *in vitro*. eIF3h phosphorylation is not required for eIF3 complex formation. We demonstrated that eIF3h is essential for TAV to activate reinitiation after long ORF translation. Protoplasts derived from *eif3h-1* mutant failed to support TAV function in reinitiation, which is restored only upon overexpression of recombinant eIF3h indifferent to its phosphorylation status. *eif3h-1* mutant defective in reinitiation was found resistant to CaMV infection suggesting that eIF3h is critical for virus amplification. In contrast, viruses that evolve translation initiation dependent on either cap or the internal ribosome entry site infect reinitiation deficient mutant. Thus, we conclude that TAV exploits the basic cell reinitiation machinery, particularly TOR and eIF3h, to overcome cellular barriers to reinitiation after long ORF translation.

2.1.2 Introduction

Cap-dependent translation initiation requires multiple translation initiation factors (eIFs). A ternary complex (TC, eIF2/GTP/Met-tRNAi^{Met}), together with eIF3, eIF1, eIF1A, binds the 40S ribosomal subunit (40S) to form a 43S preinitiation complex (43S PIC) (BENNE AND HERSHEY 1978). After loading on the mRNA cap-structure, which is facilitated by the heterotrimeric eIF4F complex, the 43S PIC scans along the mRNA until the 48S PIC forms at an AUG start codon in optimal initiation context (KOZAK 1999; PISAREV *et al.* 2007). After 60S joining, translation elongation begins. eIF3 is a critical factor required at all steps of translation initiation, playing a critical role in TC recruitment to 40S, binding of the 43S PIC to the mRNA, and recognition of the start codon (HINNEBUSCH 2006). In higher eukaryotes, including plants, eIF3 is an 700-800 kDa multisubunit complex made of 13 different subunits (eIF3a–eIF3m) (DES GEORGES *et al.* 2015; SMITH *et al.* 2016)five subunits—eIF3a, eIF3b, eIF3c, eIF3g and eIF3i—forming the core of eIF3 in all eukaryotes (HINNEBUSCH 2006). Recently, eIF3 subunit h was implicated in assembly of subunits e, d, k and l into the functional eIF3 complex (SMITH *et al.* 2016). eIF3 is involved in intensive interaction networks with other eIFs (see (VALASEK 2012)). Thus, translation initiation at the 5'-end of mRNA is regulated at multiple levels.

Initiation further downstream after termination of translation of an ORF, so-called reinitiation of translation, is limited in eukaryotes but can occur if the preceding translated ORF is short [sORF, less than ~30 codons; (MORRIS AND GEBALLE 2000; VON ARNIM *et al.* 2014)]. Reinitiation efficiency is modulated by many parameters such as the distance between ORFs, protein factors, and RNA *cis*-elements (VON ARNIM *et al.* 2014). Upstream ORFs (uORFs) are common in mammals and plants, being present in at least 30%–45% of full-length mRNAs (CALVO *et al.* 2009; ZHOU *et al.* 2010), many of which are translated (INGOLIA *et al.* 2009). Accumulating data suggest that uORFs play an important role in down-regulation of translation their associated mRNA in mammals (SOMERS *et al.* 2013) and plants (TRAN AND PLAXTON 2008). Several canonical translation initiation factors, such eIF4F, eIF4A and elongation factor 2 (eEF2), have been suggested to promote reinitiation after uORF translation in mammals and yeast (POYRY *et al.* 2004; SKABKIN *et al.* 2013). eIF3 participates in promoting reinitiation after translation of a short ORF (HINNEBUSCH 2006), and after long ORF translation in some rare cases in plant (PARK *et al.* 2001) and mammalian (POYRY *et al.* 2007) viruses. In plants, the 60S ribosomal protein L24B (NISHIMURA *et al.* 2005; ZHOU *et al.* 2010) and eIF3 subunit h (KIM *et al.* 2004) promote translation reinitiation on uORF-containing mRNAs, as exemplified by mRNAs coding for the *Arabidopsis*

transcriptional factors bZIP11, ARF3 and ARF5. *eif3h-1* and *rpl24b* (*short valve 1*, *stv1*) *Arabidopsis* mutants exhibit developmental defects in part similar to those revealed in plants that undertranslate mRNAs for transcription factors bZIP11 and the auxin-response factors [ARFs, (NISHIMURA *et al.* 2005; ZHOU *et al.* 2010)]. Thus, although the functions of eIF3h and eL24 in reinitiation remain to be identified, they likely differ (TIRUNEH *et al.* 2013).

Target-of-rapamycin (TOR) protein kinase—the key component of a nutrient- and hormone-dependent signalling pathway controlling cell growth—has been revealed as a main controller of protein synthesis in mammals. TOR positively regulates cap-dependent translation initiation via mTOR complex 1 (mTORC1) via phosphorylation of its two major targets, i.e., the 4E-BPs that regulate cap-dependent translation-initiation (GINGRAS *et al.* 1999) and S6Ks [40S ribosomal protein S6 kinases; (MA AND BLENIS 2009)]. In mammals, eIF3 serves as a binding platform for S6K1 phosphorylation by mTOR (HOLZ *et al.* 2005).

In plants, TOR encoded by a single *TOR* gene (MENAND *et al.* 2002; MAHFOUZ *et al.* 2006) was implicated in phosphorylation of S6K1 at T449 (SCHEPETILNIKOV *et al.* 2011; XIONG AND SHEEN 2012). TOR is activated in response to glucose (XIONG *et al.* 2013), the plant hormone auxin (SCHEPETILNIKOV *et al.* 2013), and the pathogenicity factor, Cauliflower mosaic virus (CaMV) protein TAV (SCHEPETILNIKOV *et al.* 2011). *Arabidopsis* TOR inactivation triggers a significant reduction in active ribosome levels [polysomes; (DEPROST *et al.* 2007)], suggesting a role for TOR in plant protein synthesis control. Accordingly, *Arabidopsis* TOR is required for translation of uORF-containing mRNAs (SCHEPETILNIKOV *et al.* 2013).

eIF3h is an intrinsic protein required for reinitiation events by promoting reinitiation competence of the translating ribosome, while being dispensable for initiation at the 5'-end of the mRNA (KIM *et al.* 2004; ROY *et al.* 2010). eIF3h can be phosphorylated at S178 in a TOR-responsive manner (SCHEPETILNIKOV *et al.* 2013). To promote reinitiation events, active TOR binds preinitiation complexes and polyribosomes to maintain the phosphorylation status of eIF3h (SCHEPETILNIKOV *et al.* 2013). Phosphorylation of eIF3h up-regulates its function in translation of uORF-containing mRNAs.

An unusual case of reinitiation after long ORF translation is found in *Cauliflower mosaic virus* (CaMV), which depends on a CaMV reinitiation factor—transactivator/viroplasmin (TAV) and several cellular proteins, including eIF3 and reinitiation supporting protein RISP (BONNEVILLE *et al.* 1989; RYABOVA *et al.* 2006). TAV functions on both the viral polycistronic 35S pregenomic RNA and artificial bicistronic RNAs together with RISP via interaction with the host translation machinery—TAV and RISP interact with eIF3 and 60S ribosomal protein L24 (PARK *et al.* 2001). Moreover, TAV

binds and promotes TOR activation (SCHEPETILNIKOV *et al.* 2011). All these factors are found in polysomes in TAV-expressing or CaMV-infected cells. We previously proposed that TAV enters the host translational machinery at the 60S-joining step via interaction with 40S-bound eIF3, and prevents dissociation of eIF3/RISP from the translating ribosomes during the long elongation event, positioning eIF3/RISP for reinitiation at the downstream ORF (THIEBEAULD *et al.* 2009).

Here, we studied the role of the N- and C-terminal domains of eIF3h in its integration into the eIF3 complex and binding to polyribosomes. Strikingly, eIF3h is critically important for TAV-activated reinitiation after long ORF translation, suggesting that it is a basic translation reinitiation factor. Interestingly *eif3h-1* mutant plants are resistant to CaMV infection.

2.1.3 Results

Integration of eIF3h into the eIF3 complex depends on its C-terminal domain

A mutant allele of *eif3h-1* carrying a T-DNA insertion that truncates the eIF3h protein at the C-terminus displays defects in translation reinitiation of mRNA that harbors uORFs within their 5'-UTRs (KIM *et al.* 2004; ZHOU *et al.* 2010; SCHEPETILNIKOV *et al.* 2013). To understand the mechanism of eIF3h function in reinitiation events *in planta*, we first attempted to dissect the eIF3h protein sequence to determine the domain(s) required for eIF3h function in eIF3 assembly and reinitiation. Based on two published C-terminally truncated mutants [*eif3h-1* and *eif3h-2*; (KIM *et al.* 2004)], we employed a series of eIF3h deletion mutants—eIF3hΔC1 and eIF3hΔC2 lacking 83 or 19 amino acids (aa) at the C-terminus, respectively, and eIF3hΔN1 and eIF3hΔN2 lacking 40 or 20 N-terminal aa, respectively (Fig. 1A). The central eIF3h MOV34/MPN (Mpr1-Pad1-N-terminus) domain is shared by eIF3f and MPN proteases (LINGARAJU *et al.* 2014), indicating that MPN is not responsible for a specific function of eIF3h in reinitiation. Indeed, within the COP9 signalosome, the eIF3h MPN domain participates in structural stabilization, and both proteins function as a heterodimer (LINGARAJU *et al.* 2014). Thus, we first analyzed whether *Arabidopsis* eIF3h deletion mutants can interact with eIF3f in the yeast two-hybrid system. The results (Fig. 1B) show that both proteins indeed interact, and that their interaction was not affected by deletion of either the N-terminal 20 aa (AD-eIF3hΔN2) or 40 aa (AD-eIF3hΔN1) residues, whereas a larger C-terminal fragment deletion (AD-eIF3hΔC1) abolished interaction with eIF3f (BD-eIF3f). The eIF3h and eIF3f interaction was confirmed by the GST pull-down assay (Fig. 1C). Because *in planta* pull-down analysis using anti eIF3h antibodies revealed accumulation and immunoprecipitation of both full length and truncated eIF3h from WT and *eif3h-1* plants (Fig. 1D), we used an IP assay to analyze whether both WT or C-terminally truncated eIF3h associate with the core eIF3 subunit c (Fig. 1E *Upper panel*). As expected, eIF3h co-immunoprecipitated with eIF3c, while the ΔC1-deletion variant was missing from the eIF3c-containing complex. Surprisingly, antibodies against eIF3h failed to pull-down the eIF3c subunit in WT and the *eif3h-1* mutant. According to the mammalian 43S PIC cryo-EM structure (DES GEORGES *et al.* 2015) the core eIF3c, eIF3h and eIF3f subunits (these subunits taken from the 43S PIC model are presented in Fig. 1F) interact via their α-helical domains within so called the eIF3 helical bundle, and deletion of eIF3h C1 could indeed abolish eIF3h association with eIF3. However, the inability of anti

eIF3h antibodies to pull down eIF3c from WT plants might suggest that either eIF3h is not accessible for antibody recognition or it represents a eIF3 subunit claster within eIF3.

Considering the role of TOR-responsive eIF3h phosphorylation at S178 in reinitiation of translation (SCHEPETILNIKOV *et al.* 2013), we next asked whether eIF3h phosphorylation is required for eIF3 complex assembly. We used the phytohormone auxin as an upstream TOR effector, and the inhibitor Torin-1 (THOREEN *et al.* 2009) to inhibit TOR activation. Thus, 7 days after germination (dag) seedlings were treated with the auxin analogue 1-naphthylacetic acid (NAA) or Torin-1 for 8 hours. Figure 1E (*Central panel*) shows coimmunoprecipitation of endogenous eIF3c with endogenous eIF3h under both auxin- and Torin-1-treated conditions. eIF3h phosphorylation was visualized by phospho-specific anti-(R/KxR/KxxS/T-P) antibodies. Note that eIF3h was phosphorylated in response to NAA, while its phosphorylation was below the limit of detection of our antibodies upon Torin-1 treatment. IP analysis of *eif3h-1* confirmed that deletion of the C1 fragment abolished its association with eIF3c-containing complexes, but not eIF3hΔC1 phosphorylation in response to auxin (Fig. 1E *Bottom panel*). Therefore, eIF3h integration into eIF3 requires its C-terminus, but is not sensitive to eIF3h phosphorylation.

We asked whether S6K1, which was implicated in phosphorylation of eIF3h at S178 (SCHEPETILNIKOV *et al.* 2013), binds eIF3h. Yeast two-hybrid system and GST pull-down results both revealed S6K1 association with eIF3h (Fig. 2A, B). Despite deletion of the C2 fragment, eIF3hΔC2 binds S6K1; furthermore, the ΔN2 deletion improved binding. The bigger deletions (ΔN1 and ΔC1) somewhat reduced, but did not abolish, eIF3h interaction with S6K1. Surprisingly, the yeast two-hybrid system detected interactions between eIF3h and the N-terminal half of TOR, which harbors HEAT repeat domains. This interaction was insensitive to both eIF3h C- and N-terminal domain truncations (Fig. 2C). We explained this result by supposing that eIF3h bound to the HEAT repeat domain of TOR might be positioned more favorably for phosphorylation by S6K1.

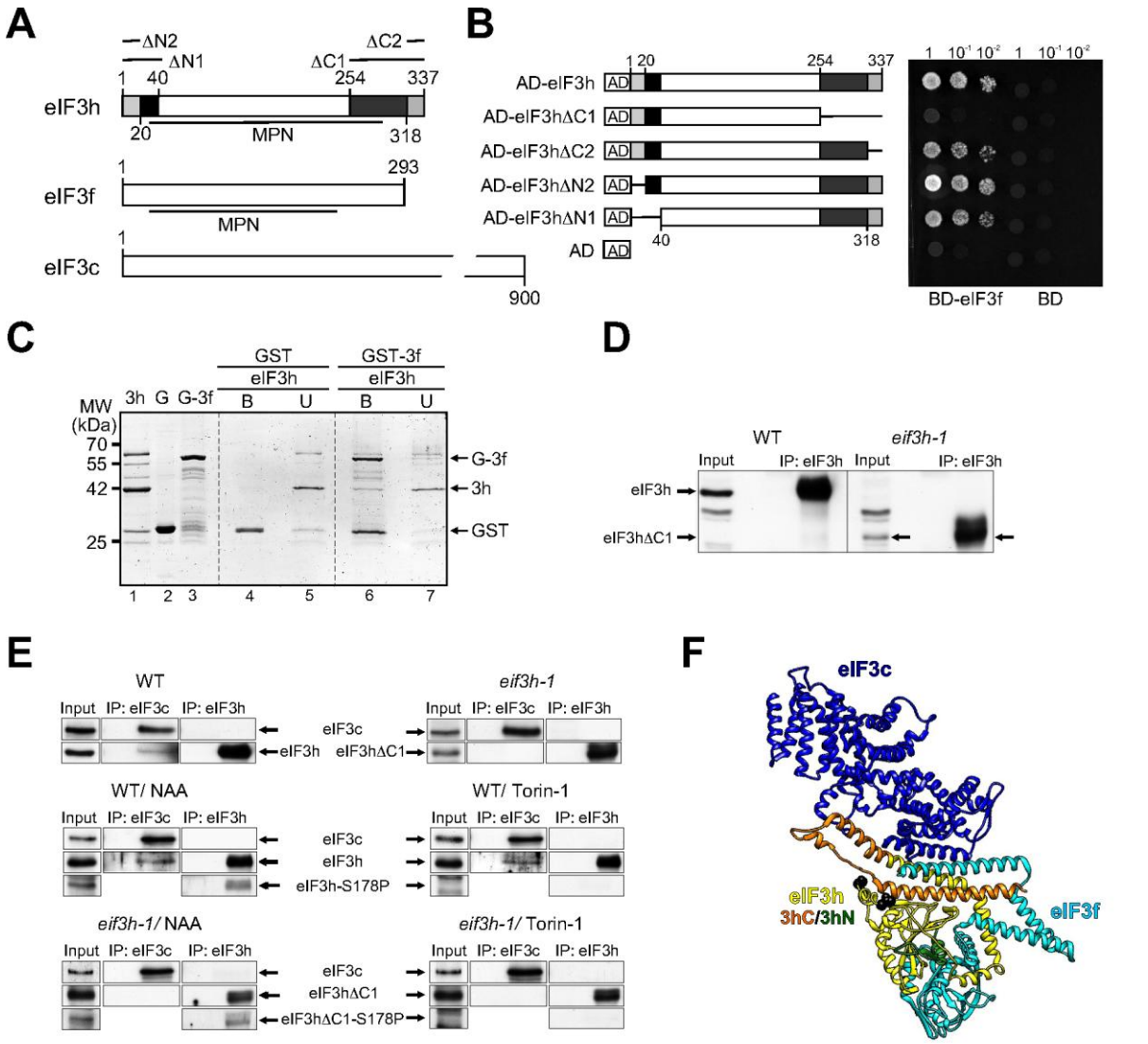

Figure 1. Characterization of eIF3h phosphorylation and interaction network

(A) Schematic representation of eIF3f, eIF3c, eIF3h and its domains—MPN, N1, N2 and C1, C2.

(B) *Left* Schematic representation of *Arabidopsis* eIF3h and its mutants fused to the Gal4 activation domain (AD). Yeast two-hybrid interactions between Gal4 binding domain (BD)—BD-eIF3f and AD-eIF3h and its deletion variants are presented. Equal OD_{600} units and 1/10 and 1/100 dilutions were spotted from left to right, and incubated for 2 days.

(C) GST pull-down assay—eIF3f-tagged GST, and GST alone, were assayed for interaction with recombinant eIF3h as indicated on the left panel. GST-fusion protein bound (B) and unbound (U) fractions were stained by Coomassie blue.

(D) Immunoprecipitation (IP) experiments with anti-eIF3h antibodies on crude extracts of WT and *eif3h-1* transgenic plants; for western blots, 10% of the input and 100% of IP fractions were analyzed with anti-eIF3h polyclonal antibodies (ABs).

(E) IP experiments with anti-eIF3c and anti-eIF3h antibodies on crude extracts of WT and *eif3h-1* transgenic plants treated with either NAA or Torin-1. For western blots, 10% of the input and 100% of IP fractions were analyzed with anti-eIF3h, -eIF3c, and phospho-specific anti-(R/KxR/KxxS/T-P) polyclonal antibodies (ABs).

(F) Contacts between three eIF3 subunits—c, f and h. Their complex is taken from the 43S PIC model showing solvent-side view of eIF3 bound to the DHX29-bound 43S complex (des Georges et al., 2015). eIF3c, eIF3f are presented in dark and light blue, respectively. eIF3h C1 domain is shown in orange, central—in yellow and N-terminus—in green (the eIF3h N-terminal 30 amino acids are not resolved).

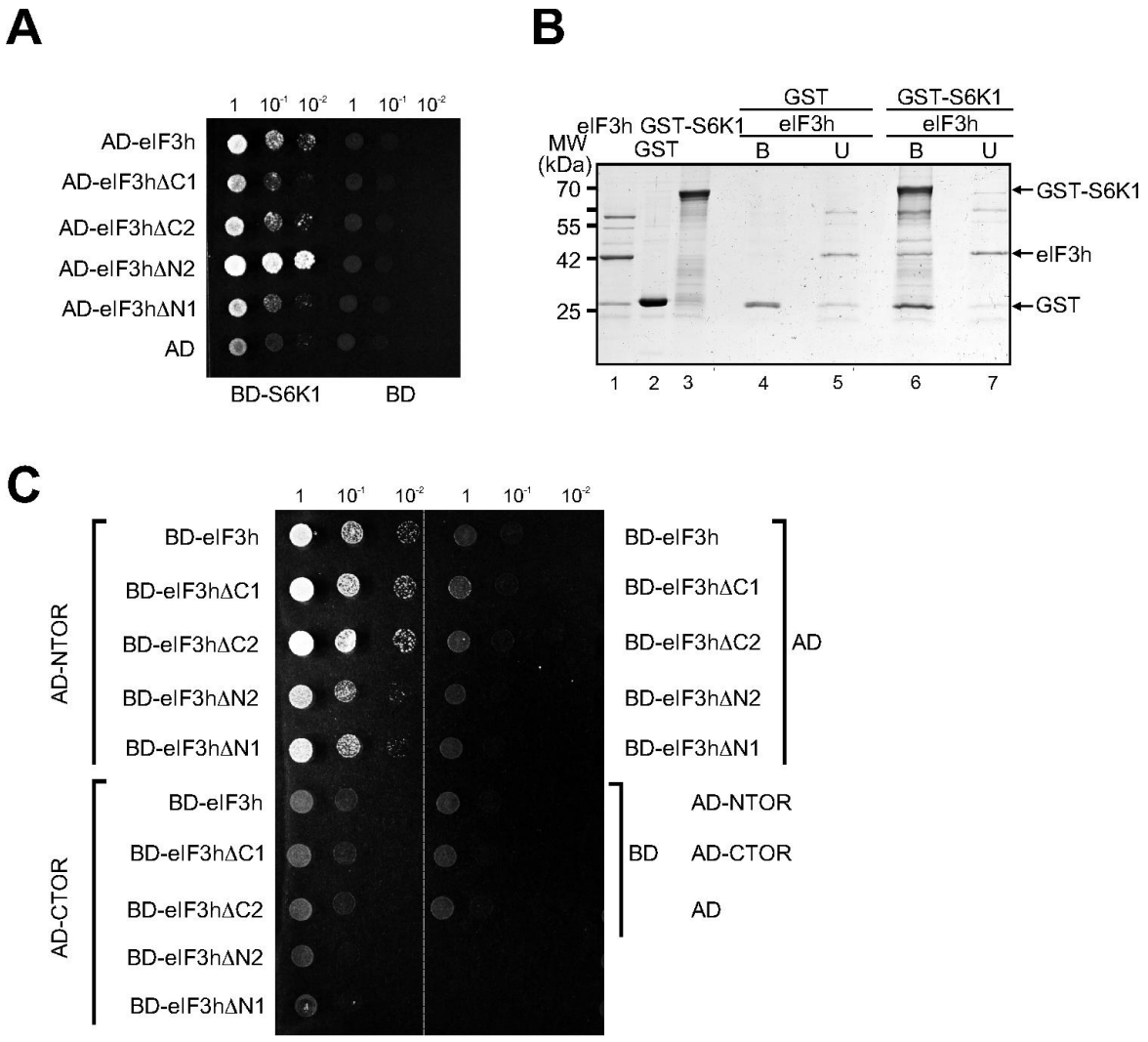

Figure 2. eIF3h interacts with S6K1 and the HEAT repeat domain of TOR
(A) Yeast two-hybrid interactions between BD-S6K1 and BD with AD-eIF3h and its deletion variants. Equal OD_{600} units and 1/10 and 1/100 dilutions were spotted from left to right and incubated for 2 days. (B) GST pull-down assay—S6K1-tagged GST, and GST alone were assayed for interaction with recombinant eIF3h as indicated on the left panel. GST-fusion protein bound (B) and unbound (U) fractions were stained by Coomassie blue. (C) Yeast two-hybrid interactions between AD, AD-NTOR, AD-CTOR and BD, BD-eIF3h and its deletion variants.

eIF3h promotes eIF3c binding to polysomes in response to TOR activation

Strikingly, the *eif3h-1* mutant that harbors an incomplete eIF3 (lacking eIF3h) exhibits strong defects in reinitiation, but not in initiation of translation *per se* (KIM *et al.* 2004). Thus, we tested eIF3 association with polysomes, using antibodies against the core eIF3 subunit, eIF3c. According to our previous findings, both eIF3 and TOR, when phosphorylated, accumulate in polysomes isolated from TAV transgenic plants or plants treated by auxin (SCHEPETILNIKOV *et al.* 2011; SCHEPETILNIKOV *et al.* 2013) respectively. We tested both eIF3 and TOR in polysome gradient fractions in extracts obtained from *Arabidopsis* 7 dag WT or *eif3h-1* mutant seedlings treated with NAA or Torin-1 for 8 hours (Fig. 3). Total levels of eIF3h and TOR, and their phosphorylation status, were measured by western blot. The levels of TOR phosphorylated at S2424 were monitored using anti-(mTOR-S2448-P) antibodies [the mTOR S2448 epitope can be aligned with the S2424 epitope in *Arabidopsis* TOR (SCHEPETILNIKOV *et al.* 2013)].

As expected, for WT plants, auxin triggered TOR phosphorylation after 8 h of NAA application, as well as association with polysomes, while Torin-1 caused TOR dephosphorylation and dissociation from polysomes. Accordingly, in response to NAA, eIF3, as manifested by both subunits c and h phosphorylated at S178, co-migrates with 80S monosomes, 40S/ 60S ribosomal subunits, and polysomes (Fig. 3A *Left panel*), while Torin-1 greatly impaired eIF3 complex formation with polysomes (Fig. 3A *Right panel*). We noted that phosphorylated TOR could be detected in 40S fractions following Torin-1 treatment—most likely due to incomplete TOR inactivation by Torin-1, which may explain why Torin-1 had no major effect on the first initiation event (SCHEPETILNIKOV *et al.* 2013), suggesting that active TOR binds primarily to 43S or 48S preinitiation complexes during translation initiation.

A drastic contrast in loading of eIF3 into polysomes was observed in *eif3h-1* mutant-derived polysomes (Fig. 3B). Although TOR was phosphorylated and found in polysomes under auxin-stimulated conditions in the *eif3h-1* mutant, eIF3c association with polysomes was abolished. Here, it was impossible to detect the C-terminally truncated eIF3h (eIF3hΔC1) within the gradient (data not shown). Torin-1 induced dephosphorylation of TOR and its dissociation from polysomes. As expected, full-length eIF3h or eIF3h-P signals were not detected in *eif3h-1*-derived polysomes, suggesting specific eIF3h association with polysomes (Fig. 3B). Thus, a defect in loading of eIF3 as manifested by its core subunit c might be the main reason why the *eif3h-1* mutant cannot promote efficient reinitiation events.

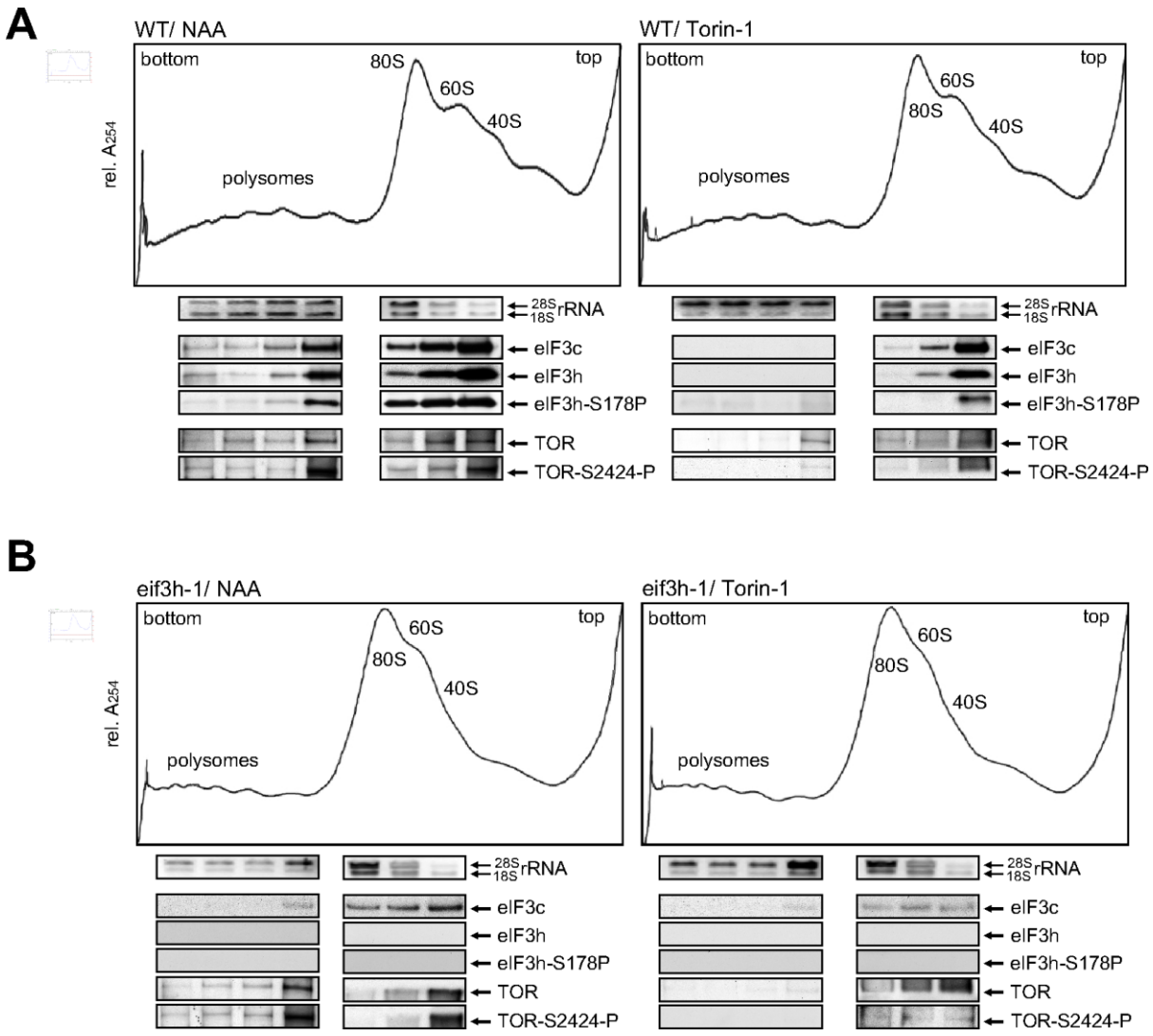

Figure 3. Characterization of eIF3c loading on polysomes in WT and *eif3h-1* plants
(A, B) *Upper panels* Ribosomal profiles of polyribosomes (polysomes) and ribosomal species from wild type WT (A) and *eif3h-1* treated with NAA or Torin-1 (B). *Bottom panels* 1 ml aliquot fractions were precipitated with 10% TCA, and analyzed by western blot using corresponding antibodies (*Lower panels*); or analyzed by agarose gel electrophoresis (*Upper panels*). Positions of 18S and 28S rRNAs are indicated. A minimum of three replicate experiments were performed for all sucrose gradients presented; all repeats gave reproducible results.

eIF3h is required for TAV to promote virus-activated reinitiation of translation

To activate reinitiation after long ORF translation, TAV binds and activates TOR, and, in addition, promotes accumulation of eIF3-containing complexes in polysomes (SCHEPETILNIKOV *et al.* 2011). Indeed, TAV transgenic plants are characterized by increased loading of eIF3 into polysomes. Knowing that eIF3h is critical in cellular cases of reinitiation after uORF translation, we tested whether TAV can overcome the requirement of eIF3h in reinitiation after long ORF translation in *Arabidopsis* mesophyll protoplasts prepared from *eif3h-1* compared with protoplasts from WT plants.

We next tested TAV transactivation capacity using transient expression of mono- and bi-cistronic reporter constructs—pmonoGFP contains a single GFP ORF, while pbiGUS contains two consecutive ORFs: CaMV ORF VII and β-glucuronidase [GUS; Fig. 4A; (BONNEVILLE *et al.* 1989)]—in protoplasts prepared from *eif3h-1* and WT plants (Fig. 4A). In WT protoplasts, translation of the GUS ORF was precluded by upstream long ORF VII and activated only upon TAV overexpression (Fig. 4A). Interestingly, eIF3h overexpression led to improved TAV-transactivation levels in WT. Strikingly, the eIF3hΔC1-containing mutant failed to activate GUS ORF translation, despite high levels of TAV overexpression. In contrast, together with TAV, overexpression of eIF3h boosted GUS ORF translation. *biGUS* RNA transcript length and levels monitored semi-quantitative RT-PCR were found non-affected (data not shown). These data strongly indicate that eIF3h is required for reinitiation after short ORF, and TAV-mediated long ORF, translation.

This finding opens an avenue to study the effect of eIF3h deletion mutants on the transactivation function of TAV. However, only entire eIF3h, but not its C- or N-terminal deletion mutants could support reinitiation in *eif3h-1* plants (Fig. 4B), highlighting the critical importance of eIF3h integration into eIF3. Although phosphorylation of eIF3h is critical for reinitiation after uORF translation, it seems not required for TAV to activate reinitiation after long ORF translation (Fig. 4C). Therefore, we conclude that eIF3h is an essential partner of TAV in activation of reinitiation after long ORF translation.

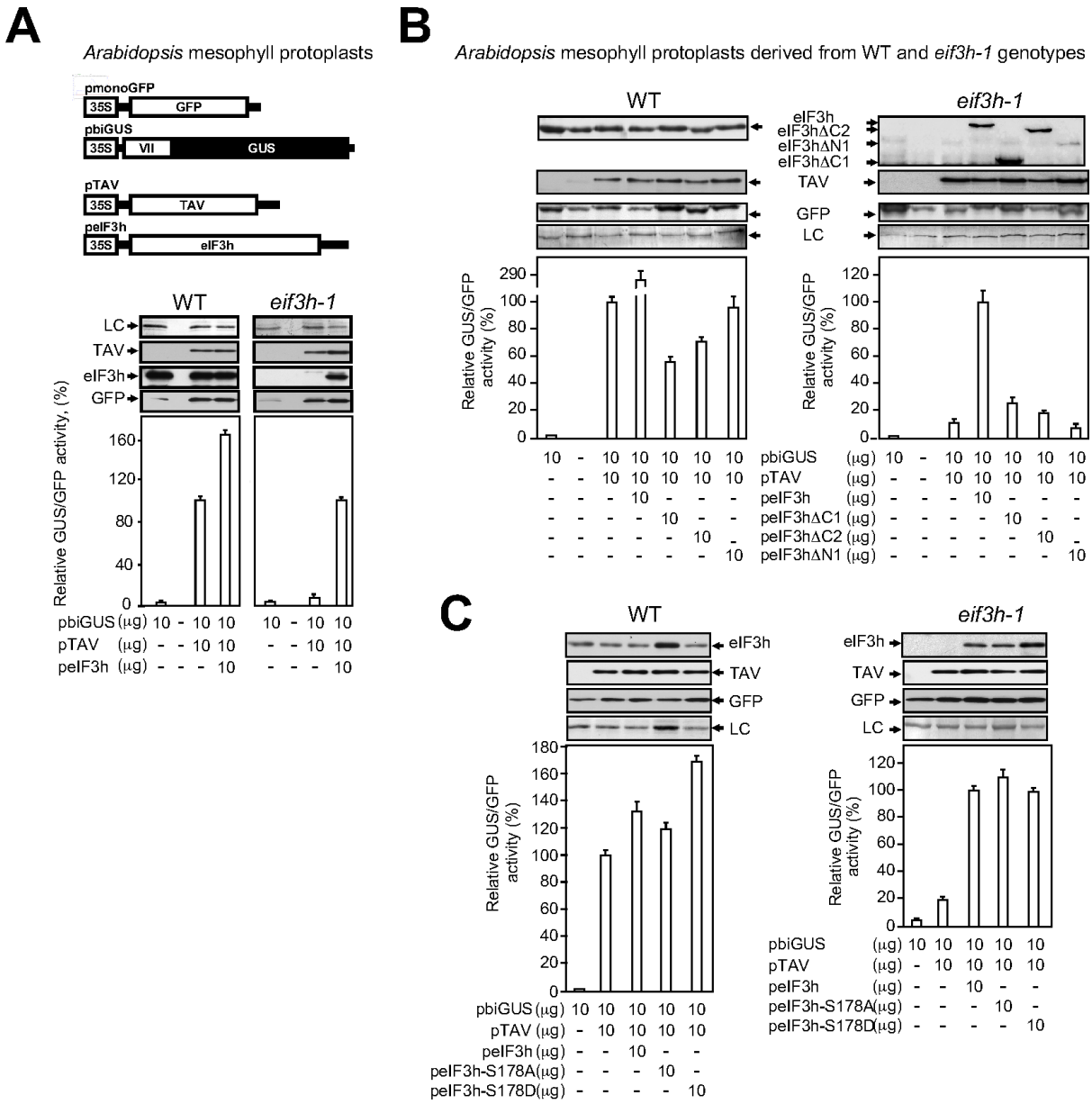

Figure 4. TAV-mediated transactivation is efficient in mesophyll protoplasts prepared from WT but abolished in *eif3h-1* mutant plants

Activity of GUS synthesized in protoplasts transfected with pTAV was set as 100% (110,000 RFU). GUS and GFP activities are shown as black and open bars, respectively. TAV, eIF3h and GFP expression levels were analyzed by immunoblot. *biGUS* mRNA levels were analyzed by qPCR (Data not shown). The data shown are the means of three independent assays: error bars indicate SD.

eIF3h is a host factor critically required for CaMV amplification

We wondered whether CaMV infection of the *eif3h-1* mutant would still trigger eIF3 loading on polysomes. Thus, we infected 36 *Arabidopsis* plants and the same number of *eif3h-1* plants with a CaMV infectious clone by agroinfiltration in two independent experiments. Although appearance of vein-clearing symptoms indicative of systemic infection at 10 dpi was obvious for WT plants, *eif3h-1* plants displayed no symptoms at either 10 dpi or 23 dpi (Fig. 5A). In total, almost 100% of WT plants displayed typical CaMV symptoms, whereas no *eif3h-1* plants expressed CaMV symptoms. Analysis of virus replication kinetics (Fig. 5B) revealed no accumulation of TAV, coat protein precursor or its processed variants in *eif3h-1* plants, in contrast to WT plants, which expressed both viral proteins.

Since the *eif3h-1* mutant is deficient only in reinitiation of translation, while cap-dependent initiation of translation is well supported, we tested whether *eif3h-1* plants would be susceptible to infection with viruses exploiting different translation mechanisms. Oilseed Rape Mosaic Virus (ORMV) likely uses a translation initiation strategy common to Tobamoviruses, i.e., the translation mechanism is similar to that of cap- and polyA-containing mRNAs, where the ORMV 3'-UTR functionally substitutes for a polyA-tail (GALLIE AND KOBAYASHI 1994). To test whether *eif3h-1* plants are susceptible to ORMV, 36 WT and 36 *eif3h-1* plants were mechanically inoculated with ORMV particles; we noted symptom development at 10 dpi for both genotypes (Figs 5C), and accumulation of RNA-dependent RNA polymerase (RdRp) was evident for WT and *eif3h-1* plants (Fig. 5D), strongly suggesting that eIF3h truncation did not significantly down-regulate ORMV replication. These results strongly suggest that eIF3h is dispensable for viral cap-dependent initiation of translation.

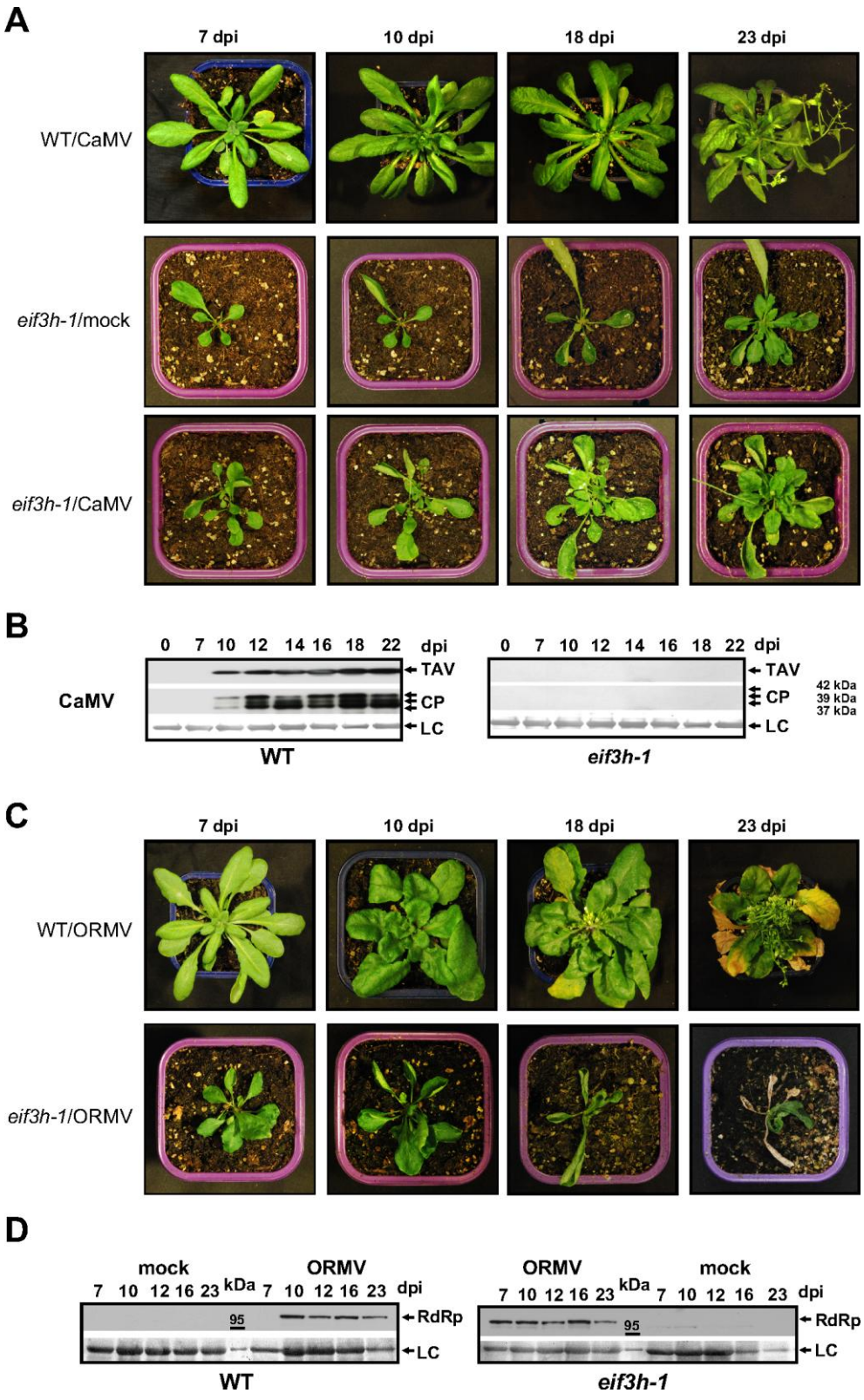

Figure 5. *eif3h-1* plants are resistant to CaMV
(A) Analysis of *eif3h-1* mutant plants (*central panels*) and CaMV disease symptoms in wild type (WT; *upper panels*) and *eif3h-1* (*bottom panels*). (B) TAV and CP proteins accumulate in CaMV-infected WT (*left panel*), but not in *eif3h-1* plants (*right panel*). (C) Analysis of *Oilseed Rape Mosaic Virus* (ORMV) disease symptoms in WT (*upper panels*) and the *eif3h-1* (*bottom panels*). (D) RNA-dependent RNA polymerase (RdRp) accumulate in ORMV-infected WT (*left panel*), and in *eif3h-1* plants (*right panel*).

Turnip mosaic virus (TuMV) is a Potyvirus of the family Potyviridae. These viruses have a VPg in place of the cap structure at the 5'-end of mRNA. Lacking a cap, TuMV initiates translation of a genomic RNA via an internal ribosome entry site (IRES) that recruits 43S PIC via VPg-bound eIF4G (BASSO *et al.* 1994; MIYOSHI *et al.* 2006). To test whether internal initiation requires eIF3h, WT and *eif3h-1* plants were agroinfiltrated with infectious TuMV clone carrying a GFP ORF placed between ORF1 and ORF2 (GARCIA-RUIZ *et al.* 2015). All plants tested were fully susceptible to TuMV, with TuMV symptoms, GFP fluorescence and accumulation detected at 10 dpi for WT and mutant plants (Fig. 6). Thus, eIF3h is likely dispensable for the internal initiation strategy of Potyviridae. We concluded that *eif3h-1* resistance to CaMV is specific to the translation reinitiation mechanism, and likely developed due to either defects in eIF3h or incomplete eIF3, which limits TAV-activated reinitiation, and thus CaMV replication, in *Arabidopsis* plants.

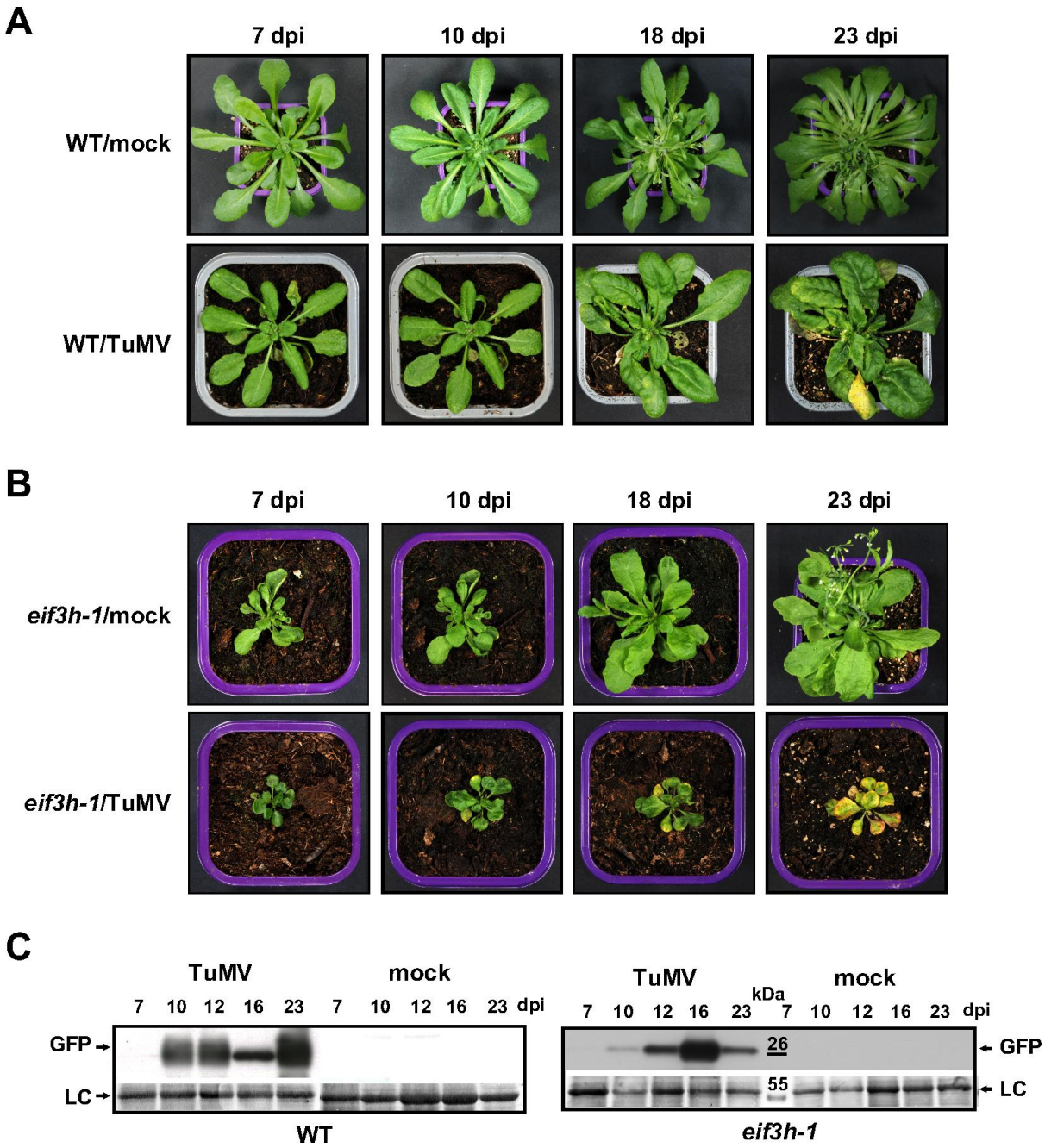

Figure 6. *eif3h-1* plants are susceptible to *Turnip mosaic virus* (TuMV)
(A-B) Analysis of WT (A, *upper panels*) and *eif3h-1* mutant plants (B, *upper panels*) and TuMV disease symptoms in wild type (A, *bottom panels*) and the *eif3h-1* (B, *bottom panels*). (C) GFP proteins accumulate in TuMV-infected wild type (*left panel*), and in *eif3h-1* plants (*right panel*).

2.1.4 Discussion

Translation of mRNAs that harbor short uORFs within their 5' UTRs is down-regulated by normally inefficient reinitiation events. Translation of their main ORF depends on the participation of certain eIFs supporting reinitiation that are recruited during the first cap-dependent initiation event at the uORF and then not released during the short time required for uORF translation (KOZAK 2001). These "reinitation supporting factors" remain associated with post-termination ribosomes and can regenerate reinitiation-competent 40S complexes. In plants, eIF3 subunit h, if phosphorylated, supports reinitiation events while being dispensable for initiation events at the mRNA cap-structure. The mechanism of eIF3h function in reinitiation is not yet understood. We now show that eIF3h, if phosphorylated in response to TOR activation, can play a role in recruitment of eIF3 into polysomes. Moreover, eIF3h plays a role in an exceptional case of translation restart controlled by the CaMV reinitiation factor TAV, which can promote translation of consecutive multiple long ORFs on the same RNA via reinitiation in *Arabidopsis* and other host plants. Our findings strongly suggest that, as in reinitiation after short ORF translation, eIF3h is critical factor for TAV in promoting a polycistronic-like mode of translation, strongly suggesting that TAV exploits the existing cellular reinitiation machinery for viral purposes.

Our findings confirm that, under auxin treatment, TOR was active and interacted with the 40S preinitiation complexes and actively translating ribosomes (polysomes; Fig. 3A). These results correlate well with our previous findings that TOR phosphorylated at S2424 and eIF3 accumulate in polysomes in response to either auxin or TAV (SCHEPETILNIKOV *et al.* 2011; SCHEPETILNIKOV *et al.* 2013). Loading of TOR-P and eIF3 on polysomes correlates with efficient translation of uORF-containing mRNAs, or virus-activated reinitiation after long ORF translation, if TAV is present. Surprisingly, the association of phosphorylated TOR with polysomes does not guarantee eIF3 recruitment to translating ribosomes if eIF3 has lost subunit h (Fig. 3B). If eIF3h is lost, eIF3c, while maintaining its binding to 43S PIC, loses its capacity to interact with polysomes (Fig. 3B), which correlates well with efficient initiation and inefficient reinitiation events in *eif3h-1*. So, it is likely that eIF3h plays a role in eIF3 retention on 40S after the 60S joining step and, importantly, during a several elongation cycles. Note that phosphorylation of eIF3h is critical for eIF3 retention on polysomes. It was shown that eIF3h seems to be essential to assemble recombinant human eIF3 (SMITH *et al.* 2013). Furthermore, removing eIF3h causes the k and l subunits to dissociate from eIF3 (SMITH *et al.* 2016), and can influence the assembly of subunits d, e, k, and l into human eIF3. If removal of eIF3h changes eIF3 compactness, its retention on polysomes by TAV via

contacts with the eIF3 subunit g (PARK *et al.* 2001) can be also affected. Similarly, eIF3 retention on 80S during a few elongation cycles failed in eif3h-1 mutant (Fig. 1E, bottom panels).

Deletion of 40 N-terminal amino acids abolished TAV-controlled reinitiation after long ORF translation (Fig. 4B). Indeed, the recent solving of mammalian 43S PIC structure (DES GEORGES *et al.* 2015) suggests that the N-terminus of eIF3h is exposed to the environment and can contact polysomes via an as yet unknown component that is critical for reinitiation.

This report identifies eIF3h as an important host factor critical for CaMV amplification. Many recessive resistance genes encode translation initiation factors—eIF4E and eIF4G, their isoforms, eIFiso4E and eIFiso4G and other translation factors eIF4A-like helicases, eIF3, eEF1A and eEF1B (SANFACON 2015). Thus, resistance genes in plants provide excellent tools for breeding programs to control plant diseases caused by pathogenic viruses. These factors seem to be recruited by RNA viruses not only to translate their viral RNAs, but also to regulate their replication and potentiate their local and systemic movement. Thus, we cannot exclude that eIF3h might participate in other steps of CaMV replication.

2.1.5 Materials and methods

Expression constructs antibodies

The constructs pmonoGFP, pTAV, peIF3h, peIF3h-S178A, peIF3h-S178D were described in (THIEBEAULD *et al.* 2009) and (SCHEPETILNIKOV *et al.* 2011). PCR products corresponding to eIF3 subunit h (At1g10840.1) (eIF3h full length, aa 1-337) and its deletion mutants (eIF3h-ΔC1, aa 1-254; eIF3h-ΔC2, aa 1-318, eIF3h-ΔN1, aa 39-337, eIF3h-ΔN2, aa 20-337) were amplified from an *Arabidopsis thaliana* cDNA library and cloned as in-frame fusions with the BD domain into the pGBKT7 vector, and with the AD domain into the pGADT7 (Clontech®) for yeast two-hybrid assay, and in the corresponding vector for transient protoplast expression. PCR products corresponding to eIF3 subunit f (AT2G39990) (aa 1-293) were amplified from an *A. thaliana* cDNA library and cloned as in-frame fusion with the BD domain into the pGBKT7 vector (Clontech®). PCR products corresponding to S6K1 were amplified from S6K1 cDNA (At3G08730) and cloned into the pGBKT7 as in-frame fusions with the BD-domain. PCR products corresponding to NTOR, CTOR were amplified from AtTOR cDNA (At1G50030), and cloned into the pGADT7 as in-frame fusions with the AD-domain to obtain pGAD-NTOR and pGAD-CTOR. Detailed description of plasmid constructions, oligos and antibodies is presented in the Materials and Methods.

Pull-down experiments

PCR products corresponding to eIF3f and S6K1 were inserted into pGEX-6P1 (Pharmacia Biotech) as in-frame fusions with the GST-domain (SCHEPETILNIKOV *et al.* 2011). pGEX-6P-1, pGEX-eIF3f and pGEX-S6K1 were used for expression and purification of GST alone, eIF3f and S6K1 fusion proteins with GST domain at the N-terminus. Glutathione-*S*-transferase pull-down assays were carried out as described in (PARK *et al.* 2001). Co-immunoprecipitation experiments were performed as described in (THIEBEAULD *et al.* 2009) and (Supplemental Data).

Yeast two-hybrid assay

GAL4-based yeast two-hybrid protein interaction assays were performed according to (THIEBEAULD *et al.* 2009).

Arabidopsis protoplasts

Arabidopsis protoplasts were prepared from 3- to 4-week-old plantlets (mesophyll protoplasts) transfected with plasmid DNA by the PEG method as described in (Supplemental Data).

Polyribosome isolation

Polyribosomes were isolated from 7-day-old *Arabidopsis* samples and analyzed by density sucrose centrifugation according to (SCHEPETILNIKOV *et al.* 2011).

Real-time and semi-quantitative PCR analyses

Quantitative PCR analysis was performed according to the SYBR Green qPCR kit protocol (Supplemental Data).

Plant material, growth conditions and expression vectors

In this study, *Arabidopsis thaliana* ecotype Columbia (Col-0) was used as a wild-type model. Dr Albrecht G. von Arnim (University of Tennessee-Knoxville, USA) kindly provided Col-0 *eif3h-1* homozygous mutant lines. A recessive mutant allele (eif3h-1) carried a T-DNA insertion in the 10th exon downstream of Ser254; a truncated eIF3h-related protein was detected in this allele (KIM *et al.* 2004).

Plant growth conditions

Arabidopsis seeds were cultured horizontally on MS agar medium (Murashige and Skoog medium with MSMO-salt mixture; Sigma®). WT Col-0 and *eif3h-1* mutant plants were incubated at 4°C in the dark for 1 and 7 days, respectively. Plants were then grown in the greenhouse under the following conditions: 16 hrs light, 21°C - 8 hrs darkness, 17°C (i*n vitro* assay).

Seeds were sown in small pots containing humid fresh *Arabidopsis* culture soil. *Arabidopsis thaliana* plants were grown under the following conditions: 16 hrs of light – 8 hrs of darkness at a temperature ranging between 18 °C and 25 °C under normal greenhouse conditions.

Viral infection

Infection by CaMV virus was performed by agrobacterium-mediated transient transformation of *Arabidopsis* young leaves with pBTCW vector [binary agro-vector containing a full length

genomic copy of CaMV, isolate CM1841, kindly provided by Dr Kappei Kobayashi (KOBAYASHI AND HOHN 2003; LAIRD *et al.* 2013)]. Images of plants were taken (Canon EOS 350D digital) at 7 dpi, 10 dpi, 18 dpi, 23 dpi. Small discs (3 mm diameter) were collected from leaves, and examined by western blot with corresponding antibodies. Infection by TuMV virus was performed by agroinfiltration using construct pCB-TuMV-GFP permitting the transient expression of TuMV polyprotein fused to GFP in *Arabidopsis thaliana* (kindly provided by Dr James Carrington, Danforth Plant Science Center). Polyprotein production was monitored by western blot with anti GFP antibodies. Mechanical inoculation with ORMV viral particles (kindly provided by Manfred Heinlein, Institut de biologie moléculaire des plantes, IBMP; Strasbourg France) was used to infect Arabidopsis. Five-week-old plants were mechanically inoculated on two leaves chosen randomly (C_{stock} = 1 µg/1 µl C_{final} = 50ng/1 µl, 150 ng/leaf) previously scrubbed with Celite to generate small wounds to facilitate the entry of viral particles. Samples were collected and analyzed by immunoblot with specific antibodies against RNA-dependent RNA polymerase (RdRp) (kindly provided by Michail Pooggin).

2.1.6 Acknowledgments

We thank K. Browning for anti-eIF3c antibodies, and A. von Arnim for *eif3h-1* line and anti eIF3h antibodies. This work was supported by the French Agence Nationale de la Recherché—BLAN-2011_BSV6 010 03 and ANR-14-CE19-0007—funding to L.R., and by a 1.5 year PhD fellowship from the Lebanon government ministries to J.M.

2.1.7 References

Basso, J., P. Dallaire, P. J. Charest, Y. Devantier and J. F. Laliberte, 1994 Evidence for an internal ribosome entry site within the 5' non-translated region of turnip mosaic potyvirus RNA. J Gen Virol 75 (Pt 11)**:** 3157-3165.

Benne, R., and J. W. Hershey, 1978 The mechanism of action of protein synthesis initiation factors from rabbit reticulocytes. J Biol Chem 253**:** 3078-3087.

Bonneville, J. M., H. Sanfacon, J. Futterer and T. Hohn, 1989 Posttranscriptional trans-activation in cauliflower mosaic virus. Cell 59**:** 1135-1143.

Calvo, S. E., D. J. Pagliarini and V. K. Mootha, 2009 Upstream open reading frames cause widespread reduction of protein expression and are polymorphic among humans. Proc Natl Acad Sci U S A 106**:** 7507-7512.

Deprost, D., L. Yao, R. Sormani, M. Moreau, G. Leterreux *et al.*, 2007 The Arabidopsis TOR kinase links plant growth, yield, stress resistance and mRNA translation. EMBO Rep 8**:** 864-870.

des Georges, A., V. Dhote, L. Kuhn, C. U. Hellen, T. V. Pestova *et al.*, 2015 Structure of mammalian eIF3 in the context of the 43S preinitiation complex. Nature 525**:** 491-495.

Gallie, D. R., and M. Kobayashi, 1994 The role of the 3'-untranslated region of non-polyadenylated plant viral mRNAs in regulating translational efficiency. Gene 142**:** 159-165.

Garcia-Ruiz, H., A. Carbonell, J. S. Hoyer, N. Fahlgren, K. B. Gilbert *et al.*, 2015 Roles and programming of Arabidopsis ARGONAUTE proteins during Turnip mosaic virus infection. PLoS Pathog 11**:** e1004755.

Gingras, A. C., S. P. Gygi, B. Raught, R. D. Polakiewicz, R. T. Abraham *et al.*, 1999 Regulation of 4E-BP1 phosphorylation: a novel two-step mechanism. Genes Dev 13**:** 1422-1437.

Hinnebusch, A. G., 2006 eIF3: a versatile scaffold for translation initiation complexes. Trends Biochem Sci 31**:** 553-562.

Holz, M. K., B. A. Ballif, S. P. Gygi and J. Blenis, 2005 mTOR and S6K1 mediate assembly of the translation preinitiation complex through dynamic protein interchange and ordered phosphorylation events. Cell 123**:** 569-580.

Ingolia, N. T., S. Ghaemmaghami, J. R. Newman and J. S. Weissman, 2009 Genome-wide analysis in vivo of translation with nucleotide resolution using ribosome profiling. Science 324**:** 218-223.

Kim, T. H., B. H. Kim, A. Yahalom, D. A. Chamovitz and A. G. von Arnim, 2004 Translational regulation via 5' mRNA leader sequences revealed by mutational

analysis of the Arabidopsis translation initiation factor subunit eIF3h. Plant Cell 16**:** 3341-3356.

Kobayashi, K., and T. Hohn, 2003 Dissection of cauliflower mosaic virus transactivator/viroplasmin reveals distinct essential functions in basic virus replication. J Virol 77**:** 8577-8583.

Kozak, M., 1999 Initiation of translation in prokaryotes and eukaryotes. Gene 234**:** 187-208.

Kozak, M., 2001 Constraints on reinitiation of translation in mammals. Nucleic Acids Res 29**:** 5226-5232.

Laird, J., C. McInally, C. Carr, S. Doddiah, G. Yates *et al.*, 2013 Identification of the domains of cauliflower mosaic virus protein P6 responsible for suppression of RNA silencing and salicylic acid signalling. J Gen Virol 94**:** 2777-2789.

Lingaraju, G. M., R. D. Bunker, S. Cavadini, D. Hess, U. Hassiepen *et al.*, 2014 Crystal structure of the human COP9 signalosome. Nature 512**:** 161-165.

Ma, X. M., and J. Blenis, 2009 Molecular mechanisms of mTOR-mediated translational control. Nat Rev Mol Cell Biol 10**:** 307-318.

Mahfouz, M. M., S. Kim, A. J. Delauney and D. P. Verma, 2006 Arabidopsis TARGET OF RAPAMYCIN interacts with RAPTOR, which regulates the activity of S6 kinase in response to osmotic stress signals. Plant Cell 18**:** 477-490.

Menand, B., T. Desnos, L. Nussaume, F. Berger, D. Bouchez *et al.*, 2002 Expression and disruption of the Arabidopsis TOR (target of rapamycin) gene. Proc Natl Acad Sci U S A 99**:** 6422-6427.

Miyoshi, H., N. Suehiro, K. Tomoo, S. Muto, T. Takahashi *et al.*, 2006 Binding analyses for the interaction between plant virus genome-linked protein (VPg) and plant translational initiation factors. Biochimie 88**:** 329-340.

Morris, D. R., and A. P. Geballe, 2000 Upstream open reading frames as regulators of mRNA translation. Mol Cell Biol 20**:** 8635-8642.

Nishimura, T., T. Wada, K. T. Yamamoto and K. Okada, 2005 The Arabidopsis STV1 protein, responsible for translation reinitiation, is required for auxin-mediated gynoecium patterning. Plant Cell 17**:** 2940-2953.

Park, H. S., A. Himmelbach, K. S. Browning, T. Hohn and L. A. Ryabova, 2001 A plant viral "reinitiation" factor interacts with the host translational machinery. Cell 106**:** 723-733.

Pisarev, A. V., A. Unbehaun, C. U. Hellen and T. V. Pestova, 2007 Assembly and analysis of eukaryotic translation initiation complexes. Methods Enzymol 430**:** 147-177.

Poyry, T. A., A. Kaminski, E. J. Connell, C. S. Fraser and R. J. Jackson, 2007 The mechanism of an exceptional case of reinitiation after translation of a long ORF

reveals why such events do not generally occur in mammalian mRNA translation. Genes Dev 21**:** 3149-3162.

Poyry, T. A., A. Kaminski and R. J. Jackson, 2004 What determines whether mammalian ribosomes resume scanning after translation of a short upstream open reading frame? Genes Dev 18**:** 62-75.

Roy, B., J. N. Vaughn, B. H. Kim, F. Zhou, M. A. Gilchrist *et al.*, 2010 The h subunit of eIF3 promotes reinitiation competence during translation of mRNAs harboring upstream open reading frames. RNA 16**:** 748-761.

Ryabova, L. A., M. M. Pooggin and T. Hohn, 2006 Translation reinitiation and leaky scanning in plant viruses. Virus Res 119**:** 52-62.

Sanfacon, H., 2015 Plant Translation Factors and Virus Resistance. Viruses 7**:** 3392-3419.

Schepetilnikov, M., M. Dimitrova, E. Mancera-Martinez, A. Geldreich, M. Keller *et al.*, 2013 TOR and S6K1 promote translation reinitiation of uORF-containing mRNAs via phosphorylation of eIF3h. EMBO J 32**:** 1087-1102.

Schepetilnikov, M., K. Kobayashi, A. Geldreich, C. Caranta, C. Robaglia *et al.*, 2011 Viral factor TAV recruits TOR/S6K1 signalling to activate reinitiation after long ORF translation. EMBO J 30**:** 1343-1356.

Skabkin, M. A., O. V. Skabkina, C. U. Hellen and T. V. Pestova, 2013 Reinitiation and other unconventional posttermination events during eukaryotic translation. Mol Cell 51**:** 249-264.

Smith, M. D., L. Arake-Tacca, A. Nitido, E. Montabana, A. Park *et al.*, 2016 Assembly of eIF3 Mediated by Mutually Dependent Subunit Insertion. Structure 24**:** 886-896.

Smith, M. D., Y. Gu, J. Querol-Audi, J. M. Vogan, A. Nitido *et al.*, 2013 Human-like eukaryotic translation initiation factor 3 from Neurospora crassa. PLoS One 8**:** e78715.

Somers, J., T. Poyry and A. E. Willis, 2013 A perspective on mammalian upstream open reading frame function. Int J Biochem Cell Biol 45**:** 1690-1700.

Thiebeauld, O., M. Schepetilnikov, H. S. Park, A. Geldreich, K. Kobayashi *et al.*, 2009 A new plant protein interacts with eIF3 and 60S to enhance virus-activated translation re-initiation. EMBO J 28**:** 3171-3184.

Thoreen, C. C., S. A. Kang, J. W. Chang, Q. Liu, J. Zhang *et al.*, 2009 An ATP-competitive mammalian target of rapamycin inhibitor reveals rapamycin-resistant functions of mTORC1. J Biol Chem 284**:** 8023-8032.

Tiruneh, B. S., B. H. Kim, D. R. Gallie, B. Roy and A. G. von Arnim, 2013 The global translation profile in a ribosomal protein mutant resembles that of an eIF3 mutant. BMC Biol 11**:** 123.

Tran, H. T., and W. C. Plaxton, 2008 Proteomic analysis of alterations in the secretome of Arabidopsis thaliana suspension cells subjected to nutritional phosphate deficiency. Proteomics 8**:** 4317-4326.

Valasek, L. S., 2012 'Ribozoomin'--translation initiation from the perspective of the ribosome-bound eukaryotic initiation factors (eIFs). Curr Protein Pept Sci 13**:** 305-330.

von Arnim, A. G., Q. Jia and J. N. Vaughn, 2014 Regulation of plant translation by upstream open reading frames. Plant Sci 214**:** 1-12.

Xiong, Y., M. McCormack, L. Li, Q. Hall, C. Xiang *et al.*, 2013 Glucose-TOR signalling reprograms the transcriptome and activates meristems. Nature 496**:** 181-186.

Xiong, Y., and J. Sheen, 2012 Rapamycin and glucose-target of rapamycin (TOR) protein signaling in plants. J Biol Chem 287**:** 2836-2842.

Zhou, F., B. Roy and A. G. von Arnim, 2010 Translation reinitiation and development are compromised in similar ways by mutations in translation initiation factor eIF3h and the ribosomal protein RPL24. BMC Plant Biol 10**:** 193.

2.2 Article 2: GTPase ROP2 promotes translation reinitiation at upstream ORFs via activation of TOR

Mikhail Schepetilnikov[1], Joelle Makarian[1], Ola Srour[1], Angèle Geldreich[1], Zhenbiao Yang[2], Johana Chicher[3], Philippe Hammann[3] and Lyubov A. Ryabova[1]*

[1] Institut de Biologie Moléculaire des Plantes, Centre National de la Recherche Scientifique, UPR 2357, Université de Strasbourg, Strasbourg, France
[2] Center for Plant Cell Biology, Department of Botany and Plant Sciences, University of California, Riverside, CA, USA
[3] Platforme Proteómique Strasbourg-Esplanade, Centre National de la Recherche Scientifique, FRC 1589, Université de Strasbourg, Strasbourg, France

GTPase ROP2 promotes translation reinitiation at upstream ORFs via activation of TOR

Mikhail Schepetilnikov[1], Joelle Makarian[1], Ola Srour[1], Angèle Geldreich[1], Zhenbiao Yang[2], Johana Chicher[3], Philippe Hammann[3] and Lyubov A. Ryabova[1]*

[1] Institut de Biologie Moléculaire des Plantes, Centre National de la Recherche Scientifique, UPR 2357, Université de Strasbourg, Strasbourg, France

[2] Center for Plant Cell Biology, Department of Botany and Plant Sciences, University of California, Riverside, CA, USA

[3] Platforme Proteómique Strasbourg-Esplanade, Centre National de la Recherche Scientifique, FRC 1589, Université de Strasbourg, Strasbourg, France

*To whom correspondence should be addressed:

lyuba.ryabova@ibmp-cnrs.unistra.fr

Tel: +33 (0)3 67 15 53 31

Fax: +33 (0)3 67 15 53 00

Running title: GTPase ROP2 activates TOR

Keywords: phytohormone auxin/ phosphorylation/ S6K1/ endosomes/ signal transduction

2.2.1 Abstract

Target-of-rapamycin (TOR) promotes reinitiation at upstream ORFs (uORFs), which play an important roles in stem cell regulation and organogenesis in plants. Here, we report that, through TOR, small ROP2 GTPase, if activated by the phytohormone auxin, can control reinitiation of uORF-containing mRNAs. Plants with high levels of active ROP2, including those expressing constitutively active ROP2 (*CA-ROP2*), contain high active TOR levels. Moreover, ROP2 physically interacts with, and, when GTP-bound, activate TOR *in vitro*. TOR activation in response to auxin was abolished in ROP-deficient *rop2rop6ROP4 RNAi* plants. GFP-TOR can associate with endosome-like structures in ROP2-overexpressing plants, indicating that endosomes mediate ROP2 effects on TOR activation. *CA-ROP2* is efficient in loading uORF-containing mRNAs onto polysomes and their translation in protoplasts, with both processes being sensitive to the TOR inhibitor AZD-8055. TOR inactivation abolishes ROP2 effects on translation reinitiation at uORFs, but not its effects on cytoskeleton or intracellular trafficking. These findings imply a mode of translation control whereby, as an upstream effector of TOR, ROP2 coordinates TOR function in translation reinitiation pathways in response to auxin.

2.2.2 Introduction

Target-of-rapamycin (TOR) is a main sensor of cell growth in response to nutrients, energy status and growth factors, and is conserved from humans to yeasts and plants. Mammalian TOR (mTOR) occurs in two structurally and functionally distinct complexes: TOR complex 1 (TORC1) and TOR complex 2 (TORC2) (Zoncu *et al,* 2011; Shimobayashi & Hall, 2014). mTORC1—comprising mTOR, raptor, and mLST8—is sensitive to the immunosuppressant drug rapamycin, and regulates cell growth by activating ribosome biogenesis, transcription, and protein synthesis (Hara *et al,* 2002; Loewith *et al,* 2002). mTORC2 mediates cell metabolism and cytoskeletal organization (Cybulski & Hall, 2009). The mTORC1 pathway promotes 5′-cap-dependent translation via phosphorylation of ribosomal protein S6 kinases (mS6Ks) and eIF4E-binding proteins (m4E-BPs) (Ma & Blenis, 2009; Sonenberg & Hinnebusch, 2009). The key eukaryotic translation initiation factor 3 (eIF3) (Hinnebusch, 2006) serves as a scaffold for mS6K phosphorylation by mTOR (Ma & Blenis, 2009). When activated, TOR binds and phosphorylates eIF3-bound S6K1, triggering its dissociation from eIF3 and further activation (Holz *et al,* 2005). The pathways leading to mTOR activation seem to depend on a group of small GTPases, including Rheb (Ras homologue enriched in brain), Rac1 (Saci *et al,* 2011) and Rag (Betz & Hall, 2013), that play a variety of roles within cells (Tee & Blenis, 2005; Sancak et al. 2008). The ribosome is an upstream mTORC2 effector in yeast and mammals, and thus can trigger its activation (Zinzalla *et al,* 2011).

Plant TOR has multifaceted roles in plant growth and homeostasis. The *Arabidopsis* genome contains a single essential *TOR* gene, down-regulation of which correlates with decreased plant size, resistance to stress (Deprost *et al,* 2007; Menand *et al,* 2002) and elevated life span (Ren *et al,* 2012). *Arabidopsis* RAPTOR and LST8 are structural and functional components of the TORC1 complex (Dobrenel *et al,* 2011; Mahfouz *et al,* 2006; Moreau *et al,* 2012). The best-characterized substrate of TORC1 in plant translation is S6K1 (Schepetilnikov *et al,* 2011; Xiong & Sheen, 2012); indeed, *Arabidopsis* plants silenced for TOR expression display significantly reduced polysome abundance (Deprost *et al,* 2007), suggesting a role for TOR in plant translational control.

We have previously characterized a novel regulatory TOR function in plant translation (Schepetilnikov *et al,* 2013). TOR is critically required for translation reinitiation of mRNAs that harbor upstream open reading frames within their leader regions (uORF-mRNAs). Such mRNAs encode many potent proteins such as transcription factors, protein kinases, cytokines and growth factors (Schepetilnikov *et al,* 2013); defects in translation of uORF-mRNAs result in severe developmental anomalies (Zhou *et al,* 2010). Reinitiation is usually less efficient than initiation at

the first ORF and occurs mainly after translation of short uORFs (Kozak, 2001), thus the latter can be used to down-modulate the production of critical effector proteins. Mutants of subunit h of the important reinitiation factor eIF3 (eIF3h) compromise translation reinitiation on uORF-mRNAs without affecting initiation events (Kim *et al,* 2004), and eIF3h functions in reinitiation under the control of TOR (Schepetilnikov *et al,* 2013). To promote reinitiation events, active TOR binds preinitiation complexes and polyribosomes to maintain the phosphorylation status of eIF3h (Schepetilnikov *et al,* 2013). Recently, it was demonstrated that translational control at uORFs plays a key role in *Arabidopsis* stem cell regulation and organogenesis (Zhou *et al,* 2014). Plant TOR is activated in response to glucose (Xiong *et al,* 2013), the plant hormone auxin (Schepetilnikov *et al,* 2013), and the pathogenicity factor, Cauliflower mosaic virus (CaMV) protein TAV (Schepetilnikov *et al,* 2011) via as yet uncharacterized signal transduction pathways. Auxin is an important regulator of plant developmental processes that can act via activation of members of a multigenic family of 11 small ROP (Rho-like GTPases from plants) GTPases (Winge *et al,* 1997; Vanneste & Friml, 2009). ROPs function in cellular signaling by regulating, among other things, cell shape and auxin responses (Xu *et al,* 2010). Indeed, ROPs, particularly ROPs 2 and 6 in *Arabidopsis*, are activated by auxin (Xu *et al,* 2010). Given that auxin has been suggested as an upstream signal that can trigger ribosomal protein S6 (rpS6) kinase phosphorylation (Beltrán-Peña *et al,* 2002; Turck *et al,* 2004), and was directly implicated in TOR phosphorylation and activation of the TOR pathway towards translation (Schepetilnikov *et al,* 2013), we focus on the relationships and possible links between small ROP GTPases and TOR.

Here, we report that ROP2 and TOR interact physically *in vitro*, and that ROP2 GTPase, if active, triggers TOR phosphorylation, activating the TOR signaling pathway and translation of a highly controlled class of mRNAs harboring regulatory uORFs. Our results uncover a novel mechanism of translation reinitiation control involving small GTPase ROP2 via TOR.

2.2.3 Results

TOR associates with ROP2 via direct binding

Given that auxin activates both TOR protein kinase (Schepetilnikov et al, 2013), and plasma membrane-associated ROPs—particularly ROPs 2 and 6 in *Arabidopsis* (Xu et al, 2010; Fig 1A)—we asked whether TOR and ROPs interact. In *Arabidopsis*, RAC/ROPs are encoded by 11 genes that comprise a closely related, multigenic family; ROPs 2, 4 and 6 form a distinct subgroup in a phylogenetic tree based on 11 *Arabidopsis* ROP sequences (Fig 1B). First, using the yeast two-hybrid system, we found specific interactions of TOR with ROPs 2, 4 and 6 (Fig 1C). We selected ROP2—the most abundant of the ROP GTPases according to the Genevestigator database (Fig EV1A)—to further examine its association with TOR. Strikingly, GST-ROP2 binds recombinant TOR physically in a GST pull-down assay, but interacts neither with *Arabidopsis* GTPase Sar1b, which is unrelated to Rho GTPases and functions in ER-Golgi trafficking (Bar-Peled & Raikhel, 1997; Jones *et al,* 2003), nor with GST alone, and only weakly with human GTPase Rheb (Fig 1D), indicating plant-specificity in TOR binding. Although ROPs shuttle between a GTP-bound active form and a GDP-bound inactive form, our GST pull-down approach suggested that *Arabidopsis* TOR can interact with GTP, the non-hydrolyzable analogue guanylyl-imidodiphosphate (GMP-PNP), and GDP-bound GST-ROP2 (Appendix Fig S1A). Third, we determined that TOR and ROP2 coimmunoprecipitate; endogenous ROPs coimmunoprecipitated with green fluorescent protein-tagged TOR (GFP-TOR) in *35S:GFP-TOR* expressing *Arabidopsis*, but not with GFP (*35S:GFP* line; Fig 1E; production of complete TOR in the *35S:GFP-TOR* transgenic line was confirmed by sequence coverage identified from MS/MS data; Appendix Fig S1B). *In planta*, endogenous ROPs coimmunoprecipitated with endogenous TOR using anti-TOR, but not control rabbit serum (NRS, Fig 1F). Thus, ROP2 was identified as a direct TOR interactor *in vitro* that associates with TOR-containing complexes in Arabidopsis.

We next delineated the region of TOR responsible for binding ROP2: the N-terminal half of TOR (NTOR), but not the TOR C-terminus, interacts with ROP2 in the yeast two-hybrid system (Fig 1G). To determine whether GTP charging is critical for ROP2 binding to TOR, we assayed NTOR interactions with both constitutively active GTP-bound ROP2 (CA-ROP2) and the dominant negative nucleotide-free ROP2 (DN-ROP2). CA-ROP2 carries a ROP2-Q64L mutation that abolishes GTP hydrolysis, thus keeping ROP2 in the GTP-bound active state, while a mutation in the consensus aspartate in the G4 motif (ROP2-D121N) results in lowered nucleotide affinity (Berken & Wittinghofer, 2008; Wu *et al,* 2001) (Fig 1A). Our results indicate that nucleotide-free DN-ROP2 binds to both TOR and NTOR in the

yeast two-hybrid system (Fig 1G). Moreover, CA-ROP2 binds TOR and NTOR only weakly or not at all in our conditions. Accordingly, TOR interacts reproducibly more strongly with nucleotide-free ROP2 than with ROP2 or CA-ROP2 GST fusions in GST pull-down assays (Fig 1H). This is similar to the human GTPase Rheb, whose binding affinity to TOR is reduced by GTP charging to enable the TOR complex to adopt a configuration that is catalytically active, when GTP-bound Rheb activates mTOR (Long *et al,* 2005). Rac1, another member of the Rho family of GTPases, which also binds directly to mTOR in GTP-bound state independent manner through the C-terminal RKR stretch of aminoacids (Saci *et al,* 2011), facilitates mTOR localization to cellular membranes. A similar motif involving the four basic lysine residues (motif I) is found at the C-terminus of ROPs 1-6 (Fig EV1B) upstream of a CxxL (x = aliphatic amino acid) geranylgeranylation motif (motif II) required for plasma membrane targeting (Fu *et al,* 2005, 2009; Sorek *et al,* 2011; Xu *et al,* 2014). Deletion of motif II alone did not affect binding of ROP2 to TOR (Fig EV1C), while deleting a longer fragment involving both motifs I and II impaired this interaction, suggesting that ROP2 binds TOR through the C-terminal polylysine stretch of amino acids.

TOR is up-regulated in plants with elevated levels of GTP-bound ROP2

To study whether ROP2 and TOR can functionally interact, we examined the effect of ROP2 on TOR phosphorylation status. To test TOR activation, we measured levels of TOR phosphorylated at S2424 using anti-(mTOR-S2448-P) antibodies [mTOR S2448 epitope can be aligned with the S2424 epitope in *Arabidopsis* TOR (Schepetilnikov *et al,* 2013)]. Anti-(mTOR-S2448-P) antibodies specifically recognize both wild type *Arabidopsis* TOR and its phosphorylation mimic TOR-S2424D transiently expressed in *Arabidopsis* suspension culture protoplasts (Appendix Fig S2A). In contrast, a TOR-specific phosphorylation site knockout (S2424A) diminished TOR recognition to endogenous levels. Accordingly, phosphorylation of S6K1 overexpressed in protoplasts, at the TOR-specific hydrophobic motif residue T449 [anti-(mS6K1-T389-P) antibodies] (Schepetilnikov *et al,* 2011; Xiong & Sheen, 2012), increased strongly upon overexpression of TOR or a TOR phosphorylation mimic. Unlike TOR-S2424D, overexpression of TOR-S2424A did not promote S6K1 phosphorylation at T449, suggesting that phosphorylation of S2424 contributes to *Arabidopsis* TOR activation. These results demonstrate that mTOR-S2448-P antiserum is specific for TOR phosphorylated at S2424.

We demonstrated earlier that external auxin treatment of *Arabidopsis* seedlings promotes TOR activation (Schepetilnikov *et al,* 2013). As expected, incubation of 7 days

after germination (dag) seedlings with auxin analogue 1-naphthylacetic acid (NAA) promoted TOR phosphorylation that was abolished by a second generation TOR inhibitor, AZD-8055, regardless of NAA treatment (Fig EV2A). AZD-8055 binds to the TOR kinase domain within the ATP-binding pocket and inactivates TOR (Chresta *et al,* 2010; Montane & Menand, 2013). To examine how levels of active GTP-bound ROPs are regulated by auxin treatment, we used a pull-down assay with a ROP-interactive CRIB motif-containing protein 1 (Ric1) that specifically targets activated forms of RAC/ROPs, and compared our results to those obtained with *CA-ROP2* (Wu *et al,* 2000; Miyawaki & Yang, 2014). Indeed, Ric1 fused to GST (GST-Ric1), but not GST alone, interacted preferentially with recombinant ROP2 charged with the non-hydrolyzable GTP analogue GMP-PNP, but not with ROP2 preincubated with GDP (Appendix Fig S2B). However, this approach did not display significant differences in active ROPs-GTP levels upon prolonged incubation of 7 dag seedlings with NAA in our experimental conditions (Fig EV2A). Next, we examined *yuc1D* (renamed from yucca; Zhao *et al,* 2001), and *curlyfolia1D* (*cuf1D*; Cui *et al,* 2013) plants characterized by high spatial auxin accumulation, which both exhibited pointed and slightly curled downward leaves (Fig EV2B). Here, high TOR phosphorylation levels in extracts from *yuc1D* and *cuf1D* associated with elevated levels of ROPs-GTP as compared with that of WT plants, where a statistically more significant increase of active ROP2 levels was demonstrated in *cuf1D* (Fig EV2C).

Thus, to further establish functional interaction of ROP2 and TOR *in planta*, we employed *Arabidopsis* mutants *cuf1D* and *CA-ROP2*, the latter being transgenic for constitutively active GTP-bound ROP2 (CA-ROP2). Note that the phenotypes of *CA-ROP2* and *cuf1D* are similar (Fig 2A). We correlated endogenous GTP-bound ROP levels pulled down by GST-Ric1 from *cuf1D* and WT, or *CA-ROP2* and WT extracts (Fig 2B). As expected, *CA-ROP2* displayed strongly elevated GTP-bound ROP2 levels due to ROP2 mutant overexpression. GTP-bound ROP2 levels in the *cuf1D* mutant were elevated as compared to WT plants. There were no obvious differences in the levels of mRNA encoding ROP and TORC1 complex components between *cuf1D* and WT plants (Fig 2C), suggesting that GTP-bound ROP levels are elevated through a posttranslational mechanism.

Next, both mutants characterized by high levels of GTP-bound ROPs were used to assess the phosphorylation status of TOR and its downstream target S6K1. We confirmed that phosphorylation of TOR at S2424 in *CA-ROP2* as well as in *cuf1D* extracts prepared from 7 dag seedlings was greatly elevated as compared with WT extracts (Fig 2D). We also observed a significant increase in S6K1 phosphorylation at the TOR-responsive motif residue

T449 in *cuf1D* and *CA-ROP2* as compared with WT plants. This further confirms that TOR signaling is up-regulated in extracts with high GTP-bound ROP2 levels. There was no significant difference in TOR protein levels between mutants and the corresponding WT extracts (Fig 2D). Accordingly, TOR phosphorylation at S2424 was abolished by AZD-8055 in WT and *CA-ROP2* seedlings (Fig 2E). Given that AZD-8055 treatment of WT and *CA-ROP2* plants only slightly altered GTP-bound total ROP levels (Fig 2E, right panel), TOR could be considered dispensable for ROP activation.

To show directly that ROP2 induces TOR signaling activation in response to auxin treatment, we depleted ROPs 2, 4 and 6 (Fig 3A and B; Ren *et al*, 2016). First, we found that knockout of only ROP2 substantially reduces the level of ROPs immunoprecipitated by TOR to levels similar to that observed in *rop2 rop6* and *rop2 rop6 ROP4 RNAi* plants, strongly suggesting that ROP2 plays a pivotal role in TOR association (Fig 3C). Time-course analysis revealed that the levels of phosphorylated TOR in WT plants increased 8-fold in response to auxin (Fig 3D). Importantly, induction of TOR by auxin was abolished in *rop2 rop6 ROP4 RNAi*, although the initial level of phosphorylated TOR in ROP-deficient extract was somewhat higher than in WT plants, possibly due to induction of other TOR upstream effectors (Fig 3D). Taken together, these results demonstrate that ROP2 largely mediates the activation of TOR in response to auxin.

We also crossed *CA-ROP2* with the *GFP-TOR* line (Fig 4) to test how GFP-TOR phosphorylation is affected by high CA-ROP2 levels *in planta*. Although the phenotype of *GFP-TOR/CA-ROP2* resembles that of *CA-ROP2* (Fig 4A), there was no obvious difference in TORC1 component mRNA levels other than the expected increase in ROP2 mRNA levels (Fig 4B). Note that we used specific primers to discriminate between GFP-TOR and endogenous TOR mRNAs (Appendix Fig S3). However, the TOR phosphorylation level in *CA-ROP2/GFP-TOR* was elevated by about 9-fold above that in *GFP-TOR* (Fig 4C), again showing that GTP-bound ROP2 boosts TOR-phosphorylation.

To assay kinase activity of TOR immunoprecipitated from either *GFP-TOR/CA-ROP2* or *GFP-TOR* extracts (TOR IP), we compared recombinant S6K1 phosphorylation at TOR-responsive T449 *in vitro* using equal amounts of total TOR IP. Consistently, a higher kinase activity of GFP-TOR was found in *GFP-TOR/CA-ROP2* (Fig 4D). Taken together, these results suggest that GTP-bound ROP2 is a putative candidate to impact TOR signaling activation.

When active, ROP2, together with its binding partner RIC4, interacts with the actin cytoskeleton and promotes the lobing of epidermal pavement cells in *Arabidopsis* leaves,

increasing their circularity (Fu *et al,* 2002; Fig 4E cf *CA-ROP2* vs WT). In *GFP-TOR*, the size of the epidermal pavement cells is reproducibly increased as expected for a TOR overexpressor (Menand *et al,* 2002), while their shape remains unaffected (Fig 4E cf. WT versus *GFP-TOR*). Accordingly, *CA-ROP2/GFP-TOR* cells are reproducibly bigger, but their circularity is similar to that in *CA-ROP2*. Moreover, GFP-TOR overexpression, as well as its activation by CA-ROP2, did not influence further the lobe-promoting ROP2 function in cytoskeleton rearrangements, but rather promoted cell growth.

ROP2 promotes TOR accumulation close to the cell periphery

ROPs associate closely with plasma membrane due to a prenylation motif II at the C-terminus (Fu *et al,* 2005; 2009; Sorek *et al,* 2011; Xu *et al,* 2014). Results showing that ROP2 interacts physically and functionally with TOR suggest that ROP2 may function in regulating relocation of TOR to the plasma membrane. Microscopic observation showed that transiently expressed GFP-TOR was distributed diffusely in the cytoplasm in *N. benthamiana* cells, mainly at the cell periphery, but appeared as multiple dots upon co-expression with myc-ROP2, and especially with myc-CA-ROP2 (Fig 5A). Moreover, the number and size of GFP-TOR dots increased upon co-expression of myc-DN-ROP2 (Fig 5A, bottom panels). To locate GFP-TOR dots between the cell periphery and the perinuclear region, we realized a series of confocal cross-sections, 0.95 μM in depth, from the top to the central section of cells overexpressing both GFP-TOR and myc-DN-ROP2 (Appendix Fig S5A). GFP-TOR dots close to the cell periphery/plasma membrane disappeared from view and reappeared progressively towards the central section, strongly suggesting GFP-TOR localization proximal to the plasma membrane. Note the levels of myc-tagged ROP2, DN-ROP2 and CA-ROP2 production in *N. benthamiana* (Fig 5B).

Next, we investigated the subcellular co-localization of GFP-TOR and red fluorescent protein-tagged ROP2 (RFP-ROP2) expressed transiently in *N. benthamiana* cells. GFP-TOR was distributed diffusely, mainly at the cell periphery (Fig 5C). In contrast, when GFP-TOR was co-expressed together with RFP-ROP2 or RFP-CA-ROP2, GFP-TOR appeared as small dots on the periphery of epidermal cells, close to the plasma membrane (Fig 5D). Although ROP2 overexpression induced GFP-TOR association with subcellular structures, neither RFP-ROP2 nor RFP-CA-ROP2 were found co-localized with GFP-TOR. In contrast, the dominant-negative ROP2 mutant (RFP-DN-ROP2), while promoting formation of GFP-TOR-containing particles, associated within these subcellular structures (Fig 5D). Moreover, nucleotide-free ROP2, DN-ROP2 exhibits tight TOR binding activity, and it appears that TOR is trapped by

DN-ROP2, suggesting that nucleotide charging is required for dissociation of ROP2 from the TOR complex. In control experiments, GFP or RFP fused to different ROP2 variants, either alone or in different combinations, did not reveal similar structures in epidermal cells (Appendix Fig S5B and S5C). In addition, neither Rheb, CA- and DN-Rheb (Appendix Fig S5D), nor Sar1b, CA- and DN-Sar1b derivatives were able to induce GFP-TOR association with subcellular structures (Appendix Fig S5E).

To elucidate the role of C-terminal motifs I and II, we investigated the subcellular co-localization of RFP-ROP2ΔII and RFP-ROP2Δ(I+II) with GFP-TOR. The ROP2 deletion mutant lacking the C-terminal CAFL (motif II) that interacted strongly with TOR *in vitro* (Fig EV1C), failed to promote formation of GFP-TOR-containing particles when co-expressed as an RFP-fusion together with GFP-TOR (Fig 5F). With a ROP2 construct lacking motif I responsible for TOR interaction (Fig EV1C), no GFP-TOR association with subcellular structures was seen. In addition, microscopic observation showed that both the polybasic domain and prenylation motif of ROP2 are responsible for ROP2 attachment to the plasma membrane. Indeed, co-localization with the plasma membrane (PM) was somewhat disturbed upon transient expression of a C-terminal RFP-ROP2 deletion mutant (Fig 5E and EV3A). Thus, ROP2 motif I is involved in TOR binding, while motif II is required for targeting of TOR into subcellular structures.

In planta, punctuate dots have been observed by fluorescence microscopy in the root cells of WT seedlings either treated by external auxin (Fig EV3B) or GTP-bound ROP2 expressing *GFP-TOR/CA-ROP2* seedlings (Fig 5G). Analysis of intracellular distribution of TOR suggested the presence of TOR mainly in supernatant (S100) and partially in microsomal (P100) fractions (Fig EV3C). Although NAA treatment of *Arabidopsis* seedlings had no significant effect on TOR intracellular distribution, active TOR-P levels in microsomes were drastically increased. Likewise, the level of active TOR-P in microsomes isolated from *GFP-TOR/CA-ROP2* was increased significantly as compared with *GFP-TOR* (Fig 5H). Taken together, our results suggest that the appearance of punctuate dots correlates with elevated levels of active TOR in microsomes.

We also tracked whether the dominant negative Sar1b-DN mutant that prevents COPII vesicle formation and blocks protein exit from the ER to the Golgi apparatus (Andreeva *et al,* 2000) can also trigger formation of GFP-TOR punctuate dots. Overexpression of myc-Sar1b-DN in *N. benthamiana* cells inhibits vesicle trafficking and leads to redistribution of Golgi markers to a polygonal network resembling ER structures (Fig EV3D). However, myc-DN-

Sar1b failed to replace myc-DN-ROP2 in GFP-TOR punctuate dot induction, and, vice versa, myc-DN-ROP2 overexpression provokes formation of GFP-TOR aggregates that are not co-localized with RFP-Golgi marker, but failed to affect Golgi transport (Fig EV3D and EV3E). Thus, we concluded that ROP2 is highly specific for TOR association.

GFP-TOR co-localizes to endosomes in response to ROP2 overexpression

To establish the nature of the mobile intercellular particles to which TOR relocates upon ROP2 overexpression, several RFP-fused marker constructs were overexpressed transiently together with GFP-TOR and FLAG-CA-ROP2 in *N. benthamiana* leaves (Fig EV4). Only one out of seven different markers—a transiently expressed RFP-RabC1 that specifically labels endosomes (Rutherford & Moore, 2002)—co-localized with GFP-TOR upon co-expression of either FLAG-ROP2, or FLAG-CA-ROP2, or FLAG-DN-ROP2, indicating that TOR can associate with endosomes (Fig 6A).

To confirm these results in *Arabidopsis*, we used *35S:GFP-TOR* and *35S:RFP-RabC1* lines stably producing GFP-TOR and RFP-RabC1, respectively. Consistent with results in *N. benthamiana*, GFP-TOR co-localized mostly with the endosome-like structures revealed by RFP-RabC1 when GFP-TOR and FLAG-CA-ROP2 were transiently co-expressed in *35S:RFP-RabC1* (Fig 6B), confirming GFP-TOR association with endosomes. The reciprocal combination, e.g. RFP-Rab1C and FLAG-CA-ROP2 expressed transiently in an *Arabidopsis* line transgenic for GFP-TOR, displayed RFP and GFP labeled particles that were mostly co-localized (Fig 6C). We conclude that TOR is targeted by ROP2 to endosome-like structures that quickly dissociate during or after TOR association with endosomes. GFP-TOR can be visualized on endosomes with the DN-ROP2 mutant.

We next determined the effect of brefeldin A (BFA) on the distribution of FM4-64 fluorescent endocytosis marker and GFP-TOR. BFA inhibits the formation of exocytic vesicles but does not block plasma membrane (PM) internalization through endocytosis (Richter *et al*, 2007). If GFP-TOR associates with endocytic compartments, it would be integrated into aggregates of endomembranes together with FM4-64 in the presence of BFA. Here, in BFA-treated cells that retained accumulation of GFP-TOR, selected internalized FM4-64 aggregates were found co-localized with GFP-TOR (Fig 6D). These results further support our hypothesis that GFP-TOR is relocated to endosomes in response to ROP2 activation.

uORF-mRNA loading on polysomes is under the control of CA-ROP2, which functions through TOR

Translation of a special class of uORF-mRNAs via reinitiation requires TOR activation in response to the phytohormone auxin (Schepetilnikov *et al*, 2013). To establish the role of active ROP2 in the control of translation reinitiation, we performed comparative polysome profile analysis in WT and *CA-ROP2* seedling-derived extracts (Fig 7C). *CA-ROP2* plants are characterized by a slightly increased ratio of polysomes to fraction of monosomes and ribosomal subunits as compared with WT and AZD-8055-treated *CA-ROP2* plants (Fig 7A). To monitor polysomal loading of uORF-mRNAs in different ROP2 activation conditions, we selected several endogenous uORF-mRNAs, such as *ARF3*, *ARF5* and *bZIP11*, translation of which includes one or more reinitiation event depending on the uORF configuration within their leader regions, as well as uORF-less mRNAs encoding actin and glycerol-3-phosphate dehydrogenase C2 (GAPC2, Fig 7B). To avoid translation repression of *bZIP11* by sucrose, seedlings were grown on agar medium containing 30 mM sucrose (Wiese *et al*, 2004).

mRNA distribution within polysomal profiles from extracts of WT seedlings and *CA-ROP2* seedlings grown without or with AZD-8055 was monitored in parallel experiments by quantitative RT–PCR (qRT–PCR) for each indicated endogenous mRNA, and results were normalized to an rRNA and a housekeeping gene, *EXP*, levels of which were stably maintained in all conditions tested. As shown in Fig 7D, efficient GAPC2 mRNA loading on polysomes was barely affected by high active ROP2 levels or by TOR inactivation. In contrast, a somewhat toxic effect of CA-ROP2 on loading of actin mRNA into polysomes was apparent. Polysomal accumulation of *bZIP11*, *ARF3* and *ARF5* mRNAs carrying long leaders with uORFs was reproducibly elevated in *CA-ROP2*-derived extracts as compared with WT extracts. Surprisingly, although, the translation/reinitiation events within *bZIP11*, *ARF3* and *ARF5* 5'-UTRs impede or block ribosomal movement towards the main ORF, causing inefficient translation of uORF-mRNAs in WT conditions (Zhou et al, 2010), the high polysome/non-polysome ratio gives a false impression of their efficient translation. Possibly, the increased abundance of initiating/reinitiating 40S, and likely uORF-translating 80S, within their leaders would shift these mRNAs towards 80S or even light polysomal fractions. The abundant appearance of uORF-mRNAs in both polysomal and non-polysomal fractions in *CA-ROP2* reflects main ORF translation at much higher levels due to improved reinitiation at uORFs, while a few 40S can still occupy the leader region *in planta* (Fig 7D). *ARF5* mRNA loading, which is nearly negligible in WT seedlings (6 uORFs inhibits *ARF5* mRNA translation by 16-fold; Zhou et al, 2010) was improved drastically upon TOR

activation in *CA-ROP2*. As expected, TOR inactivation by AZD-8055 abolished cell reinitiation ability. There was no significant effect of AZD-8055 on total mRNA levels in *CA-ROP2* and WT extracts, except that levels of *bZIP11* mRNA were surprisingly high upon AZD-8055 treatment (Fig EV5D), although this did not improve *bZIP11* mRNA loading. AZD-8055 treatment diminished further loading of *bZIP11* and *ARF3* mRNAs on WT polysomes, while *ARF5* loading remained low under our WT+AZD-8055 conditions (Fig EV5B).

Cell reinitiation efficiency depends on retention of active TOR in polyribosomes after the preceding initiation event (Schepetilnikov *et al,* 2013). Here, the phosphorylation level of TOR found in WT extract 80S and ribosomal subunit fractions was below the limit of detection of our antibodies (Fig EV5C). In contrast, in *CA-ROP2* plants, TOR is phosphorylated and associates not only with 80S and ribosomal subunit fractions but also with light polysomes, which contain two or three translating ribosomes on average on the same mRNA. Application of a TOR inhibitor resulted in TOR inactivation and dissociation from polyribosomal profiles (Fig EV5C). Therefore, uORF-mRNA abundance in polysomes is regulated by GTP-bound ROP2 in a TOR-responsive manner for several ARF-encoded genes, and also for auxin-unrelated *bZIP11,* suggesting that GTP-bound ROP2 up-regulates the translation capacity of reinitiation-dependent mRNAs via TOR.

CA-ROP2 up-regulates translation of uORF-containing mRNAs in Arabidopsis protoplasts

Our results suggest that active ROP2 promotes uORF-mRNA accumulation in polysomes in a TOR-responsive manner. We tested whether CA-ROP2 seedlings can drive efficient reinitiation of translation. As expected, TOR phosphorylation status was elevated in *CA-ROP2*–derived mesophyll protoplasts as compared with WT protoplasts, and nearly abolished by AZD-8055 after overnight incubation of protoplasts (Fig 8A).

Next, we compared the transient expression of several reporter genes that harbor a β-glucuronidase (GUS) ORF downstream of short 60-nt-, *ARF3*- or *ARF5*-containing leaders (Fig 8B) in mesophyll protoplasts prepared from WT or *CA-ROP2* seedlings. Mesophyll protoplasts were transformed with one of the above plasmids, and a plasmid containing a single GFP ORF downstream of the TEV IRES (Zeenko & Gallie, 2005) as a control for transformation efficiency.

Under the conditions used, the *ARF5* and *ARF3* leaders fused to the GUS ORF in their authentic initiation context reduced GUS ORF translation by about 80% and 85%,

respectively, compared with that of the short-GUS mRNA (Fig 8C) in WT protoplasts. *ARF3*- and *ARF5*-dependent GUS/GFP levels were dramatically increased by 3- to 4-fold in protoplasts prepared from *CA-ROP2* as compared with WT protoplasts, while GUS/GFP levels did not change significantly upon short leader-dependent expression (Fig 8C). GUS-containing mRNA levels as well as GFP levels in either WT or *CA-ROP2* protoplasts were similar during protoplast incubation. *CA-ROP2*-sensitive induction of *ARF3*- and *ARF5*-dependent GUS ORF expression was blocked by treatment with AZD-8055 (Fig 8C). Thus, the CA-ROP2 effect on uORF-mRNA translation is AZD-8055 sensitive and thus TOR responsive.

We next monitored translation reinitiation efficiencies of short-GUS- and ARF5-GUS-containing reporters in mesophyll protoplasts transfected with either ROP2 (WT-ROP2), or CA-ROP2, or DN-ROP2-expression vectors. As can be seen in Fig 8D, ROP2, and especially CA-ROP2, proteins, but not DN-ROP2, were found active in promoting reinitiation at uORFs of ARF5 mRNA. Indeed, the translation efficiency of the ARF5 leader-containing mRNA was increased up to three-fold in CA-ROP2 expressing protoplasts, while DN-ROP2 GTPase failed to increase translation of either short-GUS, or ARF5-GUS mRNAs.

2.2.4 Discussion

Recent results have revealed a role for auxin in TOR signaling activation in plants (Schepetilnikov *et al,* 2013). Moreover, a recent publication confirmed that TOR plays an important role in auxin signaling transduction in *Arabidopsis* (Deng *et al,* 2016). These results prompted us to address the question of which TOR pathway intermediate compounds can transmit signals from auxin or other TOR upstream effectors (environmental changes, glucose and amino acids) to promote protein synthesis via TOR in plants. Our investigations *in vitro* and *in planta* have demonstrated that the small GTPase ROP2 promotes TOR activation in response to auxin; active TOR can up-regulate translation reinitiation at uORFs. Several lines of evidence support this conclusion: first, ROP2 interacts directly with TOR *in vitro*, and both proteins co-immunoprecipitate in plant extracts (Figs 1, EV1C). Second, plants characterized by high active ROP or CA-ROP2 contain increased levels of active TOR and S6K1 (Fig 2D). Third, inactivation of TOR by AZD-8055 abolishes ROP2 effects on TOR and its downstream signaling, but TOR is dispensable for the active status of ROP2 and other ROPs, strongly suggesting that ROP2 is upstream of TOR (Fig 2D). Importantly, TOR activation in response to auxin was abolished in *rop2rop6ROP4 RNAi* extracts (Fig 3). Fourth, GTP-bound ROP2 dramatically stimulates translation reinitiation of uORF-mRNAs in a manner sensitive to the TOR inhibitor AZD-8055 (Figs 7, 8A). Strikingly, CA-ROP2 GTPase, but not the dominant negative DN-ROP2, is active in reinitiation at uORFs (Fig 8D). Another interesting phenomenon revealed by our data is the connection between ROP2-containing TOR complexes and endosome-like structures in the cytoplasm.

ROPs—orthologs of mammalian Rho and Rac (Berken & Wittinghofer, 2008)—are promising candidates for regulating the TOR signaling pathway—the main growth-related pathway in eukaryotes. In addition, a connection between auxin and ROP activation has been established (Miyawaki & Yang, 2014), placing ROPs downstream of auxin. Our data suggest that, in addition to ROP2, TOR is able to interact specifically with ROP4 and ROP6, but additional studies are needed to determine the role of these latter ROPs in TOR regulation. ROP2 is expressed in all vegetative tissues, belongs to the largest ROP subgroup (Li *et al*, 1998; 2001) and, according to our data, when active, contributes to TOR signaling activation in an AZD-8055-sensitive manner. We cannot exclude the possibility that ROP6 and ROP2, which functions in cell expansion on different sides of the membrane (Xu *et al*., 2010), exert differential effects on TOR signaling.

ROP2 associates with TOR or TOR-containing complexes *in vitro* and *in planta* (Figs 1, EV1C). According to our results, only some TOR-binding characteristics of ROP2

resemble those of human Rho-related GTPase Rheb, although both bind physically and activate TOR in the GTP-bound state. However, the ROP2–TOR interaction is plant specific; ROP2 binds to the heat repeat domain of *Arabidopsis* TOR, while Rheb binds within the kinase domain of mTOR (Long *et al*, 2005). This may explain the weak interaction of Rheb with *Arabidopsis* TOR under our conditions. ROP2 binding to TOR can occur via the C-terminal basic stretch of aminoacids (motif I), and *in vitro* does not require ROP2 charging, but GTP somewhat negatively modulates this interaction (this study and Long *et al*, 2005). Consistently, only WT ROP2 or CA-ROP2 are active in promoting reinitiation at uORFs in protoplasts. These results suggest that TOR/GTP-ROP2 complex formation in *Arabidopsis*, albeit possibly transient, is a necessary prerequisite for the physiological activation of TOR kinase. Strikingly, *Arabidopsis* GFP-TOR, when activated by ROP2, can relocate to endosome-like structures labeled by RabC1. The closest RabC1 GTPase mammalian homologue, Rab18, is also associated with endosomes, especially in epithelial cells, and can function in recycling to the plasma membrane (Rutherford & Moore, 2002). Since the TOR cofactor LST8 was also localized on RabC1-labelled endosomes or endosome-like structures (Moreau *et al*, 2012), we suggest that endosomes are sites of TOR complex localization. Although nucleotide-free ROP2 (DN-ROP2) promotes targeting of TOR to endosomes (Figs 5,6), it remains endosome associated, indicating formation of inactive complexes, from which DN-ROP2 is unable to dissociate. Thus, we conclude that ROP2 targeting to endosomes is an intermediate step in ROP2 recycling. In plants, the auxin-related ROP2 pathway plays a role in the promotion of endosomal trafficking from early endosomes during PIN1 internalization (Dhonukshe *et al*, 2007; 2008; Nagawa *et al*, 2012). In turn, disruption of membrane trafficking can influence auxin signaling at the level of translation (Rosado *et al*, 2012). In mammals, Rag GTPases are responsible for lysosomal recruitment of mTOR by targeting its cofactor RAPTOR (Bar-Peled & Sabatini, 2014), while our experiments did not reveal interactions between ROP2 and Arabidopsis RAPTOR (data not shown). Interestingly, although both ROP2 and human Rac1 bind TOR via their polybasic domain, ROP2 activates TOR in a way similar to human Rheb. This can reflect the situation in plants, which contain only a single family of Rho-like GTPases.

Consistent with our findings, a subset of ROP GTPases function in auxin signaling to downstream responsive genes (Tao, 2002), indicating that the active ROP2 status can be translated into specific auxin-dependent responses. Auxin is under the control of various environmental and developmental signals that trigger local auxin biosynthesis or its intercellular polar distribution. High auxin maxima trigger the cell transcription machinery

towards expression of auxin-responsive genes via release of repression of the ARF family (Vanneste & Friml, 2009). In the cytosol, ROP2 can trigger TOR activation in response to auxin, or other as yet uncharacterized signals, to induce translation of a highly regulated class of mRNAs containing regulatory uORFs.

Our results provide a new paradigm for translation regulation of a specific class of messages loaded with short uORFs within their leader regions that are responsive to small GTPase ROP2. When overexpressed in protoplasts, active ROP2 renders protoplasts high-reinitiation-permissive. Our results explain this phenomenon via the model presented in Fig 9. Auxin mediates recycling of ROP2-GDP to ROP2-GTP. ROP2 can bind TOR directly via its polybasic domain. GTP-bound ROP2 forms a transient, but potentially active, complex with TOR, which triggers phosphorylation events and conformational changes that result in TOR activation. Although GTP-bound ROP2 interacts somewhat weakly with TOR, the configuration of GTP-charged ROP2 enables TOR to adopt a form that is both catalytically active and capable of producing signaling *in planta*. TOR activation could occur upon complex formation with ROP2 on endosomes. ROP2 then dissociates from TOR and requires recycling. Several GEFs can recycle ROPs (Oda & Fukuda, 2014). Active TOR is loaded on eIF3-containing preinitiation complexes (Holz et al., 2005) and polysomes, where it activates S6K1, and both promote translation reinitiation of uORF-mRNAs (Schepetilnikov *et al,* 2013). In our model, ROP2 is activated in response to auxin signals that are transported via an as yet uncharacterized receptor.

Our findings, together with the observation that TOR is required for virus-controlled polycistronic translation—a process normally strictly prohibited in eukaryotes—in CaMV (Schepetilnikov *et al,* 2011) suggests that TOR up-regulation of reinitiation at uORFs could be as harmful in plants as in mammals, where up-regulation of the protein synthesizing machinery contributes to the development of cancer (Ruggero & Pandolfi, 2003). Notwithstanding that auxin regulates a range of distinct effectors, these findings further corroborate the idea that translation reinitiation is achieved via crosstalk between the TOR kinase and ROP2 signaling pathways. The developmental abnormalities identified in rpl24b and *eif3h-1* mutants due to defects in reinitiation at uORFs are largely similar to auxin-related developmental defects (Zhou *et al,* 2010). Thus, TOR can play an important role in modulating auxin responses during plant development. Further studies are needed to understand the roles of ROP2 in TOR activation as well as to identify other TOR effectors in plants.

2.2.5 Materials and Methods

Cell shape analysis and chemical treatment

Interdigitation analysis of *Arabidopsis* pavement cells was performed as described in the Appendix Supplementary Methods. For microscopic observation of GFP-TOR in endosomes, root cells of *GFP-TOR* transgenic plants were treated with 90 µM brifeldin A (BFA; Sigma) for 30 min and stained with 10 µM FM4-64 dye (Sigma).

Time-course experiments

To study the dynamics of TOR-P accumulation upon auxin treatment *in planta* (Fig 3), 7-dag Col0 WT and rop2rop6ROP4 RNAi transgenic seedlings cultured on MS agar plates were transferred into fresh liquid MS medium and incubated for 2–3 hours at 24°C under constant light conditions to avoid additional stress. Seedlings were then transferred to fresh liquid MS medium with or without 100 nM NAA and samples were harvested at 0, 30, 60, 90 and 120 min after induction. The samples for TOR-P analysis were taken 8 hours after incubation with or without 100 nM NAA, or 1µM AZD. TOR levels and phosphorylation status were determined by western blot with specific antibodies.

***In vitro* kinase assay**

Immunoprecipitated GFP-TOR complexes from *GFP-TOR* and *GFP-TOR/CA-ROP2* 7 dag transgenic seedlings were compared for their phosphotransferase activity towards rec S6K1 as a substrate. Kinase reactions were stopped after 0, 5, 10, 15, and 20 min of incubation at 30°C, and incorporation of phosphate was analyzed by immunoblotting with anti-mS6K1-P-T389 antibodies (Cell Signaling). For TOR immunoprecipitation details, see Appendix Supplementary Methods.

Polyribosome analysis

Polysomes were isolated from 7 dag *Arabidopsis* wild-type Col-0 WT and *CA-ROP2* seedlings grown on MS agar plates supplemented (or not) with 0.5 µM AZD-8055. To monitor *ARFs*, *bZIP11*, *GAPC2* and *ACTIN* mRNA loading into polysomes, total RNA isolated from polysomal fractions as indicated were analyzed by qRT-PCR. mRNAs were monitored in sub/ polysomal fractions, and transcript levels for each mRNA were normalized to maximum mean in monosomal fraction (set as 100%). For gene-specific primer sequences, see Appendix Supplementary Methods.

Protoplast assays

Transient expression was analysed in *Arabidopsis* mesophyll protoplasts from WT and *CA-R0P2* 2-week transgenic seedlings. For plasmid construction, transfection and qRT-PCR protocol details, see Appendix Supplementary Methods.

Yeast two-hybrid assay

Yeast two-hybrid protein interaction assays were performed according to Park *et al,* (2001) Constructs containing NTOR, CTOR and TOR fused to the GAL4 AD-domain and ROP1-6, CA-ROP2 and DN-ROP2 fused to the BD-domain were co-transformed into AH109 cells. Transformants were selected onto SD-Leu-Trp plates. Surviving yeast colonies were picked as primary positives and transferred on SD-Leu-Trp-His selection plates to score protein interaction. The assays and dilutions were performed in triplicate. For plasmid construction details, see Appendix Supplementary Methods.

GST pull-down assay

To analyze activation of ROP2 *in vivo* in total plant extracts treated or not with 1 µM AZD-8055. We utilized a biochemical assay, in which GTP-bound active ROP2 was pulled down by use of GST-Ric1 attached to glutathione-agarose beads.

Binding of TOR to GST-fused Sar1b, or Rheb, or ROP2, or ROP2ΔII, or ROP2Δ(I+II) or GST alone, respectively (Fig 1D, H and Fig EV1C) was carried out as described in Appendix Supplementary Methods.

2.2.6 Acknowledgments

We are grateful to Y. Hu for *cuf1D* and Y. Zhao for *yuc1D* lines, A. Komar (*DAPCEL Inc*) for recombinant TOR design, and N. Baumberger for helpful assistance in protein analysis. We thank A. von Arnim for comments on the manuscript and C. Meyer for helpful discussions. This work was supported by French Agence Nationale de la Recherché—BLAN-2011_BSV6 010 03 and ANR-14-CE19-0007—funding to L.R.

Author contributions

MS and LR conceived the project. MS performed the experiments and data analysis. LR and MS wrote the paper. JM, OS and AG participated in experiments. ZY provided material, JC and PH performed MS-MS and data analysis.

Conflict on interest - The authors declare that they have no conflict of interest.

2.2.7 References

Andreeva AV, Zheng H, Saint-Jore CM, Kutuzov MA, Evans DE & Hawes CR (2000) Organization of transport from endoplasmic reticulum to Golgi in higher plants. *Biochem. Soc. Trans* 28: 505–512

Bar-Peled L & Sabatini DM (2014) Regulation of mTORC1 by amino acids. *Trends Cell Biol* 24: 400–406

Bar-Peled M & Raikhel NV (1997) Characterization of AtSEC12 and AtSAR1. Proteins likely involved in endoplasmic reticulum and Golgi transport. *Plant Physiol.* 114: 315–324

Beltrán-Peña E, Aguilar R, Ortíz-López A, Dinkova TD & De Jiménez ES (2002) Auxin stimulates S6 ribosomal protein phosphorylation in maize thereby affecting protein synthesis regulation. *Physiol Plant* 115: 291–297

Berken A & Wittinghofer A (2008) Structure and function of Rho-type molecular switches in plants. *Plant Physiol. Biochem.* 46: 380–393

Betz C & Hall MN (2013) Where is mTOR and what is it doing there? *J. Cell Biol.* 203: 563–574

Chiang GG & Abraham RT (2005) Phosphorylation of mammalian target of rapamycin (mTOR) at Ser-2448 is mediated by p70S6 kinase. *J. Biol. Chem.* 280: 25485–25490

Chresta CM, Davies BR, Hickson I, Harding T, Cosulich S, Critchlow SE, Vincent JP, Ellston R, Jones D, Sini P, James D, Howard Z, Dudley P, Hughes G, Smith L, Maguire S, Hummersone M, Malagu K, Menear K, Jenkins R, et al (2010) AZD8055 is a potent, selective, and orally bioavailable ATP-competitive mammalian target of rapamycin kinase inhibitor with in vitro and in vivo antitumor activity. *Cancer Res.* 70: 288–298

Cui D, Zhao J, Jing Y, Fan M, Liu J, Wang Z, Xin W & Hu Y (2013) The Arabidopsis IDD14, IDD15, and IDD16 Cooperatively Regulate Lateral Organ Morphogenesis and Gravitropism by Promoting Auxin Biosynthesis and Transport. *PLoS Genet.* 9: e1003759

Cybulski N & Hall MN (2009) TOR complex 2: a signaling pathway of its own. *Trends Biochem. Sci.* 34: 620–627

Deng K, Yu L, Zheng X, Zhang K, Wang W, Dong P, Zhang J & Ren M (2016) Target of Rapamycin Is a Key Player for Auxin Signaling Transduction in Arabidopsis. *Front Plant Sci* 7: 291

Deprost D, Yao L, Sormani R, Moreau M, Leterreux G, Nicolai M, Bedu M, Robaglia C & Meyer C (2007) The Arabidopsis TOR kinase links plant growth, yield, stress resistance and mRNA translation. *EMBO Rep* 8: 864–870

Dhonukshe P, Aniento F, Hwang I, Robinson DG, Mravec J, Stierhof Y-D & Friml J (2007) Clathrin-mediated constitutive endocytosis of PIN auxin efflux carriers in Arabidopsis. *Current Biology* 17: 520–527

Dhonukshe P, Tanaka H, Goh T, Ebine K, Mähönen AP, Prasad K, Blilou I, Geldner N, Xu J,

Uemura T, Chory J, Ueda T, Nakano A, Scheres B & Friml J (2008) Generation of cell polarity in plants links endocytosis, auxin distribution and cell fate decisions. *Nature* 456: 962–966

Dobrenel T, Marchive C, Sormani R, Moreau M, Mozzo M, Montané MH, Menand B, Robaglia C & Meyer C (2011) Regulation of plant growth and metabolism by the TOR kinase. *Biochem. Soc. Trans.* 39: 477–481

Fu Y, Gu Y, Zheng Z, Wasteneys G & Yang Z (2005) Arabidopsis interdigitating cell growth requires two antagonistic pathways with opposing action on cell morphogenesis. *Cell* 120: 687–700

Fu Y, Li H & Yang Z (2002) The ROP2 GTPase controls the formation of cortical fine F-actin and the early phase of directional cell expansion during Arabidopsis organogenesis. *Plant Cell* 14: 777–794

Fu Y, Xu T, Zhu L, Wen M & Yang Z (2009) A ROP GTPase signaling pathway controls cortical microtubule ordering and cell expansion in Arabidopsis. *Curr. Biol.* 19: 1827–1832

Hara K, Maruki Y, Long X, Yoshino K-I, Oshiro N, Hidayat S, Tokunaga C, Avruch J & Yonezawa K (2002) Raptor, a binding partner of target of rapamycin (TOR), mediates TOR action. *Cell* 110: 177–189

Hinnebusch A (2006) eIF3: a versatile scaffold for translation initiation complexes. *Trends Biochem. Sci.* 31: 553–562

Holz MK, Ballif BA, Gygi SP & Blenis J (2005) mTOR and S6K1 mediate assembly of the translation preinitiation complex through dynamic protein interchange and ordered phosphorylation events. *Cell* 123: 569–580

Jones B, Jones EL, Bonney SA, Patel HN, Mensenkamp AR, Eichenbaum-Voline S, Rudling M, Myrdal U, Annesi G, Naik S, Meadows N, Quattrone A, Islam SA, Naoumova RP, Angelin B, Infante R, Levy E, Roy CC, Freemont PS, Scott J, et al (2003) Mutations in a Sar1 GTPase of COPII vesicles are associated with lipid absorption disorders. *Nature Genetics* 34: 29–31

Kim TH, Kim BH, Yahalom A, Chamovitz DA & Arnim von AG (2004) Translational regulation via 5' mRNA leader sequences revealed by mutational analysis of the Arabidopsis translation initiation factor subunit eIF3h. *Plant Cell* 16: 3341–3356

Kozak M (2001) Constraints on reinitiation of translation in mammals. *Nucleic Acids Res* 29: 5226–5232

Li H, Shen JJ, Zheng ZL, Lin Y & Yang Z (2001) The Rop GTPase switch controls multiple developmental processes in Arabidopsis. *Plant Physiol.* 126: 670–684

Li H, Wu G, Ware D, Davis KR & Yang Z (1998) Arabidopsis Rho-related GTPases: differential gene expression in pollen and polar localization in fission yeast. *Plant Physiol.* 118: 407–417

Loewith R, Jacinto E, Wullschleger S, Lorberg A, Crespo JL, Bonenfant D, Oppliger W,

Jenoe P & Hall MN (2002) Two TOR complexes, only one of which is rapamycin sensitive, have distinct roles in cell growth control. *Molecular Cell* 10: 457–468

Long X, Lin Y, Ortiz-Vega S, Yonezawa K & Avruch J (2005) Rheb Binds and Regulates the mTOR Kinase. *Current Biology* 15: 702–713

Ma XM & Blenis J (2009) Molecular mechanisms of mTOR-mediated translational control. *Nature Reviews Molecular Cell Biology* 10: 307–318

Mahfouz MM, Kim S, Delauney AJ & Verma DP (2006) Arabidopsis TARGET OF RAPAMYCIN interacts with RAPTOR, which regulates the activity of S6 kinase in response to osmotic stress signals. *Plant Cell* 18: 477–490

Menand B, Desnos T, Nussaume L, Berger F, Bouchez D, Meyer C & Robaglia C (2002) Expression and disruption of the Arabidopsis TOR (target of rapamycin) gene. *Proceedings of the National Academy of Sciences* 99: 6422–6427

Miyawaki KN & Yang Z (2014) Extracellular signals and receptor-like kinases regulating ROP GTPases in plants. *Front Plant Sci* 5: 449

Montane MH & Menand B (2013) ATP-competitive mTOR kinase inhibitors delay plant growth by triggering early differentiation of meristematic cells but no developmental patterning change. *J. Exp. Bot.*

Moreau M, Azzopardi M, Clément G, Dobrenel T, Marchive C, Renne C, Martin-Magniette M-L, Taconnat L, Renou J-P, Robaglia C & Meyer C (2012) Mutations in the Arabidopsis homolog of LST8/GβL, a partner of the target of Rapamycin kinase, impair plant growth, flowering, and metabolic adaptation to long days. *Plant Cell* 24: 463–481

Nagawa S, Xu T, Lin D, Dhonukshe P, Zhang X, Friml J, Scheres B, Fu Y & Yang Z (2012) ROP GTPase-dependent actin microfilaments promote PIN1 polarization by localized inhibition of clathrin-dependent endocytosis. *PLoS Biol.* 10: e1001299

Oda Y & Fukuda H (2014) Emerging roles of small GTPases in secondary... [Front Plant Sci. 2014] - PubMed - NCBI. *Front Plant Sci* 5: 428

Park HS, Himmelbach A, Browning KS, Hohn T & Ryabova LA (2001) A plant viral 'reinitiation' factor interacts with the host translational machinery. *Cell* 106: 723–733

Ren H, Dang X, Yang Y, Huang D, Liu M, Gao X & Lin D (2016) SPIKE1 Activates ROP GTPase to Modulate Petal Growth and Shape. *Plant Physiol.* 172: 358–371

Ren M, Venglat P, Qiu S, Feng L, Cao Y, Wang E, Xiang D, Wang J, Alexander D, Chalivendra S, Logan D, Mattoo A, Selvaraj G & Datla R (2012) Target of rapamycin signaling regulates metabolism, growth, and life span in Arabidopsis. *Plant Cell* 24: 4850–4874

Richter S, Geldner N, Schrader J, Wolters H, Stierhof Y-D, Rios G, Koncz C, Robinson DG & Jürgens G (2007) Functional diversification of closely related ARF-GEFs in protein secretion and recycling. *Nature* 448: 488–492

Rosado A, Li R, van de Ven W, Hsu E & Raikhel NV (2012) Arabidopsis ribosomal proteins control developmental programs through translational regulation of auxin response factors. *Proc. Natl. Acad. Sci. U.S.A.* 109: 19537–19544

Ruggero D & Pandolfi PP (2003) Does the ribosome translate cancer? *Nat Rev Cancer* 3: 179–192

Rutherford S & Moore I (2002) The Arabidopsis Rab GTPase family: another enigma variation. *Curr Opin Plant Biol* 5: 518–528

Saci A, Cantley LC & Carpenter CL (2011) Rac1 Regulates the Activity of mTORC1 and mTORC2 and Controls Cellular Size. *Molecular Cell* 42: 50–61

Sancak Y, Peterson TR, Shaul YD, Lindquist RA, Thoreen CC, Bar-Peled L & Sabatini DM (2008) The Rag GTPases bind raptor and mediate amino acid signaling to mTORC1. *Science* 320: 1496–1501

Schepetilnikov M, Dimitrova M, Mancera-Martínez E, Geldreich A, Keller M & Ryabova LA (2013) TOR and S6K1 promote translation reinitiation of uORF-containing mRNAs via phosphorylation of eIF3h. *EMBO J.* 32: 1087–1102

Schepetilnikov M, Kobayashi K, Geldreich A, Caranta C, Robaglia C, Keller M & Ryabova LA (2011) Viral factor TAV recruits TOR/S6K1 signalling to activate reinitiation after long ORF translation. *EMBO J.* 30: 1343–1356

Shimobayashi M & Hall MN (2014) Making new contacts: the mTOR network in metabolism and signalling crosstalk. *Nature Publishing Group* 15: 155–162

Sonenberg N & Hinnebusch AG (2009) Regulation of translation initiation in eukaryotes: mechanisms and biological targets. *Cell* 136: 731–745

Sorek N, Gutman O, Bar E, Abu-Abied M, Feng X, Running MP, Lewinsohn E, Ori N, Sadot E, Henis YI & Yalovsky S (2011) Differential effects of prenylation and s-acylation on type I and II ROPS membrane interaction and function. *Plant Physiol.* 155: 706–720

Tao LZ (2002) Plant Rac-Like GTPases Are Activated by Auxin and Mediate Auxin-Responsive Gene Expression. *Plant Cell* 14: 2745–2760

Tee AR & Blenis J (2005) mTOR, translational control and human disease. *Semin. Cell Dev. Biol.* 16: 29–37

Turck F, Zilbermann F, Kozma SC, Thomas G & Nagy F (2004) Phytohormones participate in an S6 kinase signal transduction pathway in Arabidopsis. *Plant Physiol.* 134: 1527–1535

Vanneste S & Friml J (2009) Auxin: a trigger for change in plant development. *Cell* 136: 1005–1016

Wiese A, Elzinga N, Wobbes B & Smeekens S (2004) A conserved upstream open reading frame mediates sucrose-induced repression of translation. *Plant Cell* 16: 1717–1729

Winge P, Brembu T & Bones AM (1997) Cloning and characterization of rac-like cDNAs

from Arabidopsis thaliana. *Plant Mol. Biol.* 35: 483–495

Wu G, Gu Y, Li S & Yang Z (2001) A genome-wide analysis of Arabidopsis Rop-interactive CRIB motif-containing proteins that act as Rop GTPase targets. *Plant Cell* 13: 2841–2856

Wu G, Li H & Yang Z (2000) Arabidopsis RopGAPs are a novel family of rho GTPase-activating proteins that require the Cdc42/Rac-interactive binding motif for rop-specific GTPase stimulation. *Plant Physiol.* 124: 1625–1636

Xiong Y & Sheen J (2012) Rapamycin and glucose-target of rapamycin (TOR) protein signaling in plants. *J Biol Chem* 287: 2836–2842

Xiong Y, McCormack M, Li L, Hall Q, Xiang C & Sheen J (2013) Glucose-TOR signalling reprograms the transcriptome and activates meristems. *Nature* 496: 181–186

Xu T, Dai N, Chen J, Nagawa S, Cao M, Li H, Zhou Z, Chen X, De Rycke R, Rakusová H, Wang W, Jones AM, Friml J, Patterson SE, Bleecker AB & Yang Z (2014) Cell surface ABP1-TMK auxin-sensing complex activates ROP GTPase signaling. *Science* 343: 1025–1028

Xu T, Wen M, Nagawa S, Fu Y, Chen J-G, Wu M-J, Perrot-Rechenmann C, Friml J, Jones AM & Yang Z (2010) Cell Surface- and Rho GTPase-Based Auxin Signaling Controls Cellular Interdigitation in Arabidopsis. *Cell* 143: 99–110

Zeenko V & Gallie DR (2005) Cap-independent translation of tobacco etch virus is conferred by an RNA pseudoknot in the 5'-leader. *J. Biol. Chem.* 280: 26813–26824

Zhou F, Roy B & Arnim von AG (2010) Translation reinitiation and development are compromised in similar ways by mutations in translation initiation factor eIF3h and the ribosomal protein RPL24. *BMC Plant Biology* 10: 193

Zhou F, Roy B, Dunlap JR, Enganti R & Arnim von AG (2014) Translational control of Arabidopsis meristem stability and organogenesis by the eukaryotic translation factor eIF3h. - PubMed - NCBI. *PLoS ONE* 9: e95396

Zinzalla V, Stracka D, Oppliger W & Hall MN (2011) Activation of mTORC2 by association with the ribosome. *Cell* 144: 757–768

Zoncu R, Efeyan A & Sabatini DM (2011) mTOR: from growth signal integration to cancer, diabetes and ageing. *Nature Publishing Group* 12: 21–35

2.2.8 Figure legends

Figure 1. Identification of ROP2 as a binding partner of TOR

A Schematic representation of *Arabidopsis* TOR (S2424 phosphorylation site indicated) and ROP functional domains (G domains, the positions of Q64 and D121 and C-terminal basic K/R-CaaL motifs are indicated).

B Phylogenetic tree of 11 Rop family member proteins. ROPs 2, 4 and 6 are classified in a subgroup (red).

C ROP2, ROP4 and ROP6 identified as putative TOR interactors by the yeast two-hybrid (Y2H) system. BD-ROPs 1–6 were assayed for interaction with AD-TOR. Equal OD_{600} units and 1/10 and 1/100 dilutions were spotted from left to right.

D GST pull-down assay—ROP2-, Rheb-, Sar1b-tagged GST, and GST alone were assayed for interaction with recombinant TOR as indicated on the left panel. GST-fusion protein bound (B) and unbound (U) fractions were stained by Coomassie blue.

E Immunoprecipitation (IP) experiments with anti-GFP-Trap magnetic beads on crude extracts of *GFP-TOR* and *GFP* transgenic plants; for western blots, 10% of the input and 100% of IP fractions were analyzed with anti-GFP, -TOR and -ROP antibodies (ABs).

F Endogenous TOR was immunoprecipitated from *Arabidopsis* extract with anti-TOR ABs (IP) and assayed for association with ROPs by immunoblotting. 10% of the input, 100% of IP or normal rabbit serum (NRS) were analyzed by anti-ROP antibodies.

G Y2H: TOR and its N-terminal domain (NTOR) interact with ROP2 and dominant negative ROP2 (DN-ROP2). AD-TOR, -NTOR and -CTOR were assayed for interaction with BD-ROP2 or -ROP2 mutants -CA-ROP2 and -DN-ROP2 as indicated.

H *Left panel* GST pull-down assay: ROP2-, DN-ROP2-, CA-ROP2- tagged GST and GST alone were assayed for interaction with recombinant TOR. Fractions were stained by Coomassie blue. *Right panel* Quantification of TOR binding to GST-fusion proteins. The value for TOR binding to GST-ROP2 was set as 100%.

Data information: (H) Statistical analysis is based on one-way ANOVA test. Data are presented as mean +/-SEM. ($P<0.05$, $n=3$).

Figure 2. TOR signaling is up-regulated in Arabidopsis with elevated active ROP2 levels

A Rosettes representative of WT, *cuf1D,* and *CA-ROP2* plants.

B GST-Ric1 (or GST) pull-down IP assays targeting active GTP-bound ROPs in WT, *cuf1D* and *CA-ROP2* seedlings. Active ROPs and total ROPs were detected with an anti-ROP ABs. GST-Ric1 and a loading control (LC) were stained with Coomassie blue.

C The level of endogenous mRNAs, including *actin* (*ACT*), *glycerol-3-phosphate dehydrogenase C2* (*GAPC2*), expressed protein (*EXP*) and others indicated below the bar graphs in WT and *cuf1D* was examined by qPCR. The RNA value in WT extracts was set as 100%.

D TOR and S6K1 levels and their phosphorylation status in either *cuf1D* and WT, or *CA-ROP2* and WT were analyzed by immunoblot with anti-*At*TOR ABs (anti-TOR), anti-(mTOR-S2448-P) and anti-mS6K1, anti-(mS6K1-T389-P) ABs, respectively. The density of bands on western blots were quantified and WT values were set as 100%.

E *Upper panels* Analysis of active ROPs by GST-Ric1 IP in WT and *CA-ROP2* extracts from 7 dag seedlings grown with or without 1 µM AZD-8055. Total ROPs and GST-Ric1 bound ROPs were detected using anti-ROP antibodies. GST-Ric1 and LC were stained with Coomassie blue. Input: Total ROPs, TOR total and its phosphorylation levels were analyzed by western blot. *Left panel* Quantification of ratio between ROPs-GTP and GST-Ric1. The value for ROPs-GTP in WT and *CA-ROP2* was set as 1.

Data information: (C) Values, expressed in arbitrary units, are averages of two technical replicates, and error bars indicate +/-SD. (E) Statistical analysis is based on unpaired t-test (n=3), ns, non-significant.

Figure 3. ROP2 mediates auxin signaling towards TOR

A Rosettes representative of WT, *rop2*, *rop2 rop6*, and *rop2 rop6 ROP4 RNAi* plants.

B The level of endogenous *ROP* mRNAs in different ROP-deficient plants were examined by a semiquantitative RT-PCR.

C Endogenous TOR was immunoprecipitated from WT and ROP-deficient *Arabidopsis* extracts by immunoblotting with anti-TOR ABs (IP) and assayed for association with ROPs. 10% of the input and 100% of IP were analyzed by anti-ROP antibodies.

D Time-course of TOR and TOR-P accumulation in extracts from 7-dag seedlings before (0 min) and after transfer to medium with NAA analysed by immunoblot with anti-TOR and anti-(mTOR-S2448-P) ABs. The value of TOR-P/TOR at 0 min (no incubation) for each line was set as 1.

Figure 4. GFP-TOR in CA-ROP2 background is highly phosphorylated, functionally and developmentally active

A Rosettes representative of WT, *GFP-TOR*, *CA-ROP2* and *GFP-TOR/CA-ROP2* plants.

B The level of endogenous mRNAs including endogenous TOR (TORend) and both GFP-TOR and TOR end (TOR mix) and others indicated below the bar graphs in *GFP-TOR* and *GFP-TOR/CA-ROP2* was examined by qRT-PCR. The RNA value in *GFP-TOR* extracts was set as 100%.

C Total and active ROP and TOR levels, TOR phosphorylation status in either *GFP-TOR* or *GFP-TOR/CA-ROP2* were analyzed as described in Fig 2B and D, respectively.

D *In vitro* phosphorylation kinetics of recombinant S6K1 (S6K1) using GFP-TOR immunoprecipitated from *GFP-TOR* or *GFP-TOR/CA-ROP2*. S6K1 total and phosphorylation levels were followed by western blot using anti-S6K1-T389-P or anti-S6K1 ABs. Total S6K1 was stained by Coomassie blue.

E Representative images of pavement cell (PC) morphology in the second true leaf of 21-day-old WT plants and the *GFP-TOR*, *CA-ROP2* and *GFP-TOR/CA-ROP2* mutant lines. Box and Whiskers plot *bottom panels*.

Data information: (B) Values, expressed in arbitrary units, are averages of three technical replicates, and error bars indicate SD. (E) Scale bars are 30 □m. Box and Whiskers plot (Tukey-style) of quantitative analysis of cell circularity (*left panel)* and cell sizes (*right panel)* is presented using unpaired t-test. *p<0.05; **p<0.001; ns, non-significant.

Figure 5. ROP2 determines TOR appearance as multiple dots close to the cell periphery in an ROP2 C-terminus-dependent fashion

A *Nicotiana benthamiana* epidermal cells transiently expressing GFP-TOR (*left panel*) and co-transformed (from left to right) with myc-ROP2, or myc-CA-ROP2, or myc-DN-ROP2. Quantitative analysis of GFP-TOR aggregate number (Box and Whiskers plot *left panel*) and sizes (Scatter plot *right panel*).

B Immunoblot analysis with anti-myc or anti-GFP of transiently co-expressed GFP-TOR without or with myc-ROP2, myc-CA-ROP2, or myc-DN-ROP2 in *N. benthamiana* cells.

C–F Fluorescence micrographs showing *N. benthamiana* cells transiently expressing: (C) GFP-TOR; (D) *Upper panels left* GFP-TOR, *central* RFP-ROP2, *right* merged. *Middle*

panels Left GFP-TOR, *central* RFP-CA-ROP2, *right* merged. *Bottom panels left* GFP-TOR, *central* RFP-DN-ROP2, *right* merged; (E) *left* RFP-ROP2, *central* RFP-ROP2-ΔII (CAFL), *right* RFP-ROP2Δ(I+II). (F) *Upper panels left* GFP-TOR, *central* RFP-ROP2, *right* merged. *Middle panels Left* GFP-TOR, *central* RFP-ROP2ΔII, *right* merged. *Bottom panels left* GFP-TOR, *central* RFP-ROP2Δ(I+II), *right* merged.

G Imaging fluorescence assays showing root cells of *Arabidopsis* 7 dag *GFP-TOR* and *GFP-TOR/CA-ROP2* cells.

H Intracellular disribution of TOR and active TOR. Western blot analysis of variuos fractions following microsome isolation from *GFP-TOR* and *GFP-TOR/CA-ROP2*. The total homogenate (total), nuclear fraction pellet (P10), pellet (P30), pellet (P100), supernatant (S100) were analyzed by western blot with corresponsing antibodies.

Data information: (A) Statistical analysis is based on one-way ANOVA test *left panel, p<0.05*; *right panel p<0.0001*. Scale bars are 5 μm (C–*right panel*, D-F), 10 μm (G), 20 μm (A, C–left panel).

Figure 6. TOR localizes to endosomal structures in an ROP2-sensitive fashion

A Co-localization analysis of GFP-TOR and RFP-RabC1 in *N. benthamiana* epidermal cells expressing FLAG-ROP2 (*upper* panels), FLAG-DN-ROP2 (*central panels*) and FLAG-CA-ROP2 (*bottom panels*).

B *35S:RFP-RabC1 Arabidopsis* line transiently expressing GFP-TOR and FLAG-CA-ROP2. *Left* GFP-TOR, *central* RFP-Rab1C, *right* merged.

C *35S:GFP-TOR Arabidopsis* line transiently expressing RFP-RabC1 and FLAG-CA-ROP2. *left* GFP-TOR, *central* RFP-RabC1, *right* merged.

D CLSM images of cells stained with FM4-64 treated with brefeldin A (BFA) in the root elongation zone of *GFP-TOR* 7-dag seedlings. GFP-TOR and FM4-64 were detected in the core of the BFA compartment.

Data information: Scale bars are 5 μm (A–C) and 10 μm (D).

Figure 7. GTP-ROP2 mounts up abundance of uORF-mRNA in polysomes in AZD-8055 sensitive manner

A Statistical analyses of ratio between polysomal and non-polysomal fractions obtained by sucrose gradient fractionation of extracts isolated from WT seedlings and *CA-ROP2* seedlings grown with or without 2-fold reduced concentration of AZD 8055 (0.5 μM).

B uORF (open rectangles) configuration within selected mRNAs.

C Ribosome sedimentation profiling from extracts prepared from WT (*left panel*) and *CA-ROP2* 7-dag seedlings treated (*right panel*) or not (*central panel*) with 0.5 μM AZD-8055. Positions of ribosomal subunits (60S/40S), monosomes (80S) and polysomes are indicated. 18S and 28S rRNA distribution was monitored by agarose gel electrophoresis.

D mRNA association with polyribosomes, 80S and 60S/40S ribosomes was monitored by quantitative PCR (q-PCR) in sucrose gradient fractions and presented as graph bars. The highest value of each selected polysome-bound mRNA among WT, *CA-ROP2* and *CA-ROP2+AZD* was set as 100%.

Data information: Statistical analysis is based on one-way ANOVA test. Data are presented as mean +/-SEM, $p<0.01$ n=3; ns, non-significant (A). Error bars indicate +/-SD of three replicates (D).

Figure 8. CA-ROP2 hops on reinitiation after uORF translation in AZD-8055-sensitive manner

A Phosphorylation of TOR at S2424 is augmented in CA-ROP2-overexpressing versus WT mesophyll protoplasts, and diminished in the presence of 0.5 μM AZD-8055. TOR and its phosphorylation levels were assayed by immunoblotting. The western blot density bands were quantified and WT (*left panel*) or CA-ROP2 (-AZD; *right panel*) values were set as 100%.

B GUS-containing reporters with either short, or uORF-containing (*ARF3* and *ARF5*) 5'-UTRs were used for mesophyll protoplasts transformation. pmonoGFP that contains GFP ORF downstream of Tobacco Etch Virus (TEV) IRES was used as a transfection marker.

C WT and *CA-ROP2* seedlings growing without (*CA-ROP2*) or with 1 μM AZD-8055 (*CA-ROP2+AZD*) were used to prepare mesophyll protoplasts. GUS and GFP functional levels related to the short leader were set at 100%. Both GFP fluorescence and β-glucuronidase hemiluminescence response was analysed in the same 96-well microtiter plate. GUS/GFP ratio were calculated and shown as bars for WT and CA-ROP2 without or with AZD-8055. GUS-containing mRNA levels and integrity were analyzed by sqRT–PCR; GFP levels were also analysed by immunoblotting; LC—loading control. Results shown represent the means obtained in three independent experiments. Quantification of initiation (short leader) and reinitiation (ARF3/ARF5 5'-UTRs) efficiencies for *CA-ROP2* vs WT, and *CA-ROP2* vs *CA-ROP2+AZD-8055*.

D WT mesophyll protoplasts were transfected in addition to pmonoGFP/ pshort-GUS or pARF5-GUS by the vector expressing either myc-tagged ROP2, or CA-ROP2, or DN-ROP2

under the 35S promoter. GUS/GFP ratio related to the short or ARF5 5'-UTRs was taken as 100%. GUS mRNA levels and integrity were analyzed by sqRT–PCR; ROP2 variants—by immunoblotting using anti-myc ABs (bottom panels). Results shown represent the means obtained in three independent experiments. Quantification of reinitiation (ARF5 UTR) vs initiation (short leader) efficiencies without or with ROP2, CA-ROP2 or DN-ROP2 are shown on the left.

Data information: Quantification represents the means +/-SD obtained in three independent experiments.

Figure 9. Putative model of ROP2 function in TOR activation that signals translation reinitiation

TOR was shown to be required for auxin responses, and these can converge through a small GTPase ROP2. Active ROP2 mediates TOR activation and thus controls the abundance of potent proteins in a post-transcriptional manner via selective translation mechanism—reinitiation. ROP2 recycling maintains TOR association with endosome-like structures (see Discussion for details).

2.2.9 Expanded View Figure legends

Figure EV1. Characterization of ROPs 2-6 from Arabidopsis

A ROPs 1–6 transcription profiles were taken from the Genevestigator database (https://www.genevestigator.ethz.ch).

B Alignment of the C-terminal tail patterns from Arabidopsis ROPs 1–6 from Arabidopsis and human RAC1. Two motifs are indicated: basic lysine residues (motif I); a CxxL (x = aliphatic amino acid) geranylgeranylation motif (motif II). Two deletion variants used are indicated by solid lines.

Alignment done in agreement with Blossom 62 and Jonson amino-acid substitution matrixes (similar residues are printed in reverse type).

C GST pull-down assay: ROP2-, ROP2ΔII-, ROP2Δ(I+II)-tagged GST and GST alone were assayed for interaction with recombinant TOR. Fractions were stained by Coomassie blue. *Right panel* Results shown represent the means obtained in three independent experiments. Quantification of TOR binding to GST-fusion proteins (n=3). The value for TOR binding to GST-ROP2 was set as 1.

Figure EV2. TOR phosphorylation at S2424 is elevated in response to auxin and in plants with high endogenous auxin levels

A WT seedlings were treated with either NAA-, or AZD-8055, or TOR was inactivated by AZD-8055 in seedlings treated with NAA during 8 h. Input: Total ROPs, TOR total and its phosphorylation levels were analyzed by western blot. GST-Ric1 and LC were stained with Coomassie blue. TOR levels and its phosphorylation status were analyzed by immunoblot with anti-*At*TOR ABs (anti-TOR) and anti-(mTOR-S2448-P) ABs, respectively. *Bottom* Quantification of ratio between TOR-P and TOR (n=3). The value for TOR-P/TOR in WT was set as 1. *Right panels* Analysis of active ROPs by GST-Ric1 IP in WT and treated extracts. Total ROPs and GST-Ric1 bound ROPs were detected using anti-ROP antibodies. *Bottom* Quantification of ratio between ROPs-GTP and GST-Ric1 (n=3). The value for ROPs-GTP/GST-Ric1 in WT was set as 1.

B Rosettes representative of WT, *yuc1D* and *cuf1D* plants.

C Analysis of active TOR and ROPs-GTP levels in WT, yuc1D and *cuf1D* 7 dag seedlings. Input: Total ROPs, TOR total and its phosphorylation levels were analyzed by western blot. GST-Ric1 and LC were stained with Coomassie blue. *Bottom* Quantification of ratio between TOR-P and TOR (n=3). The value for TOR-P/TOR in WT was set as 1. *Right panels* Analysis of active ROPs by GST-Ric1 IP in seedling extracts. Total ROPs and GST-

Ric1 bound ROPs were detected using anti-ROP antibodies. Quantification of ratio between ROPs-GTP and GST-Ric1 (n=3). The value for ROPs-GTP/GST-Ric1 in WT was set as 1.
Data information: Results shown represent the means obtained in three independent experiments.

Figure EV3. Appearance of GFP-TOR as punctuate dots in response to NAA treatment correlates with an increase of active TOR in microsomes

A Fluorescence micrographs showing N. benthamiana cells transiently expressing: Upper panels left GFP-BD-CVIL—plasma membrane (PM) marker, *central* RFP-ROP2, *right* merged. *Middle panels Left* GFP-BD-CVIL, *central* RFP-ROP2DII, *right* merged. *Bottom panels left* GFP-BD-CVIL, *central* RFP-ROP2Δ(I+II), *right* merged. PM marker consists of green fluorescent protein (GFP) fused to C-terminal polybasic domain (BD) and isoprenylation motif (CVIL).

B Imaging fluorescence assays showing root cells of *Arabidopsis* 7 dag *GFP* and GFP-*TOR*

seedlings before and after treatment with 100 nM NAA.

C Intracellular disribution of TOR and active TOR in WT seedlings before (*left panel*) and after treatment by 100 nM NAA during 8 h *(right panel*). Western blot analysis of variuos fractions—the total homogenate (total), nuclear fraction pellet (P10), 30,000g pellet (P30), 100,000g pellet (P100), 100,000g supernatant (S100).

D *N. benthamiana* cells transiently coexpressing GFP-TOR, or RFP-Golgi, or both with either myc-DN-Sar1b or myc-DN-ROP2.

E Immunoblot analysis with anti-myc ABs of cells.

Data information: Scale bars are 5 μm (A, D); 10 μm (B).

Figure EV4. GFP-TOR specific co-localization with RFP-RabC1 that labels endosomes

Imaging fluorescence assays showing *Nicotiana benthamiana* cells transiently co-expressing FLAGCA-ROP2 with GFP-TOR (*left panels*), and intracellular markers (*central panels*) that specifically label early endosomes (RFP-RabC1), endosomes (RFP-RabE1d), autophagosomes (RFP-ATG8a), 37 peroxisomes (mCherry-peroxi), mitochondria (mCherry-mito), late endosomes (ARF-ARA7), Golgi (GmMan1-tdTomato), (*right*) merged.

Data information: Scale bars are 5 μm.

Figure EV5. Ribosome profiling of uORF-containing mRNA in WT Arabidopsis without or with TOR inhibitor

A The level of heavy polysomes is reduced in WT *Arabidopsis* treated by AZD-8055 (AZD). Extracts prepared from 7-dag seedlings growing without (WT) and with 0.5 µM AZD-8055 on agar plates (WT+AZD) were subjected to velocity sedimentation through sucrose density gradients. Gradients were fractionated while scanning at 254 nm, and the resulting absorbance profiles are shown (WT and WT+AZD). Positions of ribosomal subunits (RS), monosomes (80S) and polysomes are indicated. rRNA distribution was monitored by agarose gel electrophoresis.

B AZD-8055 treatment down-regulates, albeit not significantly, the abundance of *bZIP11* and the already low polysomal levels of *ARF5* mRNA in WT *Arabidopsis*. Distribution of mRNAs—*Actin*, *GAPC2*, *bZIP11*, *ARF3* and *ARF5*—in fractions were analyzed by quantitative PCR (qPCR). The highest value of each polysome-bound mRNA was set as 100%.

C TOR and TOR phosphorylation status was analyzed in polysomes prepared from WT, *CA-ROP2* seedlings and *CA-ROP2* line treated by AZD-8055. Three samples from polysomes and two from 80S and ribosomal subunits were taken to monitor TOR by immunoblotting with anti-TOR (*low panels*) and phospho-TOR with anti-(mTOR-S2448-P) (*central panels*). Data shown are representative of two independent blots.

D qRT-PCR of each mRNA in total extracts. The RNA value in WT extracts *left central panels* and *CA-ROP2 right panel* was set as 100%.

Data information: Error bars indicate +/-SD of three replicates (D).

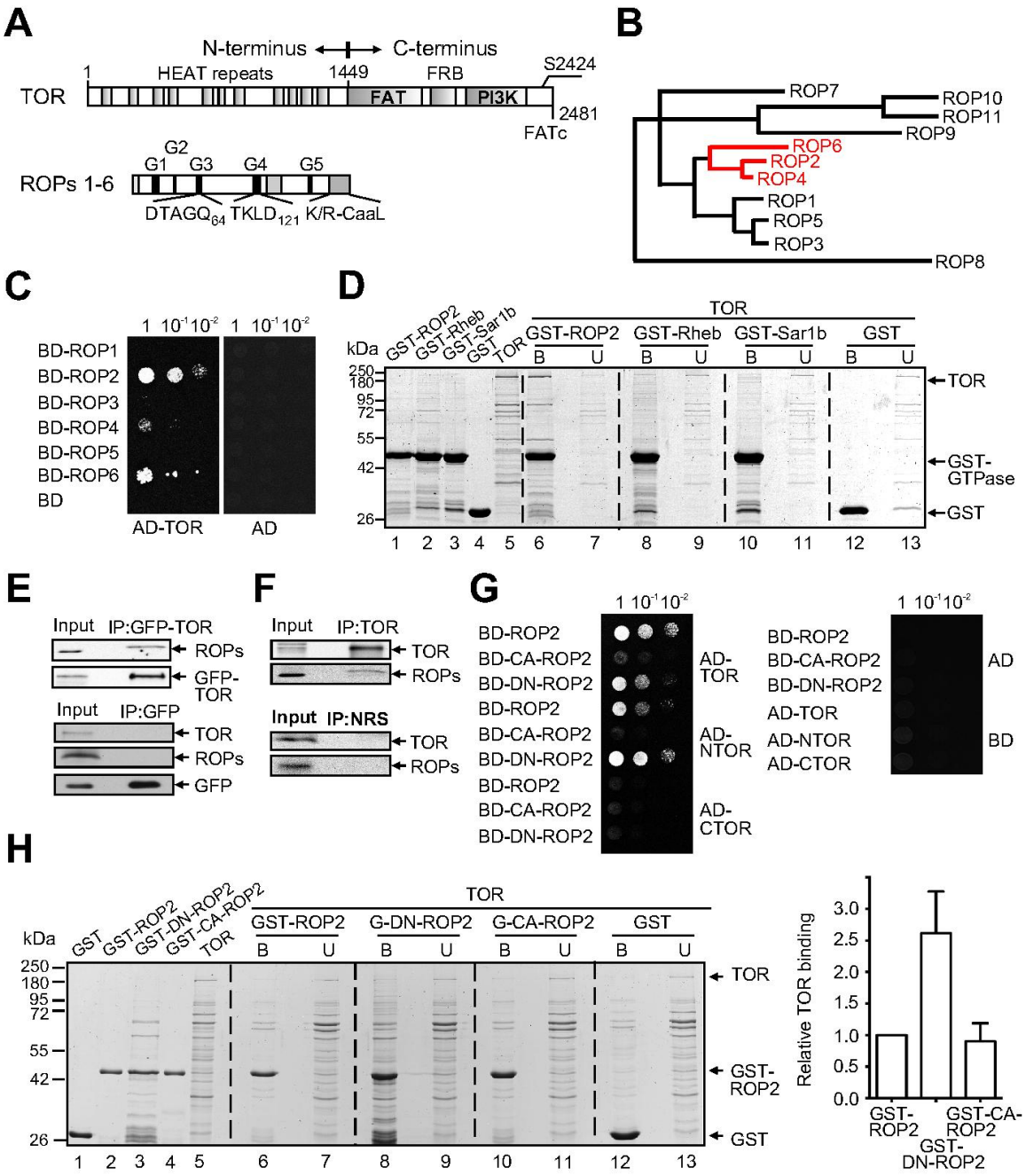
A
N-terminus
C-terminus
TOR
1
HEAT repeats
1449
FRB
S2424
FAT
PI3K
2481
FATc
ROPs 1-6
G1
G2
G3
G4
G5
DTAGQ64
TKLD121
K/R-CaaL
B
ROP7
ROP10
ROP11
ROP9
ROP6
ROP2
ROP4
ROP1
ROP5
ROP3
ROP8
C
BD-ROP1
BD-ROP2
BD-ROP3
BD-ROP4
BD-ROP5
BD-ROP6
BD
AD-TOR
AD
D
kDa
GST-ROP2
GST-Rheb
GST-Sar1b
GST
TOR
B
U
TOR
GST-GTPase
GST
E
Input
IP:GFP-TOR
ROPs
GFP-TOR
IP:GFP
TOR
GFP
F
IP:TOR
IP:NRS
G
BD-ROP2
BD-CA-ROP2
BD-DN-ROP2
AD-TOR
AD-NTOR
AD-CTOR
AD
BD
H
GST-DN-ROP2
GST-CA-ROP2
G-DN-ROP2
G-CA-ROP2
GST-ROP2
Relative TOR binding
GST-CA-ROP2
GST-DN-ROP2

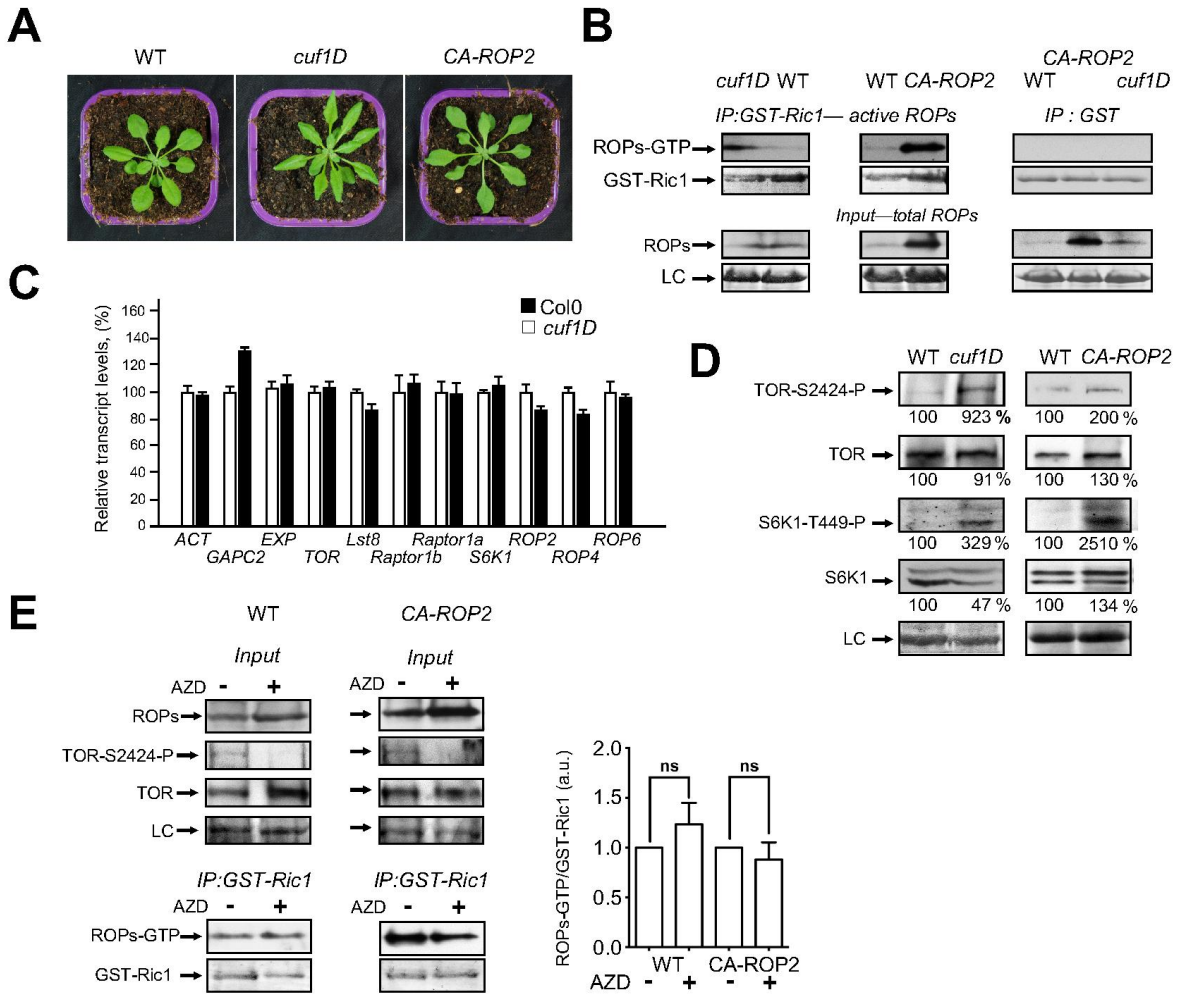
A
WT
cuf1D
CA-ROP2
B
cuf1D WT
WT CA-ROP2
CA-ROP2
WT
cuf1D
IP:GST-Ric1— active ROPs
IP : GST
ROPs-GTP
GST-Ric1
Input—total ROPs
ROPs
LC
C
Col0
cuf1D
Relative transcript levels, (%)
160
140
120
100
80
60
40
20
0
ACT
GAPC2
EXP
TOR
Lst8
Raptor1b
Raptor1a
S6K1
ROP2
ROP4
ROP6
D
WT cuf1D
WT CA-ROP2
TOR-S2424-P
100 923 %
100 200 %
TOR
100 91 %
100 130 %
S6K1-T449-P
100 329 %
100 2510 %
S6K1
100 47 %
100 134 %
LC
E
WT
CA-ROP2
Input
Input
AZD - +
AZD - +
ROPs
TOR-S2424-P
TOR
LC
IP:GST-Ric1
IP:GST-Ric1
AZD - +
AZD - +
ROPs-GTP
GST-Ric1
ROPs-GTP/GST-Ric1 (a.u.)
2.0
1.5
1.0
0.5
0.0
ns
ns
WT
CA-ROP2
AZD - + - +

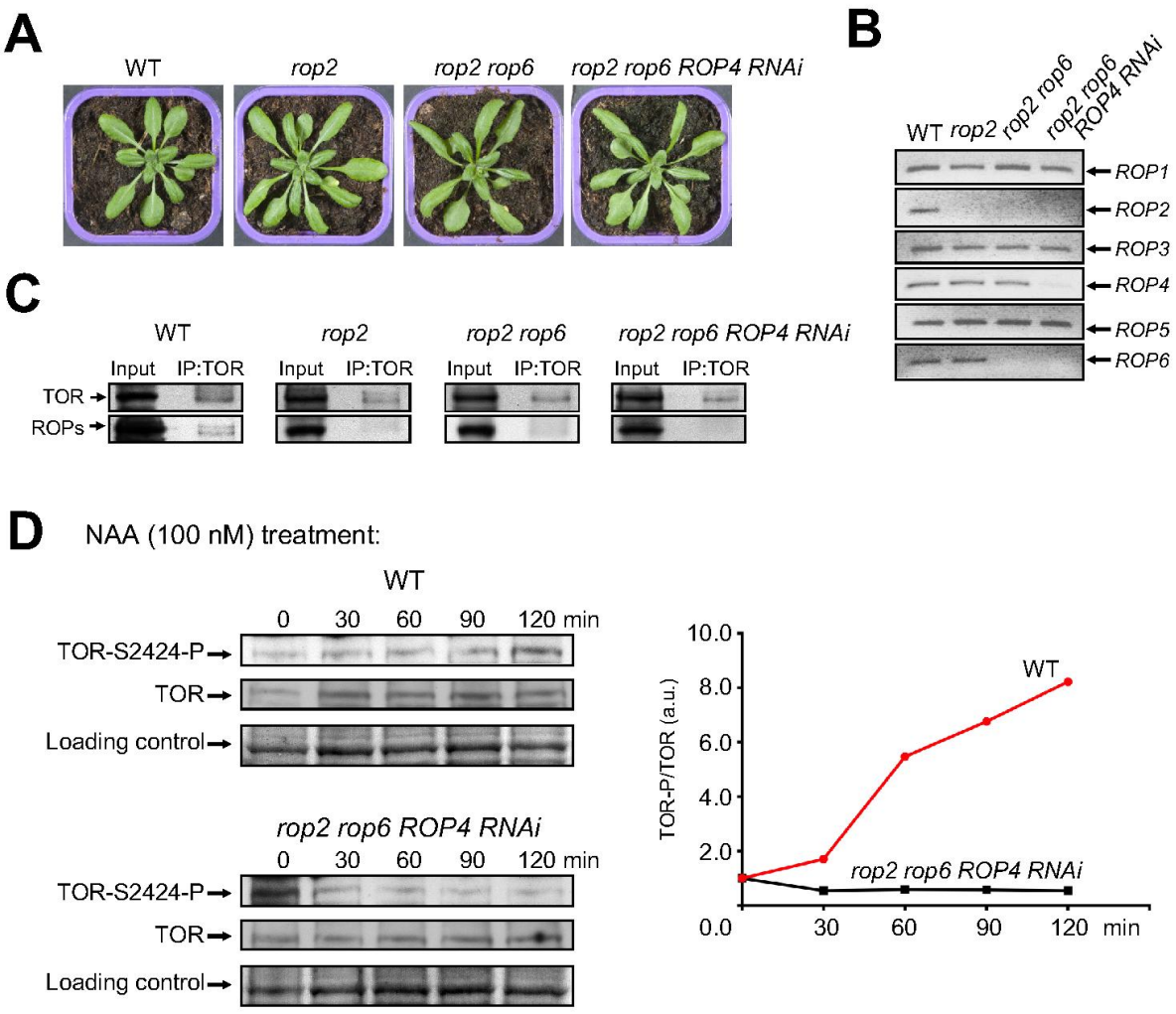
A
WT
rop2
rop2 rop6
rop2 rop6 ROP4 RNAi
B
WT rop2 rop2 rop6 rop2 rop6 ROP4 RNAi
ROP1
ROP2
ROP3
ROP4
ROP5
ROP6
C
WT
rop2
rop2 rop6
rop2 rop6 ROP4 RNAi
Input IP:TOR
TOR
ROPs
D
NAA (100 nM) treatment:
WT
0 30 60 90 120 min
TOR-S2424-P
TOR
Loading control
rop2 rop6 ROP4 RNAi
0 30 60 90 120 min
TOR-S2424-P
TOR
Loading control
TOR-P/TOR (a.u.)
10.0
8.0
6.0
4.0
2.0
0.0
30 60 90 120 min
WT
rop2 rop6 ROP4 RNAi

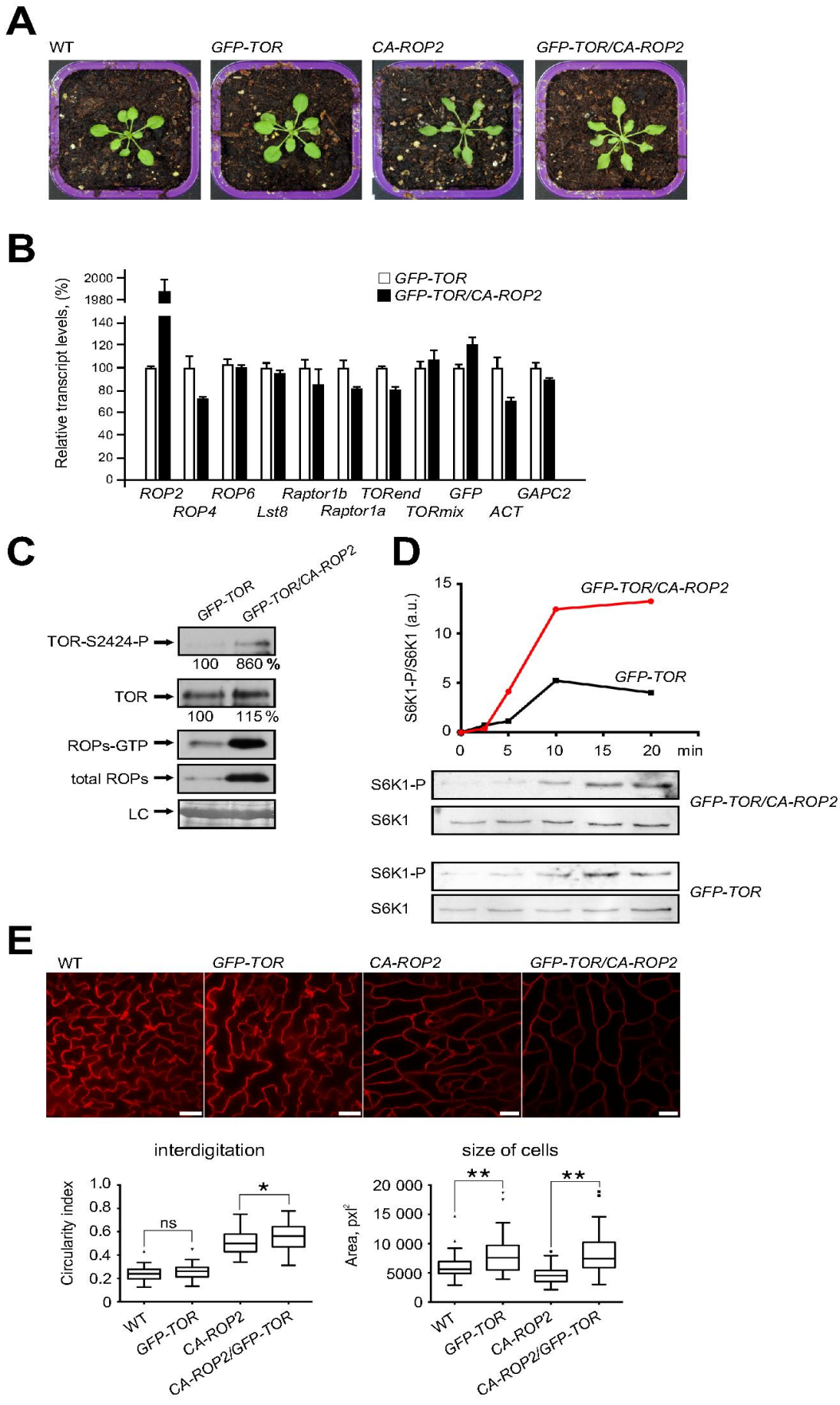
A
WT
GFP-TOR
CA-ROP2
GFP-TOR/CA-ROP2
B
GFP-TOR
GFP-TOR/CA-ROP2
Relative transcript levels, (%)
2000
1980
140
120
100
80
60
40
20
0
ROP2
ROP4
ROP6
Lst8
Raptor1b
Raptor1a
TORend
TORmix
GFP
ACT
GAPC2
C
GFP-TOR
GFP-TOR/CA-ROP2
TOR-S2424-P
100 860 %
TOR
100 115 %
ROPs-GTP
total ROPs
LC
D
GFP-TOR/CA-ROP2
GFP-TOR
S6K1-P/S6K1 (a.u.)
15
10
5
0
0 5 10 15 20 min
S6K1-P
S6K1
GFP-TOR/CA-ROP2
S6K1-P
S6K1
GFP-TOR
E
WT
GFP-TOR
CA-ROP2
GFP-TOR/CA-ROP2
interdigitation
Circularity index
1.0
0.8
0.6
0.4
0.2
0
ns
*
WT
GFP-TOR
CA-ROP2
CA-ROP2/GFP-TOR
size of cells
Area, pxl²
20 000
15 000
10 000
5000
0
**
**
WT
GFP-TOR
CA-ROP2
CA-ROP2/GFP-TOR

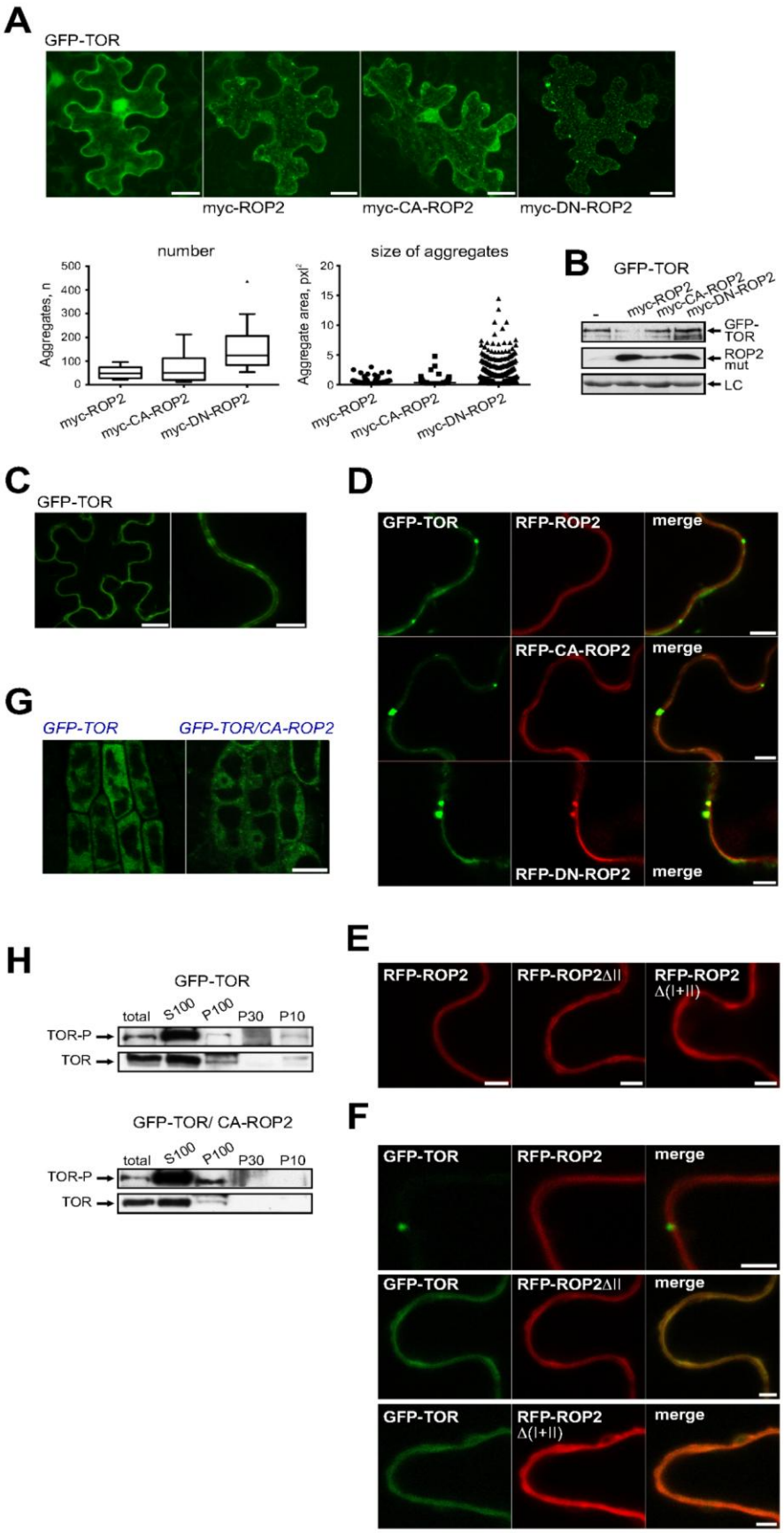
A
GFP-TOR
myc-ROP2
myc-CA-ROP2
myc-DN-ROP2
number
Aggregates, n
size of aggregates
Aggregate area, pxl²
B
GFP-TOR
myc-ROP2
myc-CA-ROP2
myc-DN-ROP2
GFP-TOR
ROP2 mut
LC
C
GFP-TOR
D
GFP-TOR
RFP-ROP2
merge
RFP-CA-ROP2
merge
RFP-DN-ROP2
merge
G
GFP-TOR
GFP-TOR/CA-ROP2
H
GFP-TOR
total
S100
P100
P30
P10
TOR-P
TOR
GFP-TOR/ CA-ROP2
E
RFP-ROP2
RFP-ROP2ΔII
RFP-ROP2 Δ(I+II)
F
GFP-TOR
RFP-ROP2
merge
RFP-ROP2ΔII
RFP-ROP2 Δ(I+II)

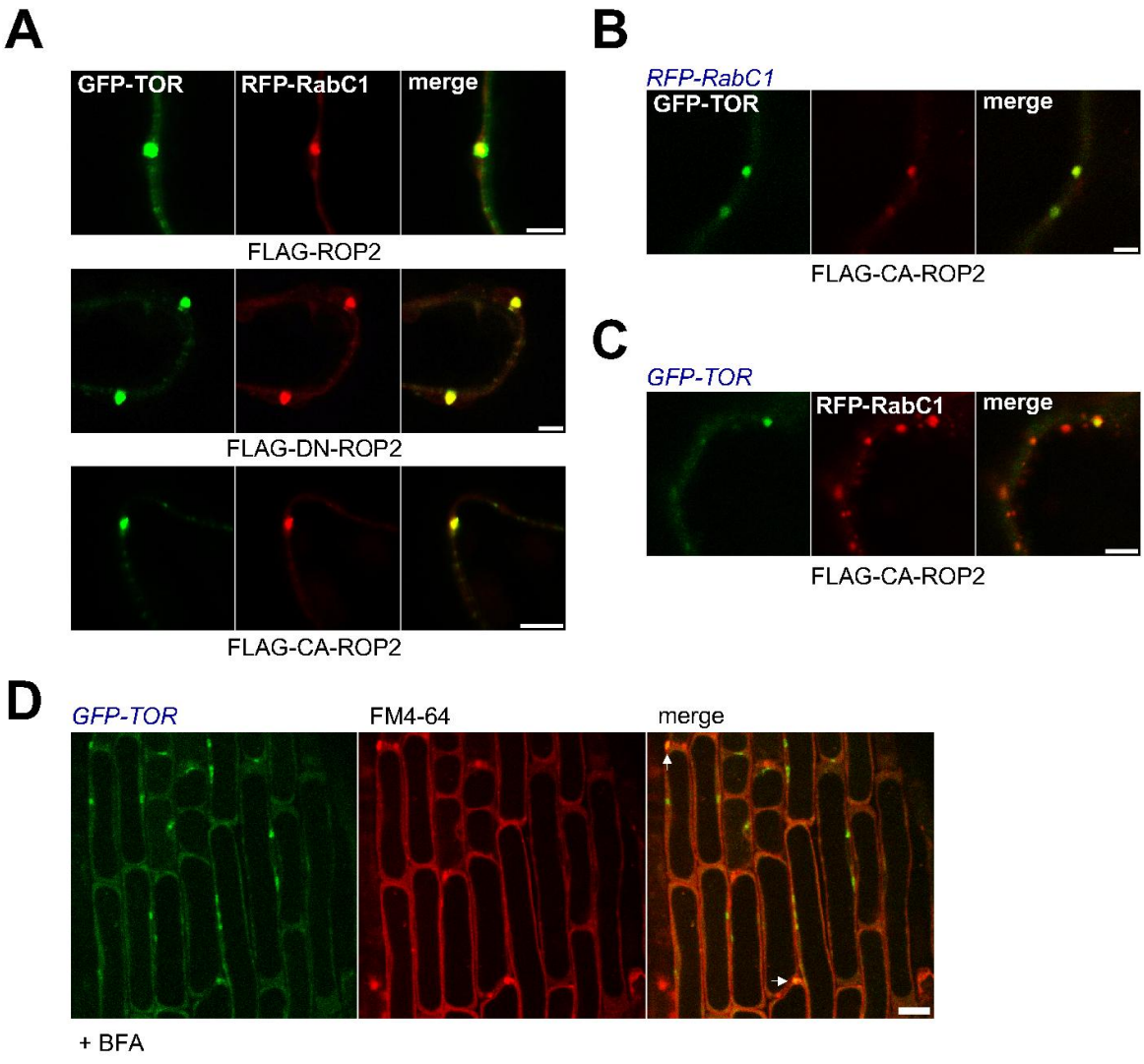
A
GFP-TOR
RFP-RabC1
merge
FLAG-ROP2
FLAG-DN-ROP2
FLAG-CA-ROP2
B
RFP-RabC1
GFP-TOR
merge
FLAG-CA-ROP2
C
GFP-TOR
RFP-RabC1
merge
FLAG-CA-ROP2
D
GFP-TOR
FM4-64
merge
+ BFA

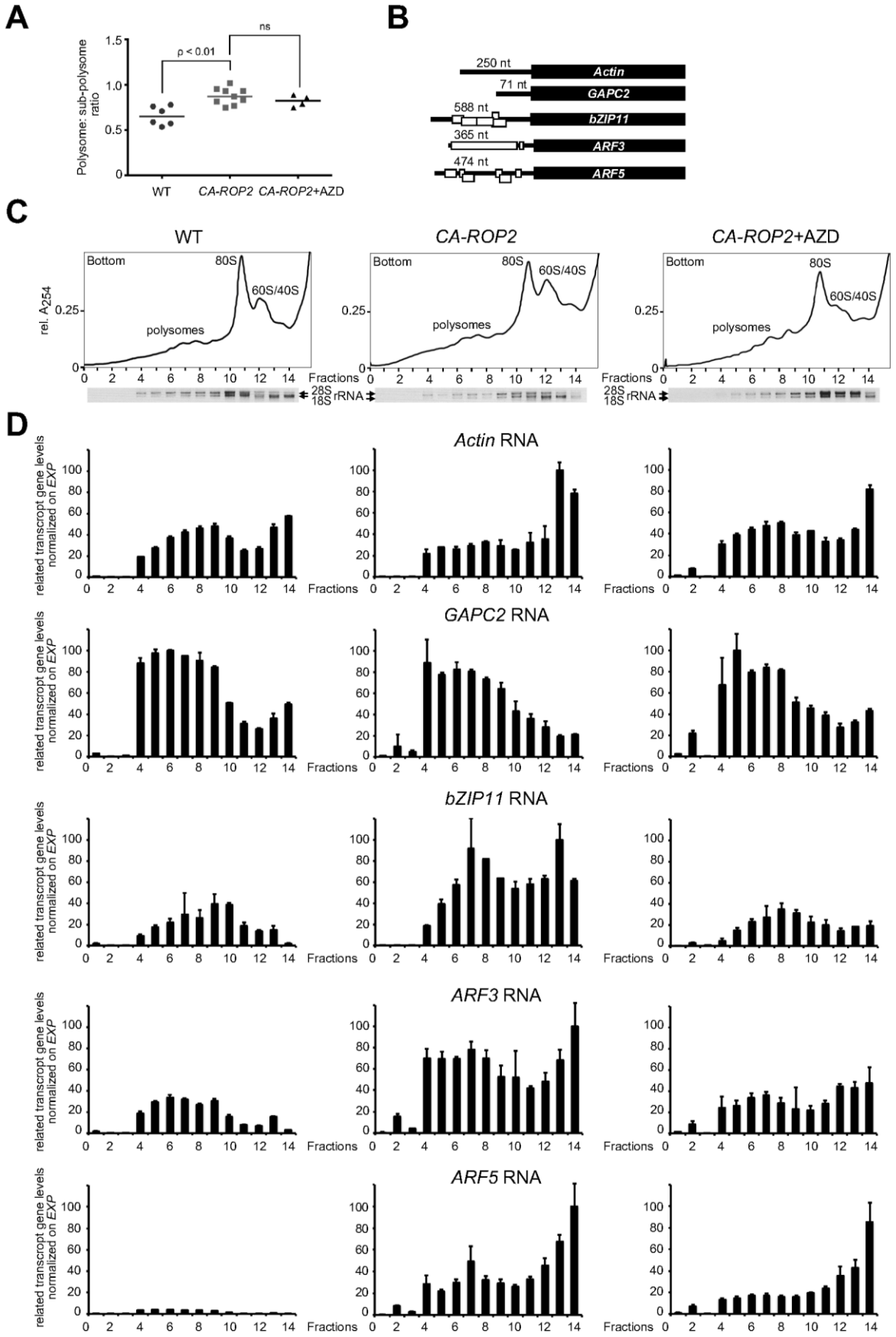
A
Polysome: sub-polysome ratio
ns
p < 0.01
WT
CA-ROP2
CA-ROP2+AZD
B
250 nt
Actin
71 nt
GAPC2
588 nt
bZIP11
365 nt
ARF3
474 nt
ARF5
C
WT
CA-ROP2
CA-ROP2+AZD
Bottom
80S
60S/40S
polysomes
rel. A254
Fractions
28S
18S rRNA
D
Actin RNA
GAPC2 RNA
bZIP11 RNA
ARF3 RNA
ARF5 RNA
related transcript gene levels normalized on EXP

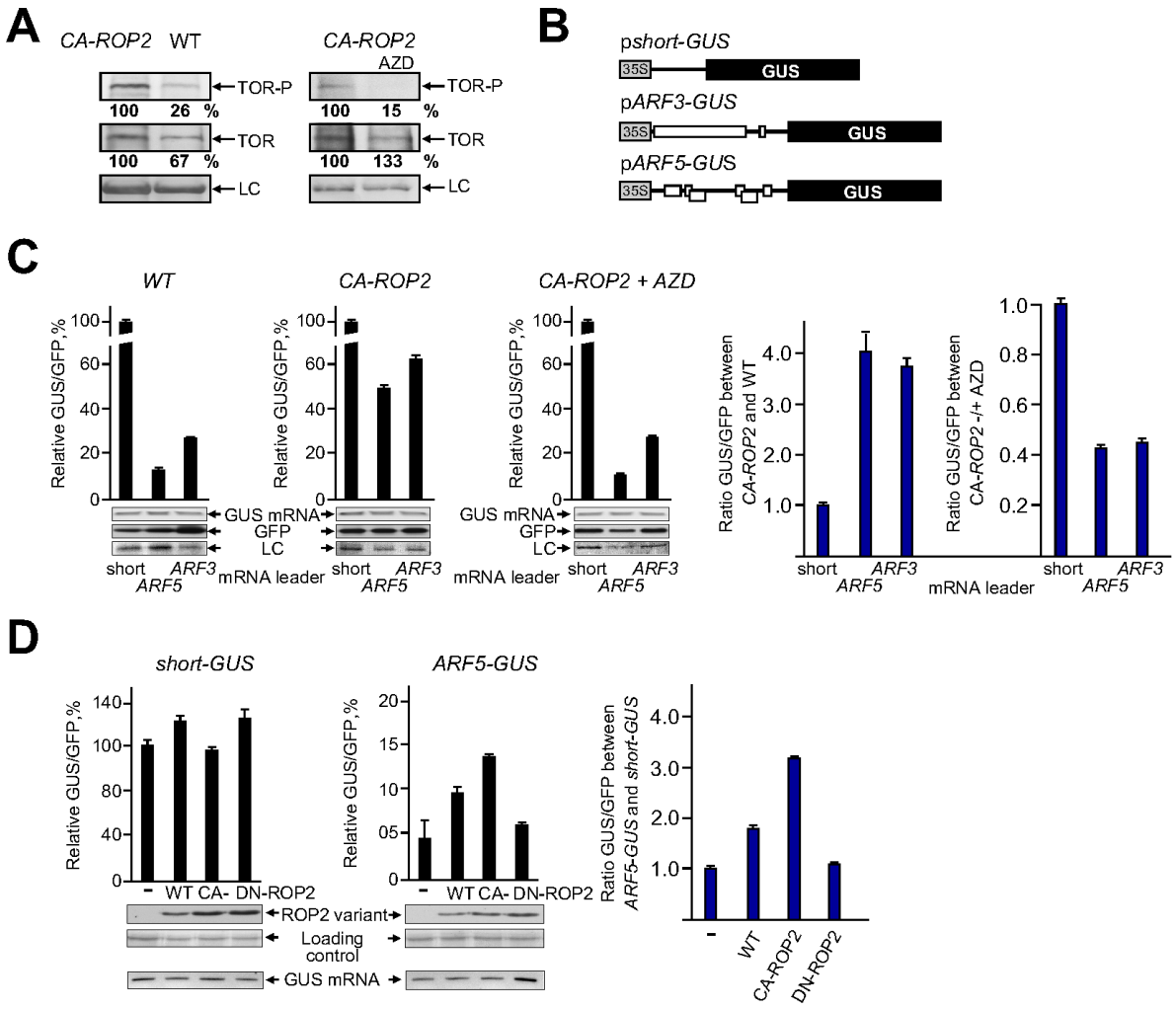
A
CA-ROP2 WT
CA-ROP2 AZD
TOR-P
100 26 %
TOR
100 67 %
LC
100 15 %
100 133 %
B
pshort-GUS
pARF3-GUS
pARF5-GUS
35S
GUS
C
WT
CA-ROP2
CA-ROP2 + AZD
Relative GUS/GFP, %
GUS mRNA
GFP
LC
short
ARF3
ARF5
mRNA leader
Ratio GUS/GFP between CA-ROP2 and WT
Ratio GUS/GFP between CA-ROP2 -/+ AZD
D
short-GUS
ARF5-GUS
Relative GUS/GFP, %
- WT CA- DN-ROP2
ROP2 variant
Loading control
GUS mRNA
Ratio GUS/GFP between ARF5-GUS and short-GUS
WT
CA-ROP2
DN-ROP2

Schepetilnikov et al_Fig.9

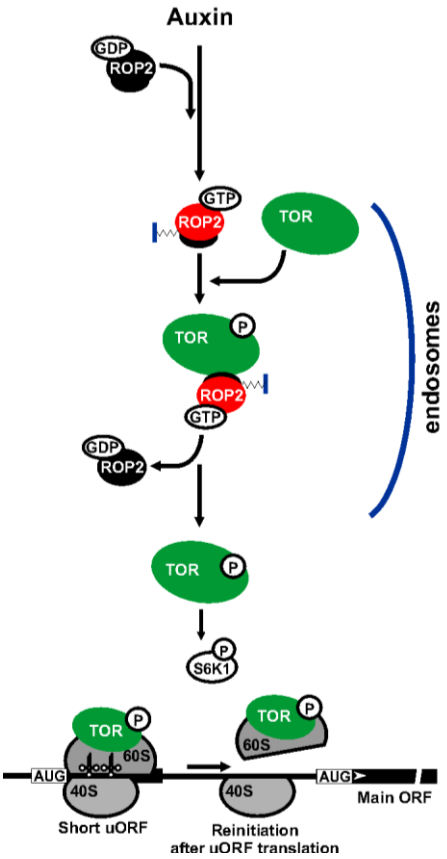

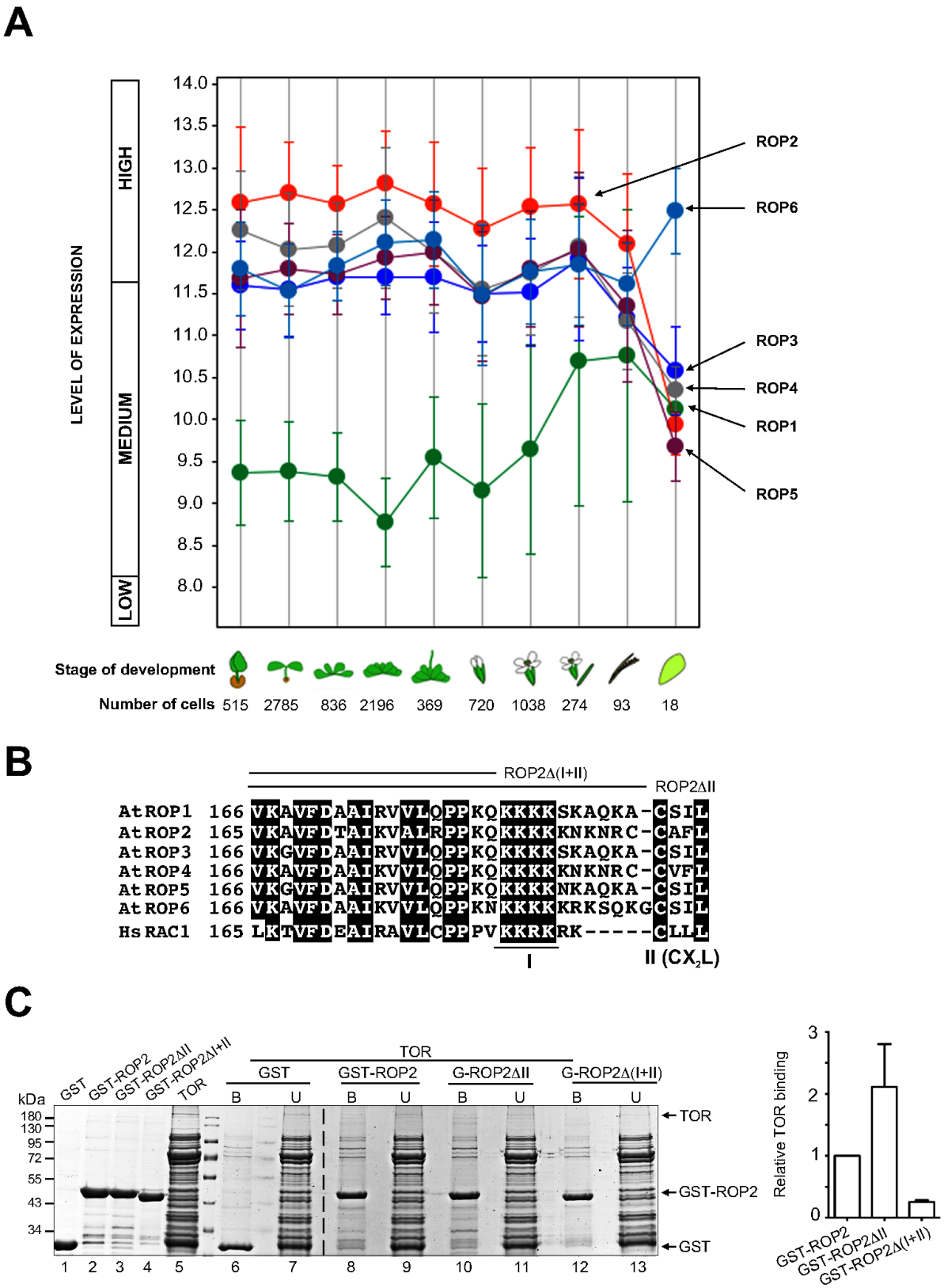
A
LEVEL OF EXPRESSION
HIGH
MEDIUM
LOW
14.0
13.5
13.0
12.5
12.0
11.5
11.0
10.5
10.0
9.5
9.0
8.5
8.0
ROP2
ROP6
ROP3
ROP4
ROP1
ROP5
Stage of development
Number of cells 515 2785 836 2196 369 720 1038 274 93 18
B
ROP2Δ(I+II)
ROP2ΔII
AtROP1 166 VKAVFDAAIRVVLQPPKQKKKKSKAQKA-CSIL
AtROP2 165 VKAVFDTAIKVALRPPKQKKKKKNKNRC-CAFL
AtROP3 166 VKGVFDAAIRVVLQPPKQKKKKSKAQKA-CSIL
AtROP4 166 VKAVFDAAIKVVLQPPKQKKKKKNKNRC-CVFL
AtROP5 166 VKGVFDAAIRVVLQPPKQKKKKNKAQKA-CSIL
AtROP6 166 VKAVFDAAIKVVLQPPKNKKKKKRKSQKG-CSIL
HsRAC1 165 LKTVFDEAIRAVLCPPPVKKRKRK-----CLLL
I
II (CX2L)
C
kDa
GST
GST-ROP2
GST-ROP2ΔII
GST-ROP2ΔI+II
TOR
TOR
GST
GST-ROP2
G-ROP2ΔII
G-ROP2Δ(I+II)
B U B U B U B U
180
130
95
72
55
43
34
TOR
GST-ROP2
GST
1 2 3 4 5 6 7 8 9 10 11 12 13
Relative TOR binding
3
2
1
0
GST-ROP2
GST-ROP2ΔII
GST-ROP2Δ(I+II)

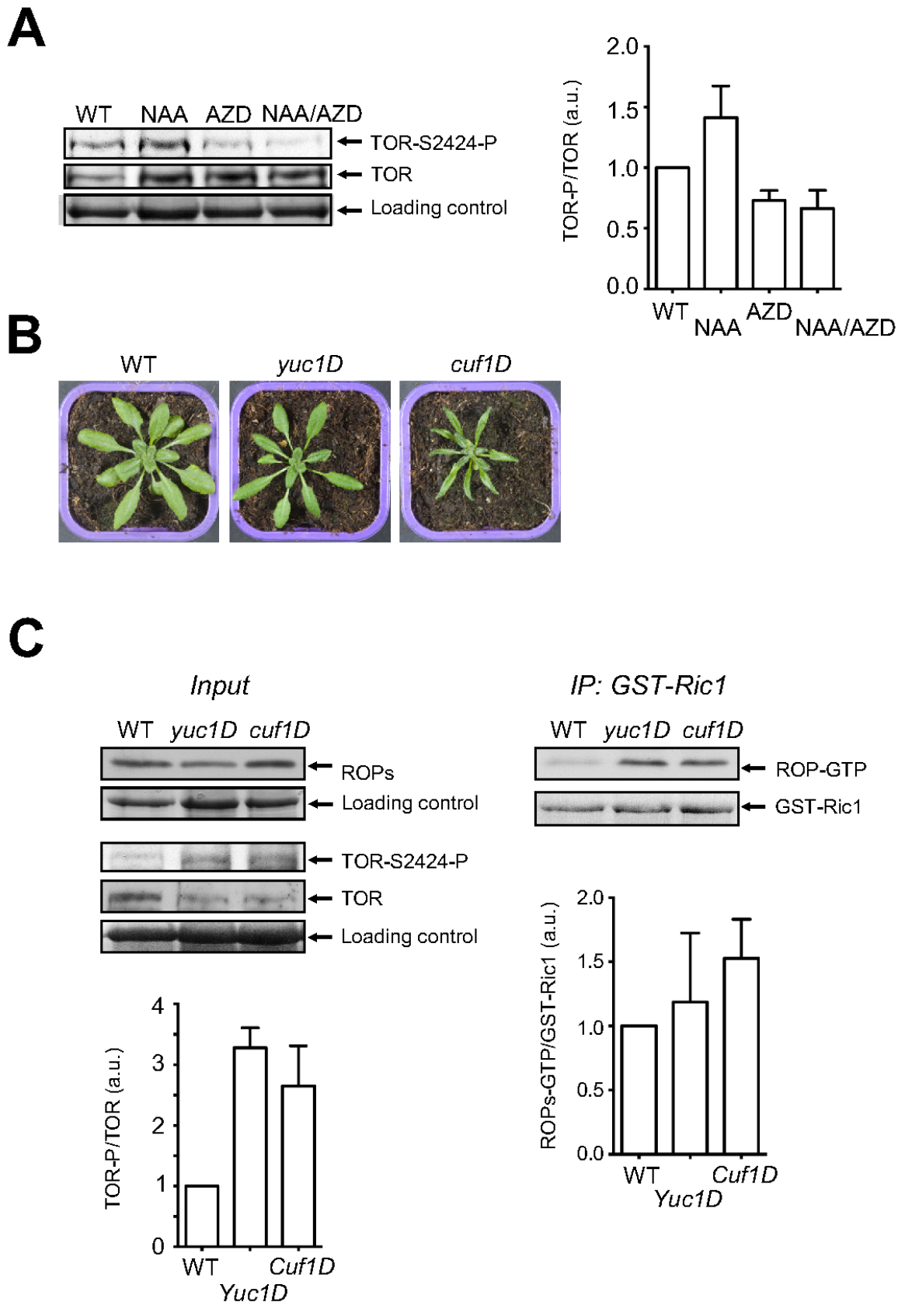
A
WT
NAA
AZD
NAA/AZD
TOR-S2424-P
TOR
Loading control
TOR-P/TOR (a.u.)
2.0
1.5
1.0
0.5
0.0
WT
NAA
AZD
NAA/AZD
B
WT
yuc1D
cuf1D
C
Input
WT
yuc1D
cuf1D
ROPs
Loading control
TOR-S2424-P
TOR
Loading control
TOR-P/TOR (a.u.)
4
3
2
1
0
WT
Cuf1D
Yuc1D
IP: GST-Ric1
WT
yuc1D
cuf1D
ROP-GTP
GST-Ric1
ROPs-GTP/GST-Ric1 (a.u.)
2.0
1.5
1.0
0.5
0.0
WT
Cuf1D
Yuc1D

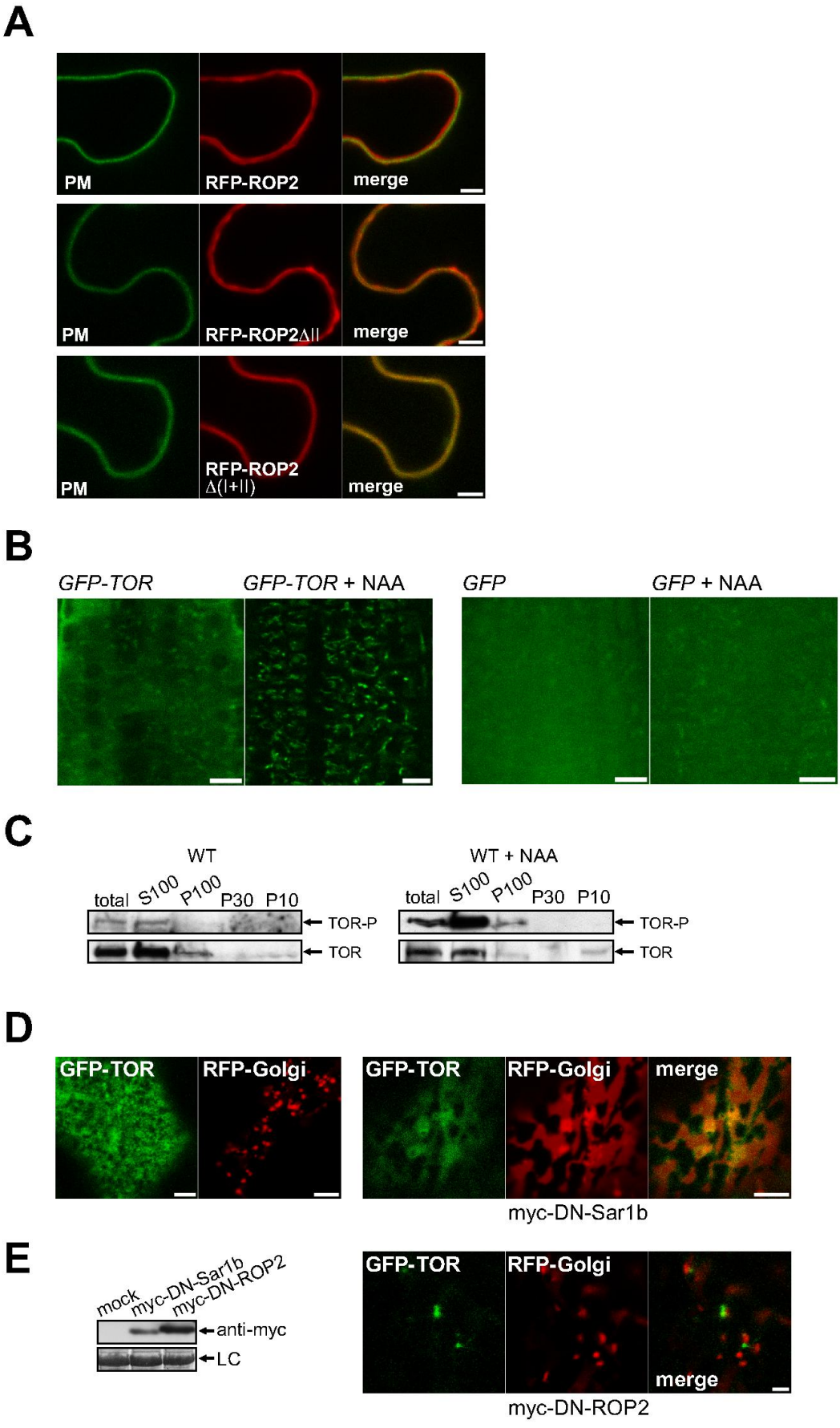
A
PM
RFP-ROP2
merge
PM
RFP-ROP2ΔII
merge
PM
RFP-ROP2
Δ(I+II)
merge
B
GFP-TOR
GFP-TOR + NAA
GFP
GFP + NAA
C
WT
total S100 P100 P30 P10
TOR-P
TOR
WT + NAA
total S100 P100 P30 P10
TOR-P
TOR
D
GFP-TOR
RFP-Golgi
GFP-TOR
RFP-Golgi
merge
myc-DN-Sar1b
E
mock
myc-DN-Sar1b
myc-DN-ROP2
anti-myc
LC
GFP-TOR
RFP-Golgi
merge
myc-DN-ROP2

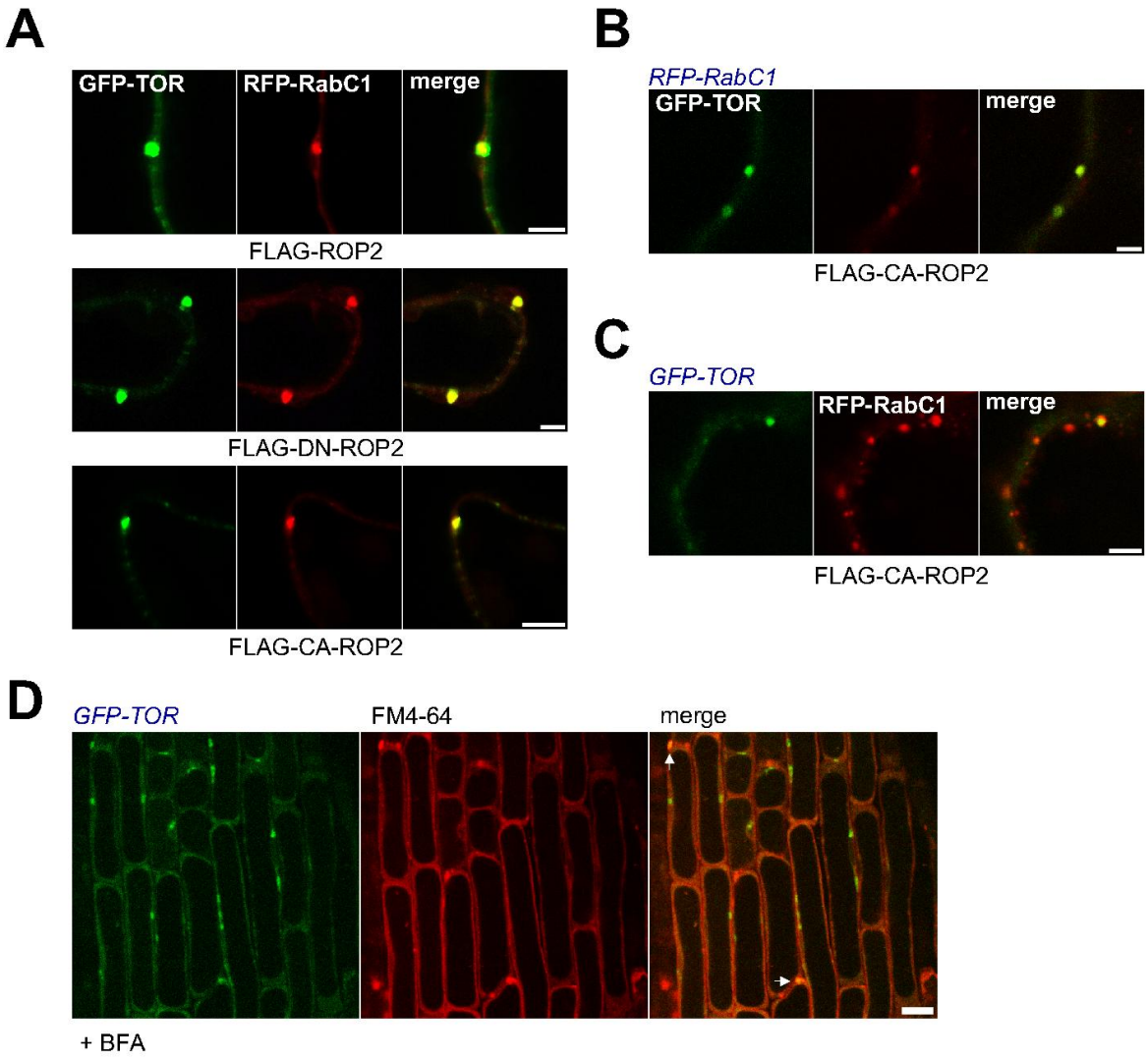
A
GFP-TOR
RFP-RabC1
merge
FLAG-ROP2
FLAG-DN-ROP2
FLAG-CA-ROP2
B
RFP-RabC1
GFP-TOR
merge
FLAG-CA-ROP2
C
GFP-TOR
RFP-RabC1
merge
FLAG-CA-ROP2
D
GFP-TOR
FM4-64
merge
+ BFA

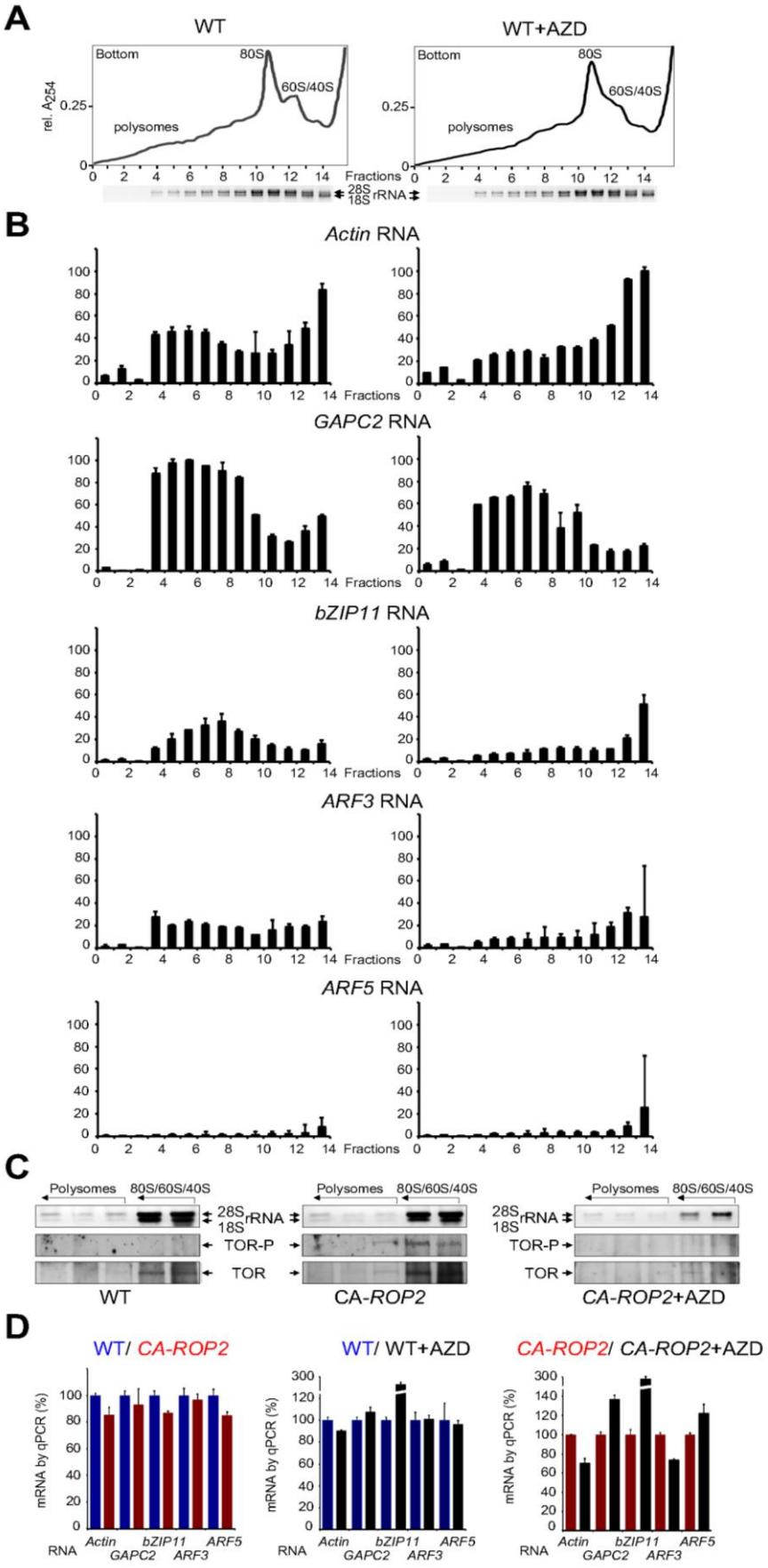
A
WT
WT+AZD
Bottom
80S
60S/40S
polysomes
rel. A254
Fractions
28S
18S rRNA
B
Actin RNA
GAPC2 RNA
bZIP11 RNA
ARF3 RNA
ARF5 RNA
C
Polysomes
80S/60S/40S
28S
18S rRNA
TOR-P
TOR
WT
CA-ROP2
CA-ROP2+AZD
D
WT/ CA-ROP2
WT/ WT+AZD
CA-ROP2/ CA-ROP2+AZD
mRNA by qPCR (%)
RNA
Actin
bZIP11
ARF5
GAPC2
ARF3

2.2.10 Appendix

GTPase ROP2 promotes translation reinitiation at upstream ORFs via activation of TOR

Mikhail Schepetilnikov[1], Joelle Makarian[1], Ola Srour[1], Angèle Geldreich[1], Zhenbiao Yang[2], Johana Chicher[3], Philippe Hammann[3] and Lyubov A. Ryabova[1]*

[1] Institut de Biologie Moléculaire des Plantes, Centre National de la Recherche Scientifique, UPR 2357, Université de Strasbourg, Strasbourg, France

[2] Center for Plant Cell Biology, Department of Botany and Plant Sciences, University of California, Riverside, CA, USA

[3] Platforme Proteómique Strasbourg-Esplanade, Centre National de la Recherche Scientifique, FRC 1589, Université de Strasbourg, Strasbourg, France

2.2.11 Table of content

2.2.12 Methods

Plant materials and growth conditions

RFP-RabC1 (N781669) and T-DNA insertion rop2 (SALK_055328C) seeds were obtained from the Nottingham Arabidopsis Stock Centre (NASC). *cuf1D* and *yuc1D* lines, a gain-of-function mutants characterized by a high level of auxin biosynthesis, were described in Cui *et al* (2013) and Zhao *et al* (2001) respectively. The double rop2rop6 and triple rop2rop6ROP4 RNAi mutant lines were described in Ren *et al* (2016). The GTP-bound constitutively active ROP2 *CA-ROP2* line were described in Li *et al* (2001). The transgenic line expressing GFP under control of the 35S promoter (35S:GFP) was kindly provided by Patrice Dunoyer (IBMP, Strasbourg, France).

To generate the *GFP-TOR* transgenic line expressing TOR kinase fused to GFP under control of the 35S promoter, stable transformation of flowering *Arabidopsis* plants was performed with *Agrobacterium tumefaciens* strain GV3101 by the floral dip method (Clough & Bent, 1998). The *Arabidopsis* homozygous *GFP-TOR/CA-ROP2* transgenic line was generated by crossing *GFP-TOR* and *CA-ROP2* lines. Transgenic lines were selected for the appropriate resistance, and the presence of the corresponding transgene was verified.

Arabidopsis lines were in Columbia (Col-0) background. Seeds were sterilized in 70% Ethanol and germinated on solid Murashige-Skoog (MS) agar plates for 3 days at +4˚C in the dark. The 7 dag *Arabidopsis* seedlings were grown under long day conditions (16h light/ 8h darkness, 22°C/ 16˚C) with illumination Neon Biolux on MS plates supplied or not with 1 μM (Fig 2, Fig 6, Fig 8 and Fig EV2) or 0.5 μM (Fig 7 and Fig EV7) of AZD-8055 (Chemdea).

Interdigitation analysis

The second true leaves from 21-day-old plants were used for interdigitation analysis of abaxial epidermal cells – pavement cells (PCs) – of the middle part of leaf blade. Cell outlines were visualized by 30 min. staining of cell walls with propidium iodide and imaged using confocal laser scanning microscopy. Cell area and circularity index were measured by ImageJ. The circularity of a pavement cell is determined by calculating 4π area/perimetr^2. The measurements were consistently conducted on PCs being at the same developmental stage. Data obtained from at least three independent experiments of 30 cells each. Unpaired t-test was performed for all comparisons to determine the *p*-values.

Polyribosome analysis

For polyribosome isolation we used 7 dag *Arabidopsis* wild-type Col-0 WT and *CA-ROP2* seedlings grown on MS agar plates supplemented (or not) with 2-fold reduced (0.5 µM) concentration of AZD 8055. Drug concentration was tested to prevent overall cytotoxic effect on mRNA polysomal loading during prolonged drug treatment. After harvesting, equal amounts of fresh material were frozen and ground in liquid nitrogen. For cytoplasmic extracts, 500 mg of powder was resuspended in ice-cold extraction buffer [200 mM Tris-HCl, pH 9, 200 mM KCl, 35 mM $MgCl_2$, 25 mM EGTA, 15.4 units/mL heparin, 18 µM cycloheximide, 0.5% NP-40, 1 mM DTT, PHOS-Stop (Roche) and protease inhibitors cocktail (Roche)]. Cell debris was removed by centrifugation. Supernatants were used to control total levels of endogenous mRNA by quantitative RT-PCR (qRT-PCR) and aliquots were loaded onto 13 mL 10% to 50% (w/w) sucrose gradients in 40 mM Tris-HCl pH 8.5, 5 mM EGTA, 20 mM KCl, 10 mM $MgCl_2$ and centrifuged at 39,000 rpm in a Beckman SW41 rotor at 4°C for 2h. Polysomal profiling was done in three independent biological replicates, each including Col-0 WT and *CA-ROP2* seedlings treated (or not) with AZD 8055. To improve translational fidelity and reproducibility, we grow seedlings on the same day under identical conditions. Samples for polysomal profiling were collected immediately the same day. Polyribosomal extract preparation, sucrose gradient sedimentation, RNA isolation and qRT-PCR analysis were performed in parallel for both wild-type Col-0 WT and *CA-ROP2* samples treated (or not) with AZD8055 inside each biological replicate.

To monitor mRNA loading into polysomes, qRT-PCR analysis of fractions of all gradients was performed at the same 384-well plate. mRNAs were monitored in sub/ polysomal fractions, and transcript levels for each mRNA were normalized to *EXP* and ribosomal RNA. For each gene levels of mRNA in each fraction were calculated as relative to fraction with maximum level of mRNA, which was set as 100. For western blot polyribosomal fractions were collected, precipitated with 2 volumes of absolute ethanol at 4°C, followed by pellet resuspension in in hot Laemmli buffer for 5 minutes at 95˚C.

Quantitative real-time PCR analyses

Total RNA was extracted using Trizol (Invitrogen). RNA samples were reverse transcribed into cDNA using SuperScript III reverse transcriptase (Invitrogen) with oligo-$(dT)_{18}$ primer (Fermentas). cDNA was quantified with gene specific primers using a SYBR Green qPCR kit (ROCHE) and SYBR Green I Master Light Cycler 480 (Roche). The level of *ROP2* (At1g20090), *ROP4* (At1g75840), *ROP6* (At1g10840), *Lst8* (At3g18140), *Raptor1a*

(At5g01770), *Raptor1b* (At3g08850), *S6K1* (At3g08730), *GFP*, *TORend*, *TORmix*, *ARF*3 (At2G33860), *ARF*5 (At1g19850), *bZIP*11 (At4G34590), *ACTIN* (At3g18780) and *GAPC2* (At1g13440) mRNAs was monitored by pairs of gene-specific primers. Transcript levels were normalized to that of *EXP* (At4g26410). For qPCR analysis of *GFP-TOR* and *GFP-TOR/CA-ROP2* transgenic lines we used specific pair of primers for endogenous TOR (TORend) and GFP-TOR transgene mRNA transcripts (see Appendix Fig S4). The TORmix probe represents set of primers designed so that two oligos hybridize to one exon sequence of *TOR* gene, which permits to detect accumulation of both *TOR* and *GFP-TOR* mRNAs. TORend set of oligos hybridize to 3`-UTR of endogenous *TOR* mRNA, thus allows qPCR amplification of only endogenous TOR. Finally, GFP probe is designed for *GFP* (green fluorescent protein) gene, which permits to detect *GFP-TOR* transcript.

The used gene-specific primer were:

ACTIN (At3g18780)	fwd: 5`-gcaccctgttcttcttaccg-3` and rev: 5`-aaccctcgtagattggcaca-3`
GAPC2 (At1g13440)	fwd: 5`-agctgcaacatacgacgaaa-3` and rev: 5`-cccttcattttgccttcaga-3`
EXP (At4g26410)	fwd: 5`-gagctgaagtggcttcaatgac-3` and rev: 5`-ggtccgacatacccatgatcc-3`
*bZIP*11 (At4G34590)	fwd: 5`-ctgcaaggagatcaagaatg-3` and rev: 5`-ggttaggtagtgttgcgttg-3`
*ARF*3 (At2G33860)	fwd: 5`-ccatatcgacccatagcgttttcag-3` and rev: 5`-cccaatgcaaaagggatagtcaaca-3`
*ARF*5 (At1g19850)	fwd: 5`-ggtcagtccatgggatatcgaaaca-3` and rev: 5`-ttcgcggaatcaggaacacgta-3`
ROP2 (At1g20090)	fwd: 5`-gaatgtagttcaaagacacagcaga-3` and rev: 5`-tggctgaagcaccactttta-3`
ROP4 (At1g75840)	fwd: 5`-atcctggtgcagtgcctatt-3` and rev: 5`-tgctttcacattctgctgagtc-3`
ROP6 (At1g10840)	fwd: 5`-ctcgttggaacaaagcttga-3` and rev: 5`-ttcttcaccctgagcggtag-3`
Lst8 (At3g18140)	fwd: 5`-ggatggagaatttcttgtaacagc-3` and rev: 5`-tgatgaccttggtacactttcac-3`
Raptor1a (At5g01770)	fwd: 5`-gatgagaatgaacggattaggg-3` and rev: 5`-agcagagagtcatcaagttcattg-3`
Raptor1b (At3g08850)	fwd: 5`-ttacagcactttctgcttctcaa-3` and rev: 5`-ctttctgatgaggccgagtc-3`
S6K1 (At3g08730)	fwd: 5`-ctcagccatcccctctga-3` and rev: 5`-ttgttgtttcccgattttaagg-3`
TORend	fwd: 5`-gaagatgaagatcccgctga-3` and rev: 5`-gcatctccaagcatatttacagc-3`
TORmix	fwd: 5`-tcacgacattggatttggaat-3` and rev: 5`-aactgctagctccaagtcacg-3`
GFP	fwd: 5`-gaagcgcgatcacatggt-3` and rev: 5`-ccatgccgagagtgatcc-3`

Semi-quantitative real-time PCR analyses

For sqRT-PCR analysis the total RNA from protoplasts was extracted using Trizol. RNA samples were reverse transcribed into cDNA using SuperScript III reverse transcriptase (Invitrogen) with oligo-$(dT)_{18}$ primer (Fermentas). sqRT-PCR was performed with the pair of specific primers to the full-length GUS reporter gene. The PCR conditions are as followed: 2 min, 98°C (first cycle); 30 s, 98°C; 30 s, 56°C; 3 min, 72°C (20 cycles).

For characterization of rop2, rop2rop6 and rop2rop6ROP4 RNAi mutant lines the sqRT-PCR was performed with the pair of specific primers to the full-length ROP1-6 reporter genes. The PCR conditions are as followed: 2 min, 98°C (first cycle); 30 s, 98°C; 30 s, 55°C; 30 s, 72°C (25 cycles). The PCR products were separated on a 1.2% agarose gel and visualized by ethidium bromide staining.

The used gene-specific primer were:

ROP1 (At3g51300)	fwd: 5`-tatacatatgagcgcttcgaggttcgt-3` and rev: 5`-tatagaattctcatagaatggagcatgccttc-3`
ROP2 (At1g20090)	fwd: 5`-tataccatggcgtcaaggtttataaag-3` and rev: 5`-tataggatcctcacaagaacgcgcaacgg-3`
ROP3 (At2g17800)	fwd: 5`-tatacatatgagcgcttcgaggttcat-3` and rev: 5`-tatagaattcttacaaaatggagcaggctttt-3`
ROP4 (At1g75840)	fwd: 5`-tatacatatgagtgcttcgaggtttat-3` and rev: 5`-tatagaattctcacaagaacacgcagcggttc-3`
ROP5 (At4g35950)	fwd: 5`-tatacatatgagcgcatcaaggttcat-3` and rev: 5`-tatagaattcttacaagatggagcaggccttt-3`
ROP6 (At1g10840)	fwd: 5`-tatacatatgagtgcttcaaggtttatc-3` and rev: 5`-tatagaattctcagagtatagaacaacctt-3`

Transient expression and imaging analysis

For transient expression assay in *N. benthamiana Agrobacterium* strain GV3101 with corresponding pBin-based constructs was grown in liquid LB media with appropriate antibiotics at +28˚C with shaking (220 rpm) for 18h. Bacteria were collected by centrifugation at 3500g for 15 minutes and were resuspended in MES buffer (10 mM $MgCl_2$, 10 mM 2-*N*-morpholino-ethanesulfonic acid (MES) pH 5.6 and 150 µM Acetosyringone). After 2-3h of incubation, OD600 was adjusted to 0.5-1.0 and suspension was infiltrated into the lower leaf surfaces of young (six- to seven-leaf-stage) *N. benthamiana* plants with a needleless syringe. After 18h of expression samples were collected for protein extraction and microscopic observation. Fluorescence was detected using a confocal microscope Zeiss LSM780 (Jena, Germany). For confocal images processing was performed with ImageJ software and FigureJ plugin.

Plasma membrane marker GFP-BD-CVIL, which consists of green fluorescent protein

(GFP) fused to C-terminal polybasic domain (BD) and isoprenylation motif (CVIL), is described in Gerber *et al* (2009). Intracellular compartment markers that specifically label peroxisomes (mCherry-peroxi), mitochondria (mCherry-mito) and Golgi (GmMan1-tdTomato) are described in Nelson *et al.* (2007). PCR products corresponding to *Arabidopsis ROP2* (At1g20090), *Sar1b* (At1g56330), *RabC1* (At1g20090), *RabE1d* (At5g03520), *Ara7* (At4g19640), *ATG8a* (At4G21980) and human *Rheb* (NM_005614) were amplified from cDNA with pairs of gene specific primers compatible with GateWay Cloning technology (Invitrogen), cloned into pDONR-Zeo vector (Invitrogen) and then subcloned into pB7WGR2 binary vector (Karimi *et al*, 2002) as in-frame fusion with RFP tag to obtain pB7-WG-RFP-ROP2, -Sar1b, -RabC1, -RabE1d, -Ara7, -ATG8a and –Rheb. The CA- and DN-mutants of ROP2, Rheb and Sar1b were generated using site-directed PCR mutagenesis – by substitution of Gln at position 64 to Asn (CA-Q64N) and Asp at position 121 to Ala (DN-D121A) in ROP2 ORF; by substitution of Gln at position 64 to Asn (CA-Q64N) and Asp at position 60 to Ile (DN-D60I) in Rheb ORF; and by substitution of His at position 74 to Leu (CA-H74L) and Thr at position 51 to Ala (DN-T51A) in Sar1b ORF respectively. The CA-, DN- and ROP2 were subcloned using GateWay Cloning technology (Invitrogen) into pEarleyGate-202 (ABRC stock CD3-688) and pEarleyGate-203 (ABRC stock CD3-689) binary vectors as in-frame fusion with FLAG- and Myc-tags respectively to obtain pEG-202-FLAG and pEG-203-Myc-CA, -DN and -ROP2.

PCR products corresponding to ROP2 C-terminal deletions of motif II and (I+II) were amplified from ROP2 cDNA with pairs of gene specific primers compatible with GateWay Cloning technology (Invitrogen), cloned into pDONR-Zeo vector (Invitrogen) and then subcloned into pB7WGR2 binary vector (Karimi et al, 2002) as in-frame fusion with RFP tag to obtain pB7-WG-RFP-ROP2ΔII and -ROP2Δ(I+II).

For microscopic observation of GFP-TOR and GFP intracellular localization in root cells upon NAA treatment (Fig EV5), the 7-dag seedlings of *GFP-TOR* and *GFP* transgenic lines were treated in fresh liquid MS media supplemented or not with 100 nM NAA for 8 hours.

Arabidopsis protoplasts and plasmid constructions

Arabidopsis mesophyll protoplasts from WT and *CA-R0P2* 2-week transgenic seedlings were transfected with plasmid DNA by the PEG method described in Yoo *et al*, (2007). After overnight incubation at 26 °C in WI buffer (4 mM MES pH 5.7, 0.5 M Mannitol, 20 mM KCl) with or without 1 µM AZD-5088, transfected protoplasts were harvested by

centrifugation, and total protein extracts were prepared in GUS extraction buffer (50 mM NaH_2PO_4 pH 7.0, 10 mM EDTA, 0.1% NP-40). Aliquots were taken immediately for GFP (green fluorescent protein) fluorescent assay followed by GUS reporter fluorimetric assay described in Pooggin *et al,* (2000). GUS activity was measured by monitoring conversion of the β-glucuronidase substrate 4-methylumbelliferyl β-D-glucuronide (MUG) into 4-Methylumbelliferone (MU). Fluorescence was measured on a FLUO-star plate reader (BMG Labtechnologies Inc., Durham, NC) at 460nm when excited at 355nm. GUS GUS mRNA levels were monitored by semi-quantitative real-time PCR (sqRT-PCR).

The construct pS6K1, pARF3-GUS, pARF5-GUS, pmonoGUS and pmonoGFP were described previously (Schepetilnikov *et al*, 2011; 2013). PCR product corresponding to *TOR* was amplified from TOR cDNA (At1g50030) with pairs of specific primers and cloned into pmonoGUS to replace GUS and obtain pTOR construct. pTOR-S2424A and pTOR-S2424D were generated by substitution of Ser at position 2424 to Ala (S2424A) and to Asp (S2424D) respectively in TOR ORF by site-directed PCR mutagenesis. The CA-, DN- and ROP2 were subcloned using GateWay Cloning technology (Invitrogen) into pUGW18 (Nakagawa *et al*, 2007) vector suitable for transient expression in protoplasts as in-frame fusion with 4xMyc-tag to obtain pUGW-4xMyc-CA, -DN and -ROP2 respectively.

Yeast two-hybrid assay and plasmid construction

To generate pGBK-ROP1-6, corresponding PCR products were amplified from ROP1 (At3g51300), ROP2 (At1g20090), ROP3 (At2g17800), ROP4 (At1g75840), ROP5 (At4g35950) and ROP6 (At1g10840) cDNA respectively with pairs of specific primers and cloned into the pGBKT7 (Clontech) as in-frame fusion with the BD-domain. pGBKT7-CA-ROP2 and pGBKT7-DN-ROP2 were generated by substitution of Gln at position 64 to Asn (Q64N) and to Asp at position 121 to Ala (D121A), respectively, in ROP2 ORF by site-directed PCR mutagenesis. PCR products corresponding to NTOR, CTOR and full-length TOR were amplified from *At*TOR cDNA (At1G50030) with pairs of specific primers respectively and cloned into the pGADT7 (Clontech) as in-frame fusion with the AD-domain to obtain pGAD -NTOR, pGAD -CTOR and pGAD-TOR.

Subcellular fractionation

Arabidopsis seedlings were harvested after 7 days growth on MS agar plates, and 3.0 g of tissue was homogenized by gentle grinding on ice with 3 mL of isolation buffer [50 mM

HEPES pH 7.5, 50 mM KCl, 5 mM EDTA pH 8.0, 10% Sucrose (w/v), 1 mM DTT, PHOS-Stop (Roche) and protease inhibitor cocktail (Roche)]; 3 mL of homogenates were centrifuged at 10,000 *g* for 30 min at 4 °C to obtain the nuclear P10 fraction. The supernatant was recentrifuged at 30,000 *g* for 60 min at 4 °C to obtain the ER-enriched P30 fraction. The supernatant was further fractionated by centrifugation at 100,000 *g* for 60 min into supernatant (S100) and pellet (microsomal P100) fractions. P10, P30, and P100 pellets were resuspended in 1x Laemmli buffer to volumes that were 10x times those before centrifugation. Fractionated and unfractionated samples of the same volume were analyzed by western blot using GFP, TOR and phospho-TOR specific antibodies.

Immunoprecipitation and kinase assay

For immunoprecipitation, *in vitro* kinase assay, and western blot detection experiments, *Arabidopsis* seedlings were cultured at MS agar for 7 days after germination (7 dag), harvested and ground in liquid nitrogen followed by homogenization in fresh ice-cold extraction buffer [50 mM Tris pH 7.5, 150 mM KCl, 0.1% NP-40, GM-132 (Sigma), Complete protease inhibitors cocktail (Roche)]. For immunoprecipitation of TOR complexes plant samples were homogenized in extraction buffer and insoluble material was removed by centrifugation (two times of 15 min, 12000g, 4°C). Lysate was pre-cleaned by incubation with protein A-agarose beads (Roche) at 4°C for 10 min. The supernatant was then incubated with either Normal rabbit serum (RS, Sigma), or anti-*At*TOR serum prebound to A-agarose beads, or with GFP-Trap magnetic beads (Chromotek) for 1h at 4°C. Immunoprecipitates were washed three times with the extraction buffer supplemented with 300 mM KCl, eluted from the beads with 1x Laemmli buffer for 5 min at 95°C and analyzed by western blot.

For *in vitro* kinase assay GFP-TOR immunoprecipitates were washed 3 times with the extraction buffer followed by brief wash with kinase buffer-1 (50 mM HEPES pH 7.5, 50 mM KCl, 5 mM $MgCl_2$) and finally resuspended in kinase buffer-2 (50 mM HEPES pH 7.5, 50 mM KCl, 5 mM $MgCl_2$, 0.5 mM rATP). Kinase reaction was carried out at 30°C in kinase buffer-2 with small aliquots of immunoprecipitated GFP-TOR complexes in the presence of 100 ng rec S6K1 purified as described in **Protein expression, purification and GST pull-down assay.** Kinase reactions were stopped after 0, 5, 10, 15, and 20 minutes of incubation at 30˚C and incorporation of phosphate was analyzed by SDS-PAGE and immunobloting with anti-mS6K1-P-T389 antibodies (Cell Signaling). Quantification of phospho-S6K1 bands was performed using ImageJ software. The graph in Fig 3D shows kinetics of S6K1 phosphorylation by TOR kinase: X axis represents fold changes in phospho-S6K1 band

density normalized to the total S6K1 amount (a.u. arbitrary units) and X axis – time of kinase reaction in min.

Western blot assay

Rabbit anti-*At*TOR polyclonal antibodies were described in Schepetilnikov *et al.* (2011). Rabbit polyclonal anti-mS6K1 antibodies were from Santa-Cruz Biotechnology. Phospho antibodies—anti-mTOR-P-S2448 (#2971) and anti-mS6K1-P-T389 (#9205)—directed against indicated phosphorylated form of either TOR or S6K1 described in Schepetilnikov *et al.* (2011) were from Cell Signaling. For detection of ROP GTPases in *Arabidopsis* plant total extracts we used rabbit polyclonal anti-AtRac3 (Sigma) and for detection in *N. benthamiana* of transiently expressed of ROP GTPases fused to myc-tag we use anti-c-Myc (Roche). Anti-GFP (A11122) antibodies were from Molecular Probes, Life Technologies. For westernblot detection we used HRP-conjugated secondary anti-rabbit or anti-goat IgG antibodies (Sigma) and ECL kit (Roche).

Protein expression, purification and GST pull-down assay

PCR products corresponding to *Arabidopsis Ric1* (At2g33460), *ROP2* (At1g20090), *Sar1b* (At1g56330) and human *Rheb* (NM_005614) were amplified from corresponding cDNAs with pairs of gene specific primers and cloned into pGEX-6P1 (Pharmacia Biotech) as in-frame fusions with the GST-domain to obtain pGEX-Ric1, pGEX-ROP2, pGEX-Sar1b and pGEX-Rheb respectively. PCR products corresponding to ROP2 C-terminal deletions of motif II and (I+II) were amplified from corresponding ROP2 cDNAs with pairs of gene specific primers and cloned into pGEX-6P1 (Pharmacia Biotech) as in-frame fusions with the GST-domain to obtain pGEX-ROP2ΔII and pGEX-ROP2Δ(I+II). pGEX-CA-ROP2 and pGEX-DN-ROP2 were generated by substitution of Gln at position 64 to Asn (Q64N) and to Asp at position 121 to Ala (D121A) respectively in ROP2 ORF by site-directed PCR mutagenesis. PCR products corresponding to S6K1 (At3g08730) and ROP2 (At1g20090) were amplified from cDNA with pairs of gene specific primers compatible with GateWay Cloning technology (Invitrogen), cloned into pDONR-Zeo vector (Invitrogen) and then subcloned into pHGWA vector (kindly provided by Dr D. Busso, IGBMC, Strasbourg, France) as in-frame fusion with 6xHis tag to obtain pHGWA-S6K1 and pHGWA-ROP2 constructs respectively.

The *E. coli* codon-optimized TOR construct was designed by A. Komar (DAPCEL Inc) and synthesized (GenScript**)**. Codon-optimized TOR construct encoded for the full-length

TOR protein with the C-terminal 6xHis tag separated by the Gly-linker sequence was cloned into the pET3a vector (Novagen) to obtain pET3a-TOR. Proteins were expressed in BL21(DE3) pLysS (Stratagene) and purified according to manufacture protocol.

The rec S6K1-6xHis protein was expressed in BL21(DE3) pLysS (Stratagene) and affinity purified on 1mL His-Trap column according to manufacture protocol. In order to obtain high purity of rec S6K1 used as a substrate and to prevent inhibition of kinase reaction, the final step of S6K1-6xHis purification included exchange solution to kinase buffer and imidazole elimination using Zeba 5mL desalting columns.

For ROP2 activity *in vitro* test, binding of ROP2 charged or not with GDP or GMP-PNP (GTP non-hydrolyzed analog; Sigma) to TOR (Fig S1), or GST-Ric1 (Fig S2), or GST alone respectively was carried out in buffer A-150 (50 mM Tris and pH 7.5, 150 mM KCl) supplemented with 5 mM $MgCl_2$ in 200 µl reaction mixture for 1h with rotation at room temperature. Preparation of GDP or GMP-PNP-charged ROP2 is carried out in two steps. In the first step, nucleotide-free ROP2 was obtained by incubation of recombinant ROP2 in nucleotide exchange buffer (50 mM Tris pH 7.5, 150 mM KCl, 10 mM EDTA and 5 mM $MgCl_2$) for 30 minutes at room temperature. Then, nucleotide-free ROP2 was incubated with 100 µM GDP, or GMP-PNP, or no nucleotides in nucleotide-binding buffer (50 mM Tris pH 7.5, 150 mM KCl, 10 mM $MgCl_2$) for 1h at room temperature. Free nucleotides were removed by on column size exclusion chromatography.

Binding of TOR to GST-fused Sar1b, or Rheb, or ROP2, or ROP2ΔII, or ROP2Δ(I+II) or GST alone, respectively (Fig 1D and Fig EV1C) was carried out in buffer A-150 (50 mM Tris and pH 7.5, 150 mM KCl) in 200 µl reaction mixture for 1h with rotation at room temperature. Binding of TOR to GST-fused CA-ROP2, or DN-ROP2, or ROP2, or GST alone, respectively (Fig 1H), was carried out in buffer A-150 supplemented with 5 mM $MgCl_2$ in 200 µl reaction mixture for 1h with rotation at room temperature. Glutathione-Sepharose bead-bound complexes were washed three times with buffer A-300 (50 mM Tris and pH 7.5, 300 mM KCl). The presence of TOR and ROP2 in the bound fraction (B) as well as 20 µl of the unbound fraction (U) was analyzed by SDS-PAGE following Coomassie blue staining.

Mass spectrometry analysis

Samples were prepared for mass-spectrometry analyses as described in Chicher *et al.* (2015). Briefly, samples solubilized in Laemmli buffer were precipitated with 0.1M ammonium acetate in 100% methanol. After a reduction-alkylation step (Dithiothreitol 5 mM -

Iodoacetamide 10 mM), proteins were digested overnight with 1/25 (W/W) of sequencing-grade porcin trypsin (Promega). Peptide mixtures were resolubilized in water containing 0.1% FA (solvent A) before being injected on nanoLC-MS/MS (NanoLC-2DPlus system with nanoFlex ChiP module; Eksigent, ABSciex, Concord, Ontario, Canada, coupled to a TripleTOF 5600 mass spectrometer ABSciex). Peptides were eluted from the C-18 analytical column (75 µm ID x 15 cm ChromXP; Eksigent) with a 5%-40% gradient of acetonitrile (solvent B) for 90 minutes. Data were searched against a TAIR database containing the GFP-TOR sequence as well as decoy reverse sequences (TAIR10_pep_20101214). Peptides were identified with Mascot algorithm (version 2.2, Matrix Science, London, UK) through the ProteinScape 3.1 package (Bruker). They were validated with a minimum score of 30, a p-value<0.05 and proteins were validated respecting a false discovery rate FDR<1%.

Data analysis and software

To quantify the bands on western blots, we applied ImageJ software based analysis (http://rsb.info.gov/ij). The area under curve (AUC) of the specific signal was corrected for the AUC of the loading control (corresponding substrate). The highest value of phosphorylation with the wild type extract was set as 100% and other conditions were recalculated. To analyze the phylogenetic relationship between plant ROP family members we used the web service Phylogeny (Dereeper *et al*, 2008). Microscopy was done on a confocal microscope Zeiss LSM780 (Jena, Germany) and image analysis was performed with ImageJ. Data were analyzed with GraphPad Prism statistical software.

2.2.13 Appendix figures

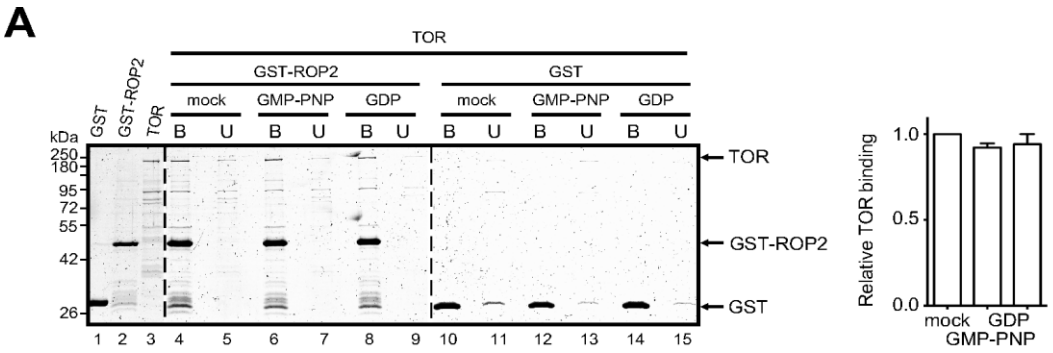

B

MVSKGEELFT	GVVPILVELD	GDVNGHKFSV	SGEGEGDATY	GKLTLKFICT	TGKLPVPWPT	LVTTLTYGVQ	CFSRYPDHMK	80
QHDFFKSAMP	EGYVQERTIF	FKDDGNYKTR	AEVKFEGDTL	VNRIELKGID	FKEDGNILGH	KLEYNYNSHN	VYIMADKQKN	160
GIKVNFKIRH	NIEDGSVQLA	DHYQQNTPIG	DGPVLLPDNH	YLSTQSALSK	DPNEKRDHMV	LLEFVTAAGI	TLGMDELYKD	240
ITSLYKKAGL	MSTSSQSFVA	GRPASMASPS	QSHRFCGPSA	TASGGGSFDT	LNRVIADLCS	RGNPKEGAPL	AFRKHVEEAV	320
RDLSGEASSR	FMEQLYDRIA	NLIESTDVAE	NMGALRAIDE	LTEIGFGENA	TKVSRFAGYM	RTVFELKRDP	EILVLASRVL	400
GHLARAGGAM	TSDEVEFQMK	TAFDWLRVDR	VEYRRFAAVL	ILKEMAENAS	TVFNVHVPEF	VDAIWVALRD	PQLQVRERAV	480
EALRACLRVI	EKRETRWRVQ	WYYRMFEATQ	DGLGRNAPVH	SIHGSLLAVG	ELLRNTGEFM	MSRYREVAEI	VLRYLEHRDR	560
LVRLSITSLL	PRIAHFLRDR	FVTNYLTICM	NHILTVLRIP	AERASGFIAL	GEMAGALDGE	LIHYLPTIMS	HLRDAIAPRK	640
GRPLLEAVAC	VGNIAKAMGS	TVETHVRDLL	DVMFSSSLSS	TLVDALDQIT	ISIPSLLPTV	QDRLLDCISL	VLSKSHYSQA	720
KPPVTIVRGS	TVGMAPQSSD	PSCSAQVQLA	LQTLARFNFK	GHDLLEFARE	SVVVYLDDED	AATRKDAALC	CCRLIANSLS	800
GITQFGSSRS	TRAGGRRRRL	VEEIVEKLLR	TAVADADVTV	RKSIFVALFG	NQCFDDYLAQ	ADSLTAIFAS	LNDEDLDVRE	880
YAISVAGRLS	EKNPAYVLPA	LRRHLIQLLT	YLELSADNKC	REESAKLLGC	LVRNCERLIL	PYVAPVQKAL	VARLSEGTGV	960
NANNNIVTGV	LVTVGDLARV	GGLAMRQYIP	ELMPLIVEAL	MDGAAVAKRE	VAVSTLGQVV	QSTGYVVTPY	KEYPLLLGLL	1040
LKLLKGDLVW	STRREVLKVL	GIMGALDPHV	HKRNQQSLSG	SHGEVPRGTG	DSGQPIPSID	ELPVELRPSF	ATSEDYYSTV	1120
AINSLMRILR	DASLLSYHKR	VVRSLMIIFK	SMGLGCVPYL	PKVLPELFHT	VRTSDENLKD	FITWGLGTLV	SIVRQHIRKY	1200
LPELLSLVSE	LWSSFTLPGP	IRPSRGLPVL	HLLEHLCLAL	NDEFRTYLPV	ILPCFIQVLG	DAERFNDYTY	VPDILHTLEV	1280
FGGTLDEHMH	LLLPALIRLF	KVDAPVAIRR	DAIKTLTRVI	PCVQVTGHIS	ALVHHLKLVL	DGKNDELRKD	AVDALCCLAH	1360
ALGEDFTIFI	ESIHKLLLKH	RLRHKEFEEI	HARWRRREPL	IVATTATQQL	SRRLPVEVIR	DPVIENEIDP	FEEGTDRNHQ	1440
VNDGRLRTAG	EASQRSTKED	WEEWMRHFSI	ELLKESPSPA	LRTCAKLAQL	QPFVGRELFA	AGFVSCWAQL	NESSQKQLVR	1520
SLEMAFSSPN	IPPEILATLL	NLAEFMEHDE	KPLPIDIRLL	GALAEKCRVF	AKALHYKEME	FEGPRSKRMD	ANPVAVVEAL	1600
IHINNQLHQH	EAAVGILTYA	QQHLDVQLKE	SWYEKLQRWD	DALKAYTLKA	SQTTNPHLVL	EATLGQMRCL	AALARWEELN	1680
NLCKEYWSPA	EPSARLEMAP	MAAQAAWNMG	EWDQMAEYVS	RLDDGDETKL	RGLASPVSSG	DGSSNGTFFR	AVLLVRRAKY	1760
DEAREYVERA	RKCLATELAA	LVLESYERAY	SNMVRVQQLS	ELEEVIEYYT	LPVGNTIAEE	RRALIRNMWT	QRIQGSKRNV	1840
EVWQALLAVR	ALVLPPTEDV	ETWLKFASLC	RKSGRISQAK	STLLKLLPFD	PEVSPENMQY	HGPPQVMLGY	LKYQWSLGEE	1920
RKRKEAFTKL	QILTRELSSV	PHSQSDILAS	MVSSKGANVP	LLARVNLKLG	TWQWALSSGL	NDGSIQEIRD	AFDKSTCYAP	2000
KWAKAWHTWA	LFNTAVMSHY	ISRGQIASQY	VVSAVTGYFY	SIACAANAKG	VDDSLQDILR	LLTLWFNHGA	TADVQTALKT	2080
GFSHVNINTW	LVVLPQIIAR	IHSNNRAVRE	LIQSLLIRIG	ENHPQALMYP	LLVACKSISN	LRRAAAQEVV	DKVRQHSGAL	2160
VDQAQLVSHE	LIRVAILWHE	MWHEALEEAS	RLYFGEHNIE	GMLKVLEPLH	DMLDEGVKKD	STTIQERAFI	EAYRHELKEA	2240
HECCCNYKIT	GKDAELTQAW	DLYYHVFKRI	DKQLASLTTL	DLESVSPELL	LCRDLELAVP	GTYRADAPVV	TISSFSRQLV	2320
VITSKQRPRK	LTIHGNDGED	YAFLLKGHED	LRQDERVMQL	FGLVNTLLEN	SRKTAEKDLS	IQRYSVIPLS	PNSGLIGWVP	2400
NCDTLHHLIR	EHRDARKIIL	NQENKHMLSF	APDYDNLPLI	AKVEVFEYAL	ENTEGNDLSR	VLWLKSRSSE	VWLERRTNYT	2480
RSLAVMSMVG	YILGLGDRHP	SNLMLHRYSG	KILHIDFGDC	FEASMNREKF	PEKVPFRLTR	MLVKAMEVSG	IEGNFRSTCE	2560
NVMQVLRTNK	DSVMAMMEAF	VHDPLINWRL	FNFNEVPQLA	LLGNNNPNAP	ADVEPDEEDE	DPADIDLPQP	QRSTREKEIL	2640
QAVNMLGDAN	EVLNERAVVV	MARMSHKLTG	RDFSSSAIPS	NPIADHNNLL	GGDSHEVEHG	LSVKVQVQKL	INQATSHENL	2720
CQNYVGWCPF	W							

Appendix Figure S1.

A **Analysis of TOR binding to ROP2 preincubated with either GMP-PNP or GDP.** ROP2 interacts with both GMP-PNP and GDP in the GST pull-down assay. GST-ROP2 and GST alone bound to glutathione beads were preincubated without (mock) or with GMP-PNP or GDP. The beads were washed and further incubated with recombinant TOR. The TOR unbound (U) and bound (B) fractions were analysed by Coomassie staining. *Right panel* Quantification of TOR binding to GST-fusion proteins. The value for TOR binding to GST-ROP2 (mock) was set as 1.

Data information: Quantification represents the means +/-SEM obtained in two independent experiments.

B **Characterization of GFP-TOR protein from the *Arabidopsis 35S:GFP-TOR* line.** Sequence coverage (highlighted in grey) for recombinant GFP-TOR obtained with trypsin digestion from 2 independent enrichment experiments (green and pink bars respectively). Tryptic and semi-tryptic peptides identified by LC-MS/MS were validated by MASCOT's identity scores (p-value < 0.05).

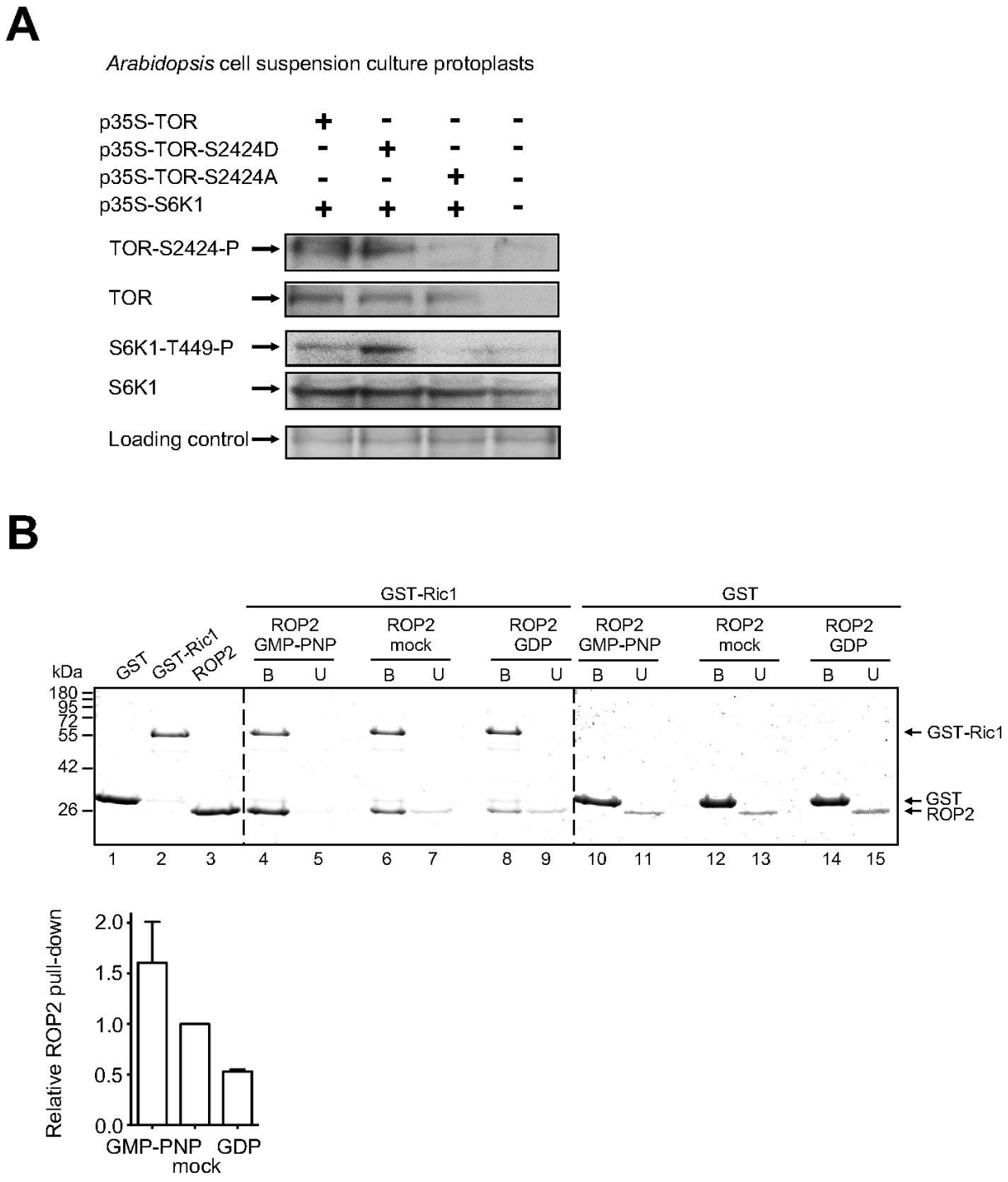
A
Arabidopsis cell suspension culture protoplasts
p35S-TOR
p35S-TOR-S2424D
p35S-TOR-S2424A
p35S-S6K1
TOR-S2424-P
TOR
S6K1-T449-P
S6K1
Loading control
B
GST-Ric1
GST
ROP2 GMP-PNP
ROP2 mock
ROP2 GDP
B U
kDa
GST
GST-Ric1
ROP2
180
95
72
55
42
26
GST-Ric1
GST
ROP2
1 2 3 4 5 6 7 8 9 10 11 12 13 14 15
Relative ROP2 pull-down
2.0
1.5
1.0
0.5
0.0
GMP-PNP
GDP
mock

Appendix Figure S2.

A **Phosphorylated S2424 (S2424-P) in *Arabidopsis* TOR is a specific target of phospho-antibodies against mammalian TOR phosphorylated S2448 (S2448-P).**

Anti-(mTOR-S2448-P) antibodies specifically recognize TOR, its phosphorylation mimic TOR-S2424D, but not TOR phosphorylation knockout TOR-S2424A transiently produced together with S6K1 in *Arabidopsis* WT protoplasts. Suspension culture protoplasts were co-transfected with plasmids expressing S6K1 under the 35S promoter (p35S-S6K1) and either p35S-TOR, p35S-TOR-S2424D, or p35S-TOR-S2424A (TOR S2424 phosphorylation site mutants) as indicated. Transiently expressed TOR and its derivatives were assayed by immunoblotting using anti-*At*TOR antibodies (anti-TOR) and anti-(mTOR-S2448-P). S6K1 levels and phosphorylation status were assayed by anti-mS6K1 and anti-(mS6K1-T389-P). Protein loading was assessed by Coomassie blue staining (LC, loading control).

B **Ric1 specifically binds active GTP-bound ROP2 *in vitro*.**

GST-Ric1 pull-down active GTP-bound ROPs. GST-Ric1 as well a GST alone bound to glutathione beads were incubated with recombinant ROP2 preincubated without (mock) or with GMP-PNP or GDP. The beads were washed, and the unbound (U) and bound (B) fractions were analysed by Coomassie staining. Recombinant GST, GST-Ric1 and ROP2 purified proteins are shown on the left panel. *Bottom panel* Quantification of ROP2 pull-down by GST-Ric1 proteins. The value for ROP2 binding to GST-Ric1 (mock) was set as 1.

Data information: Quantification represents the means +/-SEM obtained in two independent experiments.

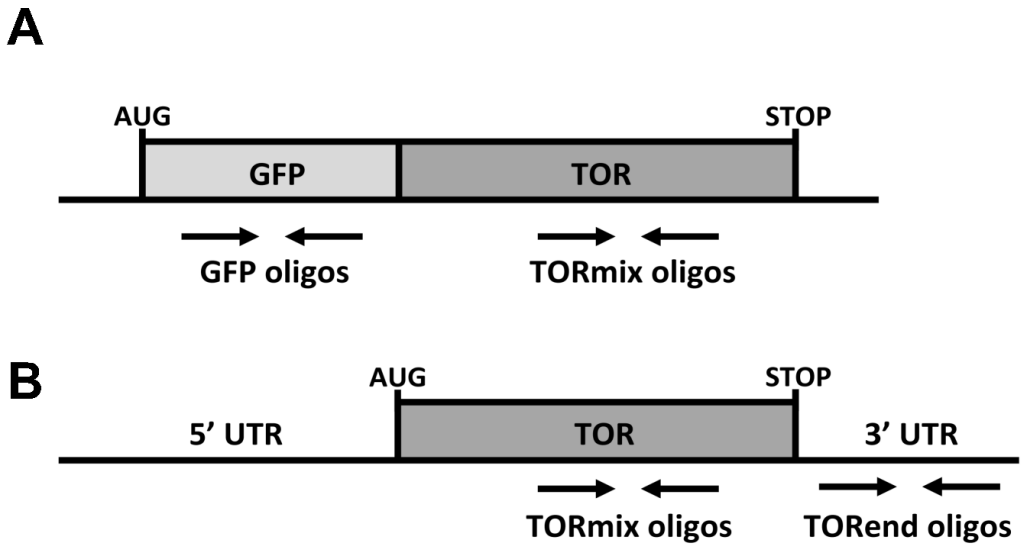

Appendix Figure S3.

Monitoring of endogenous, GFP-tagged and total TOR mRNA levels.

A, B Primer design for monitoring of *GFP-TOR* (A) and endogenous *TOR* mRNA levels (B) in *GFP-TOR/CA-ROP2* or *GFP-TOR* transgenic plants.

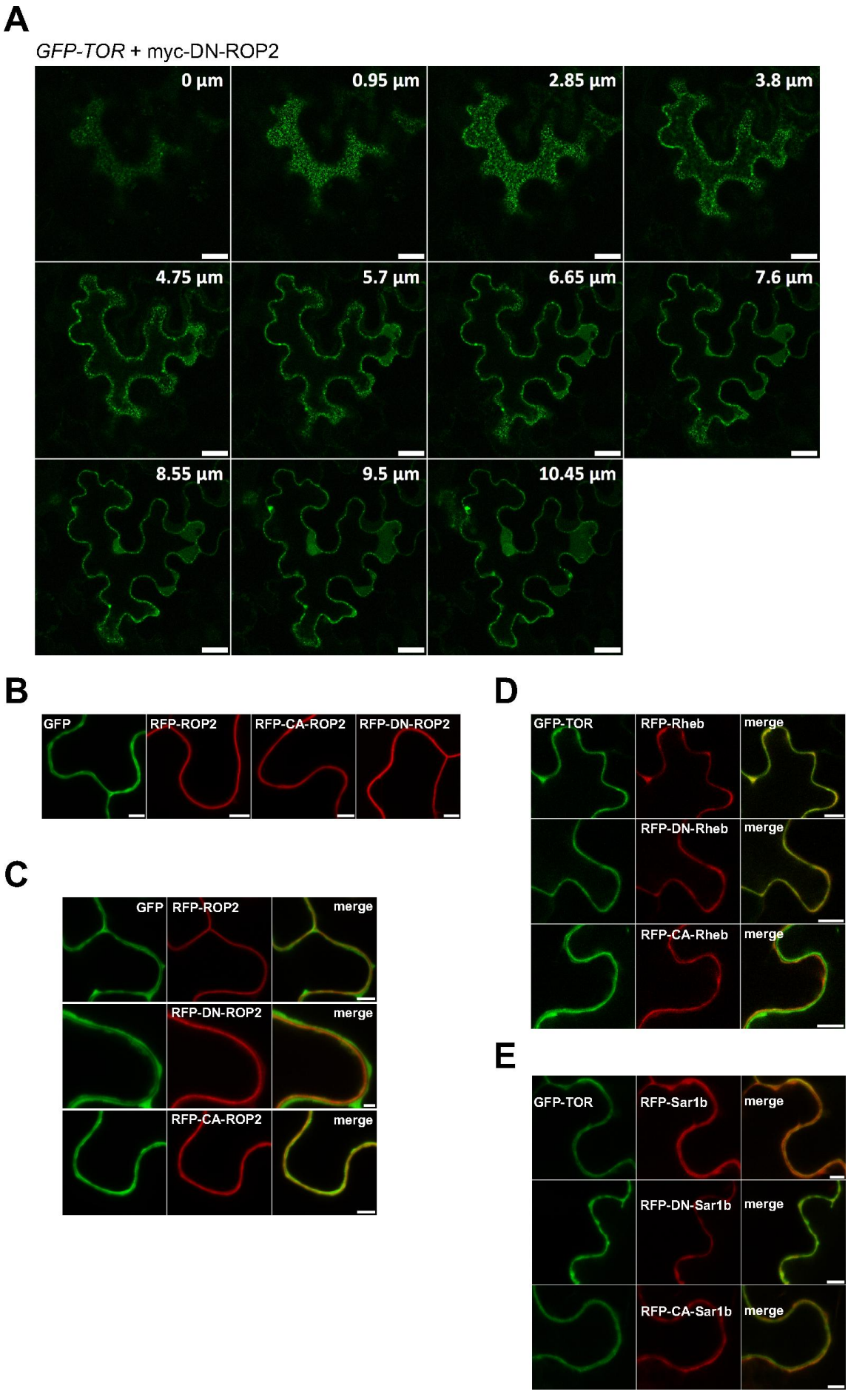
A
GFP-TOR + myc-DN-ROP2
0 µm
0.95 µm
2.85 µm
3.8 µm
4.75 µm
5.7 µm
6.65 µm
7.6 µm
8.55 µm
9.5 µm
10.45 µm
B
GFP
RFP-ROP2
RFP-CA-ROP2
RFP-DN-ROP2
C
GFP
RFP-ROP2
merge
RFP-DN-ROP2
merge
RFP-CA-ROP2
merge
D
GFP-TOR
RFP-Rheb
merge
RFP-DN-Rheb
merge
RFP-CA-Rheb
merge
E
GFP-TOR
RFP-Sar1b
merge
RFP-DN-Sar1b
merge
RFP-CA-Sar1b
merge

Appendix Figure S4.

A **Analyses of GFP-TOR dot distribution between the N. benthamiana cell periphery and the perinuclear region upon DN-ROP2 overexpression.** DN-ROP2 promotes GFP-TOR-containing multiple dot formation close to the cell periphery. Cross-section of an *Nicotiana benthamiana* epidermal cell showing the distribution of GFP-TOR punctuated dots upon overexpression of myc-DN-ROP2 in the cytoplasm. Serial sections were taken from the top at every 0.95 μm of cell depth.

Data information: Scale bars are 20 μm.

B-E **Small GTPases—Rheb and Sar1b—failed to promote GFP-TOR-containing aggregate formation in the cytoplasm of *Nicotiana benthamiana* cells.** B, C ROP2 variants failed to promote GFP-containing aggregate formation in the cytoplasm of *Nicotiana benthamiana* cells. Imaging fluorescence assays showing cells transiently expressing either GFP, or RFP-ROP2, or RFP-CA-ROP2, or RFP-DN-ROP2 (A) as well as their combination (B). *Upper panels Left* GFP (green), *central* RFP-ROP2 (red), *right* merged. *Middle panels Left* GFP (green), *central* RFP-CA-ROP2 (red), *right* merged. *Bottom panels Left* GFP (green), *central* RFP-DN-ROP2 (red), *right* merged.

D, E Sar1b and Rheb variants failed to promote GFP-TOR localization with subcellular structures in *Nicotiana benthamiana* cells. (C) *Upper panels Left* GFP-TOR (green, *1*), *central* RFP-Rheb (red, *2*), *right* merged. *Middle panels Left* GFP-TOR (green, *1*), *central* RFP-DN-Rheb (red, *2*), *right* merged. *Bottom panels Left* GFP-TOR (green, *1*), *central* RFP-CA-Rheb (red, *2*), *right* merged. (D) *Upper panels Left* GFP-TOR (green, *1*), *central* RFP-Sar1b (red, *2*), *right* merged. *Middle panels Left* GFP-TOR (green, *1*), *central* RFP-DN-Sar1b (red, *2*), *right* merged. *Bottom panels Left* GFP-TOR (green, *1*), *central* RFP-CA-Sar1b (red, *2*), *right* merged.

Data information: Scale bars are 5 μm.

2.2.14 Appendix references

Chicher J, Simonetti A, Kuhn L, Schaeffer L, Hammann P, Eriani G & Martin F (2015) Purification of mRNA-programmed translation initiation complexes suitable for mass spectrometry analysis. *Proteomics*

Clough SJ & Bent AF (1998) Floral dip: a simplified method for Agrobacterium-mediated transformation of Arabidopsis thaliana. *Plant J.* 16: 735–743

Cui D, Zhao J, Jing Y, Fan M, Liu J, Wang Z, Xin W & Hu Y (2013) The Arabidopsis IDD14, IDD15, and IDD16 Cooperatively Regulate Lateral Organ Morphogenesis and Gravitropism by Promoting Auxin Biosynthesis and Transport. *PLoS Genet.* 9: e1003759

Dereeper A, Guignon V, Blanc G, Audic S, Buffet S, Chevenet F, Dufayard JF, Guindon S, Lefort V, Lescot M, Claverie JM & Gascuel O (2008) Phylogeny.fr: robust phylogenetic analysis for the non-specialist. - PubMed - NCBI. *Nucleic Acids Res* 36: W465–W469

Karimi M, Inzé D & Depicker A (2002) GATEWAY vectors for Agrobacterium-mediated plant transformation. *Trends Plant Sci.* 7: 193–195

Li H, Shen JJ, Zheng ZL, Lin Y & Yang Z (2001) The Rop GTPase switch controls multiple developmental processes in Arabidopsis. *Plant Physiol.* 126: 670–684

Nakagawa T, Kurose T, Hino T, Tanaka K, Kawamukai M, Niwa Y, Toyooka K, Matsuoka K, Jinbo T & Kimura T (2007) Development of series of gateway binary vectors, pGWBs, for realizing efficient construction of fusion genes for plant transformation. *J. Biosci. Bioeng.* 104: 34–41

Nelson BK, Cai X & Nebenführ A (2007) A multicolored set of in vivo organelle markers for co-localization studies in Arabidopsis and other plants. *The Plant Journal* 51: 1126–1136

Pooggin MM, Hohn T & Futterer J (2000) Role of a short open reading frame in ribosome shunt on the cauliflower mosaic virus RNA leader. *J. Biol. Chem.* 275: 17288–17296

Ren H, Dang X, Yang Y, Huang D, Liu M, Gao X & Lin D (2016) SPIKE1 activates ROP GTPase to modulate petal anisotropic growth in Arabidopsis. *Plant Physiol.*: pp.00788.2016

Schepetilnikov M, Dimitrova M, Mancera-Martínez E, Geldreich A, Keller M & Ryabova LA (2013) TOR and S6K1 promote translation reinitiation of uORF-containing mRNAs via phosphorylation of eIF3h. *EMBO J.* 32: 1087–1102

Schepetilnikov M, Kobayashi K, Geldreich A, Caranta C, Robaglia C, Keller M & Ryabova LA (2011) Viral factor TAV recruits TOR/S6K1 signalling to activate reinitiation after long ORF translation. *EMBO J.* 30: 1343–1356

Yoo SD, Cho YH & Sheen J (2007) Arabidopsis mesophyll protoplasts: a versatile cell system for transient gene expression analysis. *Nat Protoc* 2: 1565–1572

Zhao Y, Christensen SK, Fankhauser C, Cashman JR, Cohen JD, Weigel D & Chory J (2001) A role for flavin monooxygenase-like enzymes in auxin biosynthesis. *Science* 291**:** 306–309

2.3 Article 3: RISP can promote reinitiation at uORFs in plants via interaction with both 40S and 60S ribosomal subunits

Eder Mancera-Martínez[1#], Ola Srour[1], Joelle Makarian[1], Odon Thiébeauld[1], Johana Chicher[2], Philippe Hammann[2], Yaser Hashem[3], Mikhail Schepetilnikov[1] and Lyubov A. Ryabova[1]*

[1]Institut de Biologie Moléculaire des Plantes, Centre National de la Recherche Scientifique, UPR 2357, Université de Strasbourg, Strasbourg, France
[2]Platforme Proteómique Strasbourg-Esplanade, Centre National de la Recherche Scientifique, FRC 1589, Université de Strasbourg, Strasbourg, France
[3]CNRS, Institut de Biologie Moléculaire et Cellulaire, Architecture et Réactivité de l'ARN UPR9002, Université de Strasbourg, 67084 Strasbourg, France

RISP can promote reinitiation at uORFs in plants via interaction with both 40S and 60S ribosomal subunits

Eder Mancera-Martínez[1#], Ola Srour[1], Joelle Makarian[1], Odon Thiébeauld[1], Johana Chicher[2], Philippe Hammann[2], Yaser Hashem[3], Mikhail Schepetilnikov[1] and Lyubov A. Ryabova[1]*

[1]Institut de Biologie Moléculaire des Plantes, Centre National de la Recherche Scientifique, UPR 2357, Université de Strasbourg, Strasbourg, France
[2]Platforme Proteómique Strasbourg-Esplanade, Centre National de la Recherche Scientifique, FRC 1589, Université de Strasbourg, Strasbourg, France
[3]CNRS, Institut de Biologie Moléculaire et Cellulaire, Architecture et Réactivité de l'ARN UPR9002, Université de Strasbourg, 67084 Strasbourg, France

#Current address: CNRS, Institut de Biologie Moléculaire et Cellulaire, Architecture et Réactivité de l'ARN UPR9002, Université de Strasbourg, 67084 Strasbourg, France.

*To whom correspondence should be addressed:
lyuba.ryabova@ibmp-cnrs.unistra.fr
Tel: +33 (0)3 67 15 53 31
Fax: +33 (0)3 88 61 44 42

Keywords: translation (re)initiation, phosphorylation via TOR, eIF2, 40S and 60S intersubunit-bridge, initiator tRNA recruitment

2.3.1 Abstract

Target-of-rapamycin (TOR) is required for translation reinitiation events in plants. TOR mediates phosphorylation of the scaffold protein reinitiation supporting protein (RISP), altering its association with eukaryotic initiation factor 3 (eIF3) and the 60S ribosomal subunit (60S) protein L24 (eL24). We show here that, in addition, RISP physically interacts with eIF2 via eIF2β and 40S via the major TOR downstream target eS6. The RISP binding is affected by mutations of a single residue, Ser267, which shown to be phosphorylated through the TOR/S6K1 pathway, that switches the RISP protein between two functionally distinct forms—the phosphorylated version of RISP (RISP-S267D) interacts preferentially with the C-terminal tails of eS6 and eL24, which are in close spatial vicinity on 80S, while the non-phosphorylatable version (RISP-S267A) prefers eIF2 and eIF3. Accordingly, we demonstrate that eIF3a/RISP-S267A/eIF2β and eS6/RISP-S267D/60S ternary complexes form *in vitro*. Transient overexpression of eIF2β in plant protoplasts up-regulates cell reinitiation capacity. An eS6 triple phosphorylation mimic, but not a phosphorylation-knockout mutant, overcomes the translation reinitiation deficiency of plants underexpressing eS6. Thus, RISP and eS6 can link 60S to 40S in response to TOR activation, indicating involvement of 80S ribosomes in reinitiation events.

2.3.2 Introduction

Translation initiation is the rate-limiting step of protein synthesis in eukaryotes and requires rapid assembly of the 43S preinitiation complex (43S PIC) composed of eukaryotic initiation factor 3 (eIF3), eIF1, eIF1A, the eIF2•GTP•Met•tRNAi^{Met} ternary complex (TC) and the 40S ribosomal subunit (40S[1,2]). eIF3 is composed of 13 distinct subunits in mammals and plants—eIF3a-eIF3m[3], and stimulates binding of tRNAi^{Met} to 43S PIC via the eIF2β subunit of a heterotrimer eIF2 that comprises eIF2α, β and γ subunits[4,5]. After translation termination, posttermination complexes are splitted by ribosome recycling factor ABCE1 and eRF1 into 60S and tRNA/mRNA-associated 40S subunits[6]. Frequently after terminating translation 40S can resume scanning and reinitiate at downstream AUGs. Reinitiation competence of ribosome depends on duration of elongation, and occurs mainly after translation of short upstream ORFs (uORFs)[7]. In this case, some eIFs, including eIF3, may remain transiently associated with ribosomes through short elongation and termination, and assist 40S scanning and *de novo* recruitment of tRNAi^{Met} and/or the 60S ribosomal subunit.

uORFs are common in mammals and plants, being present in at least 30%–45% of full-length mRNAs[8,9], where many of these are translated[10]. In eukaryotes, a target of rapamycin (TOR) signaling pathway integrates nutrient and energy sufficiency, hormones and growth factors to provide additional levels of translation initiation control via phosphorylation of several targets within the cell translation machinery[11-14]. In Arabidopsis, translation reinitiation is under control of the TOR signaling pathway[15]. Active TOR promotes translation reinitiation of mRNAs that harbour uORFs within their leader regions via phosphorylation of eIF3h that bolster the reinitiation capacity of post-terminating ribosomes, but the underlying molecular mechanisms remain enigmatic[15-17].

Reinitiation after translation of a long ORF is rare, but does occur in specific circumstances, for example, it is activated in *Cauliflower mosaic virus* (CaMV) by a single viral protein transactivator/viroplasmin (TAV)[18,19]. TAV promotes both activation of TOR and thus its downstream target S6K1 (the kinase of the 40S ribosomal protein S6, eS6), and retention of eIF3 and reinitiation supporting protein (RISP), on ribosomes throughout longer elongation[20,21]. RISP—a novel and specific target of TOR/S6K1—was identified as a TAV cofactor that assists TAV in reinitiation after long ORF translation, if phosphorylated[22]. Active TOR binds polyribosomes concomitantly with polysomal accumulation of TAV, eIF3 and RISP, with RISP being phosphorylated[21]. Strikingly, the phosphorylation status of RISP regulates its interaction with the cell translation machinery—it associates with eIF3 before

phosphorylation and, when phosphorylated, binds TAV and the 60S ribosomal protein L24 (eL24) via its C-terminal tail. Although RISP connections with either eIF3 or 60S are exploited by TAV to promote reinitiation after long ORF translation, whether RISP alone regulates gene expression when associated with the cell translation machinery remains to be determined.

Here, we present evidence that RISP functions in cellular initiation and reinitiation of translation, where its phosphorylation status is crucial for selection of partners within the cell translation machinery. Our results reveal a new role for eS6—the most studied target of TOR signaling, in supporting retention and re-use of 60S during translation reinitiation. This becomes possible since the C-terminal ends of eS6 and eL24 protrude out of 80S and, according to our data, can be connected by RISP in response to TOR activation.

2.3.3 Results

RISP interacts with intact eIF2 via subunit β

Previously, we characterized RISP as able to interact physically with eIF3 subunits a/c via its H2 helix and, when pre-bound to eIF3, with 40S, and to associate *in vitro* with the C-terminal half of the 60S ribosomal protein L24 (eL24) via its H4 helix[22] (**Fig. 1a**). *In planta*, RISP was found in preinitiation complexes containing eS6, eIF3c and eIF2β indicating that RISP together with eIF3 plays a role in initiation of translation[22]. Thus, our first objectives were to confirm whether RISP is found in eIF3-containing preinitiation complexes *in vivo*, and to investigate the possible link between RISP and eIF2 in detail.

As a first step, we elaborated a method of high-resolution mass spectrometry to identify factors that associate globally with RISP. To do this, RISP immunoprecipitated from *Arabidopsis rispa/35S:RISP-GFPox* line transgenic for GFP-tagged RISP using anti-GFP antibodies was subjected to liquid chromatography-tandem mass spectrometry analysis (LC-MS/MS). We identified 8 out of 13 eIF3 subunits, with subunits a and c being highly represented. eIF3 subunits b, h and f were also efficiently immunoprecipitated with RISP (**Supplementary Table 1**; **Supplementary Fig. 1**). We also identified TOR, already known as a direct eIF3-binding protein in mammals[23] and upstream effector of RISP[21]. Thus, several eIF3 subunits and TOR are immunoprecipitated by RISP from *Arabidopsis thaliana*.

Since eIF2 was not identified within GFP-RISP IP complexes, we assayed full-length RISP for direct binding to entire eIF2 purified from wheat germ in a GST-pull down assay (**Fig. 1b**). All three eIF2 subunits were present in the bound fraction after incubation with GST-RISP, strongly indicating GST-RISP binding to eIF2. Next, we tested the capacity of each eIF2 subunit to interact with RISP using the yeast two-hybrid assay (**Fig. 1c**). Only subunit β fused to the Gal4 binding domain (BD) interacted strongly with RISP fused to the Gal4 activation domain (AD-RISP), while α and γ were inactive, suggesting that subunit β is primarily responsible for eIF2 binding to RISP. Consistent with association of eIF2β and RISP in yeast, purified recombinant eIF2β and RISP interacted specifically in the GST pull-down assay (**Fig. 1d**). Thus, RISP associates with eIF2 via subunit β. It is known that eIF3 can promote eIF2 recruitment indirectly via eIF5, which bridges eIF3c with eIF2β in yeast and mammals[24-26], and directly, when eIF2β binds eIF3c in yeast and plants[24, 27-28] and eIF3a in yeast[29]. **Fig. 1e** shows that, as in yeast, GST-tagged eIF3a in addition to eIF3c can contact eIF2β in *Arabidopsis*.

To delineate regions of RISP involved in eIF2β binding, we performed a dissection based on predicted tertiary structure. A 3D model of *Arabidopsis* RISP, generated by

RaptorX[30], predicts, with high probability, four coiled-coil structure domains (**Fig. 1a**). The archaebacterial aIF2β[31] exhibits strong conservation with *Arabidopsis* eIF2β despite the fact that eIF2β has an N-terminal extension of 114 aminoacids. The aIF2β N-terminal α-helix is connected by a flexible linker to a central α-β domain, followed by a C-terminal zinc-binding domain (**Fig. 2b**). The 3D structure of aIF2β suggests possible folding of the conserved C-terminal part of the *Arabidopsis* subunit (C-terminus, aa 114–268). Accordingly, the eIF2β sequence was dissected into a C-terminal part, the N-terminus, and a short central α-helix (aa 121-144) that is also present within aIF2β (**Fig. 2b**).

RISP and eIF2β truncation and deletion mutants (different colors in **Fig. 2**) fused to the AD or BD domain were tested to delineate regions important for binding. The N-terminal part of RISP (aa 1–190) binds eIF2β strongly, while the C-terminal part (aa 190–389) did not bind (**Fig. 2c**). Binding was stronger between eIF2β and RISP lacking H1, but an internal deletion of H2 (aa 120–190) abolished RISP binding to eIF2β. Thus, RISP domain H2 seems to be a key contact for eIF2 subunit β. eIF2β-C binds RISP as strongly as full-length eIF2β, while the N-terminus (aa 1–121) does not (**Fig. 2c**). However, elongation of the eIF2β N-terminal fragment by an additional 23 aa (aa 1–144; eIF2β-NΔ124) restored the interaction, suggesting that a segment spanning residues 121–144 is required for RISP binding. On the 3D structure of aIF2β (**Fig. 2b**) the N-terminal alpha helix shown in black corresponds to this putative RISP binding fragment (aa 121–144). Thus, results from the yeast two-hybrid system suggest that the eIF2β α-helix downstream of two blocks of lysine residues is responsible for RISP H2 binding. Interestingly, the H2 helix is implicated in binding of eIF3a/c and eIF2β.

Phosphorylation of RISP at Ser267 decreases its binding to eIF2β

RISP is phosphorylated at Ser267 within the motif RGRLES—a pattern (R/KxR/KxxS/T) found in many Akt or S6K1 substrates—by S6K1 in a TOR-responsive manner[21]. Earlier results revealed that RISP phosphorylation can reduce its binding to eIF3c[21]. To gain a better understanding of how RISP phosphorylation changes its binding characteristics to eIF2β, we tested RISP phosphorylation mutants—the phospho-knockout mutant S267A and mimic S267D—for their binding capacities to eIF2β in a yeast two-hybrid quantitative β-galactosidase assay. As shown in **Fig. 2e**, the phosphorylation-inactive mutant RISP-S267A has a reproducibly stronger interaction with eIF2β than the phosphorylation mimic RISP-S267D or wild-type RISP that has high phosphorylation status in yeast[21]. The GST pull-down assay presented in **Fig. 2f** suggests that GST-tagged eIF2β binds RISP-S267A somewhat stronger compared with its phosphomimetic mutant (RISP-S267D) or WT (data not shown).

Overall, these data suggest that RISP, when non-phosphorylated, interacts preferentially with eIF2β and, as it was shown previously[15], the eIF3 subunit c.

To further confirm a link between RISP and eIF2β *in planta*, we analyzed their effect on translation initiation and reinitiation in plant protoplasts prepared from *Arabidopsis* suspension cultures. To address this question, we monitored translation of a β-glucuronidase (GUS) reporter ORF downstream of either of a short synthetic leader (*short GUS*; marker of the frequency of translation initiation events), or the auxin responsive factor 5 (ARF5) leader carrying six uORFs (*ARF5-GUS*), where GUS ORF translation would require reinitiation (**Fig. 3a**). A marker of transformation efficiency—*monoGFP* with a single GFP ORF downstream of the tobacco etch virus (TEV) 5'-leader—initiates via a cap-independent mechanism[32]. Under the conditions used, ARF5 leader uORFs reduced *GUS* ORF translation by about 70% compared with that of *shortGUS* mRNA (**Fig. 3b**). Here, overexpression of RISP-S267A up-regulates expression of both the short leader- and ARF5-containing GUS reporter by 1.5- and 2-fold, respectively. eIF2β overexpression either alone or in combination with RISP-S267A is somewhat indifferent for *shortGUS* mRNA translation (**Fig. 3c**). In contrast, eIF2β cotransfection gives a 2-fold increase only for *ARF5-GUS* translation (**Fig. 3d**), supporting earlier data that eIF2 is a limiting factor in reinitiation. Interestingly, eIF2β seems to be the most labile of the three subunits (eIF2α /β /γ) within the intact complex (Beilsten-Edmands et al., 2015), indicating that eIF2β overexpression might up-regulate cellular eIF2 levels. Moreover, the simultaneous overexpression of eIF2β and RISP-S267A or at significantly lesser extend RISP, but not RISP-S267D, impaired eIF2β-induced *ARF5-GUS* translation, indicating that RISP-S267A efficiently outcompetes for eIF2β.

Since RISP is involved in multiple interactions with eIF3 subunits a and c, and eIF2β via the same helix H2, we wanted to know whether RISP can be positioned within the 43S PIC according to the known contact points between eIF3, eIF2 and 40S. We used cryo-EM data[33-35] to generate the 43S PIC model to integrate the RISP 3D model generated by RaptorX[30] within the surroundings of eIF3a, eIF3c and eIF2β on 40S. Strikingly, placement of RISP H2 in close proximity to both the eIF3 subunit a (aa 615-640, approximately) and the subunit c (its N-terminal extension is shown in blue) on the intersubunit face might still allow contact with eIF2β (**Fig. 3e, f**).

RISP interacts with the C-terminal α-helix of ribosomal protein S6 (eS6)

RISP, when phosphorylated, can associate with the C-terminal tail of eL24, which protrudes out of 60S towards the C-terminus of eS6[36]. According to the 3D-structure of *S. cerevisiae*

and human 80S, eL24 protrudes out of 60S to form a new interaction site on the 40S subunit with eS6 and 18S rRNA[36,37]. Indeed, RISP was detected in fractions of 60S and 80S when wheat germ extract was fractionated on a sucrose gradient[22]. Since, 60S-bound eL24 and 40S-bound eS6 can form an inter-subunit bridge via their C-terminal tails; RISP binding to eL24 may influence formation of such a bridge.

To test this hypothesis, we first looked for a complex between *Arabidopsis* eL24 and eS6 *in vitro*. All attempts to reveal direct interaction between eL24 and eS6 and their deletion mutants failed (data not shown). We then tested if RISP can provide additional contacts between eL24 and eS6 using the yeast two-hybrid system (**Fig. 4**). Although AD-RISP interacts strongly with BD-S6 under our yeast two-hybrid system conditions, none of the RISP fragments assayed interacted with full-length eS6 (**Fig. 4a**), probably indicating the critical importance of RISP tertiary structure for this interaction. Taking advantage of the known 3D conformation of ribosome-bound eS6[36]; **Fig. 4b**), eS6 was dissected into three fragments. Two fragments of eS6—the central fragment, MS6 (aa 83–177) and the C-terminal alpha-helix, CS6 (aa 177–249)—bind RISP as strongly as the full-length protein (**Fig. 4c**). However, the longer C-terminal fragment of eS6, ICS6 (aa 130–249) failed to interact with RISP, indicating that the RISP binding site is somewhat concealed by a 47-aa fragment insertion in our yeast two-hybrid conditions. Since direct interaction between MS6 and the central segment of eL24 within the 80S ribosome has been suggested[37], we concentrated on characterization of the CS6 alpha-helix interaction with RISP by the GST pull-down assay. The RISP and GST-tagged CS6 interaction *in vitro* was specific (**Fig. 4d**)—RISP was present in the bound fraction after incubation with GST-CS6. Thus, our results indicate that RISP can potentially mediate the interaction between 40S and 60S ribosomal subunits by providing contacts with the C-terminal domains of eL24 and eS6, which are both solvent-exposed within 80S.

Given that RISP phosphorylation up-regulates its interaction with eL24[21], we next tested whether RISP phosphorylation would also govern its interaction with the C-terminal α-helix of eS6 in the yeast two-hybrid system. Remarkably, compared with controls, wild type RISP and the phosphorylation mimic mutant of RISP (RISP-S267D) interacted reproducibly more strongly with CS6 than the RISP phosphorylation inactive mutant (**Fig. 4e**). These results confirm that phosphorylation of RISP promotes its interaction with both the C-terminus of eS6 and, according to our earlier data, eL24.

60S retention by eS6 C-terminal α-helix requires RISP phosphorylated at S267

To further confirm the hypothesis that TOR-responsive RISP phosphorylation governs recruitment of RISP to both eL24 and eS6, while attenuating RISP binding to both eIF3 and eIF2, RISP phosphorylation mimic and phospho-knockout mutants were assayed for reconstitution experiments in the GST pull-down assay with direct targets of RISP—eIF3a, the C-terminal α-helix of eS6 and wheat germ 60S ribosomal subunits.

Although eIF2β was implicated in interaction with eIF3 via a (**Fig. 1e**) and c subunits[28], the same subunits associate with RISP[22], suggesting multiple contacts between eIF3a/ eIF3c, RISP and eIF2β. We used GST-tagged eIF3a pre-bound with either RISP-S267A or RISP-S267D mutants to demonstrate that RISP binding does not interfere with eIF2 accommodation by eIF3a. Thus, GST-eIF3a bound to glutathione beads was incubated with excess RISP, either phosphorylation mimic or knockout (**Fig. 5a**), followed by incubation of bound fractions with or without eIF2β. Although, both RISP knockout and phosphomimic remain bound to GST-eIF3a after extensive washing, the level of GST-eIF3a-bound RISP-S267A was reproducibly 2-fold higher than that for RISP-S267D (fractions 12 and 18, respectively). Accordingly, the eIF2β component was about 2-fold enriched in the eIF3a-bound RISP-S267A as compared with eIF3a/RISP-S267D. Neither eIF2β nor RISP interacted with GST alone (**Fig. 5a**, lanes 6 and 8, respectively). These results suggest that eIF3-bound RISP also has the capacity to accommodate eIF2.

Next, we assayed *in vitro* assembly of a complex between the eS6 C-terminal domain, to mimic eS6 C-terminus folding on 40S, and analyzed whether each of the RISP phosphorylation mutants can pull down the 60S ribosomal subunit. Indeed, a significant fraction of RISP-S267A and RISP-S267D was found in the GST-eCS6 bound fraction (**Fig. 5b**, lanes 8 and 14, respectively). Remarkably, RISP phosphorylation knockout (RISP-S267D) bound to GST-CS6 was able to pull down 60S, as manifested by the presence of at least two 60S ribosomal proteins in the GST-CS6-bound fraction. No 60S interacted with RISP-S267A bound to GST-CS6 (**Fig. 5b**); thus, RISP failed to bridge CS6 and 60S before being phosphorylated, but was fully able to connect the C-terminal α-helix of eS6 and 60S after phosphorylation. These results suggest that the phosphomimetic mutant of RISP promotes formation of a bridge between the C-proximal helices of eS6 and 60S likely via eL24. As TOR triggers RISP phosphorylation during translation, and, given that eS6 is a TOR major downstream target among ribosomal proteins in eukaryotes[2] and is phosphorylated**,** we next asked whether eS6 phosphorylation plays a role in (re)initiation of translation.

***Arabidopsis* plants overexpressing eS6 phosphorylation mimic (eS6-S237D/S240D/S241D) are more competent for reinitiation of translation**

Phosphoproteomic studies in *Arabidopsis* suggest significant quantitative increase in phosphorylation state of two redundant and interchangeable eS6a and eS6b proteins (*RPS6A* and *RPS6B*[38]; in response to high CO_2 and light, auxin and cytokinin availability[39-42]. First, we decided to test a role of phosphorylation of several closely spaced phosphorylation sites—S231, S237 and S240[40,41,43] in eS6 binding to RISP. Two of these sites are characterized by a pattern found in many plant S6K1 substrates (S231, DRRSES; S237, LAKKRS; **Fig. 6a**). Strikingly, phosphomimetic mutants of eCS6 at S231, or S237, or S240, display statistically more significant interactions with RISP-S267D than their phospho-knockout mutants (**Fig. 6b**).

To directly test the functional consequences of eS6 phosphorylation, we next varied intracellular concentrations of "phosphorylated" eS6 *in planta* to assess effects of eS6 phosphorylation on plant reinitiation capacities. We took advantage of T-DNA insertion *s6a* knockout mutant, where total eS6 level was reduced to S6B levels (**Fig. 6c**), and used it to obtain 35S-promoter-driven stable expression of either the S6B phosphorylation mimic mutant (*s6a/S6B*$^{S/D}$) where three closely spaced serines, S237, S240 and S241, were replaced by either D (*S237D/S240D/S241D*), or phospho-knockout mutant (*s6a/S6B*$^{S/A}$*)* with A (*S237A/S240A/S241A*; all mutant phenotypes are shown in **Fig. S2 a, b**). Western blot analysis of obtained homozygous lines suggests that low S6B levels in *s6a* mutant were nearly restored in our transgenic lines (**Fig. 6c**). However, 35S-promoter-driven expression of S6B did not significantly restore *S6a* mutant developmental defects such as growth retardation and leaf asymmetry (**Supplementary Fig. 2**).

To determine the contribution of eS6 to regulating initiation or reinitiation events, we used mesophyll protoplasts generated from WT seedlings, *s6a* and *s6a/S6B*$^{S/A}$, and *s6a/S6B*$^{S/D}$ transgenic lines, and compared their (re)initiation capacities. Initiation events were monitored with the construct containing the β-glucuronidase (GUS) ORF following a short leader (p*shortGUS*), while the impact of events undergoing reinitiation after short ORF translation were followed with reporter plasmid *ARF5-GUS* (**Fig. 6d**). We also tested whether a special case of reinitiation after long ORF translation under control of a CaMV translation transactivator/ viroplasmin (TAV) is sensitive to phosphorylation status of eS6. Here, we used the bicistronic reporter plasmid p*biGUS*, containing two consecutive ORFs: CaMV ORF VII and GUS, where GUS serves as a marker of transactivation, and with or without the reporter plasmid expressing TAV[44] (Fig. **6d**).

The levels of transiently expressed GUS from p*short-GUS* did not differ significantly in WT, *s6a*, *s6a/S6B*$^{S/D}$ and *s6a/S6B*$^{S/A}$ protoplasts (**Fig. 6d**, lane 1). In contrast, translation reinitiation on *ARF5-GUS* mRNA was reduced 3-fold in *s6a* as compared with that in WT protoplasts, strongly suggesting a role for eS6 in translation renitiation (**Fig. 6d**, lane 2). The level of reinitiation was partially restored in *s6a/S6B*$^{S/A}$, and fully restored in *s6a/S6B*$^{S/D}$-derived protoplasts. Virus-induced reinitiation after long ORF translation that is strictly dependent on TAV—upstream ORF VII blocks downstream GUS ORF expression and no GUS activity appeared in all tested protoplasts without TAV—was reduced by 2-fold (**Fig. 6d**, cf lanes 3/4 in WT and *s6a*). Strikingly, the transactivation ability of TAV was decreased further in *s6a/S6B*$^{S/A}$-derived, but fully restored in *s6a/S6B*$^{S/D}$-derived protoplasts. Thus, TAV-controlled reinitiation after long ORF translation is eS6-dependent, and requires eS6 phosphorylation. No significant differences in RNA transcript or TAV/GFP levels were seen in any of the protoplasts tested (**Fig. 6d**). These results suggest a role for eS6 in translation reinitiation, and suggest that eS6 phosphorylation is necessary for plants to acclimate to reinitiation events.

2.3.4 Discussion

uORFs within the leaders of mRNAs have been implicated in translational control of plant growth and development, including meristem maintenance[45] and responses to auxin[9,15]. Despite inhibition of main ORF translation by one or multiple uORFs, reinitiation persists by a mechanism that relies on activation of target-of-rapamycin, TOR[15], but the role of TOR has not been completely understood. We previously described a TOR downstream target, the reinitiation supporting protein, RISP, that, when phosphorylated, promotes reinitiation after long ORF translation under the control of the virus-specific translation transactivator TAV[21,22]. Here, we identified RISP as a dynamic partner for assembly of either the eIF3-containing complex with eIF2, or 40S and 60S ribosomal subunits via the eS6–eL24. Aside from eIF3 and the 60S ribosomal protein eL24[22], here we identified two additional RISP-interacting partners—eIF2, which is primarily responsible for initiator tRNA delivery, and, strikingly, the 40S ribosomal protein eS6, which, together with eL24, may form a specific bridge between the 40S and 60S ribosomal subunits[37]. These interactions appear to strengthen previously proposed RISP function in recruitment of TC and open a new attractive role for RISP in 60S joining *de novo* or retention of 60S during post-termination events. *In planta*, reinitiation defects of the eS6 deficient mutant *Arabidopsis* are restored only by overexpression of an eS6 phosphomimetic mutant, although we did not modify all eS6 C-terminal phosphorylation sites. The interaction between RISP and these two clusters of partners is governed by phosphorylation of RISP at S267 within its α-helix 3. Thus, our studies have uncovered a molecular mechanism underlying the role of phosphorylation in the dynamic interactions between RISP and its partners. When non-phosphorylated, RISP physically associates with eIF3 and eIF2, whereas after phosphorylation it can maneuver to 80S via binding to eS6 and eL24 C-terminal α-helices, which are exposed to solvent[36].

However, S267 seems not to be a critical interface for interaction with its multiple partners; we assume that phosphorylation of RISP may trigger conformational rearrangements that weaken the association with eIF3 and eIF2, and strengthen alternative interactions on 80S. Also, phosphorylation can modulate RISP–eS6 protein–protein interactions via modulating their ionic contacts. In mammals, active TOR or inactive S6K1 interact readily with eIF3, but dissociate if their active status is changed[23].

Our experimental design, which combined *in vitro* and protoplast examination of eIF3a and eIF2β binding to a RISP phosphorylation mutant, allowed us to demonstrate ternary complex formation between eIF2β•RISP•eIF3c and selection of the RISP phospho-knockout mutant as a preferential partner within the complex. Although, *in planta*, eIF2α-complexes

contain RISP[22], MS-MS analysis failed to identify eIF2 subunits in GFP-RISP-complexes suggesting possibly transient contacts, but reveal the presence of eIF3 subunits and TOR, indicating the possibility of RISP phosphorylation directly within eIF3-containing complexes, as suggested in mammals[23]. Taking into account the previous results of interaction mapping, we may locate RISP in close proximity to both eIF3a and eIF3c on 40S (**Fig. 3e, f**) in the position that is well adapted for eIF2β capture according to the recently published architecture of the 43S PIC[35]), the 48S-open/closed PIC[34] and the 40S•eIF1•eIF3 complex[33]. The latter structures suggest an extended orientation for eIF3c N-terminus and eIF3a that encircles the 40S towards to the subunit interface.

In contrast, RISP preferentially associates with eS6 and, as shown previously[15], eL24. Within the 3D structure of 80S[36,46], 40S and 60S are connected by two long protein helices extending from the left eL19 (eB12 bridge) and right sides of the 60S subunit interface eL24 (eB13, located near the main factor binding site of 60S). Strikingly, the putative RISP 3D structure is well suited for integration into the elongating 80S (**Fig. 7a**) or the putative open conformation of 80S (**Fig. 7b**), where 60S is connected to 40S via RISP-mediated interactions between eS6/eL24 C-terminal protruding ends. The latter hypothesis is of importance since it gives functional meaning to the eS6- and eL24-protruding ends. Our hypothesis of 60S retention during 80S reinitiation correlates well with *in vitro* data suggesting scanning and reinitiation by terminating 80S in mammals[6], and the crucial importance of ribosomes splitting at the termination step to allow specific recognition of downstream AUG codons in yeast[47]. However, whether RISP binding would interfere or not with the function of ribosome recycling factor, ABCE1[48], remains to be examined.

Our study has revealed a role for eS6 in plant translation reinitiation, where it can function in an ensemble with eL24. In contrast to eS6, eL24 has long been known as a reinitiation-supporting factor that is critical for 60S joining to the 48S PIC[49,50] and translation of uORF-containing mRNAs such as ARF3 and ARF5[9,51].

Based on our findings, we propose a model (**Fig. 7c**) in which RISP can mediate either 43S PIC assembly or translation reinitiation depending on its phosphorylation status. Before being phosphorylated, RISP is recruited to 43S PIC as a complex with eIF3, where RISP helix 2 contacts eIF3 subunits a and/or c (**Fig. 3e, f**). Here, the eIF3/RISP complex participates in ternary complex recruitment via eIF2 (**Fig. 3e, f**). TOR, which is present in RISP/eIF3-containing complexes, triggers phosphorylation of S6K1. One might expect that phosphorylation of RISP by activated S6K1 would proceed in close proximity to 48S PIC[23]. Although RISP is attached to eIF2-eIF3 before phosphorylation, its phosphorylation could

trigger RISP-P relocation to the eS6 C-terminus and/or eL24. An interesting possibility is that the link between RISP and eS6/eL24 could be used for the retention of RISP through elongation (RISP positioning on 80S is proposed in **Fig. 7b**) and, during resuming of scanning. These novel interactions between RISP and the 40S ribosomal protein eS6 could ensure the re-use of 60S via the eS6•RISP•eL24 interaction network (see putative model of 60S holding by scanning 40S via RISP in **Fig. 7c**). Recruitment of TC *de novo* could be achieved either via eIF3 alone or via its complex with RISP, if nonphosphorylated RISP is available. Clearly there are many layers of eS6 function in translation under the control of TOR, and many of these are yet to be explored in eukaryotes and explained at the molecular level. Thus, phosphorylation of eS6, which has attracted much attention since its discovery, seems to be important in plant translation reinitiation. Obviously, further work on the functional consequences of eS6 phosphorylation is needed to better understand the role of phosphorylation in translational control.

2.3.5 Methods

Plant materials and growth conditions. *Arabidopsis thaliana* ecotype Columbia-0 (Col-0) and *s6a*[38] were grown under standard greenhouse conditions with supplemental light on a 16 h/8 h dark cycle. *s6a* was kindly provided by T. Desnos (LBDP, Université Aix-Marseille-II, France). *rispa Arabidopsis* line was described[22]. All the plants were in Col-0 ecotype background. *s6a* line was transformed by the floral dip method with either p*GWB2-eS6B*, or p*GWB2-eS6B-S237A/S240A/S241A*, or p*GWB2-eS6B-S237D/S240D/S241D*, or p*GWB5-eS6B-cMyc*. Then *s6a/S6B*, *s6a/S6B*$^{S/D}$ and *s6a/S6B*$^{S/A}$ homozygous lines were screened based on hygromycin resistance. The *rispa* line was transformed with p*GWB5-RISP-GFP*, and two *rispa/RISP-GFPox* homozygous lines ectopically expressing RISP-GFP were isolated based on hygromycin resistance.

Protoplast assays. p*shortGUS* (or p*monoGUS*) and p*monoGFP* were described previously[21] and p*ARF5-GUS*[15]. PCR product corresponding to AteIF2β was amplified from eIF2β cDNA (At5g20920) with pairs of specific primers and cloned into p*monoGUS* to replace GUS and obtain the p*eIF2β* construct. The RISP coding sequence was subcloned under the control of the *CaMV* 35S promoter into p*TAV* (p35S-P6)[22] to obtain p*RISP*. p*RISP-S267A* and p*RISP-S267D* were generated by substitution of Ser at the position 267 to Ala (S267A) and Asp (S267D), respectively, within RISP ORF by site-directed PCR mutagenesis. Arabidopsis protoplasts from *Arabidopsis* suspension cell cultures and mesophyll protoplasts from 2-week WT, s6a, *s6a/S6B*$^{S/D}$, or *s6a/S6B*$^{S/A}$ plantlets were transfected with plasmid DNA by the PEG method[52]. 5 µg p*monoGFP* and either 5 µg p*shortGUS* or p*ARF5-GUS*, without or with increasing concentrations of p*RISP* (or phosphorylation mutants of RISP) and/ or p*eIF2β* as indicated were used for cotransformation of *Arabidopsis* suspension culture protoplasts (Fig. 3b-d). 5 µg p*monoGFP* and (1) 5 µg p*shortGUS* or (2) 10 µg p*ARF5-GUS*, or two pairs of plasmids—(3) 10 µg p*biGUS*[44] and 10 µg p*35S* or (3/4) 10 µg p*biGUS* and p*TAV* (p35S-P6)[53] were used to transform mesophyll protoplasts prepared from WT, *s6a*, *s6a/S6B*$^{S/D}$, or *s6a/S6B*$^{S/A}$ *Arabidopsis* (Fig. 6d). After over-night incubation at 26°C in WI buffer (4 mM MES pH 5.7, 0.5 M Mannitol, 20 mM KCl) transfected protoplasts were harvested by centrifugation and protein extract was prepared in GUS extraction buffer (50 mM NaH_2PO_4 pH 7.0, 10 mM EDTA, 0.1% NP-40). The aliquots were immediately taken for GUS reporter gene assays. GUS activity was measured by a fluorimetric assay using a FLUOstar OPTIMA fluorimeter (BMG Biotech)[54]. pmonoGFP expression was monitored by western blot using anti-GFP antibodies (Chromotek) and/ or by determining GFP fluorescence. The values given

are the means from at least three independent experiments. GUS mRNA levels after protoplasts incubation were determined as indicated in supplementary information.

GST pull-down assay. PCR products corresponding to RISP, eIF3aΔ (aa 1-646), eIF2β and eS6 C-ter (CS6) were inserted into pGEX-6P1 (Pharmacia Biotech) as in-frame fusions with GST. The in vitro Glutathione-S-transferase pull-down assay was performed as described previously[20]. GST pull-down assays were set up as follows: molar equivalents of purified proteins were incubated with the immobilized GST or GST-tagged protein at 4°C for 2 h under constant rotation. Binding of GST or GST-RISP to wheat eIF2, GST or GST-RISP to His-eIF2β, GST or GST-eIF2β to RISP phosphorylation mutants, and GST or GST-eIF3a to His-eIF2β was carried out in a 300 µL reaction containing 50 mM HEPES pH 7.5, 100 mM KCl, 3 mM magnesium acetate, 0.1 mM EDTA, 0.5 % v/v Igepal 360® (Sigma-Aldrich®) and cOmplete® protease inhibitor cocktail (Roche®). Sepharose beads and associated proteins (bound fraction, B) were recovered by centrifugation at 500g for 5 min and thoroughly washed as before (4 washing steps). Fifty µL of the first unbound fraction (U) solution and bound fraction were used for SDS-PAGE analysis. Binding of GST or GST-eIF3a (—GST or GST-CS6—) to RISP phosphorylation mutants—RISP-S267A or RISP-S267D—was carried out in 3-fold increased reaction mixture (900 µl) overnight at 4 °C. After intensive washing, GST-eIF3a-RISP-S267A or GST-eIF3a-RISP-S267D complexes were split into three equal fractions, washed and used for incubation with or without eIF2β, 70 pmol (—purified 60S ribosomal subunits, respectively, 100 pmol—) during 2 h at 4 °C. eIF2β– or 60S-bound complex formation was analyzed (Fig. 5). The bound fractions (B) as well as 50 µL of the unbound fraction (U) were separated by a 12% SDS-PAGE gel and stained by Coomassie™ blue.

Protein purification. Wheat germ eIF2 was kindly provided by K. Browning (University of Texas at Austin, USA). GST-fusion and His-tagged proteins were expressed in Rosetta 2 DE3 pLysS (Novagen®) and purified using Glutathione Sepharose4B beads or HisTrap HP columns (GE Healthcare®), according to supplier protocol.

Yeast two-hybrid assay. PCR products corresponding to eIF2 α, β and γ subunits were amplified from eIF2α (AT5G05470.1), eIF2β (AT5G20920.1) and eIF2γ (AT1G04170.1) cDNAs with pairs of specific primers and cloned into the pGBKT7 vector (Clontech®) as in-frame fusion with the BD-domain to obtain the pBD-eIF2 subunit variants. eIF2β and eS6

deletion mutants fused to the BD-domain in the pGBKT7 vector were produced by deletion mutagenesis of the pGBK-eIF2β and eS6 (AT5G10360.1) cDNA. RISP (AT5G61200.3) and its deletion mutants fused to AD were produced by PCR from the original pGAD-RISP[22] and cloned between the NdeI and BamHI sites of pGADT7 (Clontech®). PCR product corresponding to RISP-S267D and RISP-S267A were generated by substitution of Ser at position 267 to Asp (S267D) or to Ala (S267A) from pGAD-RISP by site-directed PCR mutagenesis and cloned into pGADT7 vector to obtain the pGAD-RISP-S267D and pGAD-RISP-S267A constructs.

Yeast two-hybrid protein interaction assays were performed according to ref. 21. Constructs containing GAL4 AD-domain and BD-domain fusion variants were co-transformed into AH109 cells. Transformants were selected onto SD-Leu-Trp plates. Surviving yeast colonies were picked as primary positives and transferred on SD-Leu-Trp-Ade selection plates to score protein interaction. β-Galactosidase activity was measured by using the Gal-Screen® assay system (Tropix® by Applied Biosystems®) The values given are the means from more than three independent experiments. Yeast expression levels of all the BD- and AD-fusion variants were monitored by immunoblot analysis with anti-HA (Sigma-Aldrich®) and anti-cMyc (Santa-Cruz Biotechnology®) antibodies of yeast cell lysates using a rapid urea/SDS lysis procedure (data not shown).

Mass spectrometry analysis. Samples were prepared for mass-spectrometry analyses as described[55]. Briefly, samples solubilized in Laemmli buffer were precipitated with 0.1 M ammonium acetate in 100% methanol. After a reduction-alkylation step (Dithiothreitol 5 mM - Iodoacetamide 10 mM), proteins were digested overnight with 1/25 (W/W) of sequencing-grade porcin trypsin (Promega). The peptide mixtures were resolubilized in water containing 0.1% FA (solvent A) before being injected on nanoLC-MS/MS (NanoLC-2DPlus system with nanoFlex ChiP module; Eksigent, ABSciex, Concord, Ontario, Canada, coupled to a TripleTOF 5600 mass spectrometer (ABSciex)). Peptides were eluted from the C-18 analytical column (75 µm ID x 15 cm ChromXP; Eksigent) with a 5%-40% gradient of acetonitrile (solvent B) for 90 minutes. Data were searched against a TAIR database containing the GFP-TOR sequence as well as decoy reverse sequences (TAIR10_pep_20101214). Peptides were identified with Mascot algorithm (version 2.2, Matrix Science, London, UK) through the ProteinScape 3.1 package (Bruker). They were validated with a minimum score of 30, a p-value<0.05 and proteins were validated respecting a false discovery rate FDR<1%.

Molecular modeling. The 3D structural model of *Arabidopsis* RISP was created using RaptorX[56] based on tropomyosin structure (PDB: 1C1G) and represented graphically by PyMOL (http://www.pymol.org).

2.3.6 Acknowledgments

We are grateful to J-M Daviere and N. Baumberger for helpful assistance in plant genetics and protein analysis, respectively. This work was supported by French Agence Nationale de la Recherche—BLAN-2011_BSV6 010 03, France—for funding L.R., and CONACYT, Service de Coopération Universitaire de l'Ambassade de France au Mexique to E. M-M. This work was supported in part by the ANR grant @RAction program 'ANR CryoEM80S' and the LABEX: ANR-10-LABX-0036_NETRNA and benefits from a funding from the state managed by the French National Research Agency as part of the Investments for the future program (to Y.H.).

2.3.7 References

1. Jackson, R. J., Hellen, C. U. T. & Pestova, T. V. The mechanism of eukaryotic translation initiation and principles of its regulation. *Nature Reviews Molecular Cell Biology* **11,** 113–127 (2010).

2. Browning, K. S. & Bailey-Serres, J. Mechanism of Cytoplasmic mRNA Translation. *The Arabidopsis Book* **13,** e0176–39 (2015).

3. Hinnebusch, A. eIF3: a versatile scaffold for translation initiation complexes. *Trends Biochem. Sci.* **31,** 553–562 (2006).

4. Flynn, A., Oldfield, S. & Proud, C. G. The role of the beta-subunit of initiation factor eIF-2 in initiation complex formation. *Biochim. Biophys. Acta* **1174,** 117–121 (1993).

5. Huang, H. K., Yoon, H., Hannig, E. M. & Donahue, T. F. GTP hydrolysis controls stringent selection of the AUG start codon during translation initiation in Saccharomyces cerevisiae. *Genes Dev* **11,** 2396–2413 (1997).

6. Skabkin, M. A., Skabkina, O. V., Hellen, C. U. T. & Pestova, T. V. Reinitiation and other unconventional posttermination events during eukaryotic translation. *Mol. Cell* **51,** 249–264 (2013).

7. Kozak, M. Constraints on reinitiation of translation in mammals. *Nucleic Acids Res* **29,** 5226–5232 (2001).

8. Calvo, S. E., Pagliarini, D. J. & Mootha, V. K. Upstream open reading frames cause widespread reduction of protein expression and are polymorphic among humans. *Proc. Natl. Acad. Sci. U.S.A.* **106,** 7507–7512 (2009).

9. Zhou, F., Roy, B. & Arnim, von, A. G. Translation reinitiation and development are compromised in similar ways by mutations in translation initiation factor eIF3h and the ribosomal protein RPL24. *BMC Plant Biology* **10,** 193 (2010).

10. Ingolia, N. T., Lareau, L. F. & Weissman, J. S. Ribosome profiling of mouse embryonic stem cells reveals the complexity and dynamics of mammalian proteomes. *Cell* **147,** 789–802 (2011).

11. Gingras, A. C., Raught, B. & Sonenberg, N. Regulation of translation initiation by FRAP/mTOR. *Genes Dev* **15,** 807–826 (2001).

12. Sengupta, S., Peterson, T. R. & Sabatini, D. M. Regulation of the mTOR complex 1 pathway by nutrients, growth factors, and stress. *Mol. Cell* **40,** 310–322 (2010).

13. Ma, X. M. & Blenis, J. Molecular mechanisms of mTOR-mediated translational control. *Nature Reviews Molecular Cell Biology* **10,** 307–318 (2009).

14. Dobrenel, T. *et al.* TOR Signaling and Nutrient Sensing. *Annu Rev Plant Biol* **67,** annurev–arplant–043014–114648 (2016).

15. Schepetilnikov, M. *et al.* TOR and S6K1 promote translation reinitiation of uORF-containing mRNAs via phosphorylation of eIF3h. *EMBO J.* **32,** 1087–1102 (2013).

16. Kim, T. H., Kim, B. H., Yahalom, A., Chamovitz, D. A. & Arnim, von, A. G. Translational regulation via 5' mRNA leader sequences revealed by mutational analysis of the Arabidopsis translation initiation factor subunit eIF3h. *Plant Cell* **16,** 3341–3356 (2004).

17. Roy, B. *et al.* The h subunit of eIF3 promotes reinitiation competence during translation of mRNAs harboring upstream open reading frames. *RNA* **16,** 748–761 (2010).

18. Futterer, J. & Hohn, T. Role of an upstream open reading frame in the translation of polycistronic mRNAs in plant cells. *Nucleic Acids Res* **20,** 3851–3857 (1992).

19. Ryabova, L. A., Pooggin, M. M. & Hohn, T. Translation reinitiation and leaky scanning in plant viruses. *Virus Res* **119,** 52–62 (2006).

20. Park, H. S., Himmelbach, A., Browning, K. S., Hohn, T. & Ryabova, L. A. A plant viral 'reinitiation' factor interacts with the host translational machinery. *Cell* **106,** 723–733 (2001).

21. Schepetilnikov, M. *et al.* Viral factor TAV recruits TOR/S6K1 signalling to activate reinitiation after long ORF translation. *EMBO J.* **30,** 1343–1356 (2011).

22. Thiebeauld, O. *et al.* A new plant protein interacts with eIF3 and 60S to enhance virus-activated translation re-initiation. *EMBO J.* **28,** 3171–3184 (2009).

23. Holz, M. K., Ballif, B. A., Gygi, S. P. & Blenis, J. mTOR and S6K1 mediate assembly of the translation preinitiation complex through dynamic protein interchange and ordered phosphorylation events. *Cell* **123,** 569–580 (2005).

24. Asano, K., Clayton, J., Shalev, A. & Hinnebusch, A. G. A multifactor complex of eukaryotic initiation factors, eIF1, eIF2, eIF3, eIF5, and initiator tRNA(Met) is an important translation initiation intermediate in vivo. *Genes Dev* **14,** 2534–2546 (2000).

25. Das, S., Maiti, T., Das, K. & Maitra, U. Specific interaction of eukaryotic translation initiation factor 5 (eIF5) with the beta-subunit of eIF2. *J. Biol. Chem.* **272,** 31712–31718 (1997).

26. Fletcher, C. M., Pestova, T. V., Hellen, C. U. & Wagner, G. Structure and interactions of the translation initiation factor eIF1. *EMBO J.* **18,** 2631–2637 (1999).

27. Dennis, M. D. & Browning, K. S. Differential phosphorylation of plant translation initiation factors by *Arabidopsis thaliana* CK2 holoenzymes. *J Biol Chem* **284,** 20602–20614 (2009).

28. Dennis, M. D., Person, M.D. & Browning, K. S. Phosphorylation of plant translation initiation factors by CK2 enhances the *in vitro* interaction of multifactor complex

components. *J Biol Chem* **284,** 20615–20628 (2009).

29. Valášek, L., Nielsen, K. H. & Hinnebusch, A. G. Direct eIF2-eIF3 contact in the multifactor complex is important for translation initiation in vivo. *EMBO J.* **21,** 5886–5898 (2002).

30. Källberg, M., Wang, H., Wang, S., Peng, J., Wang, Z., Lu, H. & Xu, J. Template-based protein structure modeling using the RaptorX web server. *Nature Protocols* **7**, 1511-1522 (2012).

31. Schmitt, E., Naveau, M. & Mechulam, Y. Eukaryotic and archaeal translation initiation factor 2: a heterotrimeric tRNA carrier. *FEBS Lett.* **584,** 405–412 (2010).

32. Zeenko, V. & Gallie, D. R. Cap-independent translation of tobacco etch virus is conferred by an RNA pseudoknot in the 5'-leader. *J. Biol. Chem.* **280,** 26813–26824 (2005).

33. Erzberger, J. P. *et al.* Molecular Architecture of the 40S · eIF1 · eIF3 Translation Initiation Complex. *Cell* **158,** 1123–1135 (2014).

34. Llácer, J. L. *et al.* Conformational Differences between Open and Closed States of the Eukaryotic Translation Initiation Complex. *Molecular Cell* (2015). doi:10.1016/j.molcel.2015.06.033

35. Georges, des, A. *et al.* Structure of mammalian eIF3 in the context of the 43S preinitiation complex. - PubMed - NCBI. *Nature* (2015).

36. Ben-Shem, A. *et al.* The Structure of the Eukaryotic Ribosome at 3.0 A Resolution. *Science* (2011). doi:10.1126/science.1212642

37. Khatter, H., Myasnikov, A. G., Natchiar, S. K. & Klaholz, B. P. Structure of the human 80S ribosome. *Nature* (2015). doi:10.1038/nature14427

38. Creff, A., Sormani, R. & Desnos, T. The two Arabidopsis RPS6 genes, encoding for cytoplasmic ribosomal proteins S6, are functionally equivalent. *Plant Mol. Biol.* **73,** 533–546 (2010).

39. Turck, F., Zilbermann, F., Kozma, S. C., Thomas, G. & Nagy, F. Phytohormones participate in an S6 kinase signal transduction pathway in Arabidopsis. *Plant Physiol.* **134,** 1527–1535 (2004).

40. Boex-Fontvieille, E. *et al.* Photosynthetic control of Arabidopsis leaf cytoplasmic translation initiation by protein phosphorylation. *PLoS ONE* **8,** e70692 (2013).

41. Turkina, M. V., Klang Årstrand, H. & Vener, A. V. Differential phosphorylation of ribosomal proteins in Arabidopsis thaliana plants during day and night. *PLoS ONE* **6,** e29307 (2011).

42. Carroll, A. J., Heazlewood, J. L., Ito, J. & Millar, A. H. Analysis of the Arabidopsis

cytosolic ribosome proteome provides detailed insights into its components and their post-translational modification. *Mol. Cell Proteomics* **7,** 347–369 (2008).

43. Reiland, S. *et al.* Large-scale Arabidopsis phosphoproteome profiling reveals novel chloroplast kinase substrates and phosphorylation networks. *Plant Physiol.* **150,** 889–903 (2009).

44. Bonneville, J. M., Sanfacon, H., Futterer, J. & Hohn, T. Posttranscriptional trans-activation in cauliflower mosaic virus. *Cell* **59,** 1135–1143 (1989).

45. Zhou, F., Roy, B., Dunlap, J. R., Enganti, R. & Arnim, von, A. G. Translational control of Arabidopsis meristem stability and organogenesis by the eukaryotic translation factor eIF3h. *PLoS ONE* **9,** e95396 (2014).

46. Anger, A. M. *et al.* Structures of the human and Drosophila 80S ribosome. *Nature* **497,** 80–85 (2013).

47. Young, D. J., Guydosh, N. R., Zhang, F., Hinnebusch, A. G. & Green, R. Rli1/ABCE1 Recycles Terminating Ribosomes and Controls Translation Reinitiation in 3′UTRs In Vivo. *Cell* **162,** 872–884 (2015).

48. Nürenberg, E. & Tampé, R. Tying up loose ends: ribosome recycling in eukaryotes and archaea. *Trends Biochem. Sci.* **38,** 64–74 (2013).

49. Baronas-Lowell, D. M. & Warner, J. R. Ribosomal protein L30 is dispensable in the yeast Saccharomyces cerevisiae. *Molecular and Cellular Biology* **10,** 5235–5243 (1990).

50. Dresios, J., Derkatch, I. L., Liebman, S. W. & Synetos, D. Yeast ribosomal protein L24 affects the kinetics of protein synthesis and ribosomal protein L39 improves translational accuracy, while mutants lacking both remain viable. *Biochemistry* **39,** 7236–7244 (2000).

51. Nishimura, T., Wada, T., Yamamoto, K. T. & Okada, K. The Arabidopsis STV1 protein, responsible for translation reinitiation, is required for auxin-mediated gynoecium patterning. *Plant Cell* **17,** 2940–2953 (2005).

52. Yoo, S. D., Cho, Y. H. & Sheen, J. Arabidopsis mesophyll protoplasts: a versatile cell system for transient gene expression analysis. *Nat Protoc* **2,** 1565–1572 (2007).

53. Kobayashi, K., Tsuge, S., Nakayashiki, H., Mise, K. & Furusawa, I. Requirement of cauliflower mosaic virus open reading frame VI product for viral gene expression and multiplication in turnip protoplasts. *Microbiol. Immunol.* **42,** 377–386 (1998).

54. Pooggin, M. M., Hohn, T. & Futterer, J. Role of a short open reading frame in ribosome shunt on the cauliflower mosaic virus RNA leader. *J. Biol. Chem.* **275,** 17288–17296 (2000).

55. Chicher, J. *et al.* Purification of mRNA-programmed translation initiation complexes suitable for mass spectrometry analysis. *Proteomics* (2015).

doi:10.1002/pmic.201400628

56. Källberg, M., Wang, H., Wang, S., Peng, J., Wang, Z., Lu, H. & Xu, J. Template-based protein structure modeling using the RaptorX web server. *Nature Protocols* **7**, 1511-1522 (2012).

2.3.8 Legend to Figures

Figure 1 RISP binds eIF2 via its subunit β. (**a**) Putative RISP 3D-structure generated by Modeller reveals α-helixes: *red* H1, *black* H2, *grey* H3 and *blue* H4. RISP binding sites for eIF3a, eIF3c, eL24 and the S267-P position are indicated. (**b**) Wheat germ-purified eIF2 was identified as a putative RISP interactor by GST pull-down assay. GST N-terminally tagged RISP can specifically pull-down all three eIF2 subunits. The unbound (U) and bound (B) glutathione bead samples were examined by SDS-PAGE and Coomassie staining. (**c**) The eIF2β subunit was selected as a RISP interactor by the yeast two-hybrid system (Y2H). Equal OD_{600} units and 1/10 and 1/100 dilutions were spotted from left to right. Gal4 activation domain (AD)-fused to RISP, but not GST alone, interacts specifically with eIF2β fused to Gal4 binding domain (BD). eIF2α and γ subunits do not display interaction with AD-RISP. (**d**) GST-RISP, but not GST alone, interacts with His-tagged eIF2β in GST pull-down assay. All fusion proteins were expressed and purified from *E. coli*. (**e**) eIF3a was shown as a eIF2β partner in *Arabidopsis* by GST pull-down. GST N-terminally tagged eIF3a pulls-down His-tagged eIF2β. The unbound (U) and bound (B) GST-eIF3a samples were revealed by Coomassie staining. Boundaries of vertically sliced images that juxtapose lanes that were non-adjacent in the gel are delineated by a discontinuous line. All the experiments were reproduced at least two times with similar results.

Figure 2 Phosphorylation state-dependent interactions of RISP with eIF2β. (**a**) Schematic representation of RISP domains shown as boxes: *red* H1; *black* H2; *grey* H3 and *blue* H4. (**b**) Except for a 114 N-terminal amino acid extension, the *Arabidopsis* eIF2β sequence is highly similar to that of archaeal eIF2β (aIF2β). The aIF2β 3D-structure is presented[31]: *blue* C-terminus homologous to *At*eIF2βC (aa 121–268); *black* central helix corresponding to aa 121–144 of *At*eIF2β; *red* N-terminal domain. (**c**) The H2 domain from RISP is sufficient to interact with *At*eIF2β in the Y2H assay. RISP deletion derivatives fused to AD (*left panel*) are depicted as boxes according to the color-code in panel a. Equal OD_{600} units and 1/10 and 1/100 dilutions were spotted from left to right. (**d**) The central domain (aa 121–144) from *At*eIF2β is required for interaction with RISP in the Y2H assay. *At*eIF2β deletion derivatives fused to BD (*left panel*) are depicted as boxes according to the color-code in panel b. (**e**) RISP phosphorylation knockout (AD-RISP-S267A) interacts more strongly with BD-eIF2β than AD-RISP and the AD-tagged RISP phosphomimetic mutant (AD-RISP-S267D) in quantitative β-galactosidase activity assay. Interactions were scored by measuring β-galactosidase activity in liquid assay. The highest value of β-galactosidase activity with AD-

RISP-S267A was set to 100%. (**f**) GST pull-down experiments confirmed that GST-eIF2β (G-2β) interacts preferentially with His-tagged RISP-S267A (RISP-A) as compared with RISP-S267D (RISP-D). GST-eIF2β and RISP mutants were purified from *E. coli*. Unbound (U) and bound (B) samples were examined by SDS-PAGE and Coomassie staining (*left panel*). Comparable quantification of interactions in bound fractions 9 and 11 (*right panel*). Boundaries of vertically sliced images that juxtapose lanes that were non-adjacent in the gel are delineated by a discontinuous line. All the experiments were reproduced at least two times with similar results. (e) Multiple comparisons (Turkey's test) are based on one-way ANOVA test. Data are presented as mean and error bars indicate SD (****P< 0.0001, n=3). (f) Values, expressed in arbitrary densitometric units, are averages of three different measurements from two biological replicates and error bars indicate SD.

Figure 3 Phosphorylation state-dependent interactions of RISP with eIF2β during translation reinitiation in *Arabidopsis* protoplasts. (**a**) Scheme of reporter plasmids used in transient expression experiments in *Arabidopsis* suspension protoplasts: p*monoGFP* (marker for transformation efficiency), p*short-GUS* (harbors 50-nt 5'-UTR, marker for initiation efficiency) and p*ARF5-GUS* (marker for reinitiation efficiency). Short upstream ORFs (uORFs) within ARF5 5'-UTR are depicted as open boxes. (**b**) Transiently expressed phosphorylation knockout mutant of RISP up-regulates initiation and reinitiation events. Protoplasts have been transformed by p*monoGFP* and either p*short GUS* (*in red*) or p*ARF5-GUS* (*in blue*) without or with the effector plasmid that codes for RISP WT or one of its phosphorylation mutants—RISP WT (RISP-S), RISP-S267D (RISP-D) and RISP-S267A (RISP-A) in amounts indicated above the panel. Both GFP fluorescence and β-glucuronidase functional activity were analysed in the same 96-well microtiter plate. Functional levels of GUS expressed from p*short-GUS* normalized to corresponding GFP levels were set at 100%. GUS-containing mRNA levels and integrity analyzed by sqRT–PCR; LC—loading control are presented below the panel. Results shown represent the means obtained in three independent experiments. (**c**) eIF2β does not increase initiation efficiency with or without RISP-A. Protoplasts have been transformed with p*monoGFP*, p*short GUS* (*red bars*) and pRISP-A in increasing amounts of the effector plasmid encoding eIF2β as indicated. Functional levels of GUS expressed from p*short-GUS* normalized to corresponding GFP levels were set at 100%. GUS-containing mRNA levels and integrity were analyzed by sqRT–PCR; GFP levels were also analysed by immunoblotting; LC—loading control. Results shown represent the means obtained in three independent experiments. (**d**) eIF2β out-

competes RISP-A, decreasing its reinitiation capacity. Protoplasts have been transformed with p*monoGFP*, p*ARF5-GUS* (*blue bars*) and eIF2β, with increasing amounts of the effector plasmid expressing RISP-S, or -A or -D as indicated. Functional levels of GUS expressed from p*ARF5-GUS* normalized to corresponding GFP levels were set at 100%. (**e**, **f**) Representative example of structural arrangement of eIF3, eIF2 and tRNA in the DHX29-bound 43S complex[35]. We show eIF3a and eIF3c extensions in red and in blue, respectively; their densities are reproduced from refs. 33,34. 40S is depicted in grey and presented as frontal (e) and intersubunit views (f). RISP, tRNAiMet, eIF3 and eIF2 subunits are colored as indicated. RISP fits well to a position on 40S in close proximity to the eIF3a C-terminus and the eIF3c N-terminus and the central domain of eIF2β. All the experiments were reproduced at least two times with similar results. (b-d) Quantification represents the means (n=3, error bars=SD) obtained in three independent experiments.

Figure 4 Phosphorylation state-dependent interactions of RISP with eS6. (**a**) The full-length RISP is required to interact with eS6 in Y2H assay. RISP deletion derivatives fused to AD (*left panel*) are depicted as boxes according to the RISP color-code. Equal OD_{600} units and 1/10 and 1/100 dilutions were spotted from left to right. (**b**) eS6 3D-structure in a ribosome-bound conformation is presented[36]: *red* N-terminal-ribosome bound domain; *black* central domain proposed to interact with the 60S ribosomal protein eL24; *blue* C-terminal α-helix that protrudes out of 40S. (**c**) The C-terminal and central domains can interact with RISP in Y2H assay. eS6 deletion derivatives fused to BD (*left panel*) are depicted as boxes according to the color-code of eS6 shown in panel b. (**d**) GST pull-down experiments confirmed that the eS6 C-terminal α-helix interacts with His-tagged RISP. GST-CS6 and RISP-His were purified from *E. coli* (*left fractions*). Unbound (U) and bound (B) samples were examined by SDS-PAGE and Coomassie staining. (**e**) BD-CS6 interacts strongly with RISP and its phosphomimetic mutant (RISP-S267D), but not with RISP-S267A in quantitative β-galactosidase activity assay. The highest value of β-galactosidase activity with AD-RISP is set to 100%. All the experiments were reproduced at least two times with similar results. (e) Multiple comparisons (Turkey's test) are based on one-way ANOVA test. Data are presented as mean and error bars indicate SD (****P< 0.0001, n=3).

Figure 5 The ternary complexes between phosphorylation knockout mutant of RISP, eIF3a and eIF2β, and phosphomimetic mutant of RISP, the eCS6 C-terminal α-helix and wheat germ 60S can be reconstructed *in vitro*. **(a)** GST pull-down experiments with RISP

phosphorylation mutants pre-bound to glutathione beads-attached GST-eIF3a or GST. After removal of unbound RISP variants (fractions 11 and 17), GST-eIF3a-RISP-S267A (fraction 12) and GST-eIF3a-RISP-S267D complexes (fraction 18) were further incubated without or with His-eIF2β. Unbound (U, fractions 15 and 21) and bound (B, fractions 14 and 20) fractions were assayed by SDS-PAGE and stained with Coomassie blue. GST, GST-eIF3a, His-RISP-S267A, His-RISP-S267D and His-eIF2β were overexpressed in *E. coli* and purified by affinity chromatography (*left panel*). Densitometric quantification of binary (His-RISP mutant/GST-eIF3a) and ternary (eIF2β/binary complex) complexes (*bottom panel*). (**b**) His-RISP phosphorylation mutants were incubated with GST-CS6 or GST-bound to glutathione beads. The glutathione-bound (B) fractions 8 and 14 were washed to remove unbound fractions (U, fractions 9 and 15) and further incubated with 60S ribosomal subunits purified from wheat germ. Unbound (U, fractions 13 and 19) and bound (B, fractions 12 and 18) samples were assayed by SDS-PAGE and stained with Coomassie blue. GST-CS6 was produced in *E. coli*. Stars indicate 60S ribosomal proteins specifically co-precipitated with the GST-CS6/RISP-S267D binary complex. All the experiments were reproduced at least two times with similar results. (a) Values, expressed in arbitrary densitometric units, are averages of three different measurements from two biological replicates and error bars indicate SD.

Figure 6 Phosphorylation of eS6 promotes its binding to RISP and reinitiation capacity of *Arabidopsis* protoplasts. (**a**) Alignment of the C-terminal tail of eS6 plant homologues. Serine phosphorylation sites—Ser231, Ser237, Ser240 and Ser241—are shown in bold. (**b**) eCS6 and its phospho-mimetic mutants (BD-CS6-S231D, BD-CS6-S237D, BD-CS6-S240D) as compared with their phosphoknockout mutants (BD-CS6-S231A, BD-CS6-S237A, BD-CS6-S240A) interact preferentially with RISP phosphorylation mimic in quantitative β-galactosidase activity assay. Interactions were scored by measuring β-galactosidase activity in liquid assay. The value of β-galactosidase activity with BD-CS6-WT and either AD-RISP or AD-RISP-S267D was set to 100%. (**c**) Western blot analysis of total eS6 levels in WT, *s6a*, *s6a/S6B*$^{S/A}$ and *s6a/ S6B*$^{S/D}$ *Arabidopsis* mutant lines were conducted on extracts from 7 dag seedlings. (**d**) Comparable analysis of initiation and reinitiation capacities of WT and *s6a*, *s6a/S6B*$^{S/A}$ and *s6a/S6B*$^{S/D}$ *Arabidopsis* plantlets in transient expression experiments in mesophyll protoplasts, where S6B$^{S/A}$ (S237A/S240A/S241A) and S6B$^{S/D}$ (S237D/S240S/S241D) contain triple S237/S240/S241 mutations. The 5 µg reporters—p*monoGFP* and either p*short-GUS* (*initiation marker*), or p*ARF5-GUS* (*reinitiation after short ORF translation marker*), or p*biGUS* without or with p*TAV* (*reinitiation after long ORF*

translation marker)—presented at the top were used for protoplast transformation. GUS/GFP ratios from in WT plants were set as 100% for each reporter plasmid in WT protoplasts. GUS/GFP activity ratios are shown in *red* (p*short-GUS*), *blue* (p*ARF5-GUS*) and *black* (p*biGUS*) bars. TAV and GFP protein levels were analyzed by immunoblot and shown in the bottom panels. GUS-containing mRNA levels were analyzed by semiquantitative RT-PCR. All the experiments were reproduced at least two times with similar results. (b) Multiple comparative tests (Turkey's test) are based on one-way ANOVA test. Data are presented as mean and error bars indicate SD (**p< *0.005*; ***p< *0.0005;* ****P< 0.0001, n=3). (d) Quantification represents the means (n=3, error bars=SD) obtained in three independent experiments.

Figure 7 Proposed scheme of RISP binding to 40S and 60S via eS6 and eL24 and RISP function during elongation and 40S posttermination scanning. (**a**) Model states that before phosphorylation, RISP can function within the 43S PIC, assisting eIF3 in TC recruitment. In response to TOR activation, RISP and eS6 are phosphorylated and, together with eL24, establish a bridge between 40S and 60S ribosomal subunits. See text for details. (**b**) Close up front view of the RISP/ elongating 80S complex highlighting the possible eS6/RISP/eL24 interaction network in the vicinity of the eB13 intersubunit bridge. The cryo-EM structure of the human 80S (see ref. 37; 40S and 60S are depicted in *grey* and *blue*, respectively) and RISP (3D model in *pink*) are presented. RISP was docked in close proximity to eS6 (*black*) and eL24 (*dark blue*) C-terminal domains. (**c**) Close-up front view of the predicted complex between RISP (atomic model) and the 40S-60S posttermination scanning complex. The predicted complex shows the atomic structure of 40S (in *grey*) and 60S (in *blue*) from the yeast 80S ribosome[36]. To build putative 80S open conformation, 60S body was rotated away from 40S by 30°. The 3D RISP model was docked with no clash in close proximity to eS6 (*black*) and eL24 (*dark blue*) C-terminal helixes.

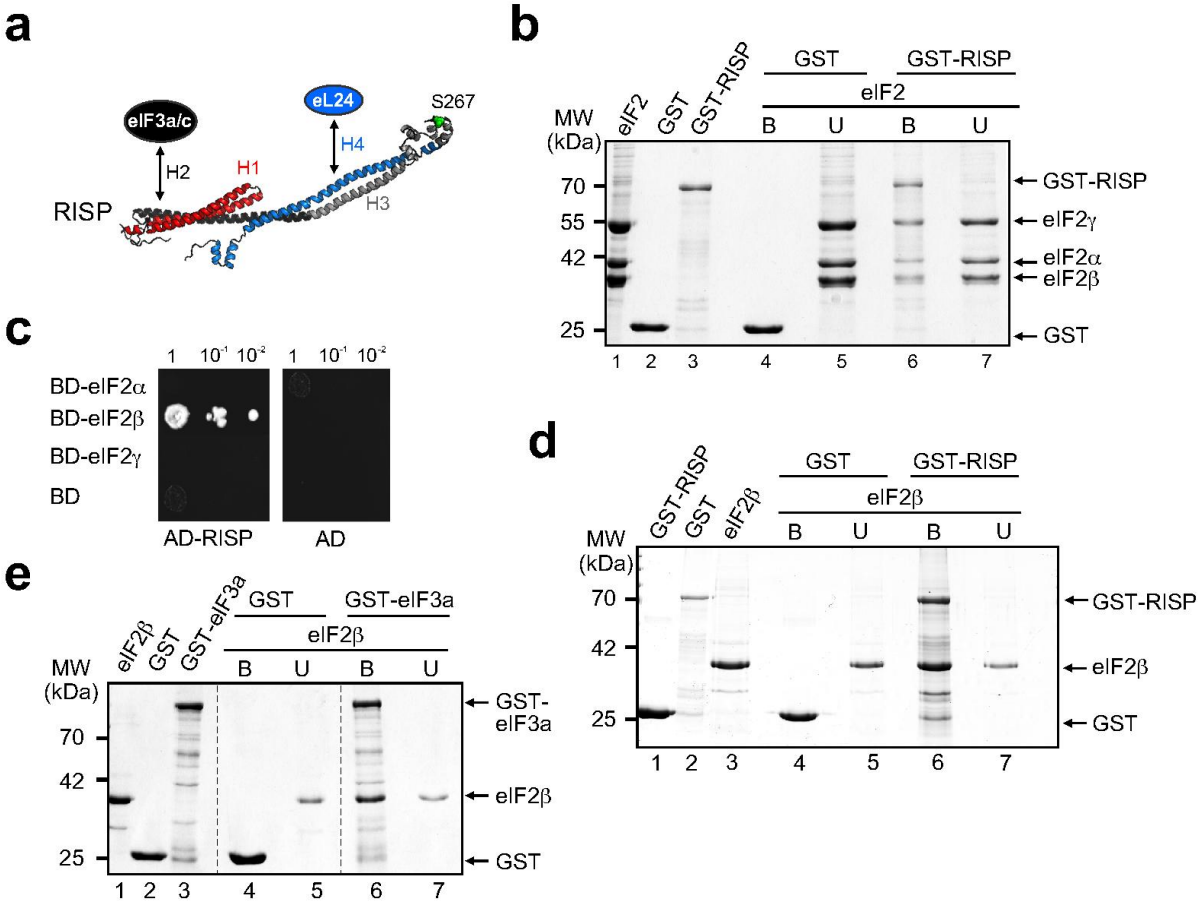
a
eIF3a/c
eL24
S267
H2
H1
H4
H3
RISP
b
GST
GST-RISP
eIF2
MW (kDa)
eIF2
GST
GST-RISP
B U B U
70
55
42
25
GST-RISP
eIF2γ
eIF2α
eIF2β
GST
1 2 3 4 5 6 7
c
1 10-1 10-2 1 10-1 10-2
BD-eIF2α
BD-eIF2β
BD-eIF2γ
BD
AD-RISP
AD
d
GST
GST-RISP
eIF2β
GST-RISP
GST
eIF2β
MW (kDa)
B U B U
70
42
25
GST-RISP
eIF2β
GST
1 2 3 4 5 6 7
e
eIF2β
GST
GST-eIF3a
GST
GST-eIF3a
eIF2β
MW (kDa)
B U B U
70
42
25
GST-eIF3a
eIF2β
GST
1 2 3 4 5 6 7

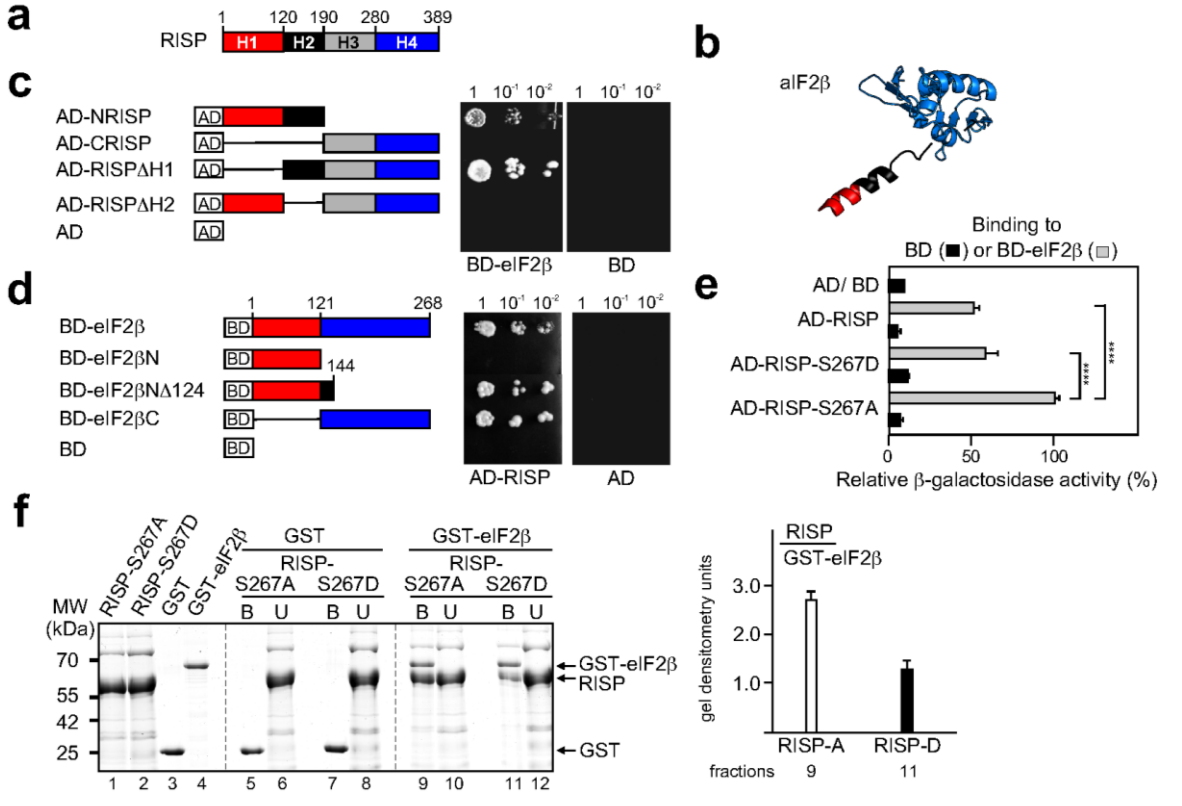
a
RISP
1 120 190 280 389
H1 H2 H3 H4
b
αIF2β
c
AD-NRISP
AD-CRISP
AD-RISPΔH1
AD-RISPΔH2
AD
1 10-1 10-2 1 10-1 10-2
BD-eIF2β
BD
d
BD-eIF2β
BD-eIF2βN
BD-eIF2βNΔ124
BD-eIF2βC
BD
1 121 268
144
AD-RISP
AD
e
Binding to
BD (■) or BD-eIF2β (□)
AD/ BD
AD-RISP
AD-RISP-S267D
AD-RISP-S267A
****
0 50 100
Relative β-galactosidase activity (%)
f
RISP-S267A
RISP-S267D
GST
GST-eIF2β
GST
RISP-S267A
RISP-S267D
GST-eIF2β
RISP-S267A
RISP-S267D
MW (kDa)
B U B U B U B U
70
55
42
25
GST-eIF2β
RISP
GST
1 2 3 4 5 6 7 8 9 10 11 12
RISP
GST-eIF2β
gel densitometry units
3.0
2.0
1.0
RISP-A
RISP-D
fractions
9
11

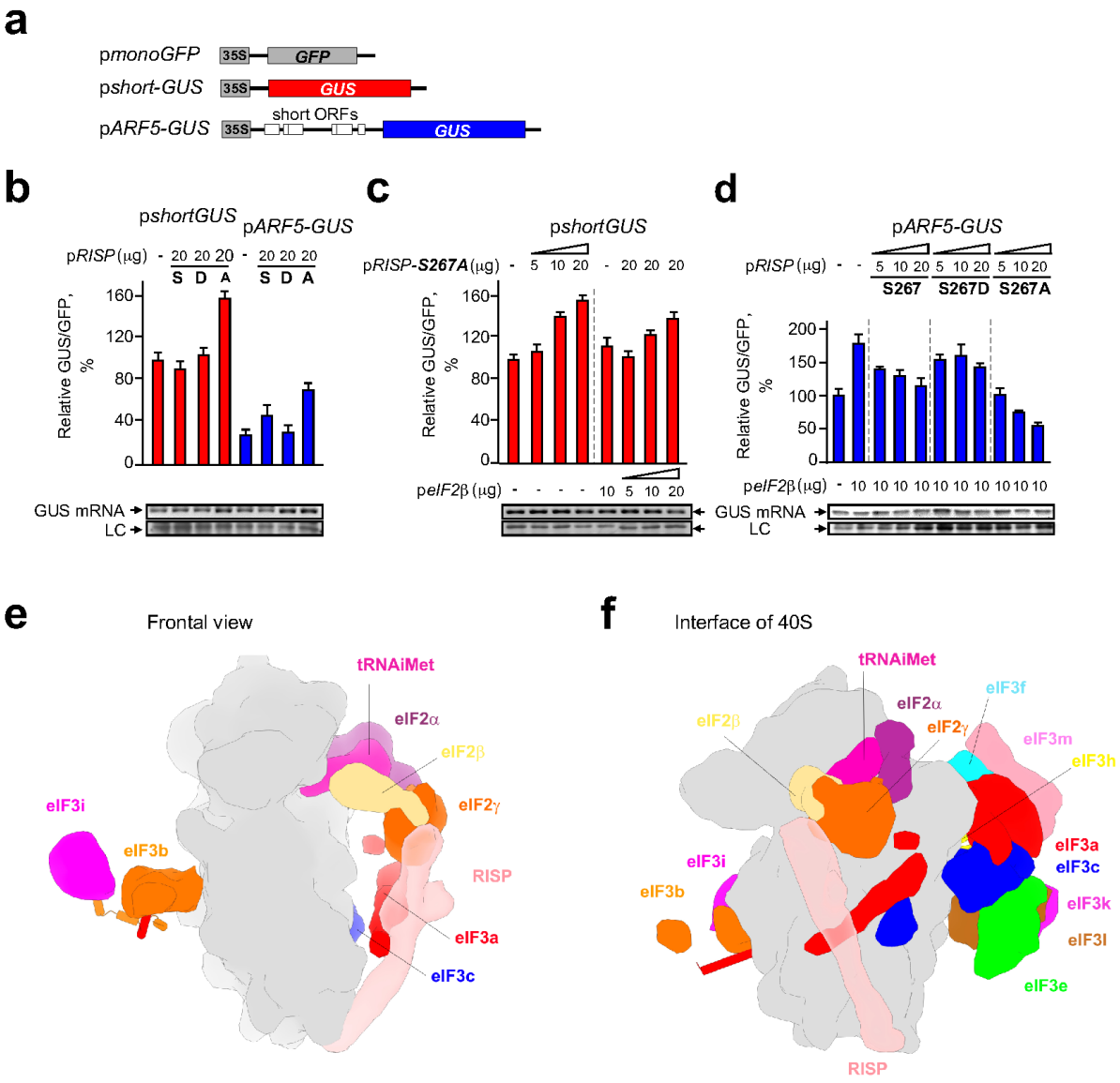
a
pmonoGFP
35S
GFP
pshort-GUS
35S
GUS
pARF5-GUS
35S
short ORFs
GUS
b
pshortGUS
pARF5-GUS
pRISP (μg)
20 20 20
S D A
20 20 20
S D A
Relative GUS/GFP, %
160
120
80
40
0
GUS mRNA
LC
c
pshortGUS
pRISP-S267A (μg)
5 10 20
20 20 20
Relative GUS/GFP, %
160
120
80
40
0
peIF2β (μg)
10 5 10 20
GUS mRNA
LC
d
pARF5-GUS
pRISP (μg)
5 10 20
5 10 20
5 10 20
S267
S267D
S267A
Relative GUS/GFP, %
200
150
100
50
0
peIF2β (μg)
10 10 10 10 10 10 10 10 10
GUS mRNA
LC
e
Frontal view
tRNAiMet
eIF2α
eIF2β
eIF2γ
eIF3i
eIF3b
RISP
eIF3a
eIF3c
f
Interface of 40S
tRNAiMet
eIF2α
eIF2β
eIF2γ
eIF3f
eIF3m
eIF3h
eIF3i
eIF3b
eIF3a
eIF3c
eIF3k
eIF3l
eIF3e
RISP

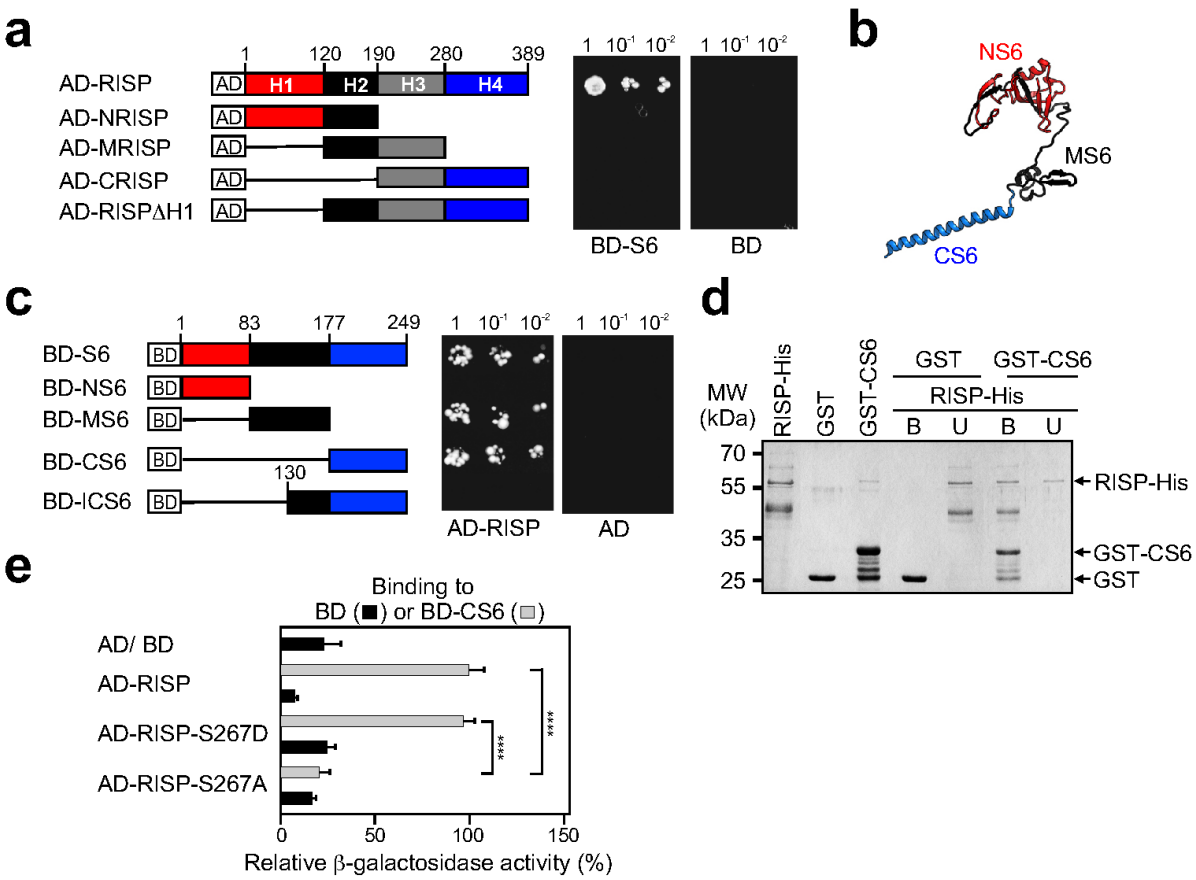
a
AD-RISP
AD-NRISP
AD-MRISP
AD-CRISP
AD-RISPΔH1
AD
H1
H2
H3
H4
1
120
190
280
389
1 10-1 10-2
BD-S6
BD
b
NS6
MS6
CS6
c
BD-S6
BD-NS6
BD-MS6
BD-CS6
BD-ICS6
BD
1
83
177
249
130
AD-RISP
AD
d
MW
(kDa)
RISP-His
GST
GST-CS6
GST
GST-CS6
RISP-His
B
U
B
U
70
55
35
25
RISP-His
GST-CS6
GST
e
Binding to
BD (■) or BD-CS6 (▫)
AD/ BD
AD-RISP
AD-RISP-S267D
AD-RISP-S267A
****
****
0
50
100
150
Relative β-galactosidase activity (%)

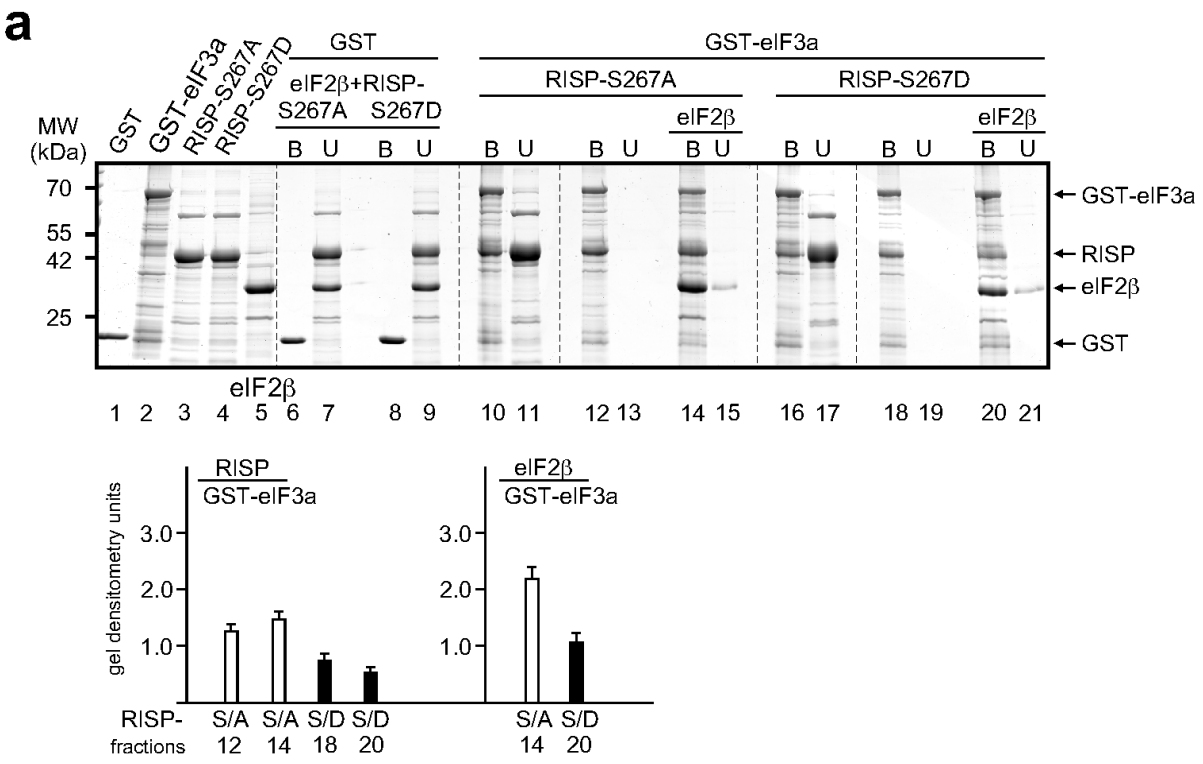
a
GST
GST-eIF3a
RISP-S267A
RISP-S267D
MW (kDa)
70
55
42
25
GST
eIF2β+RISP-S267A
eIF2β+RISP-S267D
GST-eIF3a
RISP-S267A
RISP-S267D
eIF2β
B U
GST-eIF3a
RISP
eIF2β
GST
eIF2β
1 2 3 4 5 6 7 8 9 10 11 12 13 14 15 16 17 18 19 20 21
RISP / GST-eIF3a
eIF2β / GST-eIF3a
gel densitometry units
3.0
2.0
1.0
RISP-fractions
S/A 12
S/A 14
S/D 18
S/D 20
S/A 14
S/D 20

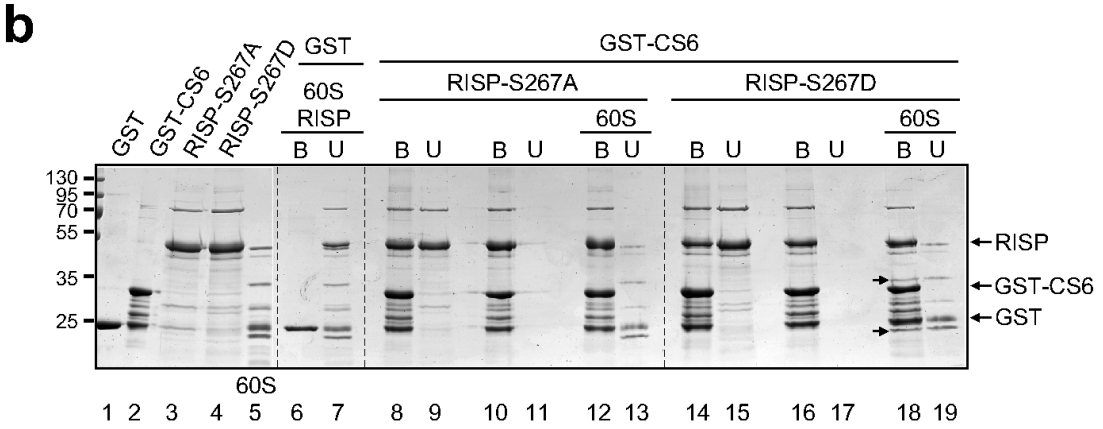
b
GST
GST-CS6
RISP-S267A
RISP-S267D
GST
60S RISP
GST-CS6
RISP-S267A
RISP-S267D
60S
B U
130
95
70
55
35
25
RISP
GST-CS6
GST
60S
1 2 3 4 5 6 7 8 9 10 11 12 13 14 15 16 17 18 19

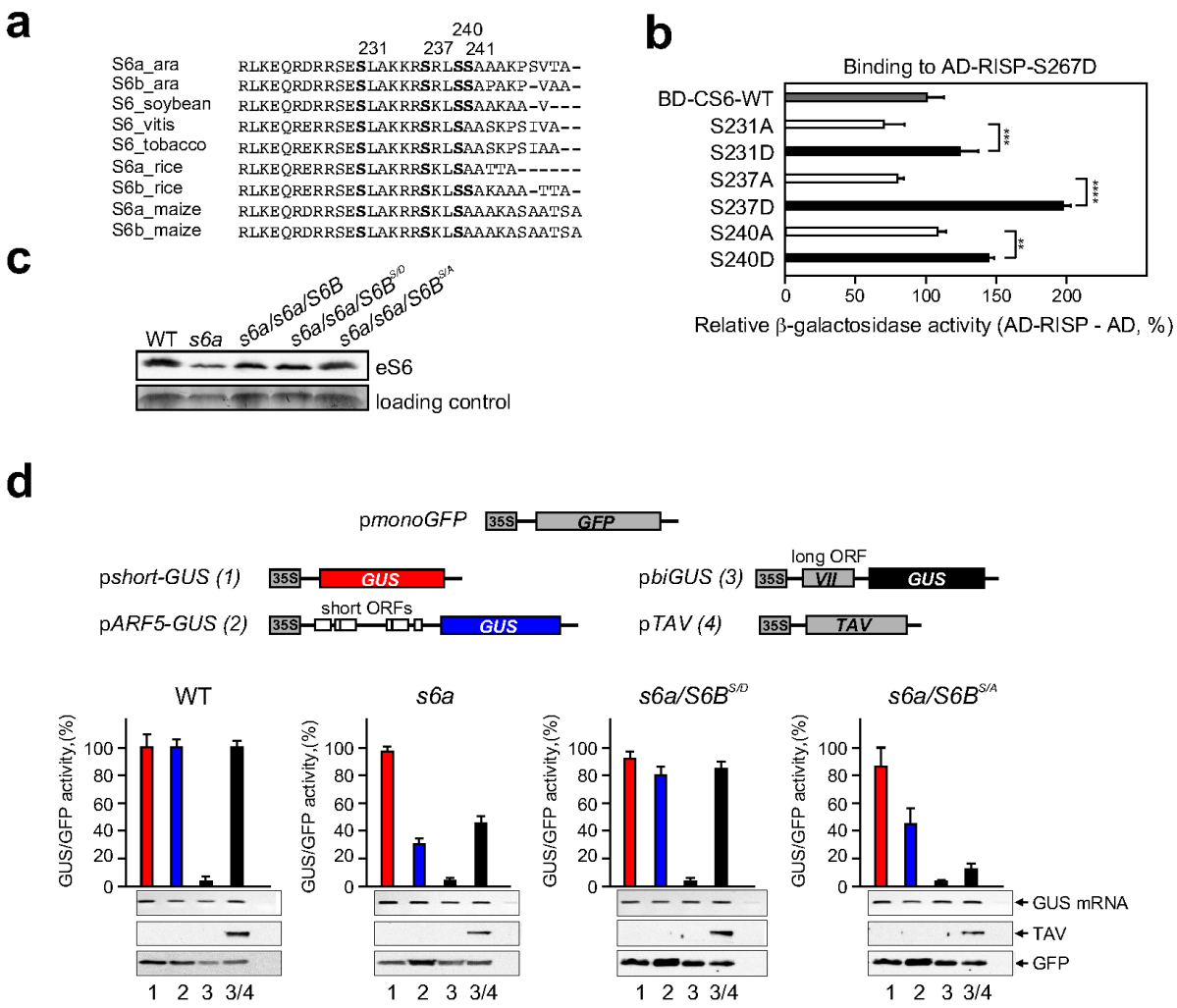
a
240
231 237 241
S6a_ara RLKEQRDRRSESLAKKRSRLSSAAAKPSVTA-
S6b_ara RLKEQRDRRSESLAKKRSRLSSAPAKP-VAA-
S6_soybean RLKEQRDRRSESLAKRRSKLSSAAKAA-V---
S6_vitis RLKEQRERRSESLAKKRSRLSAASKPSIVA--
S6_tobacco RLKEQREKRSESLAKKRSRLSAASKPSIAA--
S6a_rice RLKEQRERRSESLAKRRSKLSAATTA------
S6b_rice RLKEQRERRSESLAKRRSKLSSAKAAA-TTA-
S6a_maize RLKEQRDRRSESLAKRRSKLSAAAKASAATSA
S6b_maize RLKEQRDRRSESLAKRRSKLSAAAKASAATSA
b
Binding to AD-RISP-S267D
BD-CS6-WT
S231A
S231D
S237A
S237D
S240A
S240D
***
****
**
0 50 100 150 200
Relative β-galactosidase activity (AD-RISP - AD, %)
c
WT s6a s6a/s6a/S6B s6a/s6a/S6B^S/D s6a/s6a/S6B^S/A
eS6
loading control
d
pmonoGFP 35S GFP
pshort-GUS (1) 35S GUS
pARF5-GUS (2) 35S short ORFs GUS
pbiGUS (3) 35S long ORF VII GUS
pTAV (4) 35S TAV
WT
s6a
s6a/S6B^S/D
s6a/S6B^S/A
GUS/GFP activity,(%)
0 20 40 60 80 100
GUS mRNA
TAV
GFP
1 2 3 3/4

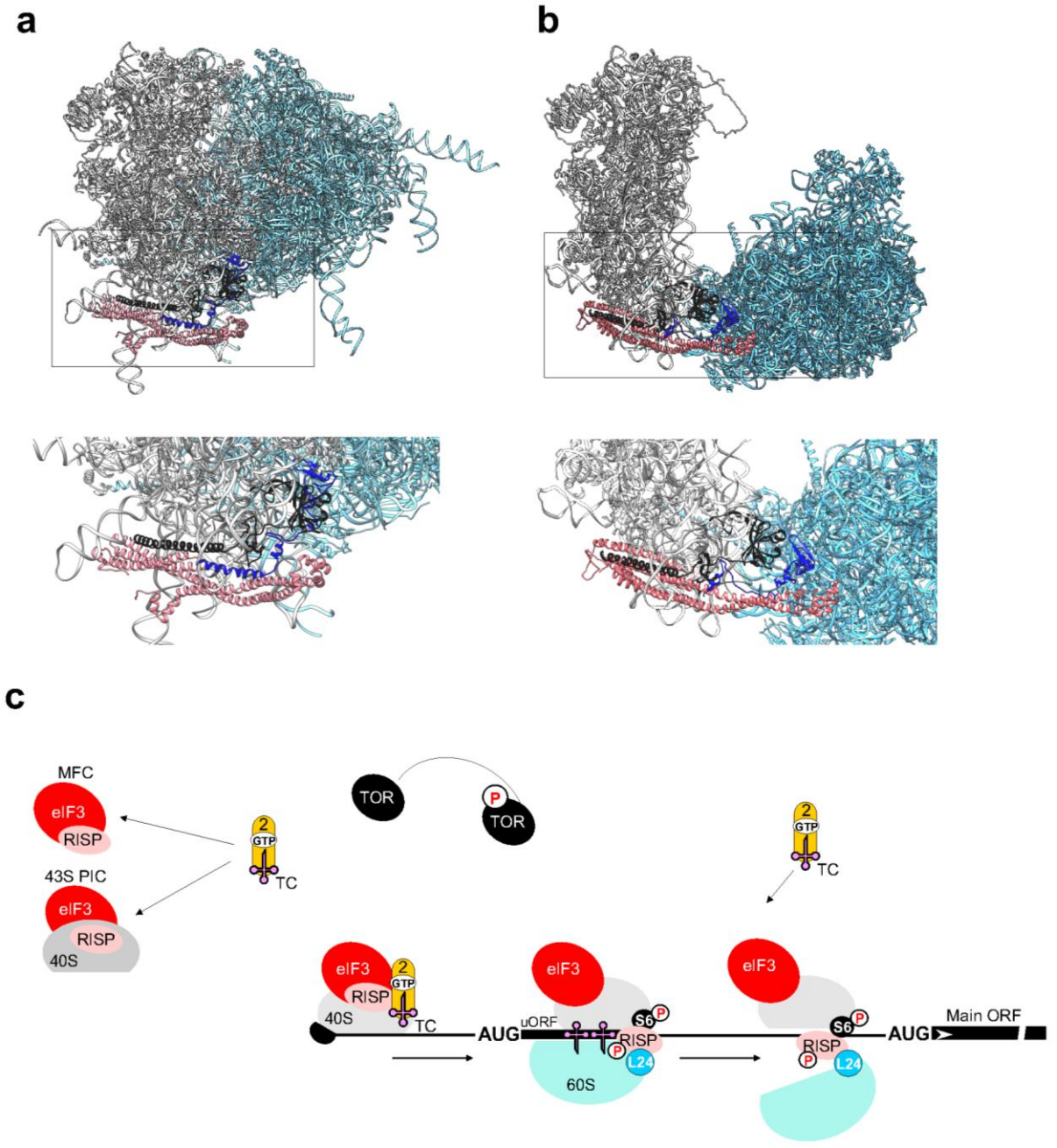
a
b
c
MFC
eIF3
RISP
43S PIC
eIF3
RISP
40S
TC
GTP
TOR
P
TOR
eIF3
RISP
40S
TC
AUG
uORF
eIF3
S6
P
RISP
P
L24
60S
eIF3
S6
P
RISP
P
L24
AUG
Main ORF

SUPPLEMENTARY INFORMATION

RISP can promote reinitiation at uORFs in plants by directly linking 40S and 60S ribosomal subunits

Eder Mancera-Martínez et al

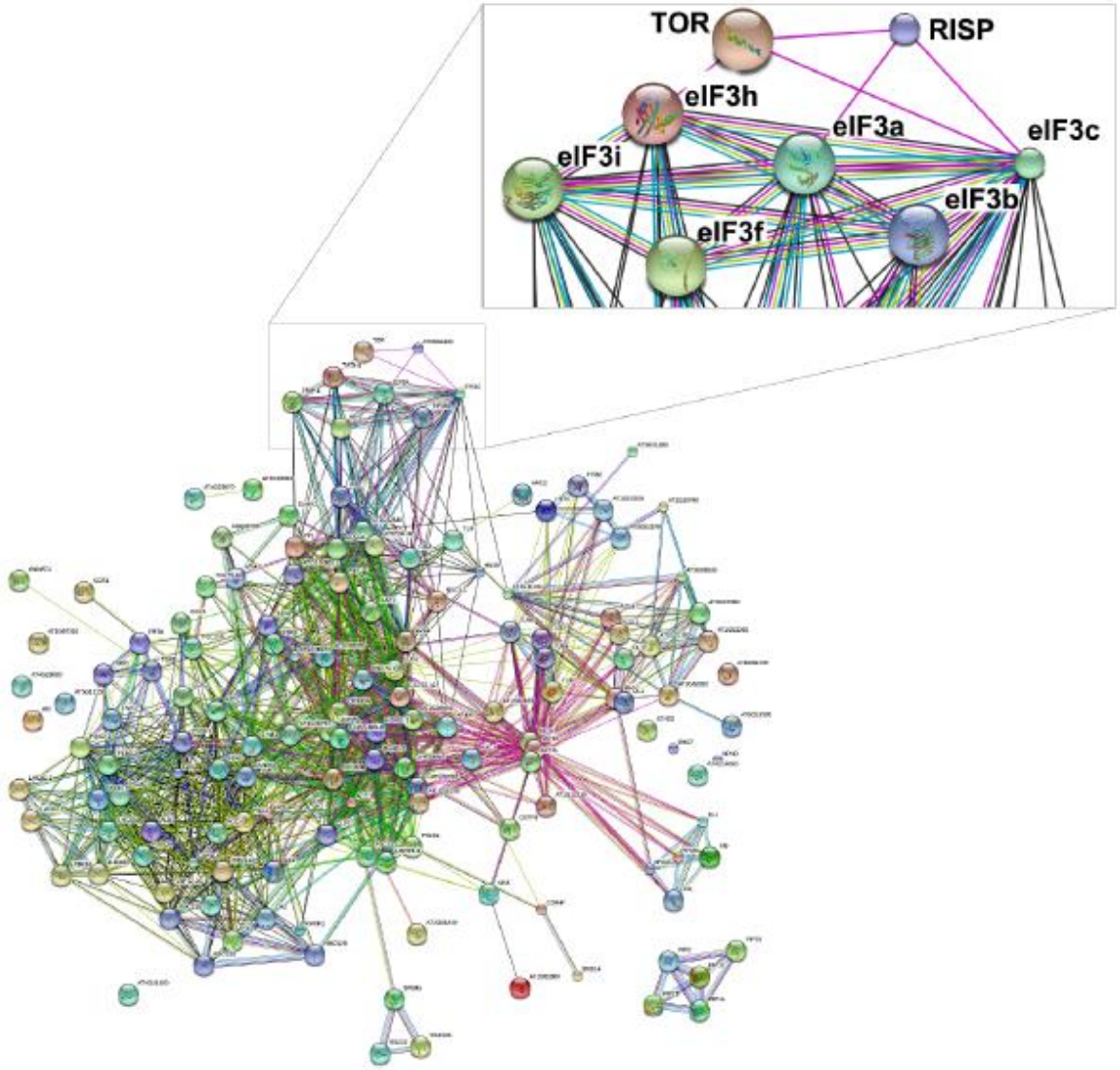

Supplementary Figure 1 Clustering of the RISP interactome using STRING v10. The 150 proteins with a spectral count ratio ≥ 2 and a minimum of 4 spectra in RISP-GFPox samples were entered into the *Arabidopsis* STRING database (see ref. 1; http://string-db.org/) and a close up view of the translation initiation-related network of RISP is presented on the top. Line colors represent the different types of evidence for the indicated association.

Supplementary Figure 2 Leaf phenotype of the eS6 mutants. (**a, b**) Picture of 10-day-old WT, *s6a*, *s6a/S6B*, *s6a/S6BS/D* and *s6a/S6BS/A Arabidopsis* seedlings. Note that the growth of leaves in *s6a* mutant is delayed. *s6a* is characterized by the pointed and asymmetric leaves. *s6a/S6BS/D* display phenotype of *s6a*. *s6a/S6BS/A* WT leaf phenotype is partly restored.

Supplementary Table 1 Quantitative assessment of 43S PIC-related proteins that associate with RISP-GFP

Accession number	Protein name	MW kDa	Spectral Count (SC)	Mascot Spectrum	P-value (n=3)
AT5G61200.3	RISP	45,3	292,8	2594,4	2.57E-05
AT3G56150.1	Initiation factor eIF3c-1	102,9	19,7	439,7	2.30E-03
AT2G46280.1	Initiation factor eIF3i-1	36,4	11,6	230,5	2.20E-04
AT4G11420.1	Initiation factor eIF3a-1	114,3	11,1	326,7	8.59E-03
AT5G27640.2	Initiation factor eIF3b-1	84,9	8,0	238,0	6.90E-04
AT2G39990.1	Initiation factor eIF3f-1	31,8	6,6	175,2	4.02E-03
AT1G10840.1	Initiation factor eIF3h-1	38,3	5,6	121,7	1.97E-03
AT1G50030.1	Target of rapamycin, TOR	279	4,4	143,4	8.39E-03

A method of high-resolution mass spectrometry was employed to identify factors that associate with RISP in *Arabidopsis rispa/RISP-GFPox* line transgenic for GFP-tagged RISP.

Reference

1. Szklarczyk, D. *et al.* STRING v10: protein-protein interaction networks, integrated over the tree of life. *Nucleic Acids Res* **43,** D447–52 (2015).

III.FINAL CONCLUSIONS AND PERSPECTIVES

During my PhD, I have studied the mechanisms of translation reinitiation in plants. Our strategy was to employ the eIF3h subunit of eukaryotic initiation factor 3 (eIF3) to better understand mechanisms of cellular reinitiation after short ORF translation and whether these mechanisms are used by Cauliflower mosaic virus for translation of its polycistronic mRNA via reinitiation after long ORF translation. The subunit h is considered to be a reinitiation factor that promotes specifically reinitiation after short upstream ORF (uORF) translation, while it is dispensable for cap-dependent initiation events.

Here we show that eIF3h, if phosphorylated, has a role in recruitment of eIF3 into actively translating ribosomes (polyribosomes) during reinitiation after uORF translation that is a prerequisite for formation of reinitiation-competent ribosomal complexes. The most frequent mechanism of reinitiation after short ORF translation depends on the participation of certain eIFs supporting reinitiation that are recruited during the first cap-dependent initiation event at the uORF and then not released during the short time required for uORF translation (KOZAK, 2001). These “reinitation supporting factors” remain associated with polysomes for a short elongation event and with post-termination ribosomes and can regenerate reinitiation-competent 40S complexes. Our experiments on dissection of eIF3h functional domains revealed that the eIF3h C-terminal domain is required for eIF3h integration into the eIF3 complex, while its N-terminus is also critical for reinitiation of translation. I suggest that eIF3h can either stabilize eIF3 binding to the 40S ribosomal

subunit, or interact with yet unknown factor that plays a role in reinitiation. To validate the second hypothesis, currently, I am doing experiments on identification of putative eIF3h partner(s). MS-MS analysis of extracts from WT seedlings and *eif3h-1* mutant plants carrying the C-terminally truncated eIF3h protein revealed two components of the host translational machinery that highly specifically precipitated by eIF3h antibodies—40S ribosomal proteins RPS15 and RPS7e. Strikingly, both that are located at the left foot of the 40S subunit in close proximity to position of eIF3h within the 43S preinitiation complex (mammalian 43S PIC; (DES GEORGES *et al.* 2015)). In light of obtained results, I predict that eIF3h interacts with the ribosomal proteins to stabilize eIF3 binding to 40S. Accordingly, eIF3h may participate in retention of eIF3 on 40S during the short elongation event. The future work is required to validate eIF3h interactions with S15 and S7e.

Although plant viruses encode a number of essential proteins (e.g., coat proteins, movement proteins, replication enzymes) their coding capacity is limited and they must rely on host factors for every stage of the infection cycle. An early and critical step of the viral amplification is synthesis of viral proteins. Viruses do not normally encode canonical translation factors, but have developed a wide array of strategies to highjack translation factors from their hosts and favor the translation of viral RNAs to the detriment of endogenous mRNAs. Cauliflower mosaic virus (CaMV) employs very unusual mechanism for translation of its polycistronic 35S pregenomic RNA (pgRNA) that activates reinitiation after long ORF translation that is normally prohibited in eukaryotes. Indeed, as identified before, translation in CaMV depends on TOR, which maintains phosphorylation of some reinitiation-promoting factors (Schepetilnikov et al., 2011; 2013). Here I show that eIF3h, a downstream target of TOR, is such reinitiation-supporting factor strictly required for CaMV infection.

I have demonstrated that Arabidopsis *eif3h-1* mutant plants carrying the eIF3h C-deletion are largely resistant to CaMV infection. This indicates that the lack of the full-length eIF3h protein is limiting factor for virus. In *eif3h-1* protoplasts, TAV-activated reinitiation after long ORF translation is abolished, but transient overexpression of eIF3h can restore TAV function in reinitiation. Although eIF3h defects can interfere with other steps of viral replication, two other viruses—ORMV and TuMV can efficiently infect *eif3h-1* mutant plants. Nevertheless, infection studies with rescue of the *eif3h-1* mutant carrying an eIF3h transgene could further validate my results.

I concluded that eIF3h is a host factor essential for CaMV amplification; eIF3h is recruited by CaMV to express its proteins via sophisticated mechanism of reinitiation. eIF3h can also participate in other steps of CaMV replication. Thus, it is of great importance to understand how eIF3h promotes the viral reinitiation mechanism and identify factors that accomplish TAV function in reinitiation. A future task will be to use this knowledge to further dissect eIF3h function *in planta*.

In our laboratory we continued to study the role of reinitiation-supporting protein (RISP) in reinitiation of translation. This ends up with a very intriguing suggestion that RPS6 phosphorylation is important for reinitiation of translation. A ribosomal protein RPS6 is a major target of the TOR signaling pathway (MAYER AND GRUMMT 2006). RPS6 and 60S ribosomal protein L24 (RPL24) participate in formation of a bridge between 40S and 60S ribosomal subunits (BEN-SHEM *et al.* 2011). Our data speaks in favor that RISP can stabilize the bridge via interaction with both RPL24 and RPS6. These data indicate a link between 60S and 40S during reinitiation of translation that can function in retention of 60S by scanning 40S ribosomes. Our results are supported by unpublished data—CaMV infection is significantly delayed in Arabidopsis S6a or S6b knockout mutant

plants. We hope that these investigations into the viral model will help to understand the mechanism behind cellular translation reinitiation after short and long ORF.

In our laboratory plant hormone auxin was identified as TOR upstream effector in plants. TOR phosphorylation in response to auxin is required to promote translation reinitiation of mRNAs that harbor uORFs within their leader regions. Now, a small GTPase ROP2 is identified as an intermediate TOR effector downstream of auxin. This means that translation reinitiation is controlled by a crosstalk between the TOR kinase and ROP2 signaling pathways. The link is further supported by observations that developmental abnormalities identified in rpl24b and *eif3h-1* mutants are largely similar to auxin-related developmental defects. Thus, TOR can play an important role in modulating auxin responses during plant development. Further studies are needed to understand mechanisms of translation reinitiation and other reinitiation-supporting factors in plants.

IV. MATERIALS AND METHODS

4.1 Materials

4.1.1 Chemical and molecular biological materials

In this study, the majority of chemicals and reagents used were ordered from BioRad Laboratories Ltd. (Marnes-la-Coquette, France), Ozyme Inc. (St Quentin en Yvelines, France), ThermoFisher Scientific Ltd. (Illkirch, France), Quiagen Ltd. (Courtaboeuf, France), Sigma-Aldrich Ltd. (Illkirch, France) and Macherey-Nagel (Hoerdt, France).

Enzymes and reagents intended for molecular biology assays were purchased from New England Biolabs Ltd. (Évry, France), Promega Ltd. (Charbonnières, France), Ozyme Inc. (St Quentin en Yvelines, France) and Roche Diagnostics Ltd. (Meylan, France).

Bacterial (*Escherichia coli* (*E.coli*), and *Agrobacterium tumefaciens*) and yeast (*Saccharomyces cerevisiae*) growth media constituents were purchased from Ozyme Inc. (St Quentin en Yvelines, France) and Sigma-Aldrich Ltd. (Illkirch, France). Antibiotics were ordered from Sigma-Aldrich Ltd. (Illkirch, France) and were reconstituted in water, 50% ethanol or DMSO stock and stored at -20˚C. The list of antibiotics used in this study is shown in Table 4.1-1. Antibiotics and their respective concentrations used in this study.

Table 4.1-1. Antibiotics and their respective concentrations used in this study

Antibiotic	[Stock]	[Final]
Ampicillin sodium salt	100 mg/ml in 50% EtOH	100 µg/ml
Kanamycin disulfate salt	50 mg/ml in dH_2O	50 µg/ml
Chloramphenicol	50 mg/ml in 50% EtOH	25 µg/ml
Rifampycin	100 mg/ml in DMSO	50 µg/ml

4.1.2 Bacterial and yeast strains

Plasmids were propagated by DH5α *E.coli* for routine cloning techniques with the following genotype: F– Φ80*lac*ZΔM15 Δ(*lac*ZYA-*arg*F) U169 *rec*A1 *end*A1 *hsd*R17 (rK–, mK+) *pho*A *sup*E44 λ– *thi*-1 *gyr*A96 *rel*A1.

BL21 (DE3) pLysS *E.coli* served for the expression of recombinant fusion proteins characterized by this genotype: F– *omp*T *hsd*SB(rB–, mB–) *gal dcm* (DE3) pLysS (CamR). Strains with DE3 denomination are lysogenic for a lambda prophage harboring an isopropyl β-d-1-thiogalactopyranoside (IPTG)-inducible T7 RNA polymerase under the lacUV5 promoter. Strains with pLysS denomination contain a plasmid (pACYC184-derived, CamR) that encodes a T7 lysozyme, which inhibits T7 RNA polymerase and in turn represses the basal expression of target genes under the control of the T7 promoter. This strain is resistant to Chloramphenicol.

The hypervirulent *Agrobacterium* strain AGL1 + virG (VAIN *et al.* 2004) carrying the pBTCW vector (WT CaMV strain CM1841) was used for agroinfiltration assays. This strain is resistant to Rifampycin (50 µg/ml).

The yeast (*Saccharomyces cerevisiae*) strain used in this study was AH109 which is diploid giving the advantage of cotransformation with two plasmids. The complete genotype

of AH109 is: *MATa, trp1-901, leu2-3, 112, ura3-52, his3-200, gal4Δ, gal80Δ, LYS2 :: $GAL1_{UAS}$-$GAL1_{TATA}$-HIS3, $GAL2_{UAS}$-$GAL2_{TATA}$-ADE2, URA3 :: $MEL1_{UAS}$- MEL1 $_{TATA}$-lacZ*

4.1.3 Bacterial and yeast growth media

The normal media used to grow bacterial cells is liquid Luria-Bertani (LB) media (1% (w/v) tryptone, 0.5% (w/v) yeast extract, 0.5% (w/v) NaCl) containing the appropriate antibiotic and 0.4% (w/v) of glucose for recombinant protein expression. To solidify the LB media, 2% (w/v) agar was added which was then autoclaved.

On the other hand, yeast cells were grown in non-selective YPD media ((1% (w/v) yeast extract, 2% (w/v) peptone, 2% (w/v) glucose or selective minimal synthetic defined (SD) media (0.675% (w/v) yeast nitrogen base deprived of amino acids, 2% (w/v) glucose)) in the absence of amino acids. Solid YPD media was also prepared by adding 2% (w/v) agar before autoclaving.

4.1.4 Antibodies for protein detection

Primary and secondary antibodies used in this study are listed in Table 4.1-4 List of antibodies.

Table 4.1-4 List of antibodies

Antibody	Description	Dilution	Reference	Buffer
Primary				
anti-HA	Mouse monoclonal antibody against residues (YPYDVPDYA) of the human influenza virus hemagglutinin	1:10000	Sigma-Aldrich	5% non-fat dried milk in PBS-T
anti-cMyc	Rabbit polyclonal IgG against residues 408-439 (EQKLISEEDL) of the human p62c-Myc protein	1:2500	Santa Cruz Biotechnology	5% non-fat dried milk in PBS-T
anti-eIF3h	Rabbit polyclonal IgG fraction against the 40kDa eIF3h	1:5000	Dr. Albert G Von Arnim (University of Tennessee-Knoxville,USA)	5% non-fat dried milk in PBS-T
anti-TAV (diluted 1:2 in glycerol	Rabbit polyclonal IgG fraction against the 70kDa recombinant TAV	1:10000	Dr. Kappei Kobayashi (Ehime University at Ehim, Japan)	5% non-fat dried milk in PBS-T
anti-CP (p37)	Rabbit polyclonal IgG fraction against the 37kDa recombinant coat protein	1:10000	Pr. Mario Keller	5% non-fat dried milk in PBS-T
anti-RdRp	Rabbit polyclonal IgG fraction against the 125 kDa recombinant RNA dependent RNA polymerase of ORMV virus	1:4000	Dr.Mikhail Pooggin (CIRAD, Montpellier, France)	5% non-fat dried milk in PBS-T
anti-GFP	Rabbit polyclonal IgG fraction	1:5000	ThermoFisher Scientific (Invitrogen)	1% non-fat dried milk in PBS-T
Secondary				
anti-mouse	HRP conjugated whole IgG from goat	1:10000	ThermoFisher Scientific	PBS-T
anti-rabbit	HRP conjugated whole IgG from goat	1:10000	ThermoFisher Scientific	PBS-T

4.2 Molecular biology methods (Plasmid cloning strategy)

4.2.1 Plasmid DNA purification from *E.coli*

DNA plasmid serving as a template for Polymerase Chain Reaction (PCR) or bacterial and yeast transformations was purified using the microcentrifugation protocol in the NucleoSpin® Plasmid Miniprep kit. Purification was performed following description in the manufacturer's instruction manual which is based on bacterial lysis and purification on silica membrane.

4.2.2 Polymerase Chain Reaction

Oligonucleotide primers designed to amplify specific DNA sequences were ordered. Phusion® High fidelity DNA polymerase with its compatible buffer is used in the PCR reaction mix having a total volume of 50µl. Amplified PCR fragments were analysed by agarose gel electrophoresis. A standard PCR mix and PCR conditions are listed in the Table 4.2.2-1. PCR reaction setup and in Table 4.2.2-2. Thermocycling conditions for PCR.

Table 4.2.2-1 PCR reaction setup

Component	50 µl Reaction
Nuclease free water	37.6 µl
5X Phusion HF Buffer	10 µl
dNTP mix of 10mM of each dATP, dCTP, dGTP, and dTTP) (C_{stock}=10mM C_{final}=0.5mM)	0.4 µl
Forward primer (C_{stock}=100µM C_{final}=0.5µM)	0.25 µl
Reverse primer (C_{stock}=100µM C_{final}=0.5µM)	0.25 µl
Phusion® DNA polymerase	0.5 µl
DNA template (50-100 ng)	1 µl

Step		Temperature	Time
Initial denaturation		98°C	30 seconds
Denaturation	**25-35cycles**	98°C	5-10 seconds
Anneal		45-72°C	10-30 seconds
Extension		72°C	15-30 seconds/kb
Final extension		72°C	5-10 minutes
Hold		4°C	

Table 4.2.2-2. Thermocycling conditions for PCR

4.2.3 Agarose gel electrophoresis

Analysis of DNA samples was done using the basic agarose gel electrophoresis. Agarose powder was weighed and added to TBE buffer (100 mM Tris, 90 mM Boric acid, 2.5 mM EDTA, pH 8.0) and dissolved by heating in a microwave. The gel solution was cooled down before adding ethidium bromide to ultimately obtain a final concentration of 0.5 µg/ml. The gel was placed in an ultraviolet (UV)-transparent plastic tray located right on top of the BioRad Mini-Cell® GT agarose gel electrophoresis unit stage. A well comb was placed near the cathode and the gel was left to solidify for 30 mins. The system was immersed in TBE buffer. 6X DNA loading dye (0.25% (w/v) bromophenol blue, 0.25% (w/v) xylene cyanol FF, 30% (v/v) glycerol) was added to the DNA samples before loading the whole volume into the wells. Five microliters of 1 kilobase pair (kb) DNA marker (GeneRuler®) was loaded in the well as a DNA standard. The gel was allowed to run at a constant electric potential of 100 volts (V). DNA bands were visualized under UV light using a UV transilluminator.

4.2.4 Gel extraction and purification of DNA

Target DNA fragments resolved by agarose gel electrophoresis were needed for subsequent procedures. DNA bands were cut from the gel using a scalpel. Extraction and purification of

the DNA from the gel was performed using the NucleoSpin® Gel and PCR Clean-up extraction kit as described in the manufacturer's instruction manual.

4.2.5 Restriction enzymes digestion of DNA

Plasmid DNA was digested by two restriction endonucleases along with their compatible buffers. A digestion mix of 50 µl total volume for plasmid DNA and of 80 µl for insert DNA were prepared in 1.5 ml Eppendorf tubes (Table 4.2.5 Restriction enzymes digestion mix) and incubated at 37°C for 2-4 hrs. Analysis of linearized DNA fragments was performed by agarose gel electrophoresis. The restriction enzyme digestions were performed using the protocol outlined in the manufacturer's instruction manual.

Table 4.2.5 Restriction enzymes digestion mix

Plasmid DNA	50µl Reaction	Insert DNA	80µl Reaction
dH_2O	Up to 50 µl	**dH_2O**	Up to 80 µl
DNA (1µg)	X µl	**DNA**	X µl
1st restriction enzyme	1 µl	**1st restriction enzyme**	1 µl
2nd restriction enzyme	1 µl	**2nd restriction enzyme**	1 µl
10X enzyme buffer	5 µl	**10X enzyme buffer**	8 µl

4.2.6 Ligation of DNA fragments

DNA fragments digested by restriction endonucleases were ligated into plasmids which were in turn digested by the same set of restriction enzymes to generate compatible ends for ligation. Linearized plasmids and inserted DNA were purified and used for ligation reactions (Table 4.2.6 DNA ligation mix). As a negative control, DNA plasmid alone without the insert DNA was included in the ligation mix. Ligation mixes were incubated for 2 hrs at room

temperature. Competent bacterial cells were transformed with the total volume of ligation mix to guarantee an optimal transformation. Successful transformations were selected on LB agar media containing the appropriate antibiotic. Afterwards, plasmid DNA carrying the insert was purified from randomly chosen colonies. For verification, purified DNA plasmids were analyzed by endonuclease digestion and visualized by agarose gel electrophoresis.

Table 4.2.6 DNA ligation mix

Component	20µl Reaction
dH_2O	Up to 20 µl
DNA insert (300ng)	X µl
Plasmid DNA (150ng)	X µl
10X T4 DNA ligase buffer	2 µl
T4 DNA ligase	1 µl

4.2.7 Plasmid construction

Plasmids for yeast two hybrid and transient protoplasts expression assays

Constructions used for transient expression in protoplasts were expressed under the control of the CaMV 35S promoter. The bicistronic reporter vector pbiGUS is constituted of two ORFs, the first one is ORF VII of CaMV and the second one is GUS reporter gene. The monocistronic reporter vector pmonoGUS where the GUS reporter is fused in-frame to ORF VII of CaMV (BONNEVILLE *et al.* 1989). The constructs pmonoGFP, pTAV, peif3h, peif3h-S178A, peif3h-S178D were described in (THIEBEAULD *et al.* 2009; SCHEPETILNIKOV *et al.* 2011). Sequences of GFP, eif3h, eif3h-S178A, eif3h-S178D were subcloned instead of TAV ORF in the vector pTAV.

PCR products corresponding to eIF3 subunit h (At1g10840.1) (eIF3h full length, aa 1-337) and its deletion mutants (eIF3h-ΔC1, aa 1-254; eIF3h-ΔC2, aa 1-318, eIF3h-ΔN1, aa 39-337, eIF3h-ΔN2, aa 20-337) were amplified from Arabidopsis thaliana cDNA library using specific primers and cloned as in-frame fusions with the BD domain into the pGBKT7 vector and with the AD domain c into the pGADT7 (Clontech®) for yeast two hybrid assay (Table 4.2.7-1,2 Primers for pGAD-eIF3h deletion mutants, Primers for pGBK-eIF3h deletion mutants) and in the pTAV vector instead of TAV ORF for transient protoplast expression (Table 4.2-7-3 Primers for pKp-eIF3h deletion mutants).

Table 4.2.7-1 Primers for pGAD-eIF3h deletion mutants

eIF3h-ΔC1	Fwd: 5' CCGGAATTCATGGCAACCATGGCTAG 3'
	Rev: 5' CCGCTCGAGTTAAGACAGGTTCCGG 3'
eIF3h-ΔC2	Fwd: 5' CCGGAATTCATGGCAACCATGGCTAG 3'
	Rev: 5' CCGCTCGAGTTAATTGATTTGGCCA 3'
eIF3h-ΔN1	Fwd: 5' CCGGAATTCATGAAGGAGTTTTCACC 3'
	Rev: 5' CCGCTCGAGTCAGTTGTCGTGCAATGC 3'
eIF3h-ΔN2	Fwd: 5' CCGGAATTCATGCCGCTTAGAGTTGTT 3'
	Rev: 5' CCGCTCGAGTCAGTTGTCGTGCAATGC 3'

Table 4.2.7-2 Primers for pGBK-eIF3h deletion mutants

eIF3h-ΔC1	Fwd: 5' CCGCATATGGCAACCATGGCTAG 3'
	Rev: 5' CCGGGATCCTTAAGACAGGTTCCGG 3'
eIF3h-ΔC2	Fwd: 5' CCGCATATGGCAACCATGGCTAG 3'
	Rev: 5' CCGGTCGACTTAATTGATTTGGCCA 3'
eIF3h-ΔN1	Fwd: 5' CCGCATATGAAGGAGTTTTCACC 3'
	Rev: 5' CCGGTCGACTCAGTTGTCGTGCAATGC 3'
eIF3h-ΔN2	Fwd: 5' CCGCATATGCCGCTTAGAGTTGTT 3'
	Rev: 5' CCGGTCGACTCAGTTGTCGTGCAATGC 3'

Table 4.2.7-3 Primers for pKp-eIF3h deletion mutants

eIF3h-ΔC1	Fwd: 5' CCGGTCGACATGGCAACCATGGCTAG 3'
	Rev: 5' CCGGGTACCTTAAGACAGGTTCCGG 3'
eIF3h-ΔC2	Fwd: 5' CCGGTCGACATGGCAACCATGGCTAG 3'
	Rev: 5' CCGGGTACCTTAATTGATTTGGCCA 3'
eIF3h-ΔN1	Fwd: 5' CCGGTCGACATGAAGGAGTTTTCACC 3'
	Rev: 5' CCGGGTACCTCAGTTGTCGTGCAATGC 3'
eIF3h-ΔN2	Fwd: 5' CCGGTCGACATGCCGCTTAGAGTTGTT 3'
	Rev: 5' CCGGGTACCTCAGTTGTCGTGCAATGC 3'

PCR product corresponding to eIF3 subunit f (AT2G39990) (eIF3f full length, aa 1-293) were amplified from *Arabidopsis thaliana* cDNA library using specific primers and cloned as in-frame fusions with the BD domain into the pGBKT7 vector (Clontech®) for yeast two hybrid assay.

PCR product corresponding to S6K1 was amplified from S6K1 cDNA (At3G08730) with pairs of specific primers and cloned into the pGBKT7 as in-frame fusion with the BD-domain.

PCR products corresponding to NTOR, CTOR were amplified from AtTOR cDNA (At1G50030) with pairs of specific primers respectively and cloned into the pGADT7 (Clontech®) as in-frame fusion with the AD-domain to obtain pGAD-NTOR and pGAD-CTOR.

Plasmids for recombinant protein expression

PCR products corresponding to eIF3f and S6K1 were inserted into pGEX-6P1 (Pharmacia Biotech) as in-frame fusions with the GST-domain (SCHEPETILNIKOV *et al.* 2011).

pGEX-6P-1, pGEX-eIF3f and pGEX-S6K1 were used for expression and purification of GST alone, eIF3f and S6K1 fusion proteins with GST domain at the N-terminus.

4.3 Protein analysis methods

4.3.1 SDS-polyacrylamide gel electrophoresis of proteins

Using sodium dodecyl sulphate polyacrylamide gel electrophoresis (SDS-PAGE), proteins were separated according to their electrophoretic mobility (LAEMMLI 1970). The preparation of the gels was performed in a vertical mould having a thickness of 1 or 1.5 mm and composed of a lower resolving region (7.5%-15% (v/v) acrylamide, 375mM Tris-HCl (pH 8.8), 0.2% (w/v) SDS) and an upper stacking region (5% (v/v) acrylamide, 150mM Tris-HCl (pH 6.8), 0.2% (w/v) SDS). Polymerization was induced by the addition of ammonium persulfate (APS) (8mM) and tetramethylenediamine (TEMED) (200nM). Then, the gels were transferred to an electrophoresis unit and immersed in running buffer (25mM Tris-base, 190mM glycine, 0.1% (w/v) SDS). Samples were then loaded into wells located within the stacking region with a constant electric potential of 100-150V throughout the gel run. Resolved proteins present within the gel were revealed with either Coomassie™ blue or immunoblot analysis. N.B: ProSieve® (Quadcolor®).

4.3.2 Coomassie™ blue staining

Coomassie™ blue staining was used to visualize the resolved proteins by SDS-PAGE. The gel was submerged in the staining solution (0.25% (w/v) Brilliant blue R-250, 40% (v/v) ethanol, 10% (v/v) acetic acid) overnight on a shaker. De-staining the gel by constant motion in several baths of a solution of 15% (v/v) ethanol, 15% (v/v) acetic acid was performed to visualize the resolved proteins.

4.3.3 Western blot transfer

Resolved proteins after SDS-PAGE were made reachable for antibody detection by transferring and immobilizing protein bands present within the acrylamide gel onto

Immobilon® PVDF membranes (0.45 µm pore size) (Millipore®, France). The protein gel and nitrocellulose membrane were placed between 2 thin sponges, 2 layers of Whatmann 3mm filter paper pre-soaked in transfer buffer (30 mM Tris base, 230 mM glycine, 20% (v/v) ethanol) as a sandwich. The sandwich was compiled inside of a BioRad Criterion® Blotter electrophoretic transfer cell, and has been run at a constant voltage of 100V for 1hr at 4°C.

4.3.4 Immunological detection of proteins

Blockage of the PVDF membrane was done in 5% non-fat dried milk (w/v) in PBS-T (140 mM NaCl, 3 mM KCl, 1.5 mM KH_2PO_4, 8 mM Na_2HPO_4, 0.1% (v/v) Tween-20) for 1hr at room temperature to avoid non-specific antibody binding to the membrane in the following steps. Membranes were washed 10 min 3 times in PBS-T previous to overnight incubation with primary antibody diluted at 4°C in PBS-T or 5% non-fat dried milk (w/v) in PBS-T. Diluted solutions of primary antibodies were poured off and membranes were washed 10 min 3 times with PBS-T in order to remove non-specifically bound primary. The appropriate secondary antibody conjugated to horseradish peroxidase (HRP) was diluted in PBS-T and incubated for 1hr at room temperature. Three times of 10 min washing in PBS-T were done to remove excess of secondary antibody and proteins were visualized using enhanced chemiluminescence (ECL) kit. Membranes were exposed on FujiFilm general purpose blue medical X-ray film (Fujifilm®) and developed in a dark room using an automatic film processor.

4.4 Yeast methods and protocols

4.4.1 Competent yeast cells preparation

One milliliter of liquid YPD was inoculated with 1-2 fresh colonies of AH109 yeast strain and vortexed vigorously then transferred to a flask containing 50 ml of YPD and incubated

overnight at 30°C 250 rpm. Overnight culture (OD_{600} = 0.2-0.3) was transferred into 300 ml of YPD and incubated for 3hrs at 30°C 250 rpm until an OD_{600} of 0.5. Cells were then placed in 50 ml Falcon tubes and centrifuged at 3000 x g for 10 min at room temperature. Cell pellets were re-suspended by vortexing in 50 ml of dH_2O. Pool cells were centrifuged at 1000 xg for 5 min. Cell pellet was re-suspended in 1.5 ml of freshly prepared 1X TE/LiAc buffer (10 mM Tris-HCl (pH 7.5), 1 mM EDTA, 100 mM Lithium acetate) and kept on ice until transformation started.

4.4.2 Competent yeast cells transformation

The lithium acetate/ single-stranded carrier DNA/polyethylene glycol protocol was used for competent yeast cells transformation. One microgram of DNA-BD/bait, 1 µg of DNA-AD/bait and 0.1 mg of herring testes carrier DNA were added to 100 µl of competent yeast cells and the mix was vortexed at high speed. For each transformation, 600 µl of PEG/LiAc solution (40% (v/v) polyethylene glycol-3350, 10 mM Tris-HCl (pH 7.5), 1 mM EDTA, 100 mM lithium acetate) were added to the mix and vortexed. The transformation mixes were shacked at 30°C for 30 min. A volume of 70 µl of DMSO was mixed with transformation reactions and heat shocked at 42°C for 15 min. Cells were chilled on ice for 2 min and centrifuged for 30 sec at 16000 x g. Cells were re-suspended in 200 µl of 1X TE buffer (10 mM Tris-HCl (pH 7.5), 1mM EDTA). The total transformation was plated onto solid selective minimal SD media deprived from the appropriate amino acids (SD-LW L: Leucine W: Tryptophan) to allow for the selection of successfully transformed cells. Colonies were grown at 30°C for 3-5 days.

4.4.3 Yeast whole cell extract preparation

Testing of BD-bait and AD-prey protein expression was performed by immunoblot analysis. The urea/SDS protein extraction method served for extraction of yeast whole cell lysates. Three colonies were cultured overnight in 1 ml of selective media (SD-LW) at 30°C 250 rpm. Overnight cultures were centrifuged 1 min at 1000 x g. Glass beads (425-600 µm) were added to the cell pellets with 150 µl of preheated urea/SDS cracking buffer (8 M urea, 5% (w/v) SDS, 40 mM Tris-HCl pH 6.8, 0.1 mM EDTA, 0.4 mg/ml bromophenol blue). Samples were incubated for 10 min at 95°C, 1500 rpm. Samples were loaded on SDS-PAGE gel followed by immunoblot analysis using antibodies against cMyc and HA epitope tags.

4.4.4 Yeast two-hybrid assay

The yeast two-hybrid technique is used to detect interaction between two targeted proteins. It is based on the possibility of reconstitution of transcription activity when two reporters, fused to Gal4 binding domain (BD) and activation domain (AD) could interact.

Thus, wild type protein and its deletion mutants fused to GAL4 AD-domain and proteins of interest (S6K1 and eIF3F) fused to GAL4 BD-domain were cotransformed into AH109 yeast strain. Afterwards, cotransformed yeast cells were plated on solid double amino acid drop-out media. Colonies picked up from positive cotransformation were cultured overnight at 30°C in the SD-LW liquid selective media. Then, cultures were set at the same optical density by water.

Finally in order to test the interaction between target proteins, a series of dilutions (10^{-1} and 10^{-2}) were prepared in a 96-well plate. Three µl of concentrated and diluted cultures were plated on the appropriate double (SD-LW) triple (-his or –ade : SD-LWH or SD-LWA) and quadruple amino acid drop outs (-his and –ade: SD-LWHA) selective agar. Agar plates were set for incubation at 30°C for 3-5 days.

To confirm expression of BD and AD fusion proteins, cell lysates were treated by 150 µl cracking buffer and resolved on SDS-PAGE gel followed by immunoblot analysis.

4.5 Purification of recombinant fusion proteins from *E.coli*

4.5.1 Transformation of competent bacterial cells

Transformation of chemical bacterial cells BL21 DE3 pLysS was performed following the traditional protocol. Competent cells were thawed on ice for 20 min. 50 µl of *E.coli* cells were mixed with 500 ng of purified DNA plasmid or total volume of DNA ligation reaction and incubated for 20 min on ice. Then, cells were heat shocked for 60 sec at 42°C to facilitate the entry of DNA into bacterial cells. 500 µl of LB media were added to the mix and cells were incubated for 1 hr at 37°C. Finally, the cells were plated on LB agar medium containing appropriate antibiotics and plates were incubated overnight at 37°C to allow the growth of the cells and the selection of successfully transformed cells.

4.5.2 Expression of recombinant fusion proteins

GST-fusion proteins were expressed in BL21 (DE3) pLysS (Novagen®) followed by purification with Glutathione Sepharose 4B batch. A single colony of *E.coli* BL21-pLysS(DE3) cells transformed with the appropriate plasmid was used to inoculate 5 ml of enriched LB medium supplemented by 0.4% glucose and containing the following antibiotics (100µg ml^{-1} of ampicillin and 25µg ml^{-1} of chloramphenicol) and incubated overnight at 37°C shaking incubator.

E.coli BL21 (DE3) pLysS cells containing the pGEX-S6K1 or pGEX-eIF3f expression plasmids were diluted in 50 ml of the same original medium and incubated at 37°C until the OD_{600} reached 0.5. Then, IPTG was added to obtain a final concentration of 0.5mM. Growth continued for an additional 1 hr at 37°C, followed by harvesting the cells by centrifugation

for 15 min at 5000 rpm at 4°C and finally resuspended in 5 ml extraction buffer (50mM Tris-HCl pH 7.5, 300mM KCl, 0.1% NP-40 (Sigma-Aldrich®) and cOmplete® protease inhibitor cocktail (Roche®)). Cells were then sonicated by one 30 sec cycle at 50% of amplification power. Lysates were clarified by centrifugation at max speed for 30 min at 4°C and filtrated through a 0.45 µm filter and processed as follows (see below).

4.5.3 Purification of GST fusion proteins (in batch)

Glutathione Sepharose beads were washed 3 times by extraction buffer. Lysate was added to the beads and incubated for 3 hrs at 4°C under constant rotation. Glutathione beads and bound recombinant GST fusion proteins were then pelleted by centrifugation at 1000 x g for 1 min followed by four washes with 1 ml of extraction buffer and one wash with 50mM Tris-HCl pH 7.5, 60 mM KCl. The pellets were then re-suspended in 300 µl of the same buffer.

4.5.4 GST-pull down assay

Molar equivalents of purified protein (eIF3h) were incubated with GST alone or GST-protein fusion (GST-S6K1 or GST-eIF3f) in total volume of 300µl Binding buffer (50 mM Tris-HCl pH 7.5, 100 mM KCl), at 4°C for 2 hrs under constant rotation. The mixtures were centrifuged at 500 x g for 5 min at 4 °C. Hundred microliter of the first supernatant (unbound fraction, U) was collected for analysis. Sepharose beads and associated proteins (bound fraction, B) were washed 5 times by 50 mM Tris-HCl pH 7.5, 750 mM NaCl, 0.1% NP-40, and then associated proteins were eluted from beads by 100 µl of 1X Laemmli buffer (4X Laemmli buffer: 250 mM Tris-HCl (pH 6.8), 40% (v/v) glycerol, 8% (w/v) SDS, 0.04% (v/v) bromophenol blue, 1% (v/v) β-mercaptoethanol). Unbound and Bound fractions were analyzed onto 12% SDS-PAGE gel and stained by Coomassie™ blue staining.

4.6 Plant *in vitro* assays

4.6.1 Plant material, growth conditions and expression vectors

In this study, as wild-type model, *Arabidopsis thaliana* ecotype Columbia (Col-0) was used. Dr Albrecht G. von Arnim (University of Tennessee-Knoxville, USA) kindly provided us with Col-0 *eif3h-1* homozygous mutant lines. A recessive mutant allele (eif3h-1) carrying a T-DNA insertion in the 10th exon downstream of Ser254. A truncated eIF3h-related protein was detected in this allele (KIM *et al.* 2004).

4.6.2 Seed sterilization

Fifty microliters of seeds were incubated in sterilization buffer (5% (v/v) bleach, 70% (v/v) ethanol) for 20 min followed by 1 min in absolute ethanol. Seeds were dried under a sterile hood for 1 hr and plated on MS-agar plates.

4.6.3 Plant growth conditions

Arabidopsis seeds were cultured horizontally on MS agar medium (Murashige and Skoog medium with MSMO-salt mixture; Sigma®). WT Col-0 and *eif3h-1* mutant plants were incubated at 4°C in the dark for 1 and 7 days, respectively. Plants were then grown in the greenhouse under the following conditions: 16 hrs light, 21°C - 8 hrs darkness, 17°C (*in vitro* assay).

Seeds were sown in small pots containing humid fresh *Arabidopsis* culture soil. *Arabidopsis thaliana* plants were grown under the following conditions: 16 hrs of light – 8 hrs of darkness at a temperature ranging between 18 °C and 25 °C under normal greenhouse conditions.

4.6.4 Viral infection

Infection by CaMV virus was performed by agrobacterium-mediated transient transformation of *Arabidopsis* young leaves with pBTCW vector [binary agro-vector containing the full length genomic copy of CaMV, isolate CM1841, kindly provided by Dr Kappei Kobayashi (KOBAYASHI AND HOHN 2003; KOBAYASHI AND HOHN 2004; LAIRD *et al.* 2013)]. The schematic presentation of this vector is shown in Figure 4.6.4-1 The schematic presentation of pBTCW vector used in CaMV infection. In brief, *Agrobacterium* (hypervirulent strain) AGL1+virG (VAIN *et al.* 2004) expressing the WT CaMV viral vector was grown for 20 hrs at 28°C in 5 ml of Luria-Bertani medium containing the following antibiotics: Kanamycin 50µg.mL^{-1} and rifampicin 100µg.mL^{-1}. Once the culture was saturated, 5 ml of it were resuspended in 95 ml of LB medium and set for incubation overnight at 28°C. Bacteria were pelleted and incubated at room temperature in an agroinfiltration buffer A (10mM $MgCl_2$ / 10mM MES pH 5.7/ 200µM acetosyringone). Finally, bacteria were diluted at the following OD (OD_{600}=0.8) and plants at the early leaf stage were infiltrated on two leaves chosen randomly. Images of plants were taken (Canon EOS 350D digital) at 7, 10, 12, 18, 23 dpi.

Small discs (3 mm diameter) were collected from leaves and placed in small Eppendorf tubes containing glass beads (425-600 µm). Plant samples were frozen in liquid nitrogen. Samples were processed on a mini-Precellys24 Homogenizer at one 7 sec cycle of 6500 x g. Proteins were extracted by 100 µl of preheated 1X Laemmli Buffer and incubated for 10 min at 95°C and analyzed by immunoblot with specific antibodies against CaMV TAV and coat protein.

Figure 4.6.4-1 The schematic presentation of pBTCW vector used in CaMV infection

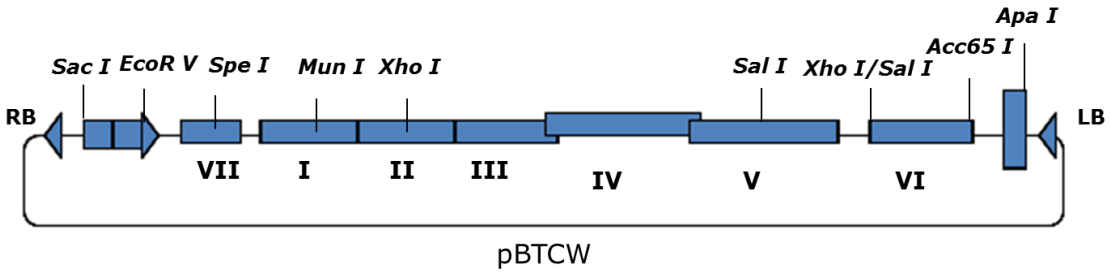

Infection by TuMV virus was performed by agroinfiltration using a construct pCB-TuMV-GFP permitting the transient expression of TuMV polyprotein fused to GFP in *Arabidopsis thaliana* kindly provided by (Dr James Carrington, Danforth Plant Science Center). Same experimental set up was performed as described above and polyprotein production was monitored by western blot with anti GFP antibodies.

Infection by ORMV virus was performed by mechanical inoculation via ORMV viral particles kindly provided by Manfred Heinlein (Institut de biologie moléculaire des plantes, Strasbourg France). Five weeks old plants were mechanically inoculated on two leaves chosen randomly (C_{stock}=1µg/1µl C_{final}=50ng/1µl, 150ng/leaf) previously scrubbed with Celite to generate small wounds to facilitate the entry of viral particles. Samples were collected and analyzed by immunoblot with specific antibodies against RdRp (RNA dependent RNA polymerase).

4.6.5 Transient expression for protoplast GUS assays

PEG mediated transfection

Mesophylls protoplasts derived from *Arabidopsis thaliana* WT or *eif3h-1* mutant plants were prepared in sterile conditions following the protocol of (YOO *et al.* 2007) modified below.

Seedlings from 7 dag plants grown on MS medium were collected and put in petri dishes containing 5ml of 45µM cell wall digestion enzyme solution (1.5% (w/v) cellulase R10 (Yakult Pharmaceutical®), 0.4% (w/v) maceroenzyme R10 (Yakult Pharmaceutical®), 0.4M

Manitol, 20mM KCl, 20mM MES (pH 5.7)). This solution should be pre-heated for 10 min at 55°C in order to deactivate the DNase, proteases and improve enzyme solubility, followed by the addition of 10mM $CaCl_2$ and 0.1% BSA and finally it is filtered before use. A scalpel is used to finely cut the seedlings. 20 ml of the digestion enzyme solution were added to the mixture. Finally, using a desiccator, digestion mixtures were vacuum infiltrated for 5 min to increase the digestion surface.

The digestion mixtures were incubated at 28°C on a shaker (50 rpm) for 4 hrs. 20 ml of W5 buffer (2mM MES (pH 5.7), 154mM NaCl, 125mM $CaCl_2$, 5mM KCl) were added to the mixture and the whole volume is then filtered through a Miracloth membrane previously immersed in W5 buffer and collected in Falcon tubes. Protoplasts were centrifuged at 1000 x g for 2 min at room temperature without break. Then, they were washed twice with 10 ml of mannitol and the pellet was resuspended in 1-5 ml of MMG buffer (0.4M mannitol, 15mM $MgCl_2$, 4mM MES (pH 5.7)) in order to get the optimal concentration of 10^6 cells ml^{-1}. For transactivation, protoplasts were transfected with 10µg of pbiGUS serving as a reinitiation marker, pmonoGFP serving as a transfection marker, pTAV, others vectors containing the genes of interest or an empty vector p35S. Transfection was performed as follows: 5-10 µg of plasmid and 100µl of protoplasts were mixed together with 110 µl of PEG solution (30% (w/v) PEG 4000 (Fluke®); 200mM mannitol; 100mM $CaCl_2$) and incubated for 15 min at room temperature. Then, 1 ml of W5 buffer was added to stop the reaction. Protoplasts were then centrifuged for 1 min at 1000 x g and the pellet was resuspended in 1 ml of WI buffer (0.5 M mannitol; 20mM KCl; 4 mM MES (pH 5.7)) and transferred into 12-well culture Greiner® plates and set for incubation in the dark for 18 hrs at 26°C. N.B: All buffers should be kept at 4°C before usage.

GUS activity quantification

When incubation was done, ¼ of the total volume of protoplasts were centrifuged for 2 min at 500 x g and pellets were dedicated for western blot to assess protein expression with specific antibodies (commercial or prepared antibodies). The remaining ¾ of the total volume of protoplasts were dedicated for GFP fluorescence and GUS assay. These protoplasts were also centrifuged for 2 min at 500 x g without break and pellets were resuspended in 180 µl of distilled water and transferred into 1.5 ml Eppendorf tubes with 20 µl of 10X GUS extraction buffer (500mM Tris-HCl (pH 7.5), 100mM EDTA (pH 8.0), 1% (v/v) Triton X-100, 1% (v/v) Igepal 360 ®). Samples were vortexed for 15 sec and incubated for 10 min at room temperature and then centrifuged for 5 min at 16000 g. Supernatants were transferred into new tubes.

GUS activity was quantified by monitoring cleavage of the β-glucuronidase substrate 4-methylumbelliferyl β-D-glucuronide (MUG) with production of MU fluorescent substrate (JEFFERSON *et al.* 1987). Samples were distributed on an opaque 96-well plate. In each well, 150 µl of sample extract were added and GFP fluorescence was measured using a FLUOstar OPTIMA fluorimeter (BMG Biotech, USA) at 485 nm when excited at 520 nm. Then, 150 µl of 2X GUS assay buffer (10X GUS extraction buffer, 2mM 4-methyllumbelliferyl β-D-glucuronide (MUG, Sigma®), 0.1% (w/v) BSA, 1mM DTT) were added to each sample extract. The reaction was performed in a dark microplate incubator (model Stat-Fax 2200, Awareness technology®) at 37°C mixed at 600 rpm. 50 µl of the reaction mix was added to 50 µl of 2X stop buffer (400 mM sodium carbonate) in the opaque plate at different time points. Standard time points correspond to 0, 15 and 30 min were established with each sample in duplicates. This time curve is used to calculate GFP/GUS relative units corresponding to the linear range slope over the time kinetic assay. GUS fluorescence was measured at 355 nm when excited at 460 nm. Values given from the fluorescence assay were

transformed to GUS relative units and then regularized by GFP protein fluorescence to outfit differences in protoplasts transfection efficacy. These values present the income from more than three independent experiments.

V. RÉSUMÉ EN FRANÇAIS

Résumé

La réinitiation de la traduction est un mécanisme permettant de traduire des ORF qui sont présents dans la région *leader* de différents ARNm cellulaires (uORF). La majorité des cas de réinitiation de la traduction chez les eucaryotes concerne des uORF de petite taille. Des stratégies alternatives ont été développées, entre autres par les virus, afin de réinitier la traduction après un long uORF. Le *virus de la mosaïque du chou-fleur* (CaMV) exprime un ARNm polycistronique codant la totalité de protéines virales. L'une d'entre elle, la protéine TAV (TransActivateur/Viroplasmine) est un facteur essentiel qui rend possible la réinitiation de la traduction après de longs ORF et qui, de plus, active la protéine kinase TOR. La sous-unité h du facteur d'initiation de la traduction eIF3, requise pour promouvoir la reinitiation après un petit ORF chez les plantes, a été identifiée comme étant une nouvelle cible de phosphorylation de la voie de signalisation de TOR. L'objectif principal de ma thèse a été d'élucider la fonction de la protéine eIF3h dans la réinitiation après un petit ORF ainsi que dans la réinitiation de la traduction, assurée par TAV, après un long ORF. Nous avons exploité les lignées transgéniques *eif3h-1* d'*Arabidopsis* exprimant la protéine eif3h tronquée de son extrémité C-terminale, qui sont déficientes pour la réinitiation mais pas pour l'initiation de la traduction. Nous avons montré que la phosphorylation de eIF3h est essentielle pour stabiliser eIF3 au niveau des ribosomes durant l'élongation, ce qui favorise la

ré-acquisition par le ribosome de facteurs nécessaires à la réinitiation de la traduction, et que la délétion de sa région Ct abolit son intégration dans le complexe eIF3. De plus, nous avons montré que eIF3h, la cible de la voie de signalisation de TOR, interagit avec S6K1. Des protoplastes préparés à partir des plantes mutantes *eif3h-1* sont incapables de promouvoir la réinitiation après de longs ORF en présence de TAV. La surexpression de eIF3h, indifféremment de son état de phosphorylation, est indispensable pour restaurer la reinitiation assurée par TAV dans les protoplastes *eif3h-1*. Par ailleurs, les plantes *eif3h-1* déficientes dans la réinitiation, sont résistantes à l'infection par le CaMV démontrant l'importance de eIF3h pour la réplication du CaMV. En revanche, ces plantes *eif3h-1* peuvent être infectées par d'autres virus dont la traduction de l'ARN génomique est coiffe- ou IRES-dépendante. Ainsi, nos résultats suggèrent que eIF3h est un facteur de reinitiation important aussi bien pour la reinitiation après un petit qu'après un long ORF (controlée par TAV), et que TAV exploite cette machinerie cellulaire, et plus particulièrement TOR et eIF3h, pour exprimer ses propres protéines par réinitiation de la traduction.

Introduction

La traduction des ARNm eucaryotes représente une étape importante de l'expression des gènes. Un contrôle efficace de la traduction des ARNm permet à la cellule de réagir rapidement pour la production des protéines nécessaires, ceci dans un contexte temporel et spatial bien défini. La traduction des ARNm eucaryotes peut être subdivisée en trois étapes principales : initiation, élongation et terminaison. Chaque étape est finement régulée par un ensemble de mécanismes, mais c'est certain que l'étape d'initiation est le processus le plus complexe soumis à une régulation fine et élaborée. Cette étape est orchestrée par de nombreux facteurs et débute par le recrutement du complexe d'initiation de la traduction eIF4F en 5' des ARNm. eIF4F est un complexe protéique composé de 3 sous-unités : eIF4A,

eIF4E et eIF4G. La sous-unité eIF4E interagit directement avec la coiffe située en 5' de l'ARNm, la sous-unité eIF4A permet de dérouler les éventuelles structures secondaires présentes dans l'ARNm en aval de la coiffe grâce à ses fonctions hélicase et ATPase-renforcée par un autre facteur eIF4B, la sous-unité eIF4G, quant à elle, joue un rôle cohésif entre différents partenaires. La petite sous-unité ribosomique 40S, accompagnée des facteurs eIF3, eIF1, eIF1A, eIF5 et du complexe ternaire eIF2-ARNti-GTP est recrutée sur l'ARNm. Une fois ce complexe 48S formé, le ribosome peut alors balayer l'ARNm grâce aux facteurs eIF1 et eIF1A à la recherche du codon initiateur. L'appariement des bases du codon initiateur AUG de l'ARNm et de l'anticodon de l'ARNtMeti, permet d'aborder la phase finale de l'initiation. Une fois l'association codon-anticodon effectuée, l'hydrolyse du GTP lié à eIF2 permet l'éjection des facteurs d'initiation de la surface du complexe d'initiation 48S. La grande sous-unité ribosomique 60S peut alors s'associer par l'intermédiaire des facteurs eIF5 et eIF5B, permettant de former un ribosome 80S actif. Une fois le complexe 80S formé, la phase d'élongation commence. Le facteur d'initiation 3 (eIF3) est un facteur critique requis à toutes les étapes de l'initiation de la traduction. Il joue un rôle capital dans la formation du complexe de pré-initiation de la traduction – le PIC 43S –, notamment en permettant le recrutement du complexe ternaire eIF2-Met-ARNtMet-GTP. Chez les eucaryotes, y compris les plantes, eIF3 est de loin le plus complexe et le plus large (700-800 kDa), il est composé de 13 sous unités, dont 5 au sein d'un « cœur » central conservé : eIF3a, eIF3b, eIF3c, eIF3g and eIF3i. Récemment, la sous-unité eIF3h a été impliquée dans l'assemblage des sous-unités e, d, k et l dans le complexe fonctionnel eIF3. eIF3 est impliqué dans des réseaux d'interaction intensive avec d'autres eIF.

Après la terminaison de la traduction, dans certains cas, la sous-unité 40S reste fixée sur l'ARNm après la traduction de l'ORF et poursuit sa migration et initie la traduction à un deuxième codon initiateur situé en aval du premier. La majorité des cas de réinitiation chez

les eucaryotes implique des uORFs de petite taille (inférieure à 30 codons) que l'on qualifiera de sORF (short ORF). L'efficacité de la réinitiation est modulée par de nombreux paramètres tels que la distance entre les ORF, les facteurs protéiques et les éléments *cis* de l'ARN. Environ 30% des ARNm des mammifères et des plantes possèdent des uORFs dans leur séquence leader dont beaucoup sont traduits. Les données d'accumulation suggèrent que les uORF jouent un rôle important dans la régulation négative de la traduction de leur ARNm associé chez les mammifères et les plantes. Plusieurs facteurs d'initiation de traduction canonique, tels eIF4F, eIF4A et le facteur d'élongation 2 (eEF2), ont été suggérés pour favoriser la réinitiation après traduction de uORF chez des mammifères et des levures. eIF3 participe à la promotion de la réinitiation après la traduction d'un court ORF, et après la traduction d'un long ORF dans quelques rares cas dans les virus des plantes et des mammifères. Dans les plantes, la protéine ribosomique 60S L24B et la sous-unité eIF3h favorisent la réinitiation de la traduction sur les ARNm contenant des uORF, comme en témoignent les ARNm codant pour les facteurs de transcription d'*Arabidopsis* bZIP11, ARF3 et ARF5.

eif3h-1 et *rpl24b Arabidopsis* présentent des défauts de développement en partie similaires à ceux révélés dans les plantes qui sous-traduisent les ARNm pour les facteurs de transcription bZIP11 et les facteurs auxine-réponse. Ainsi, bien que les fonctions de eIF3h et eL24 dans la réinitiation restent à identifier, elles diffèrent probablement.

TOR, protéine sérine/thréonine kinase, existe chez les animaux et la levure sous la forme de deux complexes, mTORC1 et mTORC2, qui régulent pour le premier, la traduction, la croissance, la prolifération cellulaire et l'autophagie et pour le second, la structuration du cytosquelette. Une fois activée par sa voie de signalisation, TOR phosphoryle la protéine kinase S6K1 et 4E-BP. Contrairement aux animaux et à la levure, la voie de signalisation

TOR et ses substrats sont beaucoup moins connus chez les plantes. Chez les mammifères, eIF3 sert de plate-forme de liaison pour la phosphorylation de S6K1 par mTOR.

Chez les plantes, TOR codé par un seul gène, a été impliqué dans la phosphorylation de S6K1 à T449. Le TOR est activé en réponse au glucose, à l'hormone végétale auxine et au facteur de pathogénicité, la protéine TAV du virus de la mosaïque du chou-fleur (CaMV). L'inactivation de *Arabidopsis* TOR déclenche une réduction significative des niveaux de ribosome actif, ce qui suggère un rôle de TOR dans la synthèse des protéines végétales. En conséquence, *Arabidopsis* TOR d' est requis pour la traduction d'ARNm contenant des uORF. eIF3h est une protéine intrinsèque requise pour les événements de réinitiation en favorisant la réinitiation de la traduction, tout en étant dispensable pour l'initiation à l'extrémité 5' de l'ARNm. eIF3h peut être phosphorylé en S178 de manière sensible à TOR. Pour favoriser les événements de réinitiation, TOR actif se lie aux complexes de préinitiation et aux polyribosomes pour maintenir le statut de phosphorylation de eIF3h. La phosphorylation de eIF3h surexprime sa fonction dans la traduction des ARNm contenant des uORF.

Un cas inhabituel de réinitiation de traduction après un long ORF est présent chez le virus de la mosaïque du chou-fleur (CaMV), grâce au facteur de réinitiation CaMV-transactivateur / viroplasmine (TAV) et de plusieurs protéines cellulaires, y compris eIF3 et la protéine RISP. TAV fonctionne à la fois sur l'ARN pré-génomique 35S polycistronique viral et les ARN bicistroniques artificiels conjointement avec RISP via l'interaction avec la machinerie de traduction de l'hôte - TAV et RISP interagissent avec la protéine ribosomale 60S L24 et eIF3. De plus, TAV se lie à TOR et favorise son activation. Tous ces facteurs se retrouvent dans les polysomes des cellules exprimant TAV ou les cellules infectées par CaMV. Nous avons proposé précédemment que TAV entre dans la machinerie de traduction de l'hôte à l'étape de l'assemblage de 60S par l'interaction avec l'eIF3 lié à 40S et empêche la dissociation de eIF3

/ RISP des ribosomes de traduction pendant le long événement d'élongation, positionnant eIF3 / RISP pour la réinitiation à l'ORF en aval.

Nous avons étudié le rôle des domaines N et C-terminaux de eIF3h dans son intégration dans le complexe eIF3 et la liaison aux polyribosomes. De façon frappante, eIF3h est d'une importance cruciale pour la réinitiation activée par TAV après la traduction d'un ORF, ce qui suggère qu'il s'agit d'un facteur de réinitiation de la traduction basique. C'est intéressant que les plantes mutantes *eif3h-1* sont résistantes à l'infection par le CaMV.

Résultats

L'intégration de eIF3h dans le complexe eIF3 dépend de son domaine C-terminal

Les lignées transgéniques *eif3h-1* d'*Arabidopsis* exprimant la protéine eif3h tronquée de son extrémité C-terminale, sont déficientes pour la réinitiation mais pas pour l'initiation de la traduction. Pour comprendre le mécanisme de la fonction eIF3h dans les événements de réinitiation *in planta*, nous avons d'abord essayé de disséquer la séquence de la protéine eIF3h pour déterminer le ou les domaines requis pour la fonction eIF3h dans l'assemblage de eIF3 et la réinitiation. Sur la base de deux mutants tronqués à l'extrémité C terminale, on a utilisé une série de mutants de délétion eIF3h -eIF3hΔC1 et eIF3hΔC2 dépourvus de 83 ou 19 acides aminés (aa) à l'extrémité C, respectivement, et eIF3hΔN1 et eIF3hΔN2 manquant de 40 ou 20 aa à l'extrémité N, respectivement (figure 1A). Le domaine central de eIF3h MOV34 / MPN est partagé par eIF3f et les protéases MPN, ce qui indique que MPN n'est pas responsable d'une fonction spécifique de eIF3h lors de la réinitiation. Ainsi, nous avons d'abord analysé si les mutants d'*Arabidopsis* eIF3h peuvent interagir avec eIF3f dans le système de double hybride chez la levure. Les résultats (figure 1B) montrent que les deux protéines interagissent effectivement et que leur interaction n'est pas affectée par la délétion des résidus 20aa (AD-eIF3hΔN2) ou 40aa (AD-eIF3hΔN1) N-terminaux, Tandis qu'une plus

grande délétion du fragment C-terminal (AD-eIF3hΔC1) a supprimé l'interaction avec eIF3f (BD-eIF3f). L'interaction eIF3h et eIF3f a été confirmée par le système de GST pull down (figure 1C).

Nous avons demandé si S6K1, qui était impliqué dans la phosphorylation de eIF3h à S178, se lie à eIF3h. Le système à double hybride chez la levure et les résultats de GST pull down ont révélé l'association de S6K1 avec eIF3h (figure 2A, B). Malgré la délétion du fragment C2, eIF3hΔC2 se lie à S6K1; De plus, la délétion de ΔN2 a amélioré la liaison. Les délétions plus grandes (ΔN1 et ΔC1) ont quelque peu réduit, mais n'ont pas supprimé, l'interaction eIF3h avec S6K1. De manière surprenante, le système à double hybride chez la levure a détecté des interactions entre eIF3h et la partie N-terminale de TOR, qui héberge des domaines de répétition HEAT. Cette interaction était insensible aux deux troncatures de domaine eIF3h C et N-terminal (figure 2C). Nous avons expliqué ce résultat en supposant que eIF3h lié au domaine de répétition HEAT de TOR pourrait être positionné plus favorablement pour la phosphorylation par S6K1.

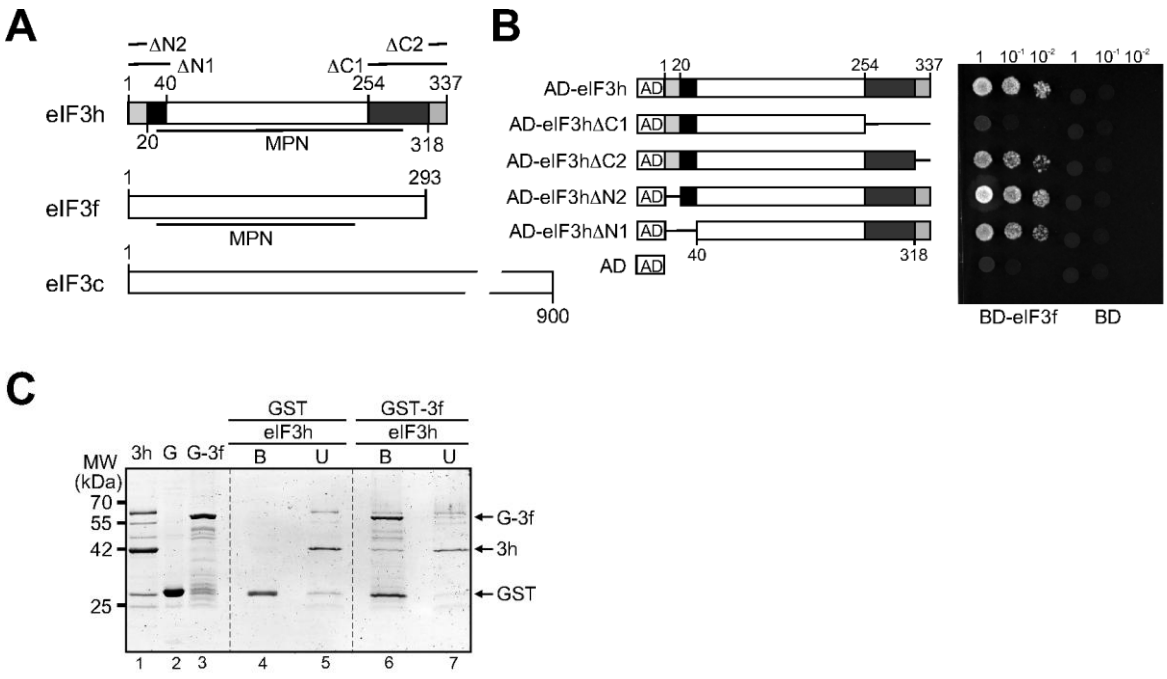

Figure 1. Caractérisation du réseau de phosphorylation et d'interaction de eIF3h
(A) Représentation schématique de eIF3f, eIF3c, eIF3h et de ses domaines - MPN, N1, N2 et C1, C2.
(B) Représentation schématique d'*Arabidopsis* eIF3h et de ses mutants fusionnés au domaine d'activation Gal4 (AD). Les interactions par double hybride de levure entre le domaine de liaison Gal4 (BD) -BD-eIF3f et AD-eIF3h et ses variantes de délétion sont présentées. Des unités égales de OD_{600} et des dilutions 1/10 et 1/100 ont été repérées de gauche à droite et incubées pendant 2 jours.
(C) L'essai de GST pull down- GST-eIF3f, et GST seul, ont été dosées pour l'interaction avec la protéine recombinante eIF3h comme indiqué sur le panneau de gauche. Les fractions liées à la protéine de fusion GST (B) et non liées (U) ont été colorées par le bleu de Coomassie.

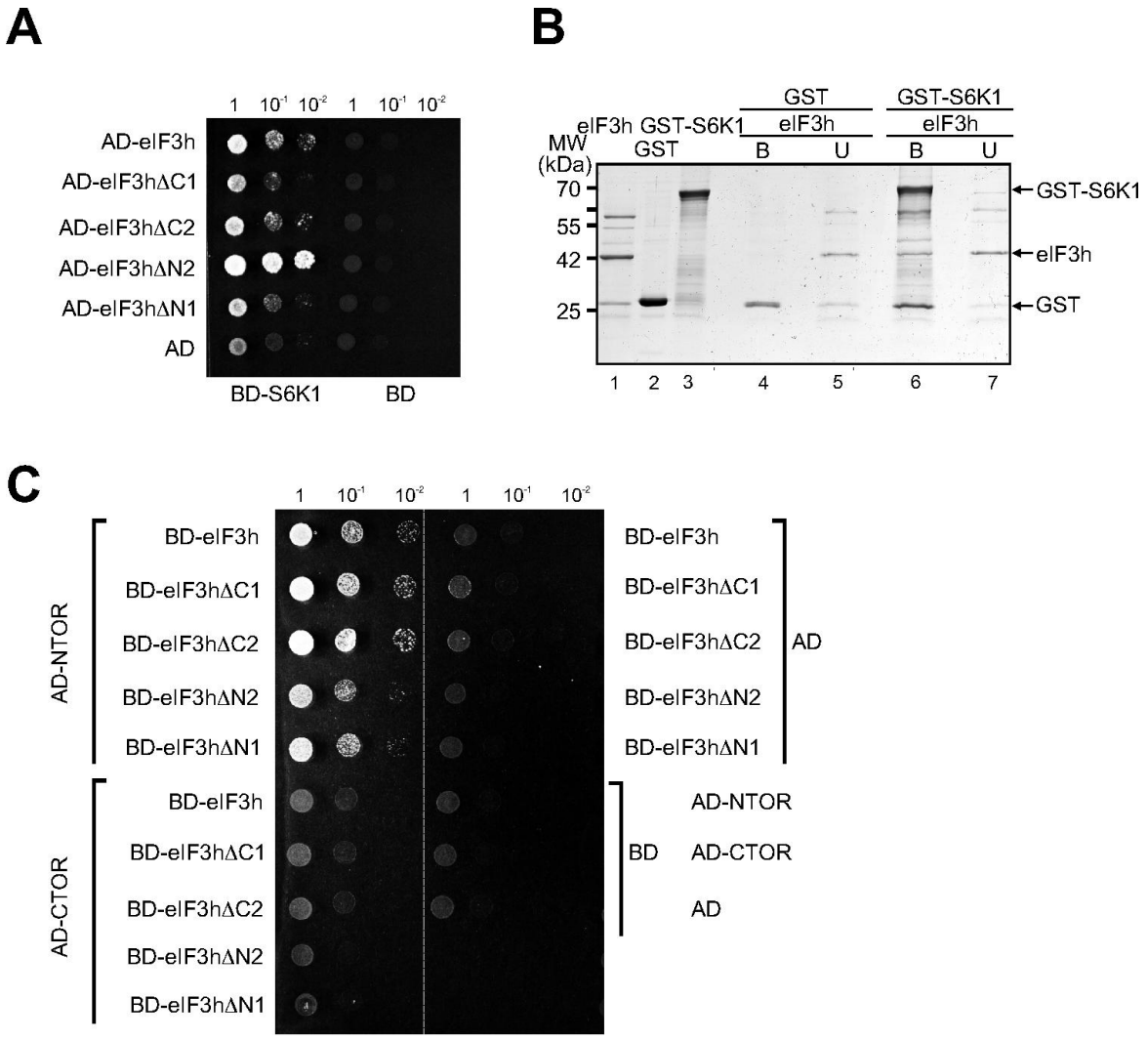

Figure 2. eIF3h interagit avec S6K1 et le domaine de répétition HEAT de TOR
(A) Interactions double hybride de levure entre BD-S6K1 et BD avec AD-eIF3h et ses variantes de délétion. Des unités égales de OD_{600} et des dilutions 1/10 et 1/100 ont été repérées de gauche à droite et incubées pendant 2 jours. (B) L'essai de GST pull down, S6K1-GST et la GST seule, ont été dosées pour l'interaction avec la protéine recombinante eIF3h comme indiqué sur le panneau de gauche. Les fractions liées à la protéine de fusion GST (B) et non liées (U) ont été colorées par le bleu de Coomassie. (C) Interactions double hybride de levure entre AD, AD-NTOR, AD-CTOR et BD, BD-eIF3h et ses variantes de délétion.

eIF3h est nécessaire pour la réinitiation de la traduction chez le virus activée par TAV

Pour activer la réinitiation de la traduction après un long ORF, TAV se lie à et active TOR, et, en outre, favorise l'accumulation de complexes contenant eIF3 dans les polysomes. En effet, les plantes transgéniques TAV sont caractérisées par un recrutement de eIF3 sur les polysomes. Connaissant que eIF3h est critique dans les cas de réinitiation cellulaire après la traduction des uORF, nous avons testé si TAV peut surmonter l'exigence de eIF3h pour la réinitiation de la traduction après un long ORF dans les protoplastes d'*Arabidopsis* préparés à partir de *eif3h-1* par rapport aux protoplastes de plantes WT.

Nous avons ensuite testé la capacité de transactivation de TAV en utilisant l'expression transitoire de constructions rapporteurs mono- et bi-cistroniques ; pmonoGFP contient un seul ORF GFP, alors que pbiGUS contient deux ORF consécutives: ORV VII de CaMV et β-glucuronidase GUS (Figue. 3A) dans des protoplastes préparés à partir de plantes *eif3h-1* et WT (figure 3A). Dans les protoplastes WT, la traduction de l'ORF GUS était empêchée par l'ORF VII situé en amont et activée seulement après surexpression de TAV (figure 3A). De façon intéressante, la surexpression eIF3h a conduit à des niveaux améliorés de transactivation médiée par TAV chez les protoplastes WT. De façon remarquable, le mutant contenant eIF3hΔC1 n'a pas activé la traduction de GUS ORF, malgré des niveaux élevés de surexpression de TAV. En revanche, en présence de TAV, la surexpression de eIF3h a stimulé la traduction ORF de GUS. Ces données indiquent fortement que eIF3h est nécessaire pour la réinitiation après un ORF court, et un ORF long, médiée par TAV.

Cette découverte ouvre la voie à l'étude de l'effet des mutants de délétion eIF3h sur la fonction de transactivation de TAV. Cependant, seul le eIF3h entier, mais pas ses mutants de délétion C ou N-terminale, pourrait soutenir la réinitiation dans les plantes *eif3h-1* (figure 3B), mettant en évidence l'importance critique de l'intégration de eIF3h dans eIF3. Bien que la phosphorylation de eIF3h soit critique pour la réinitiation après traduction de uORF, elle

ne semble pas nécessaire pour la réinitiation après un long ORF médié par TAV (figure 3C). Par conséquent, nous concluons que eIF3h est un partenaire essentiel de TAV dans l'activation de réinitiation de la traduction après un long ORF.

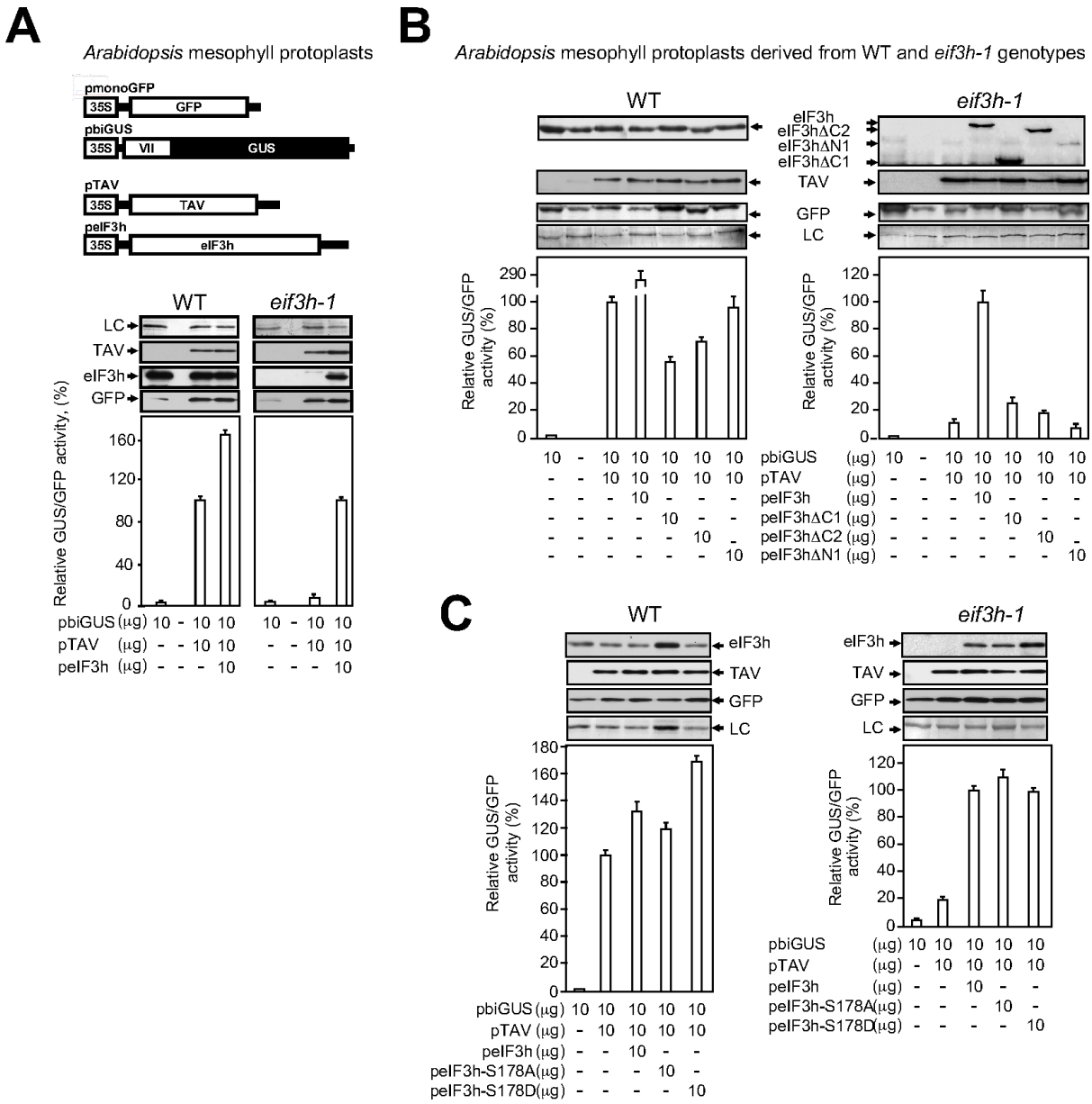

Figure 3. La transactivation médiée par TAV est efficace chez les protoplastes préparés à partir de plantes WT mais abolie chez les plantes mutantes *eif3h-1*

L'activité de GUS synthétisé dans des protoplastes transfectés par pTAV a été fixée à 100% (110 000 RFU). Les activités GUS et GFP sont respectivement représentées sous forme de barres noires et ouvertes. TAV, eIF3h et GFP ont été analysés par immunoblot. Les données montrées sont les moyennes de trois essais indépendants: les barres d'erreur indiquent SD.

eIF3h est un facteur hôte essentiel pour l'amplification du CaMV

Nous nous sommes demandé si l'infection par CaMV du mutant *eif3h-1* pourrait encore déclencher un recrutement de eIF3 sur les polysomes. Ainsi, nous avons infecté 36 plantes *Arabidopsis* et le même nombre de plantes *eif3h-1* avec un clone infectieux CaMV par agro-filtration dans deux expériences indépendantes. Bien que l'apparition de symptômes indiquant une infection systémique à 10 dpi fût évidente pour les plantes WT, les plantes *eif3h-1* ne présentaient aucun symptôme à 10 dpi ou 23 dpi (figure 4A). Au total, 100% des plantes WT présentaient des symptômes typiques de CaMV, alors qu'aucune plante *eif3h-1* ne manifestait des symptômes de CaMV. L'analyse de la cinétique de réplication du virus (figure 4B) n'a révélé aucune accumulation de TAV, et de la capside virale et ses variantes traitées dans des plantes *eif3h-1*, contrairement aux plantes WT, qui exprimaient les deux protéines virales.

Puisque les lignées transgéniques *eif3h-1* d'*Arabidopsis* exprimant la protéine eif3h tronquée de son extrémité C-terminale, sont déficientes pour la réinitiation mais pas pour l'initiation de la traduction, nous avons testé si les plantes *eif3h-1* seraient sensibles à l'infection par des virus exploitant différents mécanismes de traduction. Le virus de la mosaïque du colza (ORMV) utilise probablement une stratégie d'initiation de la traduction commune aux Tobamovirus, dont la traduction de l'ARN génomique est coiffe- dépendante. Pour tester si les plantes *eif3h-1* sont sensibles à l'ORMV, 36 plantes WT et 36 *eif3h-1* ont été inoculées mécaniquement avec des particules d'ORMV; Nous avons noté le développement des symptômes à 10 dpi pour les deux génotypes (Figure 4C), et l'accumulation d'ARN polymérase dépendante de l'ARN (RdRp) était évidente pour les plantes WT et *eif3h-1* (Figure 4D), suggérant fortement que la truncation eIF3h n'a pas significativement diminué la réplication du virus ORMV. Ces résultats suggèrent fortement que eIF3h est dispensable pour l'initiation de la traduction virale cap-dépendante.

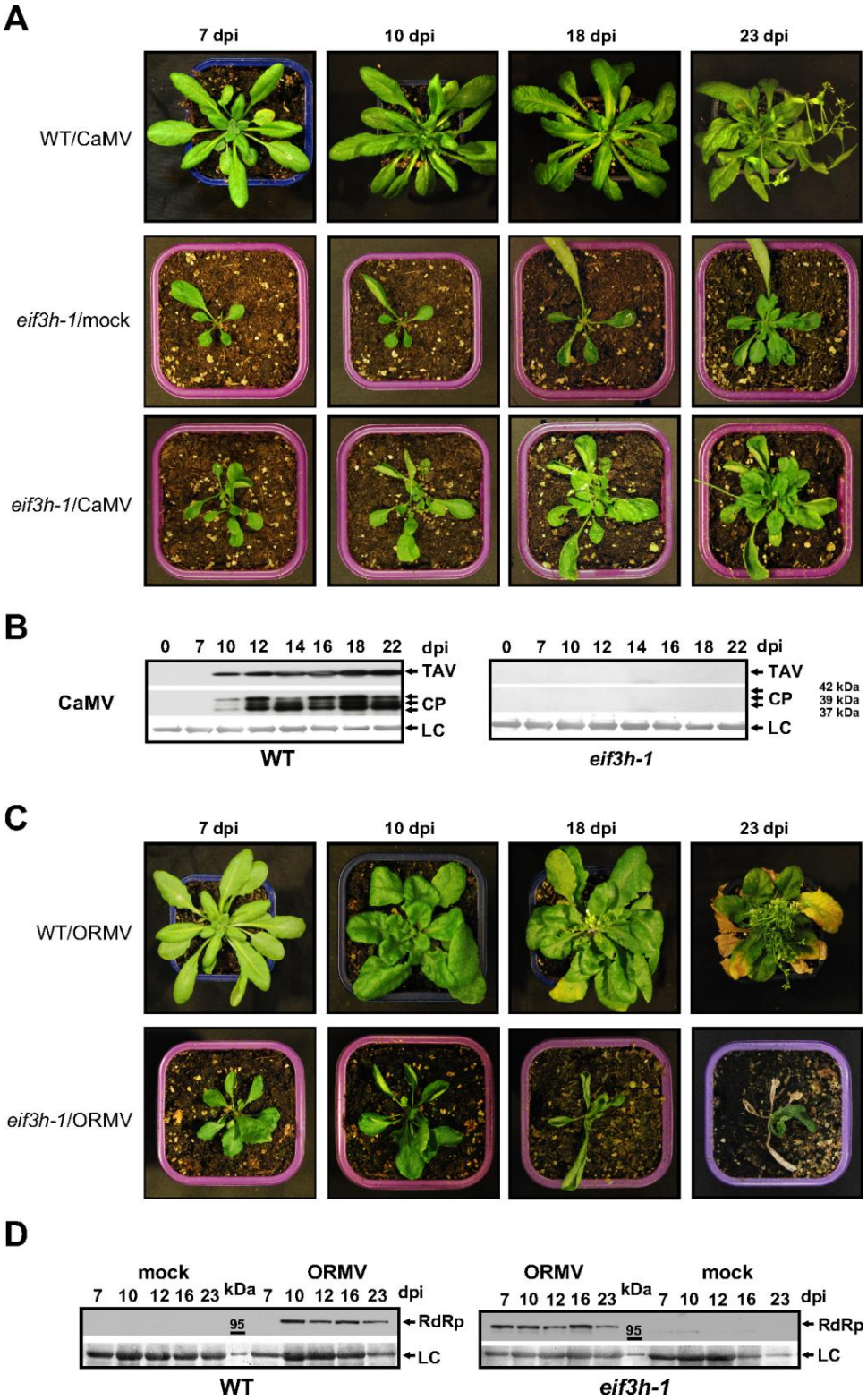

Figure 4. Les plantes *eif3h-1* sont résistantes au CaMV
(A) Analyse des plantes mutantes *eif3h-1 (panneaux centraux)* et des symptômes de la maladie de CaMV dans le type sauvage *(WT; panneaux supérieurs)* et *eif3h-1 (panneaux de fond)*. (B) Les protéines TAV et CP s'accumulent dans les plantes WT infectées par CaMV *(panneau de gauche)*, mais pas dans les plantes *eif3h-1 (panneau de droite)*. (C) Analyse des symptômes de la maladie du virus de la mosaïque du colza (ORMV) chez les WT *(panneaux supérieurs)* et les *eif3h-1 (panneaux du bas)*. (D) L'ARN polymérase ARN-dépendante (RdRp) s'accumule chez les plantes WT infectées par ORMV *(panneau gauche)*, et chez les plantes *eif3h-1 (panneau de droite)*.

Le virus de la mosaïque du navet (TuMV) est un Potyvirus de la famille des Potyviridae. Ces virus ont un VPg à la place de la coiffe à l'extrémité 5' de l'ARNm. En l'absence de cap, TuMV initie la traduction d'un ARN génomique via IRES qui recrute le PIC 43S par l'intermédiaire de l'eIF4G lié à VPg. Pour tester si l'initiation interne nécessite le facteur eIF3h, des plantes WT et *eif3h-1* ont été agro-filtrées avec un clone TuMV infectieux portant un ORF GFP placé entre ORF1 et ORF2. Toutes les plantes testées étaient entièrement sensibles au TuMV, avec des symptômes de TuMV, une fluorescence GFP et une accumulation détectées à 10 dpi pour des plantes WT et mutantes (figure 5). Ainsi, eIF3h est probablement dispensable pour la stratégie d'initiation interne de Potyviridae. Nous avons conclu que la résistance de *eif3h-1* au CaMV est spécifique au mécanisme de réinitiation de la traduction et probablement développée en raison de défauts dans eIF3h ou eIF3 incomplet, ce qui limite la réinitiation activée par TAV et donc la réplication CaMV chez des plantes d'*Arabidopsis*.

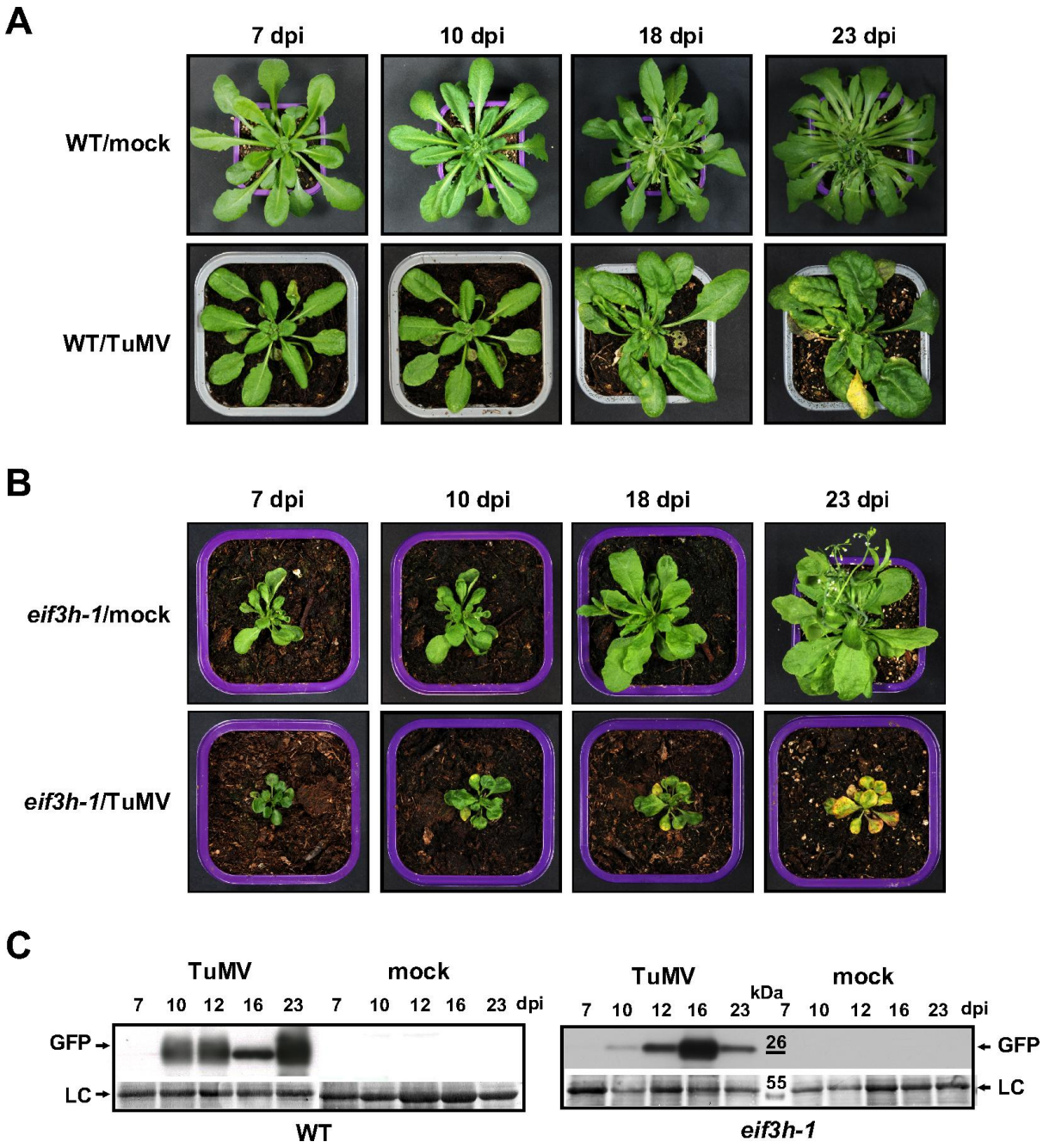

Figure 5. Les plantes *eif3h-1* sont sensibles au virus de la mosaïque du navet (TuMV)
(A-B) Analyse des plantes WT *(A, panneaux supérieurs)* et *eif3h-1 (B, panneaux supérieurs)* et les symptômes de TuMV chez les plantes de type sauvage *(A, panneaux du fond)* et *eif3h-1* (B, panneaux inférieurs). (C) La protéine GFP s'accumulent dans le type sauvage infecté par TuMV *(panneau de gauche*) et dans les plantes *eif3h-1 (panneau de droite).*

Discussion

La traduction des ARNm qui abritent des ORFs courts dans leurs UTR 5' est régularisée par des événements de réinitialisation normalement inefficaces. La traduction de leur ORF principal dépend de la participation de certains eIF soutenant la réinitiation qui sont recrutés pendant le premier événement d'initiation cap-dependent à l'uORF et ensuite non libérés pendant le temps court requis pour la traduction du uORF . Ces «facteurs supportant la réinitiation» restent associés aux ribosomes après la terminaison et peuvent régénérer des complexes de réinitiation 40S compétents. Chez les plantes, la sous-unité eIF3h, si elle est phosphorylée, supporte les événements de réinitiation tout en étant dispensable pour des événements d'initiation. Le mécanisme de fonction de eIF3h dans la réinitiation n'est pas encore compris. Nous montrons maintenant que eIF3h, s'il est phosphorylé par TOR, peut jouer un rôle dans le recrutement de eIF3 sur les polysomes. De plus, eIF3h joue un rôle dans un cas exceptionnel de réinitiation de la traduction contrôlé par le facteur de réinitiation CaMV TAV, ce qui peut favoriser la traduction de plusieurs long ORF consécutives sur le même ARN par réinitiation chez *Arabidopsis* et d'autres plantes hôtes. Nos résultats suggèrent fortement que, comme dans la réinitiation de la traduction après un court ORF, eIF3h est un facteur critique pour TAV dans la promotion d'un mode de traduction polycistronique, ce qui suggère fortement que TAV exploite cette machinerie cellulaire, et plus particulièrement TOR et eIF3h, pour exprimer ses propres protéines par réinitiation de la traduction.

La délétion de 40 acides aminés N-terminaux a aboli la réinitiation de la traduction après un long ORF contrôlée par TAV (figure 3B). En effet, la résolution récente de la structure PIC de 43S de mammifère suggère que l'extrémité N-terminale de eIF3h est exposée à l'environnement et peut entrer en contact avec des polysomes via une composante encore inconnue qui est critique pour la réinitiation.

Conclusion

Ce rapport identifie eIF3h comme un important facteur hôte critique pour l'amplification du virus de CaMV. De nombreux gènes de résistance récessive codent les facteurs d'initiation de la traduction-eIF4E et eIF4G, leurs isoformes, eIFiso4E et eIFiso4G et d'autres facteurs de traduction eIF4A-like helicases, eIF3, eEF1A et eEF1B. Ainsi, les gènes de résistance dans les plantes fournissent d'excellents outils pour les programmes de reproduction pour lutter contre les maladies des plantes causées par les virus pathogènes. Ces facteurs semblent être recrutés par les virus ARN non seulement pour traduire leurs ARN viraux, mais aussi pour réguler leur réplication et potentialiser leur mouvement local et systémique. Ainsi, nous ne pouvons pas exclure que eIF3h pourrait participer à d'autres étapes de la réplication CaMV.

VI. BIBLIOGRAPHY

Ahmadian, G., J. S. Randhawa and A. J. Easton, 2000 Expression of the ORF-2 protein of the human respiratory syncytial virus M2 gene is initiated by a ribosomal termination-dependent reinitiation mechanism. EMBO J 19**:** 2681-2689.

Aichinger, E., N. Kornet, T. Friedrich and T. Laux, 2012 Plant stem cell niches. Annu Rev Plant Biol 63**:** 615-636.

Alisch, R. S., J. L. Garcia-Perez, A. R. Muotri, F. H. Gage and J. V. Moran, 2006 Unconventional translation of mammalian LINE-1 retrotransposons. Genes Dev 20**:** 210-224.

Alkalaeva, E. Z., A. V. Pisarev, L. Y. Frolova, L. L. Kisselev and T. V. Pestova, 2006 In vitro reconstitution of eukaryotic translation reveals cooperativity between release factors eRF1 and eRF3. Cell 125**:** 1125-1136.

Allen, G. S., and J. Frank, 2007 Structural insights on the translation initiation complex: ghosts of a universal initiation complex. Mol Microbiol 63**:** 941-950.

Alone, P. V., and T. E. Dever, 2006 Direct binding of translation initiation factor eIF2gamma-G domain to its GTPase-activating and GDP-GTP exchange factors eIF5 and eIF2B epsilon. J Biol Chem 281**:** 12636-12644.

Andreou, A. Z., and D. Klostermeier, 2014 eIF4B and eIF4G jointly stimulate eIF4A ATPase and unwinding activities by modulation of the eIF4A conformational cycle. J Mol Biol 426**:** 51-61.

Atkinson, G. C., S. L. Baldauf and V. Hauryliuk, 2008 Evolution of nonstop, no-go and nonsense-mediated mRNA decay and their termination factor-derived components. BMC Evol Biol 8**:** 290.

Bailey-Serres, J., L. K. Dixon, A. D. Liddell and C. J. Leaver, 1986 Nuclear-mitochondrial interactions in cytoplasmic male-sterile sorghum. Theor Appl Genet 73**:** 252-260.

Bandyopadhyay, A., T. Matsumoto and U. Maitra, 2000 Fission yeast Int6 is not essential for global translation initiation, but deletion of int6(+) causes hypersensitivity to caffeine and affects spore formation. Mol Biol Cell 11**:** 4005-4018.

Basso, J., P. Dallaire, P. J. Charest, Y. Devantier and J. F. Laliberte, 1994 Evidence for an internal ribosome entry site within the 5' non-translated region of turnip mosaic potyvirus RNA. J Gen Virol 75 (Pt 11)**:** 3157-3165.

Benne, R., and J. W. Hershey, 1978 The mechanism of action of protein synthesis initiation factors from rabbit reticulocytes. J Biol Chem 253**:** 3078-3087.

Ben-Shem, A., N. Garreau de Loubresse, S. Melnikov, L. Jenner, G. Yusupova and M. Yusupov, 2011 The structure of the eukaryotic ribosome at 3.0 A resolution. Science 334**:** 1524-1529.

Besancon, R., S. Valsesia-Wittmann, C. Locher, C. Delloye-Bourgeois, L. Furhman *et al.*, 2009 Upstream ORF affects MYCN translation depending on exon 1b alternative splicing. BMC Cancer 9**:** 445.

Beznoskova, P., L. Cuchalova, S. Wagner, C. J. Shoemaker, S. Gunisova *et al.*, 2013 Translation initiation factors eIF3 and HCR1 control translation termination and stop codon read-through in yeast cells. PLoS Genet 9**:** e1003962.

Boex-Fontvieille, E., M. Daventure, M. Jossier, M. Zivy, M. Hodges *et al.*, 2013 Photosynthetic control of Arabidopsis leaf cytoplasmic translation initiation by protein phosphorylation. PLoS One 8**:** e70692.

Bonneville, J. M., H. Sanfacon, J. Futterer and T. Hohn, 1989 Posttranscriptional trans-activation in cauliflower mosaic virus. Cell 59**:** 1135-1143.

Brand, U., J. C. Fletcher, M. Hobe, E. M. Meyerowitz and R. Simon, 2000 Dependence of stem cell fate in Arabidopsis on a feedback loop regulated by CLV3 activity. Science 289**:** 617-619.

Browning, K. S., 1996 The plant translational apparatus. Plant Mol Biol 32**:** 107-144.

Browning, K. S., and J. Bailey-Serres, 2015 Mechanism of cytoplasmic mRNA translation. Arabidopsis Book 13**:** e0176.

Burks, E. A., P. P. Bezerra, H. Le, D. R. Gallie and K. S. Browning, 2001 Plant initiation factor 3 subunit composition resembles mammalian initiation factor 3 and has a novel subunit. J Biol Chem 276**:** 2122-2131.

Calkhoven, C. F., C. Muller and A. Leutz, 2000 Translational control of C/EBPalpha and C/EBPbeta isoform expression. Genes Dev 14**:** 1920-1932.

Calvo, S. E., D. J. Pagliarini and V. K. Mootha, 2009 Upstream open reading frames cause widespread reduction of protein expression and are polymorphic among humans. Proc Natl Acad Sci U S A 106**:** 7507-7512.

Carroll, A. J., J. L. Heazlewood, J. Ito and A. H. Millar, 2008 Analysis of the Arabidopsis cytosolic ribosome proteome provides detailed insights into its components and their post-translational modification. Mol Cell Proteomics 7**:** 347-369.

Casati, P., and V. Walbot, 2004 Crosslinking of ribosomal proteins to RNA in maize ribosomes by UV-B and its effects on translation. Plant Physiol 136**:** 3319-3332.

Cerritelli, S. M., O. Y. Fedoroff, B. R. Reid and R. J. Crouch, 1998 A common 40 amino acid motif in eukaryotic RNases H1 and caulimovirus ORF VI proteins binds to duplex RNAs. Nucleic Acids Res 26**:** 1834-1840.

Chapman, B., and C. Brown, 2004 Translation termination in Arabidopsis thaliana: characterisation of three versions of release factor 1. Gene 341**:** 219-225.

Chaudhuri, J., D. Chowdhury and U. Maitra, 1999 Distinct functions of eukaryotic translation initiation factors eIF1A and eIF3 in the formation of the 40 S ribosomal preinitiation complex. J Biol Chem 274**:** 17975-17980.

Chavatte, L., A. Seit-Nebi, V. Dubovaya and A. Favre, 2002 The invariant uridine of stop codons contacts the conserved NIKSR loop of human eRF1 in the ribosome. EMBO J 21**:** 5302-5311.

Chen, L., D. Muhlrad, V. Hauryliuk, Z. Cheng, M. K. Lim *et al.*, 2010 Structure of the Dom34-Hbs1 complex and implications for no-go decay. Nat Struct Mol Biol 17**:** 1233-1240.

Col, B., S. Oltean and R. Banerjee, 2007 Translational regulation of human methionine synthase by upstream open reading frames. Biochim Biophys Acta 1769**:** 532-540.

Conte, M. R., G. Kelly, J. Babon and C. G. Proud, 2006 Resonance assignment for the N-terminal region of the eukaryotic initiation factor 5 (eIF5). J Biomol NMR 36 Suppl 1**:** 42.

Cornu, M., V. Albert and M. N. Hall, 2013 mTOR in aging, metabolism, and cancer. Curr Opin Genet Dev 23**:** 53-62.

Csibi, A., K. Cornille, M. P. Leibovitch, A. Poupon, L. A. Tintignac *et al.*, 2010 The translation regulatory subunit eIF3f controls the kinase-dependent mTOR signaling required for muscle differentiation and hypertrophy in mouse. PLoS One 5**:** e8994.

Csibi, A., L. A. Tintignac, M. P. Leibovitch and S. A. Leibovitch, 2008 eIF3-f function in skeletal muscles: to stand at the crossroads of atrophy and hypertrophy. Cell Cycle 7**:** 1698-1701.

Cuchalova, L., T. Kouba, A. Herrmannova, I. Danyi, W. L. Chiu *et al.*, 2010 The RNA recognition motif of eukaryotic translation initiation factor 3g (eIF3g) is required for resumption of scanning of posttermination ribosomes for reinitiation on GCN4 and together with eIF3i stimulates linear scanning. Mol Cell Biol 30**:** 4671-4686.

Daubert, S. D., J. Schoelz, L. Debao and R. J. Shepherd, 1984 Expression of disease symptoms in cauliflower mosaic virus genomic hybrids. J Mol Appl Genet 2**:** 537-547.

De Tapia, M., A. Himmelbach and T. Hohn, 1993 Molecular dissection of the cauliflower mosaic virus translation transactivator. EMBO J 12**:** 3305-3314.

Dennis, M. D., M. D. Person and K. S. Browning, 2009 Phosphorylation of plant translation initiation factors by CK2 enhances the in vitro interaction of multifactor complex components. J Biol Chem 284**:** 20615-20628.

Deprost, D., H. N. Truong, C. Robaglia and C. Meyer, 2005 An Arabidopsis homolog of RAPTOR/KOG1 is essential for early embryo development. Biochem Biophys Res Commun 326**:** 844-850.

Deprost, D., L. Yao, R. Sormani, M. Moreau, G. Leterreux *et al.*, 2007 The Arabidopsis TOR kinase links plant growth, yield, stress resistance and mRNA translation. EMBO Rep 8**:** 864-870.

des Georges, A., V. Dhote, L. Kuhn, C. U. Hellen, T. V. Pestova *et al.*, 2015 Structure of mammalian eIF3 in the context of the 43S preinitiation complex. Nature 525**:** 491-495.

Dever, T. E., and R. Green, 2012 The elongation, termination, and recycling phases of translation in eukaryotes. Cold Spring Harb Perspect Biol 4**:** a013706.

Dixon, L. K., and T. Hohn, 1984 Initiation of translation of the cauliflower mosaic virus genome from a polycistronic mRNA: evidence from deletion mutagenesis. EMBO J 3**:** 2731-2736.

Dobrenel, T., C. Caldana, J. Hanson, C. Robaglia, M. Vincentz *et al.*, 2016 TOR Signaling and Nutrient Sensing. Annu Rev Plant Biol 67**:** 261-285.

Doerfel, L. K., I. Wohlgemuth, C. Kothe, F. Peske, H. Urlaub *et al.*, 2013 EF-P is essential for rapid synthesis of proteins containing consecutive proline residues. Science 339**:** 85-88.

Dong, Z., Z. Liu, P. Cui, R. Pincheira, Y. Yang *et al.*, 2009 Role of eIF3a in regulating cell cycle progression. Exp Cell Res 315**:** 1889-1894.

Dresios, J., I. L. Derkatch, S. W. Liebman and D. Synetos, 2000 Yeast ribosomal protein L24 affects the kinetics of protein synthesis and ribosomal protein L39 improves translational accuracy, while mutants lacking both remain viable. Biochemistry 39**:** 7236-7244.

Dufner, A., and G. Thomas, 1999 Ribosomal S6 kinase signaling and the control of translation. Exp Cell Res 253**:** 100-109.

Ehsan, H., W. K. Ray, B. Phinney, X. Wang, S. C. Huber *et al.*, 2005 Interaction of Arabidopsis BRASSINOSTEROID-INSENSITIVE 1 receptor kinase with a homolog of mammalian TGF-beta receptor interacting protein. Plant J 43**:** 251-261.

Evans, D. R., R. A. Singer, G. C. Johnston and A. E. Wheals, 1994 Cell-cycle mutations among the collection of Saccharomyces cerevisiae dna mutants. FEMS Microbiol Lett 116**:** 147-153.

Eyler, D. E., and R. Green, 2011 Distinct response of yeast ribosomes to a miscoding event during translation. RNA 17**:** 925-932.

Fekete, C. A., S. F. Mitchell, V. A. Cherkasova, D. Applefield, M. A. Algire *et al.*, 2007 N- and C-terminal residues of eIF1A have opposing effects on the fidelity of start codon selection. EMBO J 26**:** 1602-1614.

Fernandez, J., I. Yaman, R. Mishra, W. C. Merrick, M. D. Snider *et al.*, 2001 Internal ribosome entry site-mediated translation of a mammalian mRNA is regulated by amino acid availability. J Biol Chem 276**:** 12285-12291.

Franco, R., and M. G. Rosenfeld, 1990 Hormonally inducible phosphorylation of a nuclear pool of ribosomal protein S6. J Biol Chem 265**:** 4321-4325.

Freire, M. A., 2005 Translation initiation factor (iso) 4E interacts with BTF3, the beta subunit of the nascent polypeptide-associated complex. Gene 345**:** 271-277.

Freire, M. A., C. Tourneur, F. Granier, J. Camonis, A. El Amrani *et al.*, 2000 Plant lipoxygenase 2 is a translation initiation factor-4E-binding protein. Plant Mol Biol 44**:** 129-140.

Futterer, J., K. Gordon, P. Pfeiffer, H. Sanfacon, B. Pisan *et al.*, 1989 Differential inhibition of downstream gene expression by the cauliflower mosaic virus 35S RNA leader. Virus Genes 3**:** 45-55.

Futterer, J., K. Gordon, H. Sanfacon, J. M. Bonneville and T. Hohn, 1990 Positive and negative control of translation by the leader sequence of cauliflower mosaic virus pregenomic 35S RNA. EMBO J 9**:** 1697-1707.

Futterer, J., and T. Hohn, 1991 Translation of a polycistronic mRNA in the presence of the cauliflower mosaic virus transactivator protein. EMBO J 10**:** 3887-3896.

Futterer, J., and T. Hohn, 1996 Translation in plants--rules and exceptions. Plant Mol Biol 32**:** 159-189.

Futterer, J., Z. Kiss-Laszlo and T. Hohn, 1993 Nonlinear ribosome migration on cauliflower mosaic virus 35S RNA. Cell 73**:** 789-802.

Futterer, J., I. Potrykus, Y. Bao, L. Li, T. M. Burns *et al.*, 1996 Position-dependent ATT initiation during plant pararetrovirus rice tungro bacilliform virus translation. J Virol 70**:** 2999-3010.

Gallie, D. R., 2002 Protein-protein interactions required during translation. Plant Mol Biol 50**:** 949-970.

Gallie, D. R., 2014 The role of the poly(A) binding protein in the assembly of the Cap-binding complex during translation initiation in plants. Translation (Austin) 2**:** e959378.

Gallie, D. R., and M. Kobayashi, 1994 The role of the 3'-untranslated region of non-polyadenylated plant viral mRNAs in regulating translational efficiency. Gene 142**:** 159-165.

Garcia-Ruiz, H., A. Carbonell, J. S. Hoyer, N. Fahlgren, K. B. Gilbert *et al.*, 2015 Roles and programming of Arabidopsis ARGONAUTE proteins during Turnip mosaic virus infection. PLoS Pathog 11**:** e1004755.

Gingras, A. C., S. P. Gygi, B. Raught, R. D. Polakiewicz, R. T. Abraham *et al.*, 1999 Regulation of 4E-BP1 phosphorylation: a novel two-step mechanism. Genes Dev 13**:** 1422-1437.

Gingras, A. C., B. Raught, S. P. Gygi, A. Niedzwiecka, M. Miron *et al.*, 2001 Hierarchical phosphorylation of the translation inhibitor 4E-BP1. Genes Dev 15**:** 2852-2864.

Green, K. A., M. J. Prigge, R. B. Katzman and S. E. Clark, 2005 CORONA, a member of the class III homeodomain leucine zipper gene family in Arabidopsis, regulates stem cell specification and organogenesis. Plant Cell 17**:** 691-704.

Guo, J., D. J. Hui, W. C. Merrick and G. C. Sen, 2000 A new pathway of translational regulation mediated by eukaryotic initiation factor 3. EMBO J 19**:** 6891-6899.

Guo, Y., L. Han, M. Hymes, R. Denver and S. E. Clark, 2010 CLAVATA2 forms a distinct CLE-binding receptor complex regulating Arabidopsis stem cell specification. Plant J 63**:** 889-900.

Gutierrez, E., B. S. Shin, C. J. Woolstenhulme, J. R. Kim, P. Saini *et al.*, 2013 eIF5A promotes translation of polyproline motifs. Mol Cell 51**:** 35-45.

Hanfrey, C., K. A. Elliott, M. Franceschetti, M. J. Mayer, C. Illingworth *et al.*, 2005 A dual upstream open reading frame-based autoregulatory circuit controlling polyamine-responsive translation. J Biol Chem 280**:** 39229-39237.

Hardtke, C. S., and T. Berleth, 1998 The Arabidopsis gene MONOPTEROS encodes a transcription factor mediating embryo axis formation and vascular development. EMBO J 17**:** 1405-1411.

Harris, T. E., A. Chi, J. Shabanowitz, D. F. Hunt, R. E. Rhoads *et al.*, 2006 mTOR-dependent stimulation of the association of eIF4G and eIF3 by insulin. EMBO J 25**:** 1659-1668.

Hashem, Y., A. des Georges, V. Dhote, R. Langlois, H. Y. Liao *et al.*, 2013 Structure of the mammalian ribosomal 43S preinitiation complex bound to the scanning factor DHX29. Cell 153**:** 1108-1119.

Heitman, J., N. R. Movva and M. N. Hall, 1991 Targets for cell cycle arrest by the immunosuppressant rapamycin in yeast. Science 253**:** 905-909.

Hernandez, G., and P. Vazquez-Pianzola, 2005 Functional diversity of the eukaryotic translation initiation factors belonging to eIF4 families. Mech Dev 122**:** 865-876.

Hershey, J. W., 2015 The role of eIF3 and its individual subunits in cancer. Biochim Biophys Acta 1849**:** 792-800.

Heufler, C., K. S. Browning and J. M. Ravel, 1988 Properties of the subunits of wheat germ initiation factor 3. Biochim Biophys Acta 951**:** 182-190.

Himmelbach, A., Y. Chapdelaine and T. Hohn, 1996 Interaction between cauliflower mosaic virus inclusion body protein and capsid protein: implications for viral assembly. Virology 217**:** 147-157.

Hinnebusch, A. G., 2006 eIF3: a versatile scaffold for translation initiation complexes. Trends Biochem Sci 31**:** 553-562.

Hinnebusch, A. G., 2014 The scanning mechanism of eukaryotic translation initiation. Annu Rev Biochem 83**:** 779-812.

Hinnebusch, A. G., and J. R. Lorsch, 2012 The mechanism of eukaryotic translation initiation: new insights and challenges. Cold Spring Harb Perspect Biol 4.

Hofmann, K., and P. Bucher, 1998 The PCI domain: a common theme in three multiprotein complexes. Trends Biochem Sci 23**:** 204-205.

Holz, M. K., B. A. Ballif, S. P. Gygi and J. Blenis, 2005 mTOR and S6K1 mediate assembly of the translation preinitiation complex through dynamic protein interchange and ordered phosphorylation events. Cell 123**:** 569-580.

Howarth, A. J., R. C. Gardner, J. Messing and R. J. Shepherd, 1981 Nucleotide sequence of naturally occurring deletion mutants of cauliflower mosaic virus. Virology 112**:** 678-685.

Hull, R., and R. J. Shepherd, 1976 The coat proteins of cauliflower mosaic virus. Virology 70**:** 217-220.

Iacono, M., F. Mignone and G. Pesole, 2005 uAUG and uORFs in human and rodent 5'untranslated mRNAs. Gene 349**:** 97-105.

Imataka, H., H. S. Olsen and N. Sonenberg, 1997 A new translational regulator with homology to eukaryotic translation initiation factor 4G. EMBO J 16**:** 817-825.

Ingolia, N. T., S. Ghaemmaghami, J. R. Newman and J. S. Weissman, 2009 Genome-wide analysis in vivo of translation with nucleotide resolution using ribosome profiling. Science 324**:** 218-223.

Ivanov, I. P., J. F. Atkins and A. J. Michael, 2010 A profusion of upstream open reading frame mechanisms in polyamine-responsive translational regulation. Nucleic Acids Res 38**:** 353-359.

Jackson, R. J., C. U. Hellen and T. V. Pestova, 2012 Termination and post-termination events in eukaryotic translation. Adv Protein Chem Struct Biol 86**:** 45-93.

Jefferson, R. A., T. A. Kavanagh and M. W. Bevan, 1987 GUS fusions: beta-glucuronidase as a sensitive and versatile gene fusion marker in higher plants. EMBO J 6**:** 3901-3907.

Jennings, M. D., and G. D. Pavitt, 2010 eIF5 has GDI activity necessary for translational control by eIF2 phosphorylation. Nature 465**:** 378-381.

Jewell, J. L., and K. L. Guan, 2013 Nutrient signaling to mTOR and cell growth. Trends Biochem Sci 38**:** 233-242.

Jiang, J., and S. D. Clouse, 2001 Expression of a plant gene with sequence similarity to animal TGF-beta receptor interacting protein is regulated by brassinosteroids and required for normal plant development. Plant J 26**:** 35-45.

Jiang, J., and J. F. Laliberte, 2011 The genome-linked protein VPg of plant viruses-a protein with many partners. Curr Opin Virol 1**:** 347-354.

Joshi, B., K. Lee, D. L. Maeder and R. Jagus, 2005 Phylogenetic analysis of eIF4E-family members. BMC Evol Biol 5**:** 48.

Karniol, B., A. Yahalom, S. Kwok, T. Tsuge, M. Matsui *et al.*, 1998 The Arabidopsis homologue of an eIF3 complex subunit associates with the COP9 complex. FEBS Lett 439**:** 173-179.

Kawaguchi, R., and J. Bailey-Serres, 2002 Regulation of translational initiation in plants. Curr Opin Plant Biol 5**:** 460-465.

Kieft, J. S., A. Grech, P. Adams and J. A. Doudna, 2001 Mechanisms of internal ribosome entry in translation initiation. Cold Spring Harb Symp Quant Biol 66**:** 277-283.

Kim, B. H., X. Cai, J. N. Vaughn and A. G. von Arnim, 2007 On the functions of the h subunit of eukaryotic initiation factor 3 in late stages of translation initiation. Genome Biol 8**:** R60.

Kim, M. I., S. W. Park, S. H. Yu, H. S. Cho, H. J. Ha *et al.*, 2001 Molecular characterization of the NeIF2Bbeta gene encoding a putative eIF2B beta-subunit in Nicotiana tabacum. Mol Cells 11**:** 110-114.

Kim, T. H., B. H. Kim, A. Yahalom, D. A. Chamovitz and A. G. von Arnim, 2004 Translational regulation via 5' mRNA leader sequences revealed by mutational analysis of the Arabidopsis translation initiation factor subunit eIF3h. Plant Cell 16**:** 3341-3356.

Klann, E., and T. E. Dever, 2004 Biochemical mechanisms for translational regulation in synaptic plasticity. Nat Rev Neurosci 5**:** 931-942.

Kobayashi, K., and T. Hohn, 2003 Dissection of cauliflower mosaic virus transactivator/viroplasmin reveals distinct essential functions in basic virus replication. J Virol 77**:** 8577-8583.

Kobayashi, K., and T. Hohn, 2004 The avirulence domain of Cauliflower mosaic virus transactivator/viroplasmin is a determinant of viral virulence in susceptible hosts. Mol Plant Microbe Interact 17**:** 475-483.

Kochetov, A. V., S. Ahmad, V. Ivanisenko, O. A. Volkova, N. A. Kolchanov *et al.*, 2008 uORFs, reinitiation and alternative translation start sites in human mRNAs. FEBS Lett 582**:** 1293-1297.

Kojima, K. K., T. Matsumoto and H. Fujiwara, 2005 Eukaryotic translational coupling in UAAUG stop-start codons for the bicistronic RNA translation of the non-long terminal repeat retrotransposon SART1. Mol Cell Biol 25**:** 7675-7686.

Kolupaeva, V. G., A. Unbehaun, I. B. Lomakin, C. U. Hellen and T. V. Pestova, 2005 Binding of eukaryotic initiation factor 3 to ribosomal 40S subunits and its role in ribosomal dissociation and anti-association. RNA 11**:** 470-486.

Kovarik, P., J. Hasek, L. Valasek and H. Ruis, 1998 RPG1: an essential gene of saccharomyces cerevisiae encoding a 110-kDa protein required for passage through the G1 phase. Curr Genet 33**:** 100-109.

Kozak, M., 1984 Selection of initiation sites by eucaryotic ribosomes: effect of inserting AUG triplets upstream from the coding sequence for preproinsulin. Nucleic Acids Res 12**:** 3873-3893.

Kozak, M., 1987 Effects of intercistronic length on the efficiency of reinitiation by eucaryotic ribosomes. Mol Cell Biol 7**:** 3438-3445.

Kozak, M., 1999 Initiation of translation in prokaryotes and eukaryotes. Gene 234**:** 187-208.

Kozak, M., 2001 Constraints on reinitiation of translation in mammals. Nucleic Acids Res 29**:** 5226-5232.

Kwon, C. S., C. Chen and D. Wagner, 2005 WUSCHEL is a primary target for transcriptional regulation by SPLAYED in dynamic control of stem cell fate in Arabidopsis. Genes Dev 19**:** 992-1003.

Laemmli, U. K., 1970 Cleavage of structural proteins during the assembly of the head of bacteriophage T4. Nature 227**:** 680-685.

Laird, J., C. McInally, C. Carr, S. Doddiah, G. Yates *et al.*, 2013 Identification of the domains of cauliflower mosaic virus protein P6 responsible for suppression of RNA silencing and salicylic acid signalling. J Gen Virol 94**:** 2777-2789.

Lamphear, B. J., R. Kirchweger, T. Skern and R. E. Rhoads, 1995 Mapping of functional domains in eukaryotic protein synthesis initiation factor 4G (eIF4G) with picornaviral

proteases. Implications for cap-dependent and cap-independent translational initiation. J Biol Chem 270**:** 21975-21983.

Laplante, M., and D. M. Sabatini, 2012 mTOR Signaling. Cold Spring Harb Perspect Biol 4.

Law, G. L., A. Raney, C. Heusner and D. R. Morris, 2001 Polyamine regulation of ribosome pausing at the upstream open reading frame of S-adenosylmethionine decarboxylase. J Biol Chem 276**:** 38036-38043.

Lee, A. S., P. J. Kranzusch, J. A. Doudna and J. H. Cate, 2016 eIF3d is an mRNA cap-binding protein that is required for specialized translation initiation. Nature 536**:** 96-99.

Liko, D., and M. N. Hall, 2015 mTOR in health and in sickness. J Mol Med (Berl) 93**:** 1061-1073.

Lingaraju, G. M., R. D. Bunker, S. Cavadini, D. Hess, U. Hassiepen *et al.*, 2014 Crystal structure of the human COP9 signalosome. Nature 512**:** 161-165.

Lopez-Valenzuela, J. A., B. C. Gibbon, D. R. Holding and B. A. Larkins, 2004 Cytoskeletal proteins are coordinately increased in maize genotypes with high levels of eEF1A. Plant Physiol 135**:** 1784-1797.

Lovett, P. S., and E. J. Rogers, 1996 Ribosome regulation by the nascent peptide. Microbiol Rev 60**:** 366-385.

Luttermann, C., and G. Meyers, 2007 A bipartite sequence motif induces translation reinitiation in feline calicivirus RNA. J Biol Chem 282**:** 7056-7065.

Luttermann, C., and G. Meyers, 2009 The importance of inter- and intramolecular base pairing for translation reinitiation on a eukaryotic bicistronic mRNA. Genes Dev 23**:** 331-344.

Luukkonen, B. G., W. Tan and S. Schwartz, 1995 Efficiency of reinitiation of translation on human immunodeficiency virus type 1 mRNAs is determined by the length of the upstream open reading frame and by intercistronic distance. J Virol 69**:** 4086-4094.

Ma, X. M., and J. Blenis, 2009 Molecular mechanisms of mTOR-mediated translational control. Nat Rev Mol Cell Biol 10**:** 307-318.

Magnuson, B., B. Ekim and D. C. Fingar, 2012 Regulation and function of ribosomal protein S6 kinase (S6K) within mTOR signalling networks. Biochem J 441**:** 1-21.

Mahfouz, M. M., S. Kim, A. J. Delauney and D. P. Verma, 2006 Arabidopsis TARGET OF RAPAMYCIN interacts with RAPTOR, which regulates the activity of S6 kinase in response to osmotic stress signals. Plant Cell 18**:** 477-490.

Marchetti, A., F. Buttitta, S. Miyazaki, D. Gallahan, G. H. Smith *et al.*, 1995 Int-6, a highly conserved, widely expressed gene, is mutated by mouse mammary tumor virus in mammary preneoplasia. J Virol 69**:** 1932-1938.

Marchione, R., S. A. Leibovitch and J. L. Lenormand, 2013 The translational factor eIF3f: the ambivalent eIF3 subunit. Cell Mol Life Sci 70**:** 3603-3616.

Marintchev, A., 2013 Roles of helicases in translation initiation: a mechanistic view. Biochim Biophys Acta 1829**:** 799-809.

Martin-Marcos, P., J. S. Nanda, R. E. Luna, F. Zhang, A. K. Saini *et al.*, 2014 Enhanced eIF1 binding to the 40S ribosome impedes conformational rearrangements of the preinitiation complex and elevates initiation accuracy. RNA 20**:** 150-167.

Martineau, Y., M. C. Derry, X. Wang, A. Yanagiya, J. J. Berlanga *et al.*, 2008 Poly(A)-binding protein-interacting protein 1 binds to eukaryotic translation initiation factor 3 to stimulate translation. Mol Cell Biol 28**:** 6658-6667.

Masutani, M., N. Sonenberg, S. Yokoyama and H. Imataka, 2007 Reconstitution reveals the functional core of mammalian eIF3. EMBO J 26**:** 3373-3383.

Mayer, C and I. Grummt, 2006 Ribosome biogenesis and cell growth: mTOR coordinates transcription by all three classes of nuclear RNA polymerases. Oncogene 48**:** 6384-6391.

Melcher, M. P., 1989 Asphyxia due to a sialocyst. Arch Otolaryngol Head Neck Surg 115**:** 1254.

Menand, B., T. Desnos, L. Nussaume, F. Berger, D. Bouchez *et al.*, 2002 Expression and disruption of the Arabidopsis TOR (target of rapamycin) gene. Proc Natl Acad Sci U S A 99**:** 6422-6427.

Meyuhas, O., 2008 Physiological roles of ribosomal protein S6: one of its kind. Int Rev Cell Mol Biol 268**:** 1-37.

Miyamoto, S., P. Patel and J. W. Hershey, 2005 Changes in ribosomal binding activity of eIF3 correlate with increased translation rates during activation of T lymphocytes. J Biol Chem 280**:** 28251-28264.

Miyoshi, H., N. Suehiro, K. Tomoo, S. Muto, T. Takahashi *et al.*, 2006 Binding analyses for the interaction between plant virus genome-linked protein (VPg) and plant translational initiation factors. Biochimie 88**:** 329-340.

Montane, M. H., and B. Menand, 2013 ATP-competitive mTOR kinase inhibitors delay plant growth by triggering early differentiation of meristematic cells but no developmental patterning change. J Exp Bot 64**:** 4361-4374.

Moreau, M., M. Azzopardi, G. Clement, T. Dobrenel, C. Marchive *et al.*, 2012 Mutations in the Arabidopsis homolog of LST8/GbetaL, a partner of the target of Rapamycin kinase, impair plant growth, flowering, and metabolic adaptation to long days. Plant Cell 24**:** 463-481.

Morris-Desbois, C., V. Bochard, C. Reynaud and P. Jalinot, 1999 Interaction between the Ret finger protein and the Int-6 gene product and co-localisation into nuclear bodies. J Cell Sci 112 (Pt 19)**:** 3331-3342.

Morris, D. R., and A. P. Geballe, 2000 Upstream open reading frames as regulators of mRNA translation. Mol Cell Biol 20**:** 8635-8642.

Munzarova, V., J. Panek, S. Gunisova, I. Danyi, B. Szamecz *et al.*, 2011 Translation reinitiation relies on the interaction between eIF3a/TIF32 and progressively folded cis-acting mRNA elements preceding short uORFs. PLoS Genet 7**:** e1002137.

Myasnikov, A. G., S. Marzi, A. Simonetti, A. M. Giuliodori, C. O. Gualerzi *et al.*, 2005 Conformational transition of initiation factor 2 from the GTP- to GDP-bound state visualized on the ribosome. Nat Struct Mol Biol 12**:** 1145-1149.

Nanda, J. S., Y. N. Cheung, J. E. Takacs, P. Martin-Marcos, A. K. Saini *et al.*, 2009 eIF1 controls multiple steps in start codon recognition during eukaryotic translation initiation. J Mol Biol 394**:** 268-285.

Nanda, J. S., A. K. Saini, A. M. Munoz, A. G. Hinnebusch and J. R. Lorsch, 2013 Coordinated movements of eukaryotic translation initiation factors eIF1, eIF1A, and eIF5 trigger phosphate release from eIF2 in response to start codon recognition by the ribosomal preinitiation complex. J Biol Chem 288**:** 5316-5329.

Nishimura, T., T. Wada, K. T. Yamamoto and K. Okada, 2005 The Arabidopsis STV1 protein, responsible for translation reinitiation, is required for auxin-mediated gynoecium patterning. Plant Cell 17**:** 2940-2953.

Oikawa, K., M. Kasahara, T. Kiyosue, T. Kagawa, N. Suetsugu *et al.*, 2003 Chloroplast unusual positioning1 is essential for proper chloroplast positioning. Plant Cell 15**:** 2805-2815.

Otero, J. H., J. Suo, C. Gordon and E. C. Chang, 2010 Int6 and Moe1 interact with Cdc48 to regulate ERAD and proper chromosome segregation. Cell Cycle 9**:** 147-161.

Oyama, M., H. Kozuka-Hata, Y. Suzuki, K. Semba, T. Yamamoto *et al.*, 2007 Diversity of translation start sites may define increased complexity of the human short ORFeome. Mol Cell Proteomics 6**:** 1000-1006.

Palam, L. R., T. D. Baird and R. C. Wek, 2011 Phosphorylation of eIF2 facilitates ribosomal bypass of an inhibitory upstream ORF to enhance CHOP translation. J Biol Chem 286**:** 10939-10949.

Park, H. S., K. S. Browning, T. Hohn and L. A. Ryabova, 2004 Eucaryotic initiation factor 4B controls eIF3-mediated ribosomal entry of viral reinitiation factor. EMBO J 23**:** 1381-1391.

Park, H. S., A. Himmelbach, K. S. Browning, T. Hohn and L. A. Ryabova, 2001 A plant viral "reinitiation" factor interacts with the host translational machinery. Cell 106**:** 723-733.

Parsyan, A., Y. Svitkin, D. Shahbazian, C. Gkogkas, P. Lasko *et al.*, 2011 mRNA helicases: the tacticians of translational control. Nat Rev Mol Cell Biol 12**:** 235-245.

Paz-Aviram, T., A. Yahalom and D. A. Chamovitz, 2008 Arabidopsis eIF3e interacts with subunits of the ribosome, Cop9 signalosome and proteasome. Plant Signal Behav 3**:** 409-411.

Perez, E. A., V. J. Suman, K. M. Rowland, J. N. Ingle, M. Salim *et al.*, 2005 Two concurrent phase II trials of paclitaxel/carboplatin/trastuzumab (weekly or every-3-week schedule) as first-line therapy in women with HER2-overexpressing metastatic breast cancer: NCCTG study 983252. Clin Breast Cancer 6**:** 425-432.

Pestova, T. V., I. B. Lomakin, J. H. Lee, S. K. Choi, T. E. Dever *et al.*, 2000 The joining of ribosomal subunits in eukaryotes requires eIF5B. Nature 403**:** 332-335.

Petsch, K. A., J. Mylne and J. R. Botella, 2005 Cosuppression of eukaryotic release factor 1-1 in Arabidopsis affects cell elongation and radial cell division. Plant Physiol 139**:** 115-126.

Phan, L., L. W. Schoenfeld, L. Valasek, K. H. Nielsen and A. G. Hinnebusch, 2001 A subcomplex of three eIF3 subunits binds eIF1 and eIF5 and stimulates ribosome binding of mRNA and tRNA(i)Met. EMBO J 20**:** 2954-2965.

Pichon, X., L. A. Wilson, M. Stoneley, A. Bastide, H. A. King *et al.*, 2012 RNA binding protein/RNA element interactions and the control of translation. Curr Protein Pept Sci 13**:** 294-304.

Pick, E., K. Hofmann and M. H. Glickman, 2009 PCI complexes: Beyond the proteasome, CSN, and eIF3 Troika. Mol Cell 35**:** 260-264.

Pisarev, A. V., M. A. Skabkin, V. P. Pisareva, O. V. Skabkina, A. M. Rakotondrafara *et al.*, 2010 The role of ABCE1 in eukaryotic posttermination ribosomal recycling. Mol Cell 37**:** 196-210.

Pisarev, A. V., A. Unbehaun, C. U. Hellen and T. V. Pestova, 2007 Assembly and analysis of eukaryotic translation initiation complexes. Methods Enzymol 430**:** 147-177.

Pisareva, V. P., A. V. Pisarev, C. U. Hellen, M. V. Rodnina and T. V. Pestova, 2006 Kinetic analysis of interaction of eukaryotic release factor 3 with guanine nucleotides. J Biol Chem 281**:** 40224-40235.

Pooggin, M. M., J. Futterer, K. G. Skryabin and T. Hohn, 1999 A short open reading frame terminating in front of a stable hairpin is the conserved feature in pregenomic RNA leaders of plant pararetroviruses. J Gen Virol 80 (Pt 8)**:** 2217-2228.

Pooggin, M. M., J. Futterer, K. G. Skryabin and T. Hohn, 2001 Ribosome shunt is essential for infectivity of cauliflower mosaic virus. Proc Natl Acad Sci U S A 98**:** 886-891.

Pooggin, M. M., T. Hohn and J. Futterer, 2000 Role of a short open reading frame in ribosome shunt on the cauliflower mosaic virus RNA leader. J Biol Chem 275**:** 17288-17296.

Powell, M. L., S. Napthine, R. J. Jackson, I. Brierley and T. D. Brown, 2008 Characterization of the termination-reinitiation strategy employed in the expression of influenza B virus BM2 protein. RNA 14**:** 2394-2406.

Poyry, T. A., A. Kaminski, E. J. Connell, C. S. Fraser and R. J. Jackson, 2007 The mechanism of an exceptional case of reinitiation after translation of a long ORF reveals why such events do not generally occur in mammalian mRNA translation. Genes Dev 21**:** 3149-3162.

Poyry, T. A., A. Kaminski and R. J. Jackson, 2004 What determines whether mammalian ribosomes resume scanning after translation of a short upstream open reading frame? Genes Dev 18**:** 62-75.

Preis, A., A. Heuer, C. Barrio-Garcia, A. Hauser, D. E. Eyler *et al.*, 2014 Cryoelectron microscopic structures of eukaryotic translation termination complexes containing eRF1-eRF3 or eRF1-ABCE1. Cell Rep 8**:** 59-65.

Przemeck, G. K., J. Mattsson, C. S. Hardtke, Z. R. Sung and T. Berleth, 1996 Studies on the role of the Arabidopsis gene MONOPTEROS in vascular development and plant cell axialization. Planta 200**:** 229-237.

Rahmani, F., M. Hummel, J. Schuurmans, A. Wiese-Klinkenberg, S. Smeekens *et al.*, 2009 Sucrose control of translation mediated by an upstream open reading frame-encoded peptide. Plant Physiol 150**:** 1356-1367.

Rasheedi, S., M. Suragani, S. K. Haq, Sachchidanand, R. Bhardwaj *et al.*, 2010 Expression, purification and ligand binding properties of the recombinant translation initiation factor (PeIF5B) from Pisum sativum. Mol Cell Biochem 344**:** 33-41.

Rebbapragada, I., and J. Lykke-Andersen, 2009 Execution of nonsense-mediated mRNA decay: what defines a substrate? Curr Opin Cell Biol 21**:** 394-402.

Reiland, S., G. Messerli, K. Baerenfaller, B. Gerrits, A. Endler *et al.*, 2009 Large-scale Arabidopsis phosphoproteome profiling reveals novel chloroplast kinase substrates and phosphorylation networks. Plant Physiol 150**:** 889-903.

Ren, M., S. Qiu, P. Venglat, D. Xiang, L. Feng *et al.*, 2011 Target of rapamycin regulates development and ribosomal RNA expression through kinase domain in Arabidopsis. Plant Physiol 155**:** 1367-1382.

Ren, M., P. Venglat, S. Qiu, L. Feng, Y. Cao *et al.*, 2012 Target of rapamycin signaling regulates metabolism, growth, and life span in Arabidopsis. Plant Cell 24**:** 4850-4874.

Richardson, C. J., M. Broenstrup, D. C. Fingar, K. Julich, B. A. Ballif *et al.*, 2004 SKAR is a specific target of S6 kinase 1 in cell growth control. Curr Biol 14**:** 1540-1549.

Robaglia, C., M. Thomas and C. Meyer, 2012 Sensing nutrient and energy status by SnRK1 and TOR kinases. Curr Opin Plant Biol 15**:** 301-307.

Rodnina, M. V., 2010 Protein synthesis meets ABC ATPases: new roles for Rli1/ABCE1. EMBO Rep 11**:** 143-144.

Rodnina, M. V., and W. Wintermeyer, 2009 Recent mechanistic insights into eukaryotic ribosomes. Curr Opin Cell Biol 21**:** 435-443.

Rodnina, M. V., and W. Wintermeyer, 2016 Protein Elongation, Co-translational Folding and Targeting. J Mol Biol 428**:** 2165-2185.

Rothnie, H. M., Y. Chapdelaine and T. Hohn, 1994 Pararetroviruses and retroviruses: a comparative review of viral structure and gene expression strategies. Adv Virus Res 44**:** 1-67.

Roy, B., J. N. Vaughn, B. H. Kim, F. Zhou, M. A. Gilchrist *et al.*, 2010 The h subunit of eIF3 promotes reinitiation competence during translation of mRNAs harboring upstream open reading frames. RNA 16**:** 748-761.

Roy, B., and A. G. von Arnim, 2013 Translational Regulation of Cytoplasmic mRNAs. Arabidopsis Book 11**:** e0165.

Ruud, K. A., C. Kuhlow, D. J. Goss and K. S. Browning, 1998 Identification and characterization of a novel cap-binding protein from Arabidopsis thaliana. J Biol Chem 273**:** 10325-10330.

Ryabova, L. A., and T. Hohn, 2000 Ribosome shunting in the cauliflower mosaic virus 35S RNA leader is a special case of reinitiation of translation functioning in plant and animal systems. Genes Dev 14**:** 817-829.

Ryabova, L. A., M. M. Pooggin and T. Hohn, 2002 Viral strategies of translation initiation: ribosomal shunt and reinitiation. Prog Nucleic Acid Res Mol Biol 72**:** 1-39.

Ryabova, L. A., M. M. Pooggin and T. Hohn, 2006 Translation reinitiation and leaky scanning in plant viruses. Virus Res 119**:** 52-62.

Sachs, A. B., and R. W. Davis, 1989 The poly(A) binding protein is required for poly(A) shortening and 60S ribosomal subunit-dependent translation initiation. Cell 58**:** 857-867.

Sanchez, A. M., A. Csibi, A. Raibon, A. Docquier, J. Lagirand-Cantaloube *et al.*, 2013 eIF3f: a central regulator of the antagonism atrophy/hypertrophy in skeletal muscle. Int J Biochem Cell Biol 45**:** 2158-2162.

Sanfacon, H., 2015 Plant Translation Factors and Virus Resistance. Viruses 7**:** 3392-3419.

Sasikumar, A. N., W. B. Perez and T. G. Kinzy, 2012 The many roles of the eukaryotic elongation factor 1 complex. Wiley Interdiscip Rev RNA 3**:** 543-555.

Scharf, K. D., and L. Nover, 1982 Heat-shock-induced alterations of ribosomal protein phosphorylation in plant cell cultures. Cell 30**:** 427-437.

Schepetilnikov, M., M. Dimitrova, E. Mancera-Martinez, A. Geldreich, M. Keller *et al.*, 2013 TOR and S6K1 promote translation reinitiation of uORF-containing mRNAs via phosphorylation of eIF3h. EMBO J 32**:** 1087-1102.

Schepetilnikov, M., K. Kobayashi, A. Geldreich, C. Caranta, C. Robaglia *et al.*, 2011 Viral factor TAV recruits TOR/S6K1 signalling to activate reinitiation after long ORF translation. EMBO J 30**:** 1343-1356.

Scholthof, H. B., S. Gowda, F. C. Wu and R. J. Shepherd, 1992 The full-length transcript of a caulimovirus is a polycistronic mRNA whose genes are trans activated by the product of gene VI. J Virol 66**:** 3131-3139.

Sessions, R. A., and P. C. Zambryski, 1995 Arabidopsis gynoecium structure in the wild and in ettin mutants. Development 121**:** 1519-1532.

Shen, X., Y. Yang, W. Liu, M. Sun, J. Jiang *et al.*, 2004 Identification of the p28 subunit of eukaryotic initiation factor 3(eIF3k) as a new interaction partner of cyclin D3. FEBS Lett 573**:** 139-146.

Shi, J., A. Kahle, J. W. Hershey, B. M. Honchak, J. A. Warneke *et al.*, 2006 Decreased expression of eukaryotic initiation factor 3f deregulates translation and apoptosis in tumor cells. Oncogene 25**:** 4923-4936.

Silvera, D., S. C. Formenti and R. J. Schneider, 2010 Translational control in cancer. Nat Rev Cancer 10**:** 254-266.

Singh, B., H. Chauhan, J. P. Khurana, P. Khurana and P. Singh, 2013 Evidence for the role of wheat eukaryotic translation initiation factor 3 subunit g (TaeIF3g) in abiotic stress tolerance. Gene 532**:** 177-185.

Singh, C. R., R. Watanabe, W. Chowdhury, H. Hiraishi, M. J. Murai *et al.*, 2012 Sequential eukaryotic translation initiation factor 5 (eIF5) binding to the charged disordered segments of eIF4G and eIF2beta stabilizes the 48S preinitiation complex and promotes its shift to the initiation mode. Mol Cell Biol 32**:** 3978-3989.

Siridechadilok, B., C. S. Fraser, R. J. Hall, J. A. Doudna and E. Nogales, 2005 Structural roles for human translation factor eIF3 in initiation of protein synthesis. Science 310**:** 1513-1515.

Skabkin, M. A., O. V. Skabkina, V. Dhote, A. A. Komar, C. U. Hellen *et al.*, 2010 Activities of Ligatin and MCT-1/DENR in eukaryotic translation initiation and ribosomal recycling. Genes Dev 24**:** 1787-1801.

Skabkin, M. A., O. V. Skabkina, C. U. Hellen and T. V. Pestova, 2013 Reinitiation and other unconventional posttermination events during eukaryotic translation. Mol Cell 51**:** 249-264.

Slavoff, S. A., A. J. Mitchell, A. G. Schwaid, M. N. Cabili, J. Ma *et al.*, 2013 Peptidomic discovery of short open reading frame-encoded peptides in human cells. Nat Chem Biol 9**:** 59-64.

Smith, M. D., L. Arake-Tacca, A. Nitido, E. Montabana, A. Park *et al.*, 2016 Assembly of eIF3 Mediated by Mutually Dependent Subunit Insertion. Structure 24**:** 886-896.

Smith, M. D., Y. Gu, J. Querol-Audi, J. M. Vogan, A. Nitido *et al.*, 2013 Human-like eukaryotic translation initiation factor 3 from Neurospora crassa. PLoS One 8**:** e78715.

Sokabe, M., C. S. Fraser and J. W. Hershey, 2012 The human translation initiation multi-factor complex promotes methionyl-tRNAi binding to the 40S ribosomal subunit. Nucleic Acids Res 40**:** 905-913.

Somers, J., T. Poyry and A. E. Willis, 2013 A perspective on mammalian upstream open reading frame function. Int J Biochem Cell Biol 45**:** 1690-1700.

Sosnovtsev, S. V., G. Belliot, K. O. Chang, O. Onwudiwe and K. Y. Green, 2005 Feline calicivirus VP2 is essential for the production of infectious virions. J Virol 79**:** 4012-4024.

Spriggs, K. A., M. Bushell and A. E. Willis, 2010 Translational regulation of gene expression during conditions of cell stress. Mol Cell 40**:** 228-237.

Stansfield, I., K. M. Jones and M. F. Tuite, 1995 The end in sight: terminating translation in eukaryotes. Trends Biochem Sci 20**:** 489-491.

Sun, C., A. Todorovic, J. Querol-Audi, Y. Bai, N. Villa *et al.*, 2011 Functional reconstitution of human eukaryotic translation initiation factor 3 (eIF3). Proc Natl Acad Sci U S A 108**:** 20473-20478.

Suragani, M., S. Rasheedi, S. E. Hasnain and N. Z. Ehtesham, 2011 The translation initiation factor, PeIF5B, from Pisum sativum displays chaperone activity. Biochem Biophys Res Commun 414**:** 390-396.

Szamecz, B., E. Rutkai, L. Cuchalova, V. Munzarova, A. Herrmannova *et al.*, 2008 eIF3a cooperates with sequences 5' of uORF1 to promote resumption of scanning by post-termination ribosomes for reinitiation on GCN4 mRNA. Genes Dev 22**:** 2414-2425.

Tabuchi, T., T. Okada, T. Azuma, T. Nanmori and T. Yasuda, 2006 Posttranscriptional regulation by the upstream open reading frame of the phosphoethanolamine N-methyltransferase gene. Biosci Biotechnol Biochem 70**:** 2330-2334.

Tarun, S. Z., Jr., and A. B. Sachs, 1996 Association of the yeast poly(A) tail binding protein with translation initiation factor eIF-4G. EMBO J 15**:** 7168-7177.

Thiebeauld, O., M. Schepetilnikov, H. S. Park, A. Geldreich, K. Kobayashi *et al.*, 2009 A new plant protein interacts with eIF3 and 60S to enhance virus-activated translation re-initiation. EMBO J 28**:** 3171-3184.

Thoreen, C. C., S. A. Kang, J. W. Chang, Q. Liu, J. Zhang *et al.*, 2009 An ATP-competitive mammalian target of rapamycin inhibitor reveals rapamycin-resistant functions of mTORC1. J Biol Chem 284**:** 8023-8032.

Tiruneh, B. S., B. H. Kim, D. R. Gallie, B. Roy and A. G. von Arnim, 2013 The global translation profile in a ribosomal protein mutant resembles that of an eIF3 mutant. BMC Biol 11**:** 123.

Tiwari, S. B., G. Hagen and T. Guilfoyle, 2003 The roles of auxin response factor domains in auxin-responsive transcription. Plant Cell 15**:** 533-543.

Tran, H. T., and W. C. Plaxton, 2008 Proteomic analysis of alterations in the secretome of Arabidopsis thaliana suspension cells subjected to nutritional phosphate deficiency. Proteomics 8**:** 4317-4326.

Turck, F., F. Zilbermann, S. C. Kozma, G. Thomas and F. Nagy, 2004 Phytohormones participate in an S6 kinase signal transduction pathway in Arabidopsis. Plant Physiol 134**:** 1527-1535.

Ulmasov, T., G. Hagen and T. J. Guilfoyle, 1997 ARF1, a transcription factor that binds to auxin response elements. Science 276**:** 1865-1868.

Ulmasov, T., G. Hagen and T. J. Guilfoyle, 1999 Activation and repression of transcription by auxin-response factors. Proc Natl Acad Sci U S A 96**:** 5844-5849.

Vain, P., A. Harvey, B. Worland, S. Ross, J. W. Snape *et al.*, 2004 The effect of additional virulence genes on transformation efficiency, transgene integration and expression in rice plants using the pGreen/pSoup dual binary vector system. Transgenic Res 13**:** 593-603.

Valasek, L. S., 2012 'Ribozoomin'--translation initiation from the perspective of the ribosome-bound eukaryotic initiation factors (eIFs). Curr Protein Pept Sci 13**:** 305-330.

Vattem, K. M., and R. C. Wek, 2004 Reinitiation involving upstream ORFs regulates ATF4 mRNA translation in mammalian cells. Proc Natl Acad Sci U S A 101**:** 11269-11274.

Vezina, C., A. Kudelski and S. N. Sehgal, 1975 Rapamycin (AY-22,989), a new antifungal antibiotic. I. Taxonomy of the producing streptomycete and isolation of the active principle. J Antibiot (Tokyo) 28**:** 721-726.

Vilela, C., B. Linz, C. Rodrigues-Pousada and J. E. McCarthy, 1998 The yeast transcription factor genes YAP1 and YAP2 are subject to differential control at the levels of both translation and mRNA stability. Nucleic Acids Res 26**:** 1150-1159.

Voigts-Hoffmann, F., S. Klinge and N. Ban, 2012 Structural insights into eukaryotic ribosomes and the initiation of translation. Curr Opin Struct Biol 22**:** 768-777.

von Arnim, A. G., Q. Jia and J. N. Vaughn, 2014 Regulation of plant translation by upstream open reading frames. Plant Sci 214**:** 1-12.

Walsh, D., and I. Mohr, 2014 Coupling 40S ribosome recruitment to modification of a cap-binding initiation factor by eIF3 subunit e. Genes Dev 28**:** 835-840.

Wang, A., and S. Krishnaswamy, 2012 Eukaryotic translation initiation factor 4E-mediated recessive resistance to plant viruses and its utility in crop improvement. Mol Plant Pathol 13**:** 795-803.

Wen, F., R. Zhou, A. Shen, A. Choi, D. Uribe *et al.*, 2012 The tumor suppressive role of eIF3f and its function in translation inhibition and rRNA degradation. PLoS One 7**:** e34194.

Wiese, A., N. Elzinga, B. Wobbes and S. Smeekens, 2004 A conserved upstream open reading frame mediates sucrose-induced repression of translation. Plant Cell 16**:** 1717-1729.

Wilker, E. W., M. A. van Vugt, S. A. Artim, P. H. Huang, C. P. Petersen *et al.*, 2007 14-3-3sigma controls mitotic translation to facilitate cytokinesis. Nature 446**:** 329-332.

Wullschleger, S., R. Loewith and M. N. Hall, 2006 TOR signaling in growth and metabolism. Cell 124**:** 471-484.

Xia, C., Y. J. Wang, W. Q. Li, Y. R. Chen, Y. Deng *et al.*, 2010 The Arabidopsis eukaryotic translation initiation factor 3, subunit F (AteIF3f), is required for pollen germination and embryogenesis. Plant J 63**:** 189-202.

Xie, X., and K. L. Guan, 2011 The ribosome and TORC2: collaborators for cell growth. Cell 144**:** 640-642.

Xiong, Y., M. McCormack, L. Li, Q. Hall, C. Xiang *et al.*, 2013 Glucose-TOR signalling reprograms the transcriptome and activates meristems. Nature 496**:** 181-186.

Xiong, Y., and J. Sheen, 2012 Rapamycin and glucose-target of rapamycin (TOR) protein signaling in plants. J Biol Chem 287**:** 2836-2842.

Yahalom, A., T. H. Kim, B. Roy, R. Singer, A. G. von Arnim *et al.*, 2008 Arabidopsis eIF3e is regulated by the COP9 signalosome and has an impact on development and protein translation. Plant J 53**:** 300-311.

Yaman, I., J. Fernandez, H. Liu, M. Caprara, A. A. Komar *et al.*, 2003 The zipper model of translational control: a small upstream ORF is the switch that controls structural remodeling of an mRNA leader. Cell 113**:** 519-531.

Yang, H. S., M. H. Cho, H. Zakowicz, G. Hegamyer, N. Sonenberg *et al.*, 2004 A novel function of the MA-3 domains in transformation and translation suppressor Pdcd4 is essential for its binding to eukaryotic translation initiation factor 4A. Mol Cell Biol 24**:** 3894-3906.

Yoo, S. D., Y. H. Cho and J. Sheen, 2007 Arabidopsis mesophyll protoplasts: a versatile cell system for transient gene expression analysis. Nat Protoc 2**:** 1565-1572.

Young, D. J., N. R. Guydosh, F. Zhang, A. G. Hinnebusch and R. Green, 2015 Rli1/ABCE1 Recycles Terminating Ribosomes and Controls Translation Reinitiation in 3'UTRs In Vivo. Cell 162**:** 872-884.

Zhou, C., F. Arslan, S. Wee, S. Krishnan, A. R. Ivanov *et al.*, 2005 PCI proteins eIF3e and eIF3m define distinct translation initiation factor 3 complexes. BMC Biol 3**:** 14.

Zhou, F., B. Roy, J. R. Dunlap, R. Enganti and A. G. von Arnim, 2014 Translational control of Arabidopsis meristem stability and organogenesis by the eukaryotic translation factor eIF3h. PLoS One 9**:** e95396.

Zhou, F., B. Roy and A. G. von Arnim, 2010 Translation reinitiation and development are compromised in similar ways by mutations in translation initiation factor eIF3h and the ribosomal protein RPL24. BMC Plant Biol 10**:** 193.

Zoncu, R., L. Bar-Peled, A. Efeyan, S. Wang, Y. Sancak *et al.*, 2011 mTORC1 senses lysosomal amino acids through an inside-out mechanism that requires the vacuolar H(+)-ATPase. Science 334**:** 678-683.

UNIVERSITÉ DE STRASBOURG

Joelle MAKARIAN

Rôle du facteur d'initiation eIF3h dans la réinitiation de la traduction et dans la pathogénèse virale chez les plantes

École Doctorale des Sciences de la Vie et de la Santé STRASBOURG

Résumé

La réinitiation de la traduction est un mécanisme permettant de traduire des ORF qui sont présents dans la région *leader* de différents ARNm cellulaires (uORF). La majorité des cas de réinitiation de la traduction chez les eucaryotes concerne des uORF de petite taille. Des stratégies alternatives ont été développées, entre autres par les virus, afin de réinitier la traduction après un long uORF. Le *virus de la mosaïque du chou-fleur* (CaMV) exprime un ARNm polycistronique codant la totalité des protéines virales. L'une d'entre elle, la protéine TAV (TransActivateur/Viroplasmine) est un facteur essentiel qui rend possible la réinitiation de la traduction après de longs ORF et qui, de plus, active la protéine kinase TOR. La sous-unité h du facteur d'initiation de la traduction eIF3, requise pour promouvoir la reinitiation après un petit ORF chez les plantes, a été identifiée comme étant une nouvelle cible de phosphorylation de la voie de signalisation de TOR. L'objectif principal de ma thèse a été d'élucider la fonction de la protéine eIF3h dans la réinitiation après un petit ORF ainsi que dans la réinitiation de la traduction, assurée par TAV, après un long ORF. Nous avons exploité les lignées transgéniques *eif3h-1* d'*Arabidopsis* exprimant la protéine eif3h tronquée de son extrémité C-terminale, qui sont déficientes pour la réinitiation mais pas pour l'initiation de la traduction. Nous avons montré que la phosphorylation de eIF3h est essentielle pour stabiliser eIF3 au niveau des ribosomes durant l'élongation, ce qui favorise la ré-acquisition par le ribosome de facteurs nécessaires à la réinitiation de la traduction, et que la délétion de sa région Ct abolit son intégration dans le complexe eIF3. De plus, nous avons montré que eIF3h, la cible de la voie de signalisation de TOR, interagit avec S6K1. Des protoplastes préparés à partir des plantes mutantes *eif3h-1* sont incapables de promouvoir la réinitiation après de longs ORF en présence de TAV. La surexpression de eIF3h, indifféremment de son état de phosphorylation, est indispensable pour restaurer la reinitiation assurée par TAV dans les protoplastes *eif3h-1*. Par ailleurs, les plantes *eif3h-1* déficientes dans la réinitiation, sont résistantes à l'infection par le CaMV démontrant l'importance de eIF3h pour la réplication du CaMV. En revanche, ces plantes *eif3h-1* peuvent être infectées par d'autres virus dont la traduction de l'ARN génomique est coiffe- ou IRES-dépendante. Ainsi, nos résultats suggèrent que eIF3h est un facteur de reinitiation important aussi bien pour la reinitiation après un petit qu'après un long ORF (controlée par TAV), et que TAV exploite cette machinerie cellulaire, et plus particulièrement TOR et eIF3h, pour exprimer ses propres protéines par réinitiation de la traduction.

Mots clés : Réinitiation de la traduction, CaMV, TAV, sous-unité h de eIF3, voie de signalisation TOR

Résumé en anglais

Translation of mRNAs that harbor upstream open reading frames (uORFs) within their leader regions operates via a reinitiation mechanism. In plants, reinitiation is up regulated by the target of rapamycin (TOR) signaling via phosphorylation of the subunit h of initiation factor 3 (eIF3). The *eif3h-1* mutant expressing the C-terminally truncated eIF3h while maintaining high translation initiation efficiency is not active in reinitiation. *Cauliflower mosaic virus* (CaMV) pregenomic polycistronic RNA is translated via an exceptional mechanism of reinitiation after long ORF translation under control of CaMV protein TAV, which ensures activation of TOR. To find the link between underlying mechanisms, we examined eIF3h function in cellular and viral context. Here we show that eIF3h, if phosphorylated, has a role in recruitment of eIF3 into actively translating ribosomes that is a prerequisite for formation of reinitiation-competent ribosomal complexes. C-terminal truncation of eIF3h abolished its integration into the eIF3 complex and eIF3 loading on polysomes as manifested by the eIF3 core subunit c. We also show that eIF3h as a putative target of TOR/S6K1 binds S6K1 *in vitro*. eIF3h phosphorylation is not required for eIF3 complex formation. We demonstrated that eIF3h is essential for TAV to activate reinitiation after long ORF translation. Protoplasts derived from *eif3h-1* mutant failed to support TAV function in reinitiation, which is restored only upon overexpression of recombinant eIF3h indifferent to its phosphorylation status. *eif3h-1* mutant defective in reinitiation was found resistant to CaMV infection suggesting that eIF3h is critical for virus amplification. In contrast, viruses that evolve translation initiation dependent on either cap or the internal ribosome entry site infect reinitiation deficient mutant. Thus, we conclude that TAV exploits the basic cell reinitiation machinery, particularly TOR and eIF3h, to overcome cellular barriers to reinitiation after long ORF translation.

Keywords: Reinitiation, CaMV, eIF3 subunit h, TAV, long ORF translation, TOR signaling pathway, S6K1